Towards 100% Renewable Energy Supply for Urban Areas and the role of Smart Control

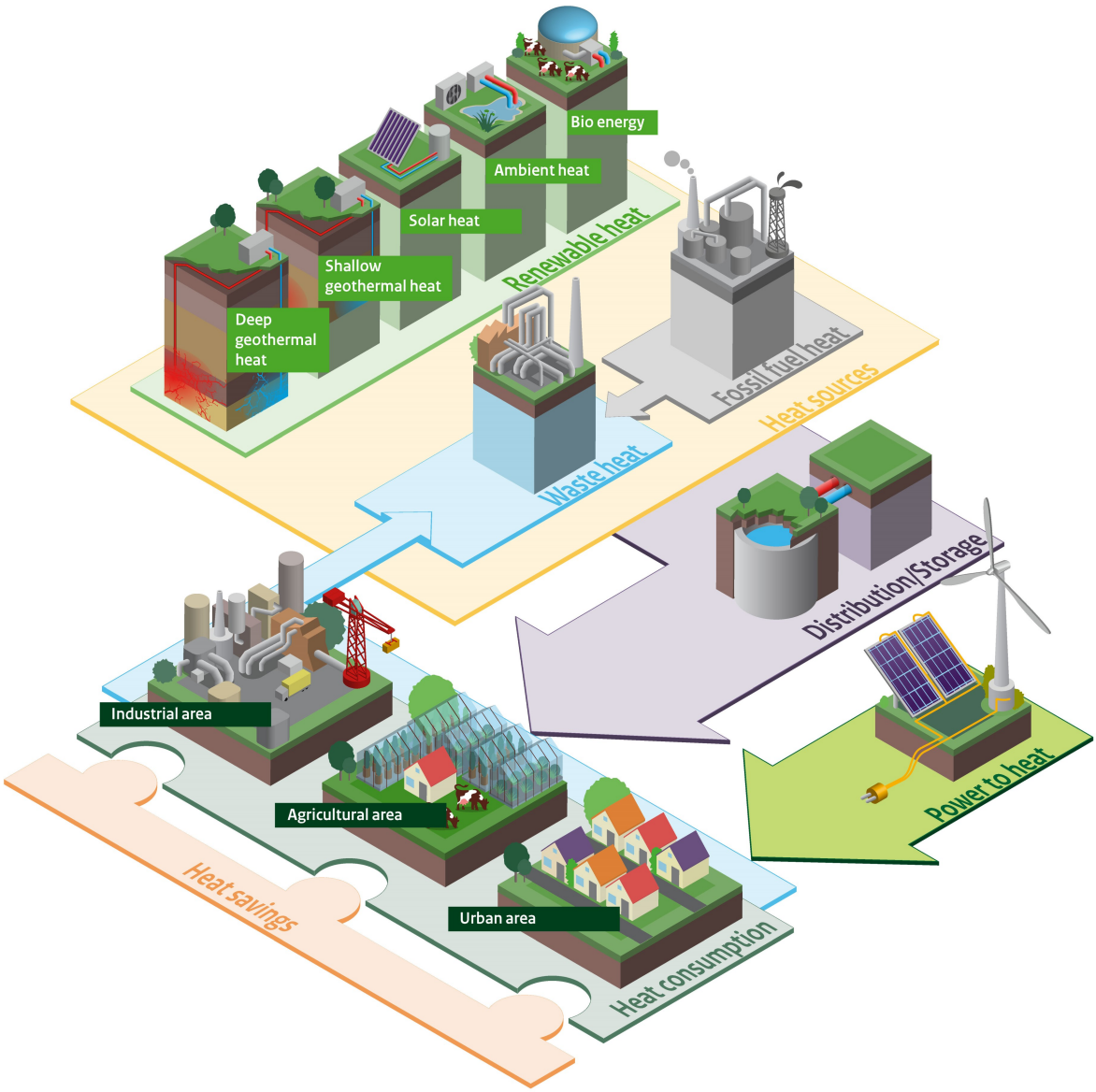

Richard Pieter van Leeuwen

Towards 100% renewable energy supply for urban areas and the role of smart control

Richard Pieter van Leeuwen

Promotie commissie:

prof.dr.ir.	G.J.M. Smit	University of Twente (promotor)
prof.dr.	J.L. Hurink	University of Twente (promotor)
prof.dr.	H. Lund	Aalborg University, Denmark
prof.ir.	W. Zeiler	Eindhoven University of Technology
prof.dr.ing.	C. Wetter	Münster University of Applied Sciences
prof.dr.	A.K.I. Remke	University of Twente & University of Münster
prof.dr.ir.	T.H. van der Meer	University of Twente
prof.dr.	P.M.G. Apers	University of Twente (voorzitter)

This research is funded by the Topsector Energie, which is part of the Netherlands Enterprise Organization (RVO) and funded by the Dutch Ministry of Economic Affairs, as part of the Topconsortia Kennis en Innovatie (TKI) program Switch2Smartgrids, Smart Grid Meppelenergie project (project number 01005).

This research is partly funded by the Dutch Technology Foundation (STW), which is part of the Netherlands Organization for Scientific Research (NWO) and partly funded by the Ministry of Economic Affairs, as part of the Personalised Climate and Ambience Control for Zero-Energy Buildings (iCARE) project (STW project number 11854).

This research is partly funded by the Euregio Twente-Münsterland, funded by the European Union, as part of the Wärme in der Euregio (WIEfm) project.

UNIVERSITY OF TWENTE.
Faculty of Electrical Engineering, Mathematics and Computer Science,
Computer Architecture for Embedded Systems (CAES) and
Discrete Mathematics and Mathematical Programming (DMMP)

Academy Life Science Engineering and Design
Research chair Renewable Energy

CTIT

Centre for Telematics and Information Technology
P.O. Box 217, 7500 AE Enschede, the Netherlands
CTIT Ph.D. thesis series no. 17-433 (ISSN 1381-3617)

ISBN 978-90-365-4346-0
ISSN 1381-3617 (CTIT Ph.D. thesis series no. 17-433)
DOI 10.3990/1.9789036543460

The cover picture "heat transition" was kindly provided by the National Expertise Center for Heat. ©Rijksoverheid rvo.nl/new

TOWARDS 100% RENEWABLE ENERGY SUPPLY FOR URBAN AREAS AND THE ROLE OF SMART CONTROL

PROEFSCHRIFT

ter verkrijging van
de graad van doctor aan de Universiteit Twente,
op gezag van de rector magnificus,
prof. dr. T.T.M. Palstra,
volgens besluit van het College voor Promoties
in het openbaar te verdedigen
op donderdag 18 mei 2017 om 14:45 uur

door

Richard Pieter van Leeuwen
geboren op 25 december 1968
te Oud-Vossemeer

Dit proefschrift is goedgekeurd door:

prof.dr.ir.	G.J.M. Smit	University of Twente (promotor)
prof.dr.	J.L. Hurink	University of Twente (promotor)

ISBN 978-90-365-4346-0

Abstract

In the Netherlands, 60% of the consumed energy is for the thermal demand of buildings and industrial processes. More than half of this is for heating purposes of the built environment, predominantly by natural gas boilers. At present, only 4.5% of the primary energy input is from renewable energy sources. Recently, integration of renewable energy in the built environment and increasing energy efficiency of buildings are receiving much attention. Policies of the Dutch government are aimed at phasing out the use of natural gas for heating buildings entirely within a time period of 40 years. This will lead to a larger amount of district heating projects and heat pump installations the coming years, using renewable sources as bio-based fuels, solar PV, wind turbines, waste heat streams and underground thermal sources.
Besides a shift from fossil towards renewable energy supply, often in the form of electrical energy generation (solar PV and wind turbines), part of the demand is also being electrified, e.g. heat pumps for the thermal demand and electric vehicles for transportation. As a consequence, the existing electricity grid experiences increasing demand and supply peaks due to fluctuating generation and fluctuating demand patterns. To overcome this, energy storage and smart control of devices can offer flexibility which may avoid problematic supply and demand peak loads.
As renewable energy is generated on decentral levels in the vicinity of the real demand, regional and local energy generation, storage technology and smart control receive increasing attention. For these decentral energy systems, renewable energy supply and expected demand patterns determine which generation and storage capacity and which control scheme is as optimal as possible. This thesis is dedicated to the development of tools for these aspects and demonstrates how smart control leads to near optimal capacities and operation of renewable energy system assets.
The thesis is centered around a smart grid demonstration project called "Meppel-energie". The purpose of this project is to demonstrate a completely renewable energy system for a new built district in which a biogas cogenerator supplies thermal energy for a district heating system and electrical energy for a group of heat pumps. The goal is to determine optimal capacities and control of generation and storage assets. Models for household space heating and cooling demand are developed, also for household hot water and electricity demand and for the state of charge of a thermal storage and electrical batteries. Of particular interest is the

possibility to store thermal energy within concrete floor heating systems for which a model is developed and effects on thermal comfort and costs for residents are investigated. Within the thesis, the models are either used to generate demand patterns or for model predictive control as part of smart control methods.
To determine optimal capacities of assets for two urban energy cases, a case specific model and a generalized system model are developed. The generalized model includes prioritization of energy generation and storage and can be applied to analyze specific urban energy cases. For one case, the hourly energy exchanges with the power grid are investigated and the possible improvements when smarter control methods are used. For this case, three possible system layouts are investigated with the goal to reach 100% renewable energy supply. The costs and environmental performance of these layouts are compared. This analysis also considers newly built districts from 2020 when Near Zero Energy Building standards are mandatory. Of special interest is the question whether to invest in district heating or in individual heating systems in such cases.
The urban energy case analysis shows that smart control, e.g. of storage devices and generators, is beneficial to keep grid exchanges within permitted boundaries or to eliminate them totally. To study this in more detail, a model predictive control method is developed for a specific case: controlling a central co-generation unit and a large group of heat pumps for the "Meppel-energie" project. The control method is verified on computational effort and performance in terms of reaching the control objectives, thermal comfort and on/off switching behavior of the devices. Next to the Meppel case, a small neighborhood of 16 houses with a central co-generation unit, solar PV, electric batteries and some flexible appliances is investigated. Of particular interest is the possibility for near off-grid operation with this energy system through smart control.
In relation to the control problem of renewable energy powered, urban energy systems, the thesis shows that smart control is effective if: (a) the control is able to forecast demand and generation of renewable sources, at least a couple of hours ahead, and (b) the control objective is aimed at making use of renewable energy sources as much as possible while maintaining acceptable comfort for residents. Also, it is demonstrated that smart control could lead to higher costs for residents than conventional control methods which should be avoided by dynamic energy tariffs. For predictions of household energy consumption, the thesis shows that there are methods available which avoid gathering privacy sensitive information from households on aggregated levels.
The urban energy case analysis demonstrates a method to determine optimal capacities of generators and storage facilities and shows which smart energy control functionality should be implemented to avoid peak grid loads. In theory this should lead to less grid related investments and prolonged service life-time of energy system related assets. Besides that, the smart heat pump control case shows that thermal comfort for residents can be improved while reducing their energy costs.

Samenvatting

In Nederland is de thermische energievraag 60% van de totale energievraag. Meer dan de helft daarvan is voor verwarming van gebouwen, hoofdzakelijk via aardgas ketels. Momenteel is slechts 4,5% van de primaire energie-input afkomstig van hernieuwbare energiebronnen. De integratie van duurzame energie in de gebouwde omgeving en het verhogen van de energie-efficiëntie van gebouwen krijgt veel aandacht. Het beleid van de Nederlandse overheid is gericht op het geheel uitfaseren van het gebruik van aardgas voor de verwarming van gebouwen binnen een periode van 40 jaar. Dit zal waarschijnlijk leiden tot een grotere hoeveelheid stadsverwarmingsprojecten en warmtepompinstallaties de komende jaren en het gebruik van hernieuwbare bronnen zoals biologische brandstoffen, zon-PV, windturbines, afvalwarmtestromen en ondergrondse thermische bronnen.
Behalve een verschuiving van fossiele naar duurzame energie, vaak in de vorm van elektrische energie (zon-PV en wind turbines), wordt ook een deel van de vraag geëlektrificeerd, b.v. warmtepompen voor de thermische behoefte en elektrische voertuigen voor transport. Een gevolg is dat het bestaande elektriciteitsnet toenemende vraag- en aanbodpieken moet verwerken als gevolg van fluctuerende opwekking en wisselende vraagpatronen. Energieopslag en intelligente aansturing van apparaten kunnen flexibiliteit bieden om deze problematische piekbelastingen te voorkomen.
Duurzame energie wordt voor een belangrijk deel opgewekt op decentraal niveau in de nabijheid van de energieverbruikers. Dit vraagt om regionale en lokale opwekking van energie, opslagtechnologie en slimme regelsystemen. Energieopwekking- en vraagpatronen bepalen welke productie- en opslagcapaciteit nodig is en welk regelsysteem zo optimaal mogelijk de energiestromen kan sturen. Dit proefschrift ontwikkelt instrumenten hiervoor en laat zien hoe slimme energieregeling kan leiden tot een vrijwel optimale capaciteit en exploitatie van duurzame energiesystemen.
Het onderzoek is uitgevoerd in het kader van het smart grid demonstratieproject "Meppelenergie". In dit nieuwbouwproject levert een biogas warmtekrachtinstallatie (WKK) thermische energie voor een stadsverwarmingsnet en elektrische energie voor woningen die zijn voorzien van warmtepompen. Het doel is hiervoor de optimale capaciteiten te bepalen en een slim regelsysteem te ontwikkelen. Hiervoor zijn modellen ontwikkeld die de warmte- en koelvraag, elektriciteitsvraag, en de status van de thermische en elektrische opslag kunnen voorspellen. Daarnaast

is een model ontwikkeld voor de opslag van thermische energie in de betonnen vloerverwarming van de woningen, waarmee tevens de effecten op de behaaglijkheid en de kosten voor de bewoners zijn onderzocht. In het proefschrift wordt getoond hoe deze modellen gebruikt kunnen worden voor model predictive control en voor het genereren van vraagpatronen.
Om zo optimaal mogelijke systeemcapaciteiten van duurzame energiesystemen te kunnen bepalen, is een capaciteitsmodel ontwikkeld. Het model bevat een prioritering van energie-opwekking en -opslag en kan worden toegepast op specifieke, gebouwde omgevingsanalyses. Binnen een integratiecasus is de uurlijkse energieuitwisseling met het elektriciteitsnet onderzocht en de mogelijke verbetering door slimme energieregeling. Voor deze casus zijn drie mogelijke energiesystemen onderzocht met als doel hiermee een zo goed mogelijk 100% duurzame energievoorziening te bereiken. Daarnaast zijn de kosten en milieuprestaties van deze systeemopties vergeleken. Ook is een variant onderzocht voor nieuw te bouwen wijken vanaf 2020 wanneer Bijna Energie Neutrale Gebouwen (BENG) verplicht zijn. Van bijzonder belang is de vraag of geïnvesteerd moet worden in stadsverwarming of in individuele verwarmingsinstallaties.
Uit de casus blijkt dat intelligente regeling van duurzame energie-opwekking en opslag, ervoor zorgt dat uitwisseling van energie met het elektriciteitsnet binnen toegestane grenzen blijft of zelfs volledig achterwege kan blijven. Om dit nader te onderzoeken, is een model predictive control methode ontwikkeld voor een specifiek geval: het regelen van een centrale WKK-installatie en een grote groep warmtepompen. Het voorgestelde regelsysteem is geverifieerd op de hoeveelheid benodigde rekentijd en op prestaties in termen van het bereiken van de doelstelling, de behaaglijkheid in de woningen en het aan/uit schakelgedrag van de WKK en warmtepompen. Naast de casus Meppelenergie, is voor een kleine woonwijk van 16 huizen de slimme energieregeling van een centrale WKK, zon-PV, elektrische batterijen en een aantal flexibele apparaten in de woningen onderzocht. Onderzocht is de mogelijkheid om dit systeem min of meer autonoom - los van het elektriciteitsnet - te laten draaien.
Met betrekking tot het algemene, regeltechnische probleem van duurzame energiesystemen voor de gebouwde omgeving laat dit proefschrift zien dat slimme energie regelsystemen effectief zijn wanneer: (a) zij in staat zijn om de energievraag en de energieproductie vanuit hernieuwbare bronnen op zijn minst een aantal uur vooruit te voorspellen, en (b) het regelsysteem als doel heeft om zoveel mogelijk gebruik te maken van de lokale, duurzame energiebronnen maar daarbij ook rekening houdt met een aanvaardbare mate van comfort voor de gebruikers. Ook wordt aangetoond dat dynamische energietarieven in geval van slimme sturing noodzakelijk zijn om hogere kosten voor gebruikers te vermijden. Als laatste is een decentrale voorspellingsmethode ontwikkeld die ervoor zorgt dat er op geaggregeerde niveaus geen privacy gevoelige informatie van de huishoudens wordt verzameld.
De ontwikkelde methoden in dit proefschrift leiden in theorie tot minder investeringen in duurzame energiesystemen en energie-opslag en een betere benutting en levensduur van de installaties.

Dankwoord

Het begon allemaal tegen het einde van 2012. Na een vergadering op de Universiteit Twente over een mogelijk project samen met Saxion, vertelde Gerard Smit dat hij een promovendus zocht om onderzoek te doen naar slimme sturing van duurzame elektriciteit én warmte. Ik kreeg meteen de proefschriften mee van Albert Molderink, Vincent Bakker en Maurice Bosman. Of daarvan de bedoeling was mij af te schrikken of juist over te halen, weet ik niet, maar ik hoefde niet erg lang na te denken. Al enige tijd had ik ideeën voor een promotie-onderzoek en was ik op zoek naar een promotor en een uitdaging zoals het project Meppelenergie waarin het gaat om integratie van duurzame energie. Er volgden nog een aantal gesprekken en het nodige lees- en schrijfwerk om mijn onderzoeksplan en promotievoorstel meer in detail vorm te geven. Dit voorstel werd zonder bezwaren door de promotiecommissie van Saxion goedgekeurd. Belangrijk daarvoor was ook de steun die mijn voorstel kreeg van Peter van Dam, directeur van de Academie Life Science Engineering en Design, en van de lectoren: Jan de Wit, Johan Wempe en Henk van Leeuwen.
In februari 2013 begon ik formeel aan mijn promotie-onderzoek. Wat een aangename verandering. Ineens was ik twee dagen per week omringd met jonge, briljante wetenschappers met een mateloze passie en energie voor hun onderzoek. Ik werd onderdeel van een voor buitenstaanders onbegrijpelijke commune onderzoekers die elkaar eraan herinneren dat het tijd voor koffie is via een briefje onder een drone die de kantoorkamers langs vliegt. Of die tijdens de koffiepauze wiskundige raadsels voor elkaar op een bord uitschrijven waardoor menige koffiepauze omslaat in een stille meditatie of juist een vurig lagerhuis debat over dit probleem. Of die een paar uur na de invoering van het nieuwste beveilingssysteem voor de deuren naar alle ruimten vol trots lieten zien dat het nieuwe systeem nog makkelijker te hacken bleek dan het oude. Kortom, waanzinning creatieve geesten die overal wel een puzzeltje in zien, bedoeld om op te lossen. Maar ook gewone mensen die net als ik graag hardlopen, schaatsen, een wandeling maken en van het goede leven houden.
Nu ik de luxe heb terug te kunnen kijken op vier jaar onderzoek en even voorbij ga aan de moeite die vooral het laatste jaar me heeft gekost, is er veel om dankbaar op terug te kijken in de afgelopen universi"tijd". De samenwerking, inspiratie en hulp van collega onderzoekers Hermen, Gerwin, Thijs, Bart, Gijs, Diego, Marco, Stefan, Vincent en Albert. Maar in het bijzonder Jirka Fink die als

post-doc onderzoeker zoveel werk heeft verricht om de ideeën die we ontwikkelden voor energieregelingen die kunnen anticiperen op basis van voorspellingen, een wiskundige basis te geven en om te zetten in werkende computer programma's.
Tijdens de afgelopen vier jaar voelde ik me verbonden met het project Meppelenergie. Hiervoor dank ik Harry van der Geest, Paul Korsten en Marco Lijflander van Rendo, Jeroen Jansen van i-NRG en Prof. Han Brezet van de TU-Delft. Ook dank aan RVO, STW en de Euregio Twente-Münsterland voor de noodzakelijke financiële ondersteuning van mijn werk.
Onderzoek doen is fascinerend, maar er moet ook erg veel gebeuren: lezen, rekenen, programmeren, publiceren en presenteren. Hoe houd je het vol? Zeker is dat ik veel steun had aan mijn inspirerende voorbeeld Jan de Wit en aan de leiding van mijn promotor Gerard Smit en co-promotor Johann Hurink. Zij zijn er meesters in om wetenschappelijke feestjes (onderzoek) te organiseren en daarvoor de gasten (onderzoekers) bij elkaar te brengen en te inspireren. Dank voor jullie vertrouwen in mij. Dank voor het op willekeurige momenten maar toch bijzonder goed getimed langslopen in de werkruimte om samen even na te denken, ideeën en concepten uit te tekenen op het bord, nooit de weg uit te stippelen maar wel helpen om op de juiste wegen uit te komen.
Dankbaar ben ik ook voor de medewerking van studenten en van collega onderzoekers van het Lectoraat Duurzame Energievoorziening van Saxion: Willem, Sandra, Simon, Ivo, Christian, Annemarie, Trynke, Edmund, Danny, Maurits en Anne Veerle. Daarnaast vele docenten en medewerkers binnen de Academie LED voor hun interesse in mijn vorderingen.
Dan mijn inspiratoren. In het leven zijn er veel mensen die een fantastische invloed op me hebben uitgeoefend en dat nog steeds doen, meestal zonder dat ze dat zelf weten. Mijn ouders Marina en Maarten van Leeuwen, Alvin "Sammy" Sint Jago en Agnes. Daarnaast dank ik mijn zussen Monique en Nathalie voor het liefdevol omzien naar onze ouders terwijl ik te druk was met schrijven tot in de nachtelijke uurtjes. Maar er zijn nog veel meer familieleden die mij inspireren door wat zij doen en hoe zij dat doen. Namen die ik in elk geval nog wil noemen zonder andere tekort te willen doen zijn Wim, Alex, Piet en Kees. Jullie hebben me laten zien dat ieder mens zijn eigen weg moet zien te vinden en zijn eigen dromen waar kan maken.
Bijzondere inspiratie kreeg ik door de gesprekken op vaak onverwachte plekken met de inmiddels helaas overleden collega Lectoren van Saxion Wim Gilijamse, Bart Meijer, Hilde de Vocht en Paul Bijleveld. Jullie waren bijzondere mensen en ik denk nog vaak aan jullie.
Aan het einde van dit lange dankwoord gaat het niet langer meer om dank en inspiratie alleen, maar vooral om liefde. Die vind ik altijd thuis bij jou Inelies, bij jullie Huub en Abel. Als er één goede reden was de afgelopen vier jaar om hard te werken om ook echt in vier jaar klaar te zijn, dan is het wel om weer meer tijd voor jullie te hebben. Huub en Abel, jullie hebben me vaak gevraagd waarom al die uren werk nodig zijn, waar ik dat voor doe. Het antwoord is dat ik geen keus heb. Dit is wat mij ten diepste bezig houdt. Dit zijn de vragen die ik als kind al had. Hoe is het toch mogelijk dat we alsmaar fossiele energiebronnen blijven

verbranden zonder stil te staan bij de gevolgen daarvan? Hoe zou de wereld eruit zien als we andere energiebronnen zouden inzetten? Nu ik wat ouder ben zijn die vragen over gegaan in de vraag: hoe krijgen we dat dan voor elkaar? Mijn proefschrift gaat over mogelijke antwoorden op die vraag. Blijf dus vragen stellen en blijf (onder)zoeken naar de antwoorden. Dat is elke moeite waard.

Richard van Leeuwen
Enschede, Mei 2017

Contents

Chapter 1

Introduction

Abstract - The Dutch government has recognized the need for energy savings and a transition towards energy from renewable sources. This thesis is dedicated to investigate integration of renewable energy for urban areas. This chapter provides a review of the most important backgrounds and trends of the present energy supply system in the Netherlands, the options for renewable energy and the current issues for integration of renewable energy. From this the problem statement of this thesis is formulated. The chapter ends with the contributions and an outline of the thesis.

1.1 Energy supply and consumption in the Netherlands

In the Netherlands, 3060 peta Joules (PJ) of primary energy (i.e. input energy from resources such as crude oil, hard coal, natural gas) is used in 2015. In Figure 1.1 the distribution of primary energy towards consumption categories is shown. The built environment includes the whole category "households", a large part of the category "government and services" and a small part (only the buildings, not the processes) of the category "industry". The final energy consumption (secondary energy, i.e. produced from primary energy) is 2070 PJ, of which 1232 PJ is consumed for the thermal demand, 353 PJ for the electrical demand and 485 PJ to drive vehicles.
The built environment (households and services, i.e. office buildings) is the largest energy consumer: 33% of the final consumption, i.e. 490 PJ or 24% for heating buildings and hot water and 195 PJ or 9% for electrical appliances. Although households consume in total more thermal energy (350 PJ) than offices (140 PJ), there are much more houses than offices and a focus on energy savings in offices is therefore more effective to reduce CO_2 emissions.
The built environment has a low temperature (LT) heat demand (below 100^oC). On the other hand, the industrial sector (478 PJ thermal demand) has a medium

[†]Major parts of this chapter have been published in [RvL:5]

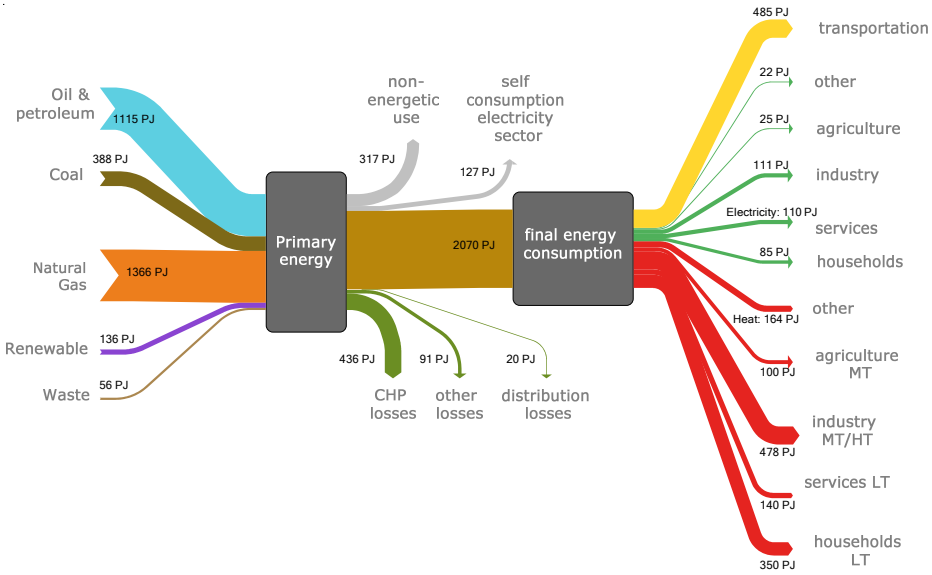

Figure 1.1 – primary energy consumption of 2015 in the Netherlands (red=heat, green=electricity)

to high temperature (MT/HT) demand ($100-500^oC$ / $500-1500^oC$). Through industrial processes this heat is converted into a LT-heat waste stream, in the range of $30-80^oC$. Other LT-heat waste streams are conversion losses of the electricity sector, which amount to 436 PJ in the same temperature range. Together, this amounts to 914 PJ which could potentially be used to supply the entire heat demand (490 PJ) of the built environment. Figure 1.1 is constructed based on information provided in [48], [162] and [161].

The Netherlands relies for more than 90% on natural gas combustion in boilers for the supply of the building related thermal demand. For the electrical energy demand, 84% is converted by natural gas and coal combustion. Due to recent low prices of coal, the share of coal increased in recent years which also led to an increase of the related CO_2 production. The remaining part of the electrical energy demand is supplied by waste co-generation plants, wind turbines and solar PV [48].

As combustion of natural gas leads to 50% less CO_2 emissions compared to combustion of coal, the Dutch energy system was relatively environmentally friendly in the past, in comparison with many countries which used predominantly coal combustion. However, large scale combustion of fossil fuels increases the CO_2 concentration in the atmosphere, which causes temperature increase (global warming) on the planet. In the last decades it has become clear that CO_2 emissions change climate systems all over the world with serious consequences to nature and population [131]. Hence, environmental policies aim to out-phase the use of fossil fuels entirely. Recently, new agreements on climate change are adopted by the

UNFCCC (United Nations Framework Convention on Climate Change) [170] with a treaty to limit global warming to 2.0 degrees and to strive for a limitation of 1.5 degrees. The treaty is signed by many governments in the world, including the Netherlands.
The European Union developed legislation and member states are committed to reach energy savings and increased renewable energy shares for 2020 (so called 20-20-20 goals: 20% energy saving, 20% renewable energy share in 2020). Road maps are also developed towards 2050 to have a completely renewable energy system [40]. The Dutch ministry of economic affairs, responsible for energy policies, has announced a shift of paradigm: initiatives towards integration of renewable energy in the heating sector will be encouraged in order to phase-out the use of natural gas completely by 2060 [83]. In [1], the Dutch government translates this vision into policy measures and proposals. An important step towards realization of the ambitions is the so called "energy agreement" between the government and the major economical sectors (energy, industry, services) (see [26] and [25]) in which targets for the short to mediate term are agreed for energy saving, increasing the share of renewable energy, finance and job creation. Part of this deal is the structural plan for large scale offshore wind turbine fields [9] and support for local urban energy initiatives [4].

1.2 Backgrounds of the energy transition

Societies predominantly use two forms of energy: work and thermal energy. Work is usually delivered either by conversion of electrical energy by electric motors or by conversion of the chemical energy stored in fuels by thermodynamic cycles. Liquid and gaseous fuels have become the dominant carriers of energy within the last 150 years since the development of combustion engines. Before that, work was delivered by steam engines which used coal or wood as fuel and before that era, work was delivered by windmills, horses and muscle power.
Traditionally, thermal energy for heating purposes is delivered by fuel combustion. Since the discovery of fire, many thousands of years ago, people used wood as fuel. Population growth, formation of larger cities during the industrial period and increasing depletion of wood reserves in many industrialized countries led to replacement of wood by coal. In the Netherlands, from the early industrial period until the 1950's, coal has been the dominant fuel for households but this ended in a relatively short time period due to the discovery and exploitation of natural gas reserves. Today, natural gas is the dominating fuel for households and industry and Dutch manufacturers of natural gas boilers and appliances have a world leading position in efficient, innovative technology. The fast Dutch transition process of replacing coal with natural gas, is a prove in itself that countries can make the transition to new energy sources in a relatively short period of time [175].
Another example which proves this for the field of renewable energy is Denmark. From the 1980's Denmark made a transition from complete dependency on fossil

fuels towards the present situation where the country has the highest share of renewable energy from wind turbines and solar energy in the world. A large part of the heating demand is supplied by district heating systems which are partly supplied by waste heat streams and renewable energy. As a result, Danish companies which produce equipment for district heating systems and wind turbines now have a strong market position in the world. Like the former Dutch transition towards natural gas, the Danish transition is made possible by a consistent governmental plan and accompanying tax regulation of the existing and new energy market, which is allowed to be executed for many years due to political stability and public consensus [145].

The traditional picture of energy supply based on fuel consumption is changed entirely by renewable energy. Dominating options like wind turbines and solar PV directly produce electrical energy, which can be stored and transformed into work with higher efficiencies than the traditional fuel combustion machines. Hence, as a side effect, integration of renewable energy partly leads to electrification of functions which are nowadays still based on fuel combustion. Examples are: electric vehicles for transportation and electric heat pumps for heating, refer to [75] and [139].

Renewable energy requires geographical space. Hence, production needs to be decentralized. Some options like solar PV are relatively easy to integrate in an urban environment while other options, like wind turbines and biomass are mostly realized some distance from urban areas. Various definitions of an urban area exist. The United Nations [171] explain that an urban area is defined differently throughout the world and defines an urban area as a population center of at least 2,000 inhabitants. When more than 100,000 people are involved, the urban area is also called a metropolitan area. In [23], sustainability quality indicators of urban environments are discussed, for instance the physical or spatial quality, the social-economic quality and the ecological quality of which energy consumption and the use of natural resources for energy generation are important parts. In this thesis, the definition of the United Nations for an urban area is interpreted towards more typical Dutch examples of city districts or village communities. The case example introduced in Chapter 3 involves a new district on the outskirts of the City of Meppel. The urban area or district contains houses but may also include other buildings like offices, schools and small companies as part of the district or in the direct vicinity.

Achieving support of local communities for large numbers of tall wind turbines or biomass cultivation and conversion does not come by itself but has to be organized by creating awareness and developing a public interest. A wider public needs to be aware of the required transition and needs to be involved in eventual benefits. Although this is often a difficult process, this is also a chance for improving social coherence [6].

When this is viewed on the scale of a country like the Netherlands, where there is a mixture of dense populated areas and agricultural areas, growing large quantities of biomass conflicts with food production for which the same agricultural land has to be used. Hence, for the integration of renewable energy, regional or

even national policies are insufficient. Together with neighboring countries, there needs to be a level playing field for energy and crop markets in order to effectively make use of the available resources.
The traditional electricity networks are a means to transport renewable electricity between large scale and often rural generation locations and urban areas. Contrary to this, in the ideal case, renewable energy generated within urban areas is to be self consumed by households and companies within the area. With smart control it is also possible to share generated electricity between households and companies. In this way, it is possible for urban areas in less dense populated areas, to become nearly energy independent from larger networks. Today, many communities in the Netherlands have the ambition to become "energy neutral" (generate and consume the same amount of energy on a yearly balance) in the coming years, which is a first step in this direction. Often such initiatives are accompanied by new collaborations between citizens and companies. The present situation in the Netherlands is that over 200 new local energy service companies (ESCO's) are established with the purpose to generate and self consume renewable energy locally [47].
In short, the energy transition is quite fundamental and involves the following transition areas:

1. Transition of energy source: a move away from fossil fuels towards renewable sources
2. Transition of energy consumption: a move to other technology which use other forms of energy, i.e. electrification of heating demand
3. Social transition: increasing citizen awareness and involvement, e.g. development of local ESCO's
4. Agricultural transition: a need to balance land use for food and biomass production
5. Tax transition: a shift to energy taxes in favor of renewable energy consumption and investments
6. Macro economic trade transition: a change of the dependence of industrial activities and jobs from fossil fuel trade towards renewable energy trade.

1.3 Changing the game in favour of renewable energy

This thesis has a focus on domestic energy consumption for heating buildings, but it should also be mentioned that in order to reach the targets, other fields where energy is consumed, i.e. transport and industry, need to receive similar attention of policy makers.
For the Dutch building sector, the following policies have been developed to lower the energy demand and diminish the use of carbon based fuels within the coming years:

1. Introduce subsequent lower EPC-levels (EPC=Energy Performance Coefficient) for new buildings. From 1995 the regulated EPC-level of new buildings is decreased in steps of 0.2 up to the level 0 (energy neutrality) to be effective from 2020. This policy is changing the house building practices in the Netherlands. Due to this legislation, heat loss from buildings is decreased by better insulation levels, heat recovery ventilation and by avoiding outside air infiltration. Besides these measures, the EPC can be lowered by installing Renewable Energy Systems (RES) as part of the house, such as solar PV and solar thermal installations and heat pumps. In this sense, energy or climate neutrality is interpreted on the basis of a yearly balance in which all energy consumed by the household is generated by the renewable energy installations of the house. The legislation also includes a method of compensation for CO_2 decreasing measures taken on a district level, e.g. connecting a house to a district heating system which generates the heat from renewable sources.
2. Execute large scale energy renovations (e.g. Stroomversnelling [92]) for existing houses. A large part of the Dutch housing stock (approx. 4 million of in total 7.7 million houses) is relatively poor insulated and older than 40 years. In the Dutch energy labeling system, these houses have labels F or G, while new houses are labeled A, A+ or A++. By renovations these houses are to be upgraded with higher insulation levels and energy saving installations like heat recovery ventilation, low temperature underfloor heating and heat pumps.
3. Introduce subsidy schemes for heat from renewable sources, i.e. heat pumps and district heating projects utilizing waste heat streams and renewable sources [127]. For all renewable heat sources, it is an advantage when the heat can be supplied with low temperatures (e.g. $30-60^oC$), as this increases efficiency of solar heating and heat pumps. This is only possible if existing buildings are renovated such that low temperature heating is made possible.
4. Stimulate investments in home solar PV, e.g. by offering feed-in tariffs which are equivalent to purchasing energy tariffs [129]. Recent years have shown a sharp cost decrease of solar PV due to achieved economies of scale through industrial innovations.
5. Increase public awareness for Renewable Energy Systems, e.g. by creating a legal level playing field for local energy corporations. The local energy corporations provide services such as buying and selling electricity, organization of local energy saving competitions and increasing local electricity production by RES such as joint solar PV or wind turbine purchase and operation projects.
6. Increase electrification of domestic energy consumption as a replacement for using fossil fuels. Electric replacements include for cooking: induction, magnetron, oven; for washing: dishwasher, electric kitchen boiler; for heating: heat pumps for space heating and domestic hot water; for transportation: electric cars. The combined impact of this increased electrification on the

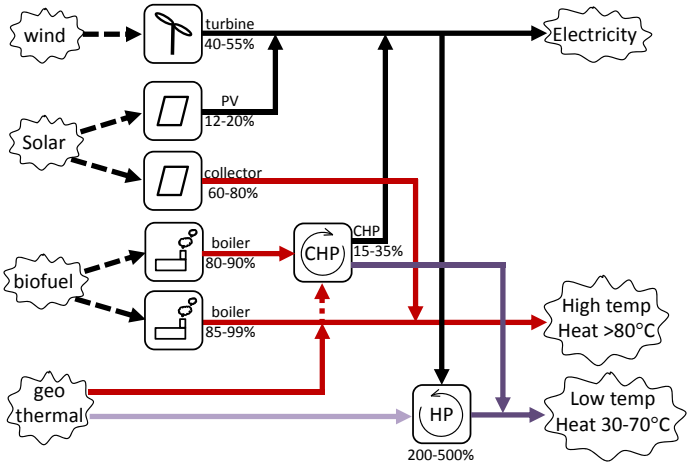

Figure 1.2 – conversion of renewable energy sources to useful energy

power demand may cause problems for existing electricity grids. Solutions which avoid grid strengthening include: local RES, smart control of flexible appliances to increase self-consumption and demandside management, refer to [123] and [139]. For this, the Dutch government financed various pilot projects within the urban energy subsidy program.

1.4 Renewable energy system aspects

At present, there are many options for the supply of renewable energy. Wind turbines, solar PV, solar thermal, biomass (solid/liquid/gas) conversion and geothermal energy are the most suitable options for countries with shallow coasts and a relatively flat landscape like the Netherlands. Other options include: water turbines for countries with mountains and tidal power for countries with oceanic coasts. The technology for all these options is well developed and there are ongoing system innovations aiming for cost decrease and higher efficiencies. Options which are presently in a research and development stage include blue energy, i.e. electric energy from the potential difference between salt and sweet water, and bio-fuels from algae or seaweed farms.

In order to replace fossil fuels entirely, complex energy systems involving many of the renewable energy options available and energy storage are needed in a coherent mixture which is able to match the entire energy demand for a large urban area or country. Figure 1.2 shows for the most suitable options mentioned, how the source energy is converted into useful energy, i.e. electricity, high temperature and low temperature heat. It also gives a first impression of the coherence between options. For each conversion, the applicable conversion efficiency range is indicated and discussed in the following.

Wind turbines convert kinetic energy present in the wind into electricity. The

theoretic maximum efficiency is given by Betz's law and is approx. 59% [178]. Friction and conversion losses from axle movement to electric power result in a somewhat lower total efficiency.
Solar PV (Photo Voltaic cells) convert solar electromagnetic radiation into electricity which is transformed by an inverter to compliant currents and voltages. Best available cell efficiencies now range between 15-25%, while the best possible cells used for outer space applications now reach 44%. Due to cable and inverter losses, system efficiencies are somewhat lower [156].
A solar collector converts solar radiation into heat. There are many collector types with vacuum tubes as the best possible technology. Efficiencies range between 50-90% depending on the absorber temperature [167].
For biomass conversion the picture first shows conversion of the chemical energy of biomass into high temperature heat which is converted into electricity and low temperature heat by a thermodynamic Combined Heat and Power (CHP) cycle. The maximum efficiency is defined by Carnot's efficiency, i.e. approx. 79%. In practice, conversion and friction losses result in total efficiencies between 15% for small installations to 40% for large installations [140]. Second, the picture shows conversion of biomass into high temperature heat which is used for industrial or domestic thermal demand.
Geothermal energy. The temperature in the earth's crust increases approx. 30^oC per kilometer. Geothermal energy from approx. 2.5-4 kilometers can be used for high temperature thermal demand or to produce electricity with a thermodynamic cycle. In some countries like Island, higher temperatures of the crust exist much closer to the surface and it is much easier to apply high temperature geothermal energy. Shallow geothermal energy from approx. 0-100 meters with an average temperature of 12^oC is used as source heat for heat pumps which transform the energy to a higher temperature [98]. Heat pumps consume electrical energy for this process. Electrical heat pumps are regarded as the most important option for the transition towards integration of renewable energy for the heating demand within the built environment [79], [152].

1.4.1 Matching renewable energy production and demand

Like the amount of energy demand, the amount of renewable energy generation fluctuates in time between moments of minor generation and moments of peak generation. To illustrate this consider solar energy. The amount of energy generation in time depends on the movement of the sun during the day and during the seasons and if there are clouds to cover the sun. This results in a fluctuating but to some extend predictable energy production in time. Moreover, energy is produced during daytime hours while domestic demand is mostly early in the morning and in the evening hours.
Wind turbines also produce fluctuating amounts of energy, depending on local wind speeds. Over the seasons, solar and wind energy are to some extend complementary on the Northern hemisphere, i.e. there is more solar energy production

during summer months than during winter months, and more on clear days than on cloudy days, while there is more wind on cloudy days and during the winter months than during the summer months [33]. But this complementary property of solar and wind energy is far from perfect, hence regions with a high penetration level of solar and/or wind energy in the total energy mix, may face large scale unbalance problems within the electricity grid if no further adjustments are made to the energy system.

Biomass conversion can be used for combined heating and power purposes. The biomass conversion process requires a more constant operation for longer periods of time, which may be difficult to match with a fluctuating demand. Conversion processes of solid biomass are the least flexible due to time consuming starting up and cooling down times, e.g. a biomass CHP or boiler. Combustion of a bio-liquid or bio-gas can be as flexible as for instance the same process with natural gas, but inflexibility may exist on the supply side of the energy source. In the Netherlands, bio-gas is produced by fermentation of sludge from waste water treatment processes or by fermentation of manure from cows and pigs, mostly combined with agricultural, energy rich waste products [72]. It is not possible to stop fermentation processes and therefore, the produced bio-gas has to be either combusted, stored or flared if there is less demand for a longer time. The generated thermal energy from bio-gas is relatively easy to store, also for longer periods of time using methods of seasonal thermal storage, refer to [184] for such methods. Other options include purification of bio-gas into methane which makes it possible to inject it into the gas grid, or gas storage either by pressurization or cooling it to liquid form. The latter options are an attractive way to integrate bio-gas into existing gas infrastructures, but the technology also increases costs considerably, refer to [148] and [180]. Although recent years have shown an increase of bio-gas production in the Netherlands, the Dutch agricultural sector is looking for more competitive alternatives for manure and agricultural waste processing like refinery in which nutrients and water are recycled and energy in gas or liquid forms is produced, refer to [59] and [172]. The possibility to include an algae production step for food, chemical and energy purposes is also investigated, refer to [185] and [186].

Last is the application of energy from geothermal sources. In the Netherlands this is mostly limited to shallow geothermal sources in a combination with heat pumps to supply thermal energy demands. In a renewable energy system, the heat pumps are powered by renewable electrical energy, for which solar and wind energy may be used or biomass conversion with a CHP.

These examples demonstrate that in most cases, renewable energy options are complementary and have to be combined to fully replace fossil fuels and to enhance stability of the energy production. However, even when options are combined, further adjustments to the energy system are necessary to solve unbalances between generation and demand. Adjustments presently available or in stages of development are:

- A large, interconnected grid with strengthened local power transmission lines. Such a grid is able to carry electric power to and from other areas and

therefore serves as an artificial "buffer". Although this solution simply seems to be a further enhancement of the existing power grid already in place in many European countries, existing grids are not designed for bi-directional current flows. Traditional power grids are designed for one direction current flows from high voltage to low voltage. Hence, besides strengthening of grid cables and switching circuits, replacement of existing transformers by expensive bi-directional transformers are required when the grid has to transport surplus renewable energy power from one part of the country to another [123]. Furthermore, larger, integrated and possibly international power grids are more complex to manage from the point of network stability and security.

- Implementation of local or regional energy storage. The goal of this solution is to level out the mismatch on a local scale by storing energy in times of surplus generation and consuming energy from the storage in times of insufficient generation. In this way, the larger grid is relieved from generation and consumption peaks. An issue is the significant cost of storage assets.
- Demand-side management, i.e. smart control of flexible, energy consuming devices. This has the same goal as the previous solution. Smart control enables direct consumption of the generated energy and therefore limits the required storage capacity. This technique is only possible for so called flexible devices, i.e. a device whose operation may be shifted in time without significant consequences. Examples are: heat pumps, electric vehicle battery chargers and washing machines [109].

Demand-side management and storage are complementary and to some extend also contribute to lower costs for grid strengthening measures. Grid operators often participate in smart grid development projects in which all solutions have a logic role in order to reach low costs for the operation of the energy system. However, when demand-side management and storage are carried out in such a way that urban regions may be islanded from the larger grid, this may threaten the profitability of existing electric power grids. In general, energy prosumers (renewable energy consumers and producers) who are part of local ESCO's, are often more interested in demand-side management and local storage than in grid strengthening measures as these local solutions are more directly related to their energy production and the self consumption of this energy [47].

Through case investigations, this thesis demonstrates that a reliable and affordable energy supply system which is 100% based on renewable sources, is only possible if mixed forms of renewable energy generation sources (for electrical and thermal power) and demand are combined in a smartly controlled environment. Such an environment consists of:

1. regional renewable energy generation from mixed sources,
2. energy conversion and storage,

3. measures to increase efficiency, i.e. reduce energy consumption and decrease temperature levels of the heat demand,
4. smart control and demand-side management to match generation and demand and minimize storage asset costs.

1.4.2 Energy conversion and storage

As introduced in the previous section and shown in Figure 1.2, energy conversion and storage are logic parts of complete renewable energy systems. Surplus renewable energy can be converted into other forms of energy which can be stored or distributed. One conversion option is power to fuel, i.e. hydrogen gas, synthetic methane gas or bio-liquids. Conversion of renewable electric energy into a combustible fuel is an attractive option as fuels are a compact way to store and distribute energy and fuels are widely applied in industry, households and the transportation sector. However, these conversion techniques are at present financially less attractive, mainly due to complex technology which has not yet reached an attractive economy of scale. Besides that, the value chain from source to application has quite a low overall efficiency. As an example the round trip efficiency of electricity from wind towards hydrogen and back into electricity is as follows: 100 units of renewable electricity result in a maximum of 70 units of hydrogen gas of which 66 units remain after storage and distribution. A maximum of 40 units electricity and 20 units heat will be available for demand supply when the hydrogen is converted back into electricity (and heat) with a fuel cell [117].

The most important subject for this thesis is power to heat. This option is usually combined with thermal storage on the scale of a single building or a district. Power to heat is possible in two ways, by electric resistance heating or a heat pump. The advantage of a heat pump is a much higher efficiency, but as shown in Figure 1.2, a low temperature heat source is required. A variety of power to heat is power to cooling. The evaporator of a heat pump is then used to convert electricity into cooling energy.
A domestic power to heat system includes a heat pump, a low temperature source, e.g. ambient air, a radiant floor heating system and a hot water storage for supply of the domestic hot water demand. A district power to heat system is similar but on a larger scale, i.e. a larger heat pump, larger thermal source and a district heating system. Experience with district heating in the Netherlands is traditionally related to large scale steam power plants (e.g. Amsterdam and Almere city heating network and many smaller city projects). More recently, de-central projects for new urban districts apply either biomass (wood) thermal conversion in boilers (e.g. muziekwijk Zwolle, [60]) or biogas co-generation (e.g. Apeldoorn [50], Zeewolde, [52] and Leeuwarden [8]). An overview of Dutch district heating projects and profitability investigation is presented in [153].

A heat storage is an attractive option due to relatively simple system technology,

modest conversion and storage investments, relatively high conversion efficiencies, wide applicability on smaller and larger scale and environmental friendliness.

For thermal storage, available techniques are:

- sensible storage, i.e. increasing the temperature of a medium; mostly water is used,
- latent storage, i.e. changing the physical phase of a material, i.e. solid to liquid, liquid to gas,
- thermochemical storage, i.e. changing the chemical composition of a material.

The described processes for these storage methods are carried out during charging and in reverse form during discharging. This thesis has its focus on sensible thermal storage with the heat capacity of a concrete floor heating or water in a tank as the storage medium.

For electrical energy storage, a variety of techniques are available. Pumped hydro storage is widely applied in the mountains of Central Europe and Norway. Compressed air energy storage (CAES) is an alternative. Pumps are used to transport the water to a higher altitude, or a compressor is used to increase the pressure of the air. In both cases, a turbine and generator are used to generate electric power. The total efficiency of both options is approx. 80%. Due to the installations and space required, pumped hydro and CAES are applicable only on a larger scale.
Chemical storage in batteries has the advantage of portability and availability for small scale applications. Within a smart grid, many stationary domestic batteries and batteries in electric vehicles together constitute a very large battery. The total efficiency of existing battery technologies is approx. 70-85%. New technologies such as redox-flow batteries and sea-salt batteries are moving out of the research phase, promising larger scale application of batteries and solving environmental issues [179] and [132].

1.4.3 Increasing energy efficiency

As introduced in Section 1.4.1, increasing energy efficiency by reducing energy consumption and temperature levels of heating demands is an important aspect of complete renewable energy systems. For this, a guiding principle exists and is called the trias energetica, which is basically a three step implementation method as shown in Figure 1.3.

The left side of Figure 1.3 shows steps dedicated to energy savings and integration of renewable energy. The right side is dedicated to another thermodynamic quantity called exergy, i.e. the amount of useful work (or electrical energy) that is potentially available from a system or process which is operating at a certain elevated temperature level. The higher this temperature level, the more work

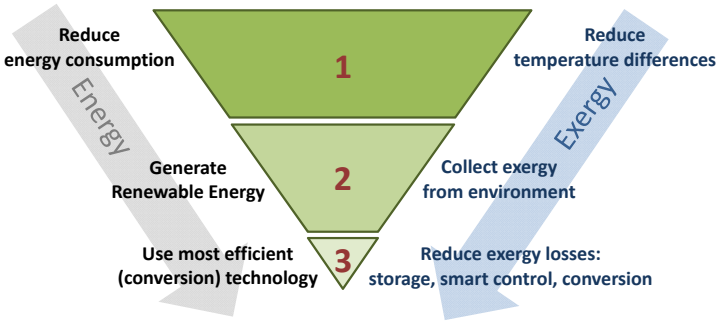

Figure 1.3 – Trias energetica principle

there is potentially available before the system reaches an equilibrium state with a surrounding, lower temperature.
The first step involves reduction of energy consumption (energy-side) and reduction of temperature differences (exergy-side). We illustrate this with the following examples for the built environment.

1. increasing building insulation reduces heat loss but also reduces the temperature difference between interior wall surfaces and the interior air,
2. heat recovery ventilation reduces heat loss but also decreases the temperature difference between inlet and outlet air flows to and from the interior,
3. reducing the surface temperature of a radiator has two effects: first, some reduction of heat loss of the entire building or district heating system. Second, when renewable heat is used e.g. a heat pump or solar thermal collector, a significant increase of efficiency is achieved.

The last example illustrates the importance of exergy for the second step of the Trias energetica: implementation of renewable energy. Besides that, implementation of the first step contributes in general positively to the energy transition in the following ways:

- on a local level, less (land) space is required for renewable energy generation when there is less local energy demand,
- lower investments are required into energy generation and storage assets,
- less CO_2 is emitted during the entire energy transition period if significant reduction of energy consumption is achieved at a relatively early stage of the energy transition period.

The second step involves the generation of energy from renewable resources (energy-side) and the collection of exergy from the environment (exergy-side). The latter can be achieved directly by wind turbines and solar PV or by thermal conversion (co-generation) of a bio-based fuel. A heat pump is a special case: exergy

(electrical energy) is used to generate heat at a useful temperature from a low temperature source. This results in less output exergy than was used as input. However, compared to a gas boiler which converts high exergy (chemical energy of a fuel) into low exergy, the exergy performance of a heat pump is better. From an exergy point of view, collecting heat with a useful temperature from waste-heat sources or from a geothermal source is preferable.
The third step involves using the most efficient conversion technology (energy-side) and the reduction of exergy losses from a system (exergy-side). Some examples to illustrate the exergy-side: for an electric vehicle, most of the electrical input (exergy) is used to drive the vehicle, hence the exergy loss is very small. Contrary, a fuel driven car wastes a large part of the exergy (fuel) input. As another example, if we assume a district as a closed system than electrical energy (exergy) generated within the district should also be consumed by the district. Exergy exported to the surrounding area is in this case regarded as exergy loss for the district. To avoid this as much as possible, energy storage and smart control may be used within the district to increase self-consumption of the generated exergy.
To illustrate the application of the Trias energetica, we consider house heating systems. In [63], optimal fuel saving options are investigated for Dutch households using the Trias energetica approach. Application of the first step leads to relatively high levels of insulation, heat recovery ventilation, good air tightness of the envelope to avoid air infiltration and measures to reduce overheating and cooling demand during the summer months. During the second step, the optimal renewable heating system for an average house is determined, i.e. a heat pump with air source and thermal storage for domestic hot water. To generate the required electricity of the households, rooftop solar PV systems are nowadays an affordable option. For the third step, it appears to be financially more attractive to co-install a highly-efficient, condensing natural gas boiler which only produces heat during moments of peak heat demand. Because of the low cost of boilers, the entire installation is smaller, and the operation cheaper and more reliable than a larger heat pump installation without a boiler.

1.4.4 Smart energy control and demand-side management

It is widely recognized that enabling technologies such as electrical energy storage, controllable electric devices and smart grids are important ingredients to match the available renewable energy with the demand [53]. As explained in Section 1.4.1, there is often a mismatch in time between renewable energy production and demand. However, part of the electric demand is to some extend flexible. As an example, heat pumps used for space heating or washing machines. These can can be controlled to consume electricity at times of production peaks. In [123] various cases of smart control are investigated with the purpose to avoid costly grid strengthening measures.
A specific solution and relatively new research area is a so called smart controlled hybrid micro-grid, i.e. an integrated low voltage power and heating grid on the scale of a single building up to the scale of a district. A hybrid micro-grid matches

supply and demand of electricity and heat locally, decreasing peak loads on the larger electricity distribution grid.
At the University of Twente, a smart grid control methodology called Triana is developed. Triana algorithms contain three steps or modules for: (1) prediction of energy demand and generation, (2) planning of flexible devices and converters and (3) real-time control of flexible devices and converters. The basic control principle, backgrounds and algorithms of Triana are explained in [22], [28], [109] and [169].

1.5 Integration of renewable energy in the built environment

The built environment contains many building categories like houses, offices, industrial buildings, public buildings like airports and hospitals etc. The research in this thesis has a focus mainly on urban areas and houses but to some extend, the research is applicable for any built area where people live or work and hence, use electric energy for domestic or work related appliances, i.e. refrigerator, computers, TV-sets, kitchen appliances etc. and thermal energy for building climate control like heating, ventilation, air conditioning and for domestic hot water.

Urban areas in the Netherlands contain a mixture of older and newer houses, offices and public buildings. As discussed in Section 1.1 natural gas boilers are today the dominant heating system for these buildings. From various examples of recently built, new districts, two approaches towards integrating renewable energy options for the thermal energy demand of buildings are distinguished:

1. Individual approach. As a power to heat concept, the individual natural gas boiler for each building is replaced by a heat pump which electrifies the heating demand. The electric demand is supplied by renewable energy from solar PV and an increasing number of regional wind turbines. For balancing energy production and demand, electric and thermal storage are part of the building energy system. This approach is adopted in some cases of new building projects [51], and renovation projects [7].
2. Collective approach. In a collective heating system, buildings are connected to a district heating system. Due to the scale of district heating stations, a wider choice of renewable sources is possible like: waste, biomass or bio-fuel conversion, solar thermal plants, power to heat, shallow and deep geothermal energy, and seasonal thermal storage. Presently, waste and biomass conversion is mainly used, for an overview of installations see [87].

Recently, district heating projects and so called all-electric buildings receive much attention. The collective approach of district heating has advantages for the integration of renewable energy, especially for existing buildings in densely populated areas [96]. However, new low-energy houses require less energy for space heating which makes individual heating systems in many cases a more attractive option, although integration of renewable energy and a suitable thermal source for heat

pumps are important drivers to consider low temperature district heating in this case [1].
A choice for one of these approaches has severe implications as it determines which options for renewable energy can be used to cover the heating demand. The individual approach relies on the capacity of electricity grids. In the ideal case of a complete renewable energy system, electricity within this approach is to be generated by wind turbines and solar PV, as the other options shown in Figure 1.2 are presently only applicable on a large, centralized scale and they also generate heat which cannot be distributed towards demand when all buildings follow the individual approach. As the electric power grid also supplies the demand for appliance usage and electric vehicles in the future, the capacity of the electricity grid needs to be increased significantly. However, the required capacity of the electric grids is diminished if buildings have a low thermal demand and low supply temperatures, while this reduces the electricity demand for heating purposes. Hence, in the individual approach, a strong focus on low building thermal demands has a positive effect on the energy costs of residents and network costs for grid owners. This coheres with the step-wise approach of the trias energetica shown in Figure 1.3.

At this stage of technological development, the collective approach enables integration of renewable energy options on larger, centralized scales and is possibly more cost-effective than the individual approach. The collective approach is less dependable on the capacity of the electricity grid. However, an additional heat grid has to be added to the energy system with its own constraints for a positive business case. For the profitability of the heat grid it is less obvious to invest in lower building heating demands as this results in lower revenues from heat sales. It seems that the only advantage to apply the trias energetica is the financial interest of the residents to save energy. Perhaps this is why the heating demand of buildings has not been an issue for most existing district heating systems. But when integration of renewable energy becomes the major direction, this will change. First as discussed in previous sections, district heating systems are more efficient when supply and return temperatures are lower [126]. Second, low approach temperatures enable more efficient heat generation by heat pumps, solar thermal energy, geothermal energy and thermal energy from waste/bio-mass/bio-fuel CHP [94]. [126] argues that low building heating demands are also positive for the business case of district heating systems using renewable energy. These aspects are also recognized internationally and a name is given to this new direction, i.e. 4th generation district heating [97]. In this concept, supply and return temperatures are as low as possible, to decrease system thermal losses and to enable integration of heat from renewable sources. Supply temperatures can be reduced further if heat pumps are used to increase the temperature at the household level, i.e. using a collective low temperature thermal source. In [130], a case for including low temperature geothermal heat into an existing district heating system is investigated and feasibility of using heat pumps for this purpose is demonstrated.
As future renewable energy systems are powered predominantly by renewable

electricity from solar-PV, wind turbines, geothermal energy and bio-fuel, district heating systems can provide large amounts of cost effective flexibility to balance energy generation and demand ([96], [1]), predominantly by "power to heat" technologies and large scale thermal storage. However, Dutch policies ([2], [1]) are more aimed at reducing the heat loss of buildings and increasing the share of renewable energy within the power grid than to stimulate district heating. Therefore, the positive role that (district) heating systems can play in the energy transition is presently overlooked by national and regional policy makers in the Netherlands. Hence, this thesis contains some cases which demonstrate the possibilities that arise when the (district) heating system plays a central role within an integrated, renewable energy system, in order to contribute to a better understanding of these possibilities.

Concluding, new building projects should focus on low building thermal demands from the start in order to reach the best possible cost levels for residents and grid operators of future, integrated renewable energy systems.
The same reasoning is of course true for existing buildings which today require high heating demands and higher supply temperatures. This is a reason for large scale house renovation projects in the Netherlands like Stroomversnelling [69].

1.6 Problem statement

As discussed in Section 1.1, the present energy supply system in the Netherlands depends largely on the consumption of fossil fuels, which through CO2 emissions has a large contribution to the global warming problem. However, Section 1.2 argues that there is an increasing sense of urgency for a transition towards a completely renewable energy supply system and that the transition involves much more than just the technology of energy systems. Past and recent examples of policies and measures to increase public awareness of the transition and investments into reducing energy consumption and renewable energy generation are discussed in Section 1.3. Section 1.4 introduces the most suitable options for renewable energy generation and concludes that for complete renewable energy systems, only a combination of options is capable to match the fluctuations between energy demand and supply. This however results in rather complex energy systems with many variables to be taken into account and to be optimized. Besides energy generation, such energy systems require various forms of energy storage and smart control.
Considering the built environment, Section 1.5 concludes that there are two approaches possible to integrate renewable energy for the building thermal energy demand, which are an individual and a collective approach. It is found that both approaches have common requirements for reducing heating demands and lowering temperatures of heating systems while this enables integration of renewable energy options much more efficiently and economically. It is also addressed that the choice for an approach should be made with great care and requires a holistic

analysis and vision on the future energy system of an urban region.
This thesis contributes to the general objective of advancing towards completely renewable or green energy systems. The complexity of multiple renewable energy system options is translated into individual or collective hybrid energy system concepts for urban regions with balanced thermal and electrical energy generation, storage and consumption. In relation to the general objective, the following overall problem statement of this thesis is formulated as:

How to determine urban energy system capacities with a high share of locally generated, renewable energy and how to control energy generation and storage in order to balance generation and demand in time?

The problem statement contains three important aspects, which at this stage are not yet addressed fully by other researchers: (a) predictive aspects of the energy storage capacity of buildings, (b) hybrid thermal/electrical smart micro grids including power to heat, and (c) system concepts for a high share of renewable energy to cover domestic energy demand. For these aspects, several research topics are determined.

The first aspect is aimed at describing energy demand, storage of energy, accuracy validation and the interplay between useful energy flow from storage, as well as the consequences for thermal comfort, associated energy losses and costs. For storage of thermal energy, the research is aimed at using the inertia of the house structure and a water tank storage. The following research questions are concluded:

1. How to model heat demand of buildings such that we can use these models for predictions and to analyze the impact of smart control?
2. How much energy can be stored without significant cost and comfort consequences within the structure of a building?
3. How to model the storage capacity and the charging and discharging process of a water tank storage that is placed in a house with sufficient accuracy?

The second aspect addresses the interplay between renewable energy production, device control, energy storage and energy consumption. The following research questions are developed:

4. How to control a CHP and a large number of heat pumps within an individual or collective energy system in such a way that there are minimum peak electrical loads within the micro grid and there are minimum electricity flows between the micro grid and the larger electricity grid?
5. How to develop the control such that it results in stable CHP or heat pump operation and delivers a high degree of thermal comfort to the inhabitants?
6. How to develop the control such that it is computationally fast and does not require privacy sensitive information of inhabitants?

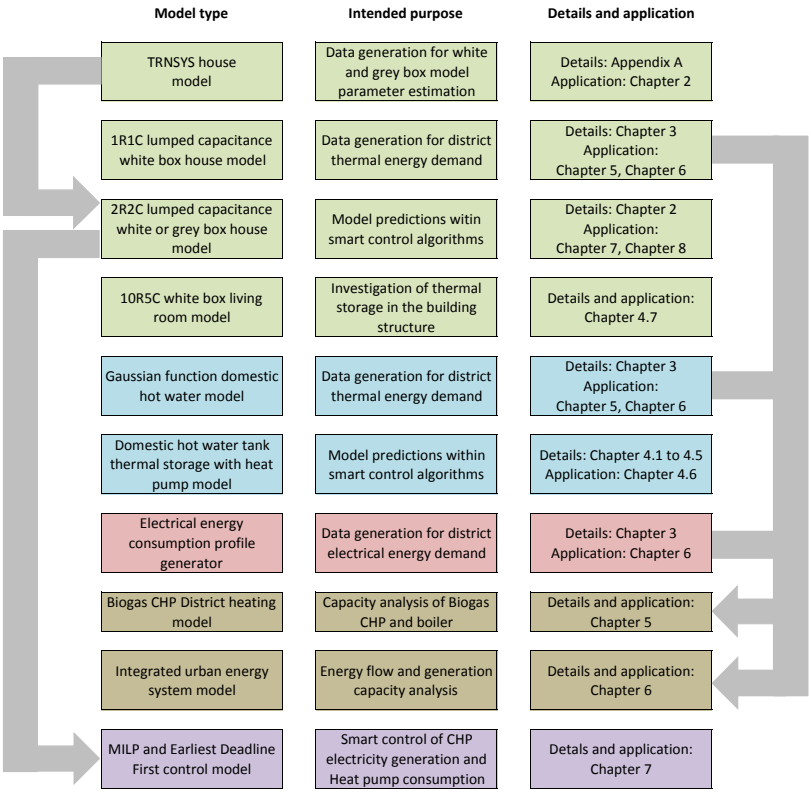

Figure 1.4 – Overview of models developed and applied in this thesis

The third aspect, integration of renewable energy into the energy demand of the building environment is investigated on the scale of a household, neighborhood and district. The following research questions are developed:

7. What are likely options for RES-integration for the thermal demand on the level of a single household, neighborhood and district and how do they compare on feasibility, costs and environmental impact?
8. To what extend is self consumption of local renewable energy and (near) off-grid operation of the urban energy system possible?

1.7 Outline of this thesis

In this thesis, various models are developed and applied in case investigations. In Figure 1.4 an overview is given of the model types, the intended purpose of the models and the chapters where details and applications of the models can be found. Following the introduction in Chapter 1, Chapter 2 investigates predictive models for building thermal energy demand. Additionally, Chapter 3 investigates

generation of demand profiles for districts. Chapter 4 investigates predictive models for the state of charge of a thermal storage for domestic hot water and electrical battery storage. Chapter 5 reports on a case investigation to determine possible migration routes for the integration of renewable energy for the thermal demand of a district. In Chapter 6, a generalized urban energy model is developed. For a specific district heating case, optimal system dimensions are determined with the model. The most feasible approaches towards integration of renewable energy are discussed and compared on economical, planning and environmental aspects. In Chapter 7, a model predictive control case is investigated for a central CHP and group of heat pumps. In Chapter 8, a case investigation is dedicated to smart control of a neighborhood of 16 houses with the purpose to reach near off-grid operation. Finally, the thesis comes to a conclusion and recommendations for future research in Chapter 9.

Chapter 2

Model for building thermal energy demand

Abstract - In this chapter, a simulation model of a house is developed which adequately describes the thermal response of a given type of house in relation to building properties, e.g. the heat storage capacity of the house, user setpoints and weather conditions. The model is used in this thesis for generation of demand profiles and for model predictive control of thermal generators and therefore sufficient accuracy but also simplicity is required.

2.1 Introduction

In Chapter 1, the most important renewable energy supply systems are introduced. Also, for the thermal energy demand of buildings, an individual and collective approach for integrating renewable energy within the built environment is introduced. It is also concluded that such integrated renewable energy supply and demand systems, require methods of smart energy control. At the University of Twente, a smart grid control methodology called Triana is developed, which consists of three steps: prediction, planning and real time control. Of specific interest is the application of this control method within the individual approach where each building has its own thermal energy generator for space heating and domestic hot water demand. The thermal energy generator can be any generator which uses renewable energy as source, e.g. a heat pump, a bio-fuel powered boiler or a CHP. For electricity networks, a large group of domestic heat pumps which often run for long periods of time, constitute a significant load. Flexibility for scheduling the heat pumps is offered by different kinds of thermal storage, e.g. a water buffer within the houses from which domestic hot water is supplied and the thermal mass of floor heating structures. In this chapter, a model is developed for prediction of thermal demand of houses for two purposes: (1) generation of

[†]Major parts of this chapter have been published in [RvL:10]

thermal demand profiles of houses and districts and (2) model predictive control of heat generators.
This chapter is structured as follows. Section 2.2 provides related work. Section 2.3 presents a general mathematical model description. In Section 2.4, a detailed simulation model is developed with the purpose to obtain simulated data from which parameters of simplified models can be estimated. In Section 2.5, the estimation approach is introduced. Parameter estimation results are presented and discussed in Section 2.6. Conclusions on which model to use for Smart Grid control are given in Section 2.9, as well as suggestions for future work.

2.2 Related work

In general, models for thermal energy demand of buildings consist of three parts [108]:

1. A model which describes the building properties, e.g. thermal capacitance and resistance of floors, walls, roofs, windows etc. This can be a set of mathematical equations based on a physical model representation (white box type), or a data driven model with a simplified physical model representation (grey box type) or without any relation to the physical world (black box type).
2. Models which describe (a) energy consumption, (b) heat transfer and (c) control of installations for heating, ventilation and air conditioning (HVAC equipment).
3. A model describing events and consequences (energy dissipation) of occupant behavior, i.e. opening doors and windows, adjusting temperature and ventilation settings, the use of electrical appliances and the number of occupants in time.

In practice, any model contains approximations and is therefore to some degree inaccurate and leads to a performance gap between predicted and real results. Performance gaps are investigated comprehensively in [101] for Dutch EPC-calculation tools and in [163] for the VABI dynamic building simulation tool. The performance of similar tools like Energyplus and TRNSYS is compared in relation to measured data in [32]. Although the model parameters were not calibrated to closer match the experimental data, the simulation tools show an excellent agreement with measured data. It is concluded that small differences are caused by the evaluation of the solar irradiance on tilted surfaces and the transient heat conduction model. In [119] a wider set of simulation tools are validated against the BESTEST validation standard [17], showing excellent agreement among simulation tools. Finally, [142] reviews tools, procedures and uncertainties on calibration of building energy simulation models. The discussed models range from detailed building simulation tools like TRNSYS to simplified data driven grey-box models. Some of the best practices mentioned in this related work like the number of days involved in the data set, RMSE (Root Mean Square Error) data fitting and methods to validate residuals are also applied in this chapter.

A relevant question for this chapter is if the predictive model is sufficiently accurate for the intended use. This has a relation with the characteristics of the buildings considered. In the near future, newly built and renovated urban districts will mainly consist of so called low-energy houses, i.e. houses which consume much less energy than traditional houses when it concerns space heating, domestic hot water, cooking and lighting. The present building standard in the Netherlands, expressed in terms of the EPC-value, is 0.4 (EPC-Energy Performance Coefficient) and houses built today are close to the low-energy intentions. For low-energy buildings, the consumption described by items 1 and 2 (listed above) decreases but also becomes better predictable because the house structure is increasingly isolated from more uncertain outside conditions (except heat gains by solar energy transmission through the glazing). However, the behavior of the inhabitants described by item 3 (above) becomes more important for the real thermal demand of households. Learning the influence and uncertainty of this in practice may be more challenging for smart control systems than the exact accuracy of models for items 1 and 2.

Thermal models for the thermal demand of buildings is a relatively well developed research area. In [108], a general overview of modeling approaches based on the principles of building physics, heating, ventilation and air conditioning systems (HVAC-systems) is given. In [90], a review of simplified thermal building models is carried out which discusses black box models like neural networks and linear parametric models, and lumped capacitance models as part of white or grey box models. Their review also highlights some important aspects when using lumped capacitance models in relation to solar gains of the interior. They also conclude on the many useful applications of simplified thermal building models in comparison to detailed building simulation models. Particularly the use of lumped capacitance, thermal networks for simulation of building heating and cooling loads is relatively simple and adequate, which is why it is chosen in this thesis for smart control purposes.

Other authors have investigated more specifically the estimation of parameters for simplified thermal network models in which only a few thermal mass and resistance terms are present. The purpose is to use these simplified models as grey-box models for model predictive control of building HVAC-systems. Early work is done by Sonderegger [160] who determines parameters from measurements of a lightweight house construction heated with electrical heaters. A single thermal mass term is used together with a mass-less zone temperature resulting in a 3R1C-model, signifying 3 resistances (R) and 1 capacity (C). Madsen [100] uses stochastic system identification techniques to find parameters for a 2R2C thermal model and uses a limited set of measurement data of a single room heated with an electric heater. The room is part of a lightweight house construction in which concrete plates are placed within the room to increase the internal thermal mass. Both authors (Sonderegger and Madsen) find quite good correlations between measurements and model predictions of room temperature for the limited dataset (5 to 10 days).

The relation between the number of parameters and accuracy of the model pre-

dictions is studied by Bacher and Madsen [20]. They use statistical maximum likelihood tests on a number of models (from 1R1C up to 5R5C) and validate the models with 6 days of measurement data of a lightweight house construction heated with electrical heaters. For this building, sufficient accuracy is reached with a 3R3C model which contains thermal mass terms for the interior, the heater and the envelope.
As the heating system concerns floor heating rather than electrical heating, a relevant study is reported by Andersen et al [16] who investigates parameter estimation for a well insulated, lightweight Arctic house heated with floor heating. They use 16 days of measured data for validation. The measured ambient conditions show a relatively constant solar energy pattern with peak radiation below 300 W/m^2 each day and ambient temperatures ranging between -10 and -30 degrees Celsius. Following the same method introduced by Bacher and Madsen they determine parameters for a 3R3C model which contains thermal mass terms for the envelope, the interior and the floor heating.

Some common aspects of this related work on model calibrations are:

- The houses concerned have rather lightweight structures, i.e. envelopes are made of wood frames, and from the inside to the outside, walls consist of gypsum board material, insulation and wood covering.
- Parameters of the simplified thermal network models are obtained from and validated against a relatively short period of measurement data.

For Dutch low-energy houses, it is interesting to determine and investigate model parameters for heating and cooling with floor heating systems. Dutch houses typically contain concrete inner walls and floors and brick outer walls. This is considerably more thermal mass than the houses investigated in related work. It is interesting to investigate if parameter estimation of simplified models also shows good results for houses with a significant larger thermal mass.
Model parameters identified from short periods of measurement data are often used as if they should be constant for all time periods. However, some parameters are likely to vary within a range, depending on e.g. the day of the year. This is for instance the case for a parameter like "window area", i.e. an important parameter through which solar energy gains are calculated. The total window area of the houses mentioned in related work is often much smaller than is the case for most Dutch houses. As the angle of the sun with the horizontal plane moves from a small angle during mid-winter to almost ninety degrees during mid-summer and various forms of shadow may occur, the window area as an estimated parameter is not likely to be constant throughout the year. This is also concluded by [32]. Other parameters which are also assumed to vary slightly throughout the year due to e.g. non-linear temperature dependency of heat transfer in relation to surface temperatures are (a) the effective thermal mass of the interior and (b) internal resistances between floor heating surfaces and the interior air. This is part of the reason why [142] suggests as best practice to evaluate much larger datasets (at

least one up to three months) to calibrate model parameters.
Concluding, a house in relation to its building physical properties, methods of temperature control, the type of heating system applied and prevailing weather conditions altogether forms a complex system. It is of interest to investigate accuracy of model predictions for cases with larger and smaller thermal mass and to verify the prediction performance of the model parameters outside a certain measurement period. These aspects are investigated in more detail in this chapter.

2.3 General model formulation

2.3.1 General model formulation

A typical Smart Grid control study for urban districts may involve hundreds of houses. To give an idea on the scale of the calculations that are carried out for such a study in the Triana simulator, the first step of the Triana method involves prediction of the upcoming heat demand for each house, for which a predictive model is used. The second step of the Triana method involves planning based on mathematical optimization [28] for the heating appliances for each house. During this step, it is also possible to evaluate the consequences on thermal comfort as a result of the proposed plannings for up to 24 hours ahead, again by using a predictive model. To limit the computational effort, basic requirements for the thermal model are: (a) preferably described within the time domain, (b) linear and (c) mathematically simple, e.g. it has the lowest possible model order. On the other hand, the dominating system dynamic parameters should be described with sufficient accuracy.
The thermal network method is adopted as it meets these requirements. In general, a thermal network of a house describes heat transfer by a number of differential equations, each representing the heat balance for a lumped thermal mass, e.g. of the interior air, of the internal house structure or of the floor heating structure. The differential equation notation can be generalized into the following continuous-time matrix notation (2.1):

$$\frac{dT}{dt} = \mathbf{A}T + \mathbf{B}q\,, \tag{2.1}$$

in which the vector T contains the thermal mass temperatures and vector q contains direct heat gains or loss terms for the thermal masses, e.g. heating input to the floor heating and solar energy gains to the zone. Matrix **A** characterizes the system dynamic parameters and contains thermal capacitance and resistance terms. Matrix **B** specifies how the direct heat gains and losses enter the respective thermal masses.

A basic model representation of the house including heating and ventilation installations is shown in Figure 2.1.
The model representation contains the following variables and parameters:

- T_a the ambient temperature

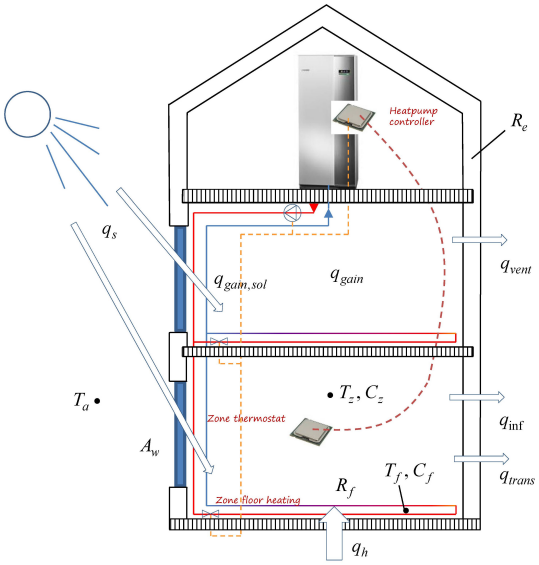

Figure 2.1 – modeling scheme of a house

- T_z the interior zone temperature
- T_f the average floor heating surface temperature
- R_f the resistance between the floor heating and interior zone thermal mass
- C_f the capacitance of the floor heating thermal mass
- C_z the capacitance of the zone thermal mass
- R_e the thermal resistance between the zone thermal mass and the ambient
- A_w the effective window area on the south side of the building
- q_s incident total solar energy on the southern vertical building plane
- $q_{gain,sol}$ the solar energy gain of the interior zone, i.e. $q_{gain,sol} = A_w \cdot q_s$
- q_h heating energy from an external source (e.g. heat pump) to the floor heating
- q_{trans} heat loss by transmission through the exterior walls and windows
- q_{gain} thermal gains by people and appliances
- q_{vent}, q_{inf} heat loss by ventilation and infiltration air streams.

2.4 Data generation

To estimate model parameters, either measurement data of real houses is required or simulated data from a detailed building simulation model. As detailed temperature and condition measurements of real houses are lacking, simulations are used.

This is justified by the small performance gap discussed in Section 2.2 between simulations with a detailed building simulation tool and measurements. For the data generation, various Dutch reference houses [10] are modeled in TRNSYS [165]. Details of the modeling process in TRNSYS are explained in Appendix A.

2.5 Estimation of Equivalent Thermal Parameters

2.5.1 Investigated models

As a first step, the accuracy of different thermal network models is investigated. The models differ in the number of lumped thermal mass and resistance terms. The amount of thermal mass terms is limited to a maximum of three. First because the results by Bacher [20] show that adding more thermal mass terms does not increase accuracy. Second because the thermal mass terms are required to have a relation with structural mass elements of the house. A house which is represented by one interior zone has three significant groups of structural mass elements (from inside to outside): floors, interior walls and outdoor facade walls. The following models are investigated (see also Figure 2.2 for model representations):

- 1R1C model, which contains one thermal mass term for the zone itself and one overall building thermal resistance. All heating inputs and direct losses are defined at the zone thermal mass.
- 2R2C model in two varieties. Besides the zone thermal mass, variety one additionally contains a thermal mass for the floor heating with connected heating input. Variety two contains a thermal mass for the interior house structure, the heating input is then defined at the zone thermal mass.
- 3R3C model in two varieties. Besides the zone thermal mass, variety one contains thermal masses for the floor heating and for the interior house structure. The heating input is defined at the floor heating thermal mass. Variety two contains a wall structural mass in between the zone thermal mass and ambient temperature, and an interior structural mass.
- 4R3C model. This is the same as the 3R3C model, variety 1, but contains an additional resistance between the floor heating and interior structural thermal mass.

Besides the parameters already explained in relation with Figure 2.1, additional parameters are:

- T_m the interior structural mass temperature
- T_w the external wall temperature
- R_m the resistance between the interior structural and zone thermal mass
- R_w the resistance between the external wall thermal mass and the ambient temperature

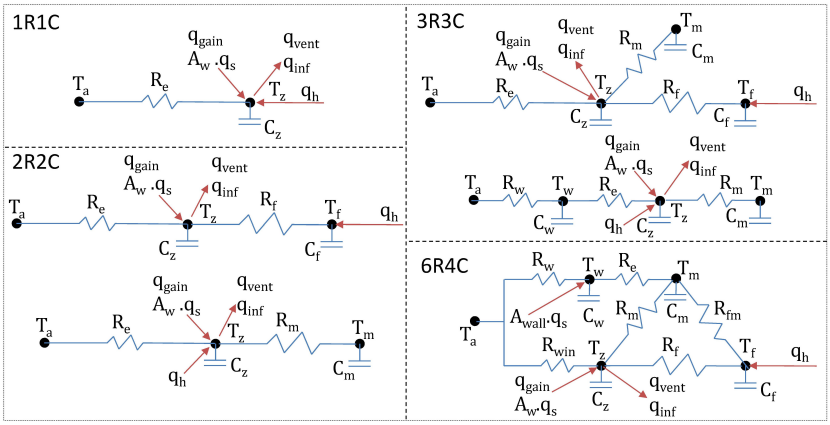

Figure 2.2 – thermal network model representations

- R_{fm} the resistance between the floor heating and interior structural thermal mass
- C_m the capacitance of the interior structural mass
- C_w the capacitance of the external wall thermal mass.

2.5.2 Estimation approach

The purpose of the estimation process is to estimate the house thermal properties, e.g. resistance and capacitance and effective window area for the presented thermal network models from TRNSYS simulation data. The TRNSYS simulations include solar gains, in order to estimate the effective window area. However, infiltration and ventilation air flows are excluded from the simulations. In practical applications of the thermal network models, heat loss by infiltration and ventilation can be expressed by additional relations which are included in the zone heat balance equation, as will be demonstrated in the following.
For each model, the number of parameters to estimate from simulated data is $r + c + 1$ in which r is the number of resistance terms and c is the number of capacitance terms. The effective window area is an additional parameter. The estimation process contains the following mathematical steps:
First consider the discrete form of Equation 2.1:

$$\begin{aligned} T_{n,t} = T_{n,t-1} + \Delta t \cdot \left(A \cdot T_{n,t-1} + B \cdot \tilde{q}_{p,t-1}\right) \\ n \in \{z, f, m, w\} \\ p \in \{h, s, vent, inf, gain\} \\ t \in [0, \ldots, \tau] \,, \end{aligned} \tag{2.2}$$

in which τ is the total number of time periods of the simulation. $T_{n,t}$ is a vector of temperatures at time point t for the zone (z), floor (f), interior (m) or external

wall mass (w), which are part of the respective thermal network models. Δt is the time step of the simulation, $\tilde{q}_{p,t-1}$ is a vector of direct heat gains and losses for the heating input (h), solar energy (s), ventilation loss (vent), infiltration loss (inf), gains by people and electric appliances (gain).
As stated, our simulations are carried out with: $\tilde{q}_{vent,t} = \tilde{q}_{inf,t} = \tilde{q}_{gain,t} = 0 \ \forall t$.
The model parameters are coefficients of matrices A and B and are found by solving a least square minimization problem, in which $\tilde{T}_{z,t}$ is a vector of measured or simulated zone temperatures. The minimization problem is formulated as:

$$MIN \sum_{t=0}^{\tau} \left(T_{z,t} - \tilde{T}_{z,t}\right)^2 . \tag{2.3}$$

To increase accuracy, the differential calculation in (2.3) is reformulated as follows by quadratic in stead of linear extrapolation:

$$\begin{aligned} T_{n,t} \quad = \quad & T_{n,t-1} + \frac{\Delta t}{2} \cdot A \cdot \left(T_{n,t-1} + T_{n,t-2}\right) + \\ & \frac{\Delta t}{2} \cdot B \cdot \left(\tilde{q}_{p,t-1} + \tilde{q}_{p,t-2}\right) . \end{aligned} \tag{2.4}$$

Indicators for the prediction accuracy of the thermal network models with the estimated parameters are:

- Residuals: $y_t = \tilde{T}_{z,t} - T_{z,t}$. The residuals should be as close to zero as possible. They are plotted in time and give a graphical impression of the accuracy and possible problematic time periods. A related parameter which is used to compare accuracy of the different thermal network models is the maximum absolute residual (MAR) value within a time period. $MAR_\tau = MAX_{t=0}^{\tau} |y_t|$.
- Mean Average Percentage Error (MAPE). Like the MAR, this is a single accuracy value for a certain time period to compare accuracy of the different thermal network models. $MAPE_\tau = \frac{1}{\tau} \sum_{t=0}^{\tau} \left| \frac{y_t}{\tilde{T}_{z,t}} \right|$.
- Auto correlation of residuals (R_{yy}). The auto correlation is plotted in time and gives an indication whether the residual signal is random or is influenced by feedback, e.g. due to some of the inputs. Formally, we have $R_{yy}(l) = \sum_t^{\tau} y_t y_{t-l}$ in which l is a time lag period and $l \in [0 \ldots \tau]$.

2.5.3 Validation case example

The estimation procedure and results are illustrated and validated with the following case example. To generate data for the case, a TRNSYS simulation is run with a simulation time step of 30 minutes for a model of a heavy structured terraced house. For details refer to Appendix A. The zone temperature is controlled by an on/off controller with a larger deadband of $\pm 0.4^o C$ in order to have more variation of the zone temperature. The inputs: ambient temperature (T_a), heating input (q_h) and south vertical plan incident solar radiation (q_s) are shown in Figure 2.3. The heating input is smaller than the value shown in Appendix A in order to have

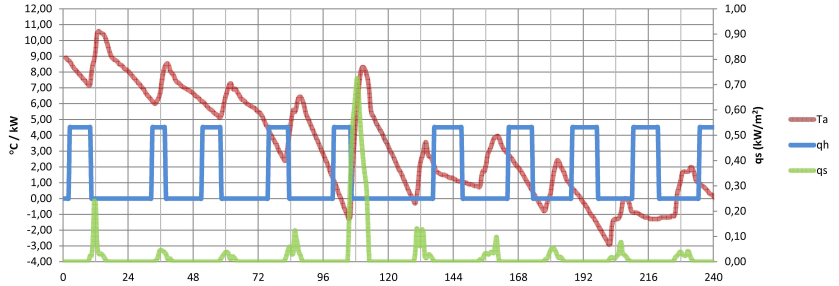

Figure 2.3 – input signals for the parameter estimation

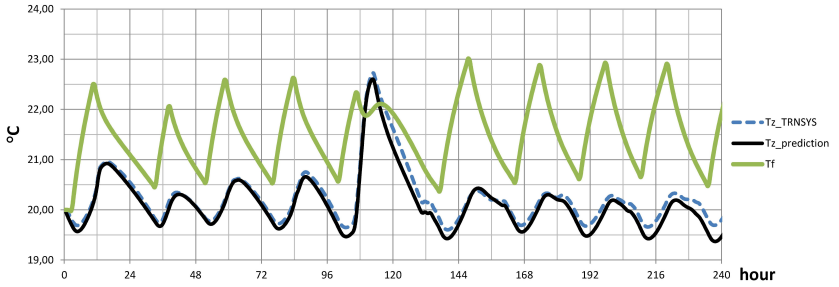

Figure 2.4 – TRNSYS and model prediction signals

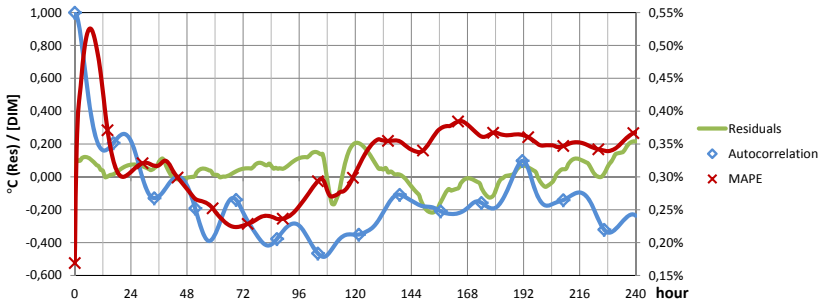

Figure 2.5 – accuracy indicators for the model parameter estimation

a slower system with less overshoot of the zone temperature. As responses, results from: TRNSYS (Tz_TRNSYS), model predictions (Tz_prediction and T_f) are shown in Figure 2.4. The accuracy indicators are shown in Figure 2.5. Parameter estimation is performed on the first 2R2C model shown in Figure 2.2.

The resulting model parameters of the estimation process are based on 10 days of simulated data and are given in Table 2.1. Direct comparison of these parameters with well known building properties such as the Rc value (unit: m^2K/W) for facade walls and the internal thermal capacitance or C_m value (unit: kJ/K), is not

possible, but the following relations apply:

- The envelope resistance R_e can be interpreted as the average thermal resistance of the entire heat loss surface of the building, including the envelope (walls and windows), the roof and the ground floor. For this house, the entire heat loss surface area is approximately 157 m^2. Multiplying this with the value of R_e and dividing by 1000 (unit conversion kW to W), results in 1.67 m^2K/W. A slightly higher value of 1.85 m^2K/W is found by calculation from building thermal resistance properties.
- In building performance calculations, the internal thermal capacitance C_m of a house is a lumped capacitance which signifies the entire internal structure. In the 2R2C model there are two lumped thermal capacitances C_z and C_f which together should be comparable with C_m. If the values for C_z and C_f are summed and multiplied by 3600 (unit conversion kWh to kJ), the result is 70840 kJ/K. This is similar to values of C_m valid for this type of house and structure.
- The effective window area A_w should approximately match the real window area of the Southern house facade multiplied by the window solar transmission factor. The estimated values appear to be slightly smaller than the real values.

parameter	estimation	unit
R_e	10.591	K/kW
C_z	7.686	kWh/K
R_f	0.996	K/kW
C_f	9.087	kWh/K
A_w	8.914	m^2
ω_s	1.603	m^2
ω_{qh}	0.00025	[ ]
ω_{Ta}	-0.004	kW/K

Table 2.1 – estimated 2R2C model parameters

Figure 2.4 and 2.5 show that due to the on/off control of the zone temperature, the zone response and residuals oscillate in time. It is observed from the auto correlation in Figure 2.5 (normalized, dimensionless [DIM]) that the dominant time period of the oscillation on the residuals is 24 hours and hence is likely to be caused by the incident solar radiation. The influence of the heating input on the residuals is also investigated but less profound.
In Figure 2.6 the prediction accuracy is shown with these parameters for a much longer, adjacent time period of 1344 hours or 56 days. In Figure 2.6, two lines are shown. The line "Residuals" signifies the residuals calculated with the model parameters given in Table 2.1. The line "Residuals_noise" signifies the same

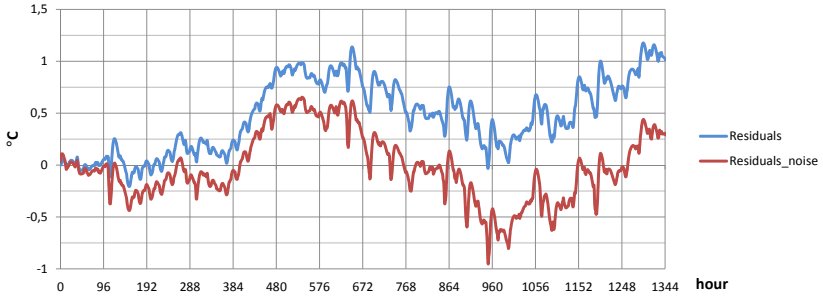

Figure 2.6 – residuals for model predictions outside the estimation period

model and parameters but with an improved accuracy which is done by adding a positive Gaussian white noise signal (W_{t-1}) multiplied with a matrix of estimated parameters ($\omega_{n,p}$) and the measured input data vector ($\tilde{q}_p$) in Equation (2.3). In general, the additional noise term is formulated as:

$$\frac{\Delta t}{C_n} W_{t-1} \omega_{n,p} \tilde{q}_{p,t-1}$$
$$\frac{\Delta t}{C_z} W_{t-1} \omega_{Ta} \left(T_{z,t-1} - \tilde{T}_{a,t-1} \right) \tag{2.5}$$

For the case example, there is one parameter ω_{qh} which is related to the equation for the floor heating temperature T_f and two parameters ω_{qs} and ω_{Ta} which are related to the equation for the zone temperature T_z. These parameters are estimated using the R and C thermal model parameters as constants and the ω parameters as variables on the data of the next 10 days. The estimated values by a similar least square minimization procedure are shown in Table 2.1. As shown in Figure 2.6, the additional noise terms clearly improve the prediction accuracy outside the original 10 day estimation and prediction period. For a period of 1344 hours or 56 days, the MAPE improves by 64% from 3.68% to 1.34%.
Investigating the obtained results more closely, the following is concluded:

- The noise parameter on the solar energy gains (ω_{qs}) is the most significant. It gives an indication on the long term inaccuracy of the estimated effective window area (A_w).
- The noise parameter for the heating input (ω_{qh}) is dimensionless. When multiplied with the heating input (on=4 kW, off=0 kW), the influence it has on the floor heating input is approximately 1 W, which is negligible.
- The noise parameter for the temperature difference between the zone and ambient temperature (ω_{Ta}). This signifies an inaccuracy on the heat transfer coefficient (U or 1/R) from the interior zone to the ambient. In terms of resistance, the reciprocal of ω_{Ta} yields 262 K/kW which yields a negligible heat transfer compared to R_e.

- Even though the eventual long term residuals still show deviations in the order of 1^oC, the resulting accuracy is regarded as sufficient but this decision depends on the application. It is observed in general, that each set of data yields slightly different parameters for simplified thermal models. Hence, the best accuracy is reached when an online parameter estimation is performed with a subsequent data time window.

2.6 Results and model order selection

Parameters for the models listed in 2.5.1 are determined using the first 10 days of simulated data by the TRNSYS model of the terraced house. During the simulations, only heat loss through the house envelope, heat gains by solar transmission and floor heating are simulated. The results are shown in Table 2.2 at the end of this chapter. The third and last columns in this table (2R2C_Cf and 2R2C_physical) are discussed in Section 2.7 where the physical interpretations of the parameters are discussed.
On the first line the MAR values for the 10 days used for the parameter estimation are shown, on the second line the MAR values for a much longer period of 1344 hours. On the third and fourth line this is repeated for the MAPE percentages. Clearly, the 1R1C and 2R2C_m models show the largest absolute residuals. The parameter Cm is constrained to a maximum of 200. So this model is less accurate and its parameters are more difficult to estimate from a limited data set.
The most accurate model is the 3R3C_f model. Even the 6R4C model is less accurate. Hence the conclusion is justified that adding more thermal mass terms than 3 does not necessarily yield better model accuracy. In fact, more thermal mass terms also increase the number of relations between the thermal masses. Due to the non-linear nature of e.g. radiation heat transfer, these relations are increasingly non-linear. This is one of the causes for inaccuracies when the model consists of a set of linear equations. The inaccuracy is best observed from the MAR and MAPE values which increase with the distance from the initial 10 day period for which the parameters are determined. External conditions like the ambient temperature and solar gains change, effecting the internal thermal masses. Also, the higher the ambient temperature, the less heating is required. The effect is a colder floor heating system which has effects on the internal thermal mass temperatures. As explained, in the real world, these effects are slightly non-linear. The TRNSYS simulations are closer to the real world situation than simulations with the linear thermal network models.

2.7 Physical interpretation of parameters

2.7.1 Comparison for houses with large internal thermal mass

In order to simulate the individual energy demand of households in a smart grid controlled district which consists of a variety of houses, parameters are needed for

each type of house. If TRNSYS simulations are needed to estimate parameters for each house type, this is an elaborate task. The effort can be reduced if the model parameters have a reasonable correlation with parameters that can be physically computed from the building structure. In [77] guidelines are given for computing physical parameters, based on an approximation of heated or cooled thermal zones by two thermal masses, i.e. one for the interior mass (interior walls, floors, ceilings) and one for the heating system (in our case radiant floor heating). The approximation is similar to the 2R2C_f model shown in Figure 2.2. The computed physical parameters are shown in the second last column of Table 2.2. The capacitance of the floor heating system is calculated by taking into account constructional details of the floor which includes a set of plastic tubes with water, a layer of concrete, and a wooden floor covering. Underneath the floor heating layer is an insulating layer which separates the floor heating from the heavier concrete floor structure. The zone capacitance is calculated by taking into account the areas of the interior walls and ceilings multiplied by a property called the structural working depth, for which guidelines are given in [77]. The structural working depth is the wall depth which accumulates and releases heat due to temperature variations within the interior. The given guidelines are based on finite element simulations. Thermal resistances are calculated by applying appropriate steady state convection, radiation and conduction heat transfer equations.
The MAR and MAPE values of the physical parameters in Table 2.2 indicate that predictions with the physical parameters are less accurate than predictions with the estimated parameters. Possible explanations for this include:

- The estimated parameters are mathematically the best possible fit for data of a certain period of time, whereas the physical parameters are not related to temperature response data.
- The physical parameters represent a simplification of a house and some of the parameters are calculated from approximate, steady state equations which are assumed to be constant and independent of the interior and ambient conditions. Hence, each physical parameter has some uncertainty for the purpose of dynamic simulations. The most uncertain parameters are R_f and C_z due to the involved heat transfer approximations. Considerably less uncertain are C_f, R_e and A_w as these are more straightforwardly calculated from building geometric information.

It is possible to find a closer correlation between the estimated parameters and the physical parameters by constraining one or more parameters during the estimation process to the pre-calculated physical value. This is investigated for each parameter and has proven to be most successful for the floor heating capacitance parameter C_f. The estimated parameters are shown in the third column 2R2C_Cf in Table 2.2. When we compare the MAR and MAPE values of this column with the values shown in the second column 2R2C_f, we conclude that the accuracy is similar. However, the correlation with physical calculations (column 2R2C_physical) has improved significantly.

If the estimated parameters are compared with the physical calculations for this specific terraced house case, the envelope resistance is lower, the zone capacitance is higher, the floor resistance is higher and the effective window area is lower. In Table 2.3, results are shown for other house cases: a corner house, a semi-detached house and a detached house. The construction (wall materials, wall thicknesses, insulation thicknesses) of the houses is similar as the terraced house case, only the geometry such as envelope and window areas, window areas and floor areas is different. EST signifies estimated parameters, PHYS the calculated physical parameters and RE signifies the relative error with the physical parameters as reference.
From the results shown in Table 2.3, it is concluded that also for other house geometries, the estimated parameters are close to the physical calculations. Furthermore, in most cases the deviations work in the same direction. Compared to the physical calculations we conclude for the estimated parameters:

- the estimated envelope resistance is mostly slightly smaller,
- the estimated zone capacitance is slightly larger,
- the floor resistance is larger and appears to have the largest difference, most likely due to inaccurate physical calculation, and
- the effective window area is slightly smaller.

2.7.2 Comparison for houses with small internal thermal mass

In order to verify the estimation method and comparison with approximate physical parameters for lighter constructed houses, the same type of houses are investigated with similar dimensions, but constructed with much lighter materials. The interior walls are in this case based on sandwich panels consisting of an insulating layer between two wooden boards, covered with plaster. The floors contain a similar type of sandwich construction and are covered by a concrete layer with the floor heating tubes. The outer walls are made of brick. In Table 2.4 the column EST shows the results for these lighter houses. The column PHYS shows the approximate physical parameters and RE the relative error with the physical parameters as reference.

From these results it is concluded that also for houses with a lighter construction, the estimated parameters are close to the physical calculations. However, for the difference between estimated parameters and physical calculations, we conclude:

- the estimated envelope resistance is smaller for the house with the smaller envelope (terraced house) and larger for the house with the bigger envelope (detached house),
- the estimated zone capacitance is similar to the physical calculation for the smaller houses (terraced and corner house) but smaller for the bigger houses (semi-detached and detached house),

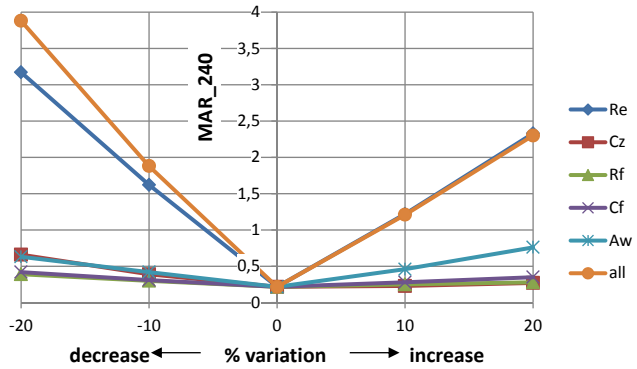

Figure 2.7 – influence of variation of model parameters on maximum residual

- like the heavier houses, the floor resistance is larger and has the largest difference, and
- the effective window area is slightly smaller and even smaller than the estimation for the heavier houses.

2.8 Model verification

In the following, two methods are discussed to verify if the model is suitable for its intended purpose. The first method involves a sensitivity analysis of the residuals in relation to small changes of the model parameters. In Figure 2.7 we show the maximum residual value for the dataset of 240 hours in relation to variations of the model parameters. The legend shows which line is related to a single parameter variation (between -20 and + 20%), while the other parameters are kept constant at their optimal value. The line "all" represents a variation of all parameters together in the same direction. This clearly shows the dominating influence of the parameter R_e (envelope thermal resistance) on the residuals and the high sensitivity of the residuals for only a few percent variation of this parameter. Hence, for successful application of the model, it is important to identify this parameter accurately from detailed calculations of the building envelope or preferably from measurements during colder periods with significant heat loss from the building.

Less dominating is the parameter A_w (effective window area) which has slightly more influence than the parameter C_z (zone thermal capacitance). The accuracy of the parameters R_f (floor heating thermal resistance) and C_f (floor heating thermal capacitance) appears to be of minor importance which is convenient as these parameters are more difficult to determine accurately from either calculations or measurements. The parameters with the largest influence are R_e and A_w and determine the heat loss through the envelope and the solar gains through the windows respectively. Accuracy of these heat flows depends also on the accuracy of

ambient temperature and solar energy predictions. Because the relation between heat loss, envelope resistance and ambient temperature is linear, the same relative accuracy of only a few percent is required for ambient temperature predictions. This is possible but only with dedicated measurements which are being done in the direct surrounding of the building. It is however more practical to use regional available weather prediction data for this. Hence, a solution is required for the longer term prediction inaccuracy of the model due to these influences. In general, from Figure 2.7 we may conclude for control purposes of the heating system that the accuracy of the "internal" part of the model is far less important than the accuracy of the "external" part of the model related to the weather predictions. Hence, a simplified "internal" model of the house will be sufficient. For a house, a model which consists of a single zone or two zones representing two building levels with different temperatures is sufficient for control purposes of the heating system.
The second verification method involves a control case to verify if the 2R2C model with the parameters close to physical calculations, can be used for model predictive control with sufficient accuracy. The quality of this control is validated with two approaches:

1. Comparison of the heat pump control obtained from two separate simulations: (a) simulation with the 2R2C model, (b) simulation with TRNSYS. For this approach, discrete time simulations with the 2R2C model and on/off heat pump control are carried out, which results in a heat pump control planning and zone temperature prediction. These results are compared with results from TRNSYS in which a similar on/off heat pump control is implemented.
2. Repeating the previous comparison for cases which include air ventilation flows.

In both approaches, the validation is carried out for two house cases: (1) a terraced house with a heavy building structure. The 2R2C model parameters are shown in Table 2.2, in the column 2R2C_Cf. (2) A semi-detached house with a light building structure. The 2R2C model parameters are shown in Table 2.4, in the column EST, section semi-detached.
For the heavy building structure case, Figure 2.8 shows the results of the on/off control simulation for a period of 10 days for the 2R2C model (predicted zone temperature: Tz_MPC and heat pump control: qh_MPC) and for the TRNSYS model (Tz_TRNSYS and qh_TRNSYS). The 2R2C discrete time simulation is performed with a time period of 0.5 hour and for the on/off controller, the same setpoint temperatures and deadbands are used as for the TRNSYS simulation. The input weather data (Ta and qs) is shown in Figure 2.3 and is obtained from the TRNSYS simulation. For the TRNSYS simulation, an equal time period of 0.5 hour is defined, but TRNSYS performs iterations between time periods in order to increase accuracy of the results. Hence, this is another source for deviations between the 2R2C and TRNSYS results, besides the obvious deviations caused by simplifications of the 2R2C model.

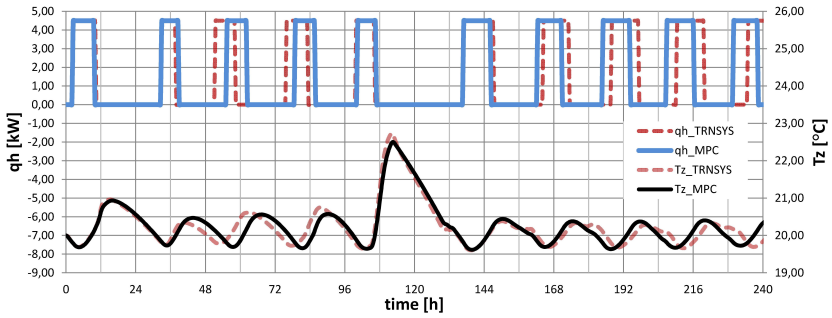

Figure 2.8 – Heat pump control simulation results for heavy building structure

The MPC results can be used for planning the heat pump control for 10 days ahead. In practice, weather predictions cannot be made with sufficient accuracy for such a long period of time. From the MPC heat pump planning and TRNSYS heat pump control, shown in the upper part of Figure 2.8, the conclusion can be drawn that the prediction is quite accurate up to the first two days ahead, then it becomes less accurate the following two days, followed by two days with more sunshine, less heat demand and more accurate predictions. The last part of the period shows that the MPC planning is becoming more out of sync with the TRNSYS results.

Considering these results and the fact that weather predictions are normally only accurate for a few days ahead, it is logic to use the MPC control to plan the heat pump only two days ahead and to synchronize the zone temperature regularly with the TRNSYS results. This is also how in the real world an MPC controller would synchronize regularly with measurement data. In practice the time interval for synchronization would be a number of times per day. In Figure 2.9, the resulting improvement of planning two days ahead is shown. In this case, the synchronization time period with the TRNSYS data is also two days, which gives satisfactory results. This synchronization is best seen on Tz_MPC at the time point 48 hours, where the temperature drops instantly to the Tz_TRNSYS value. The prediction accuracy of both the zone temperature and heat pump planning by the 2R2C model is very much improved due to the synchronization.

For a semi-detached house with light building structure, it is verified whether the same observations can be made. Figure 2.10 shows on/off control results for the same period of 10 days without synchronization of the MPC with TRNSYS zone temperature data. Notice that in this case, the MPC gives an accurate heat pump planning for the first 6 days. However, like in the heavy building case, for the last part of the period, the planning starts to be more out of sync with the TRNSYS results.

Looking at Figure 2.11, it can be stated that a 48 hour synchronization period gives only a slight improvement. Results improve to a satisfactory level when a 24 hour synchronization period is introduced. So also for a light building case, the prediction accuracy of both the zone temperature and heat pump planning by the

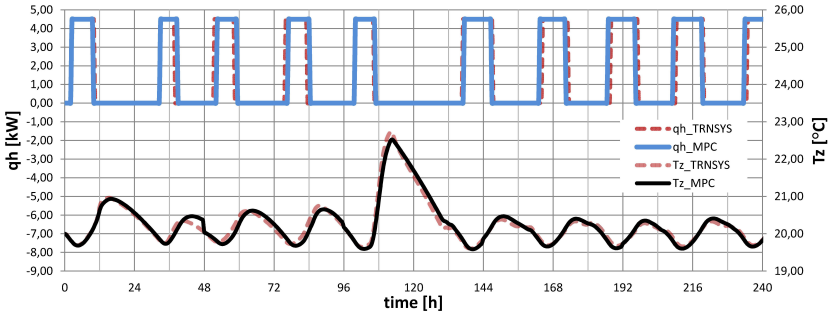

Figure 2.9 – Improved heat pump planning due to synchronization every 48 hours

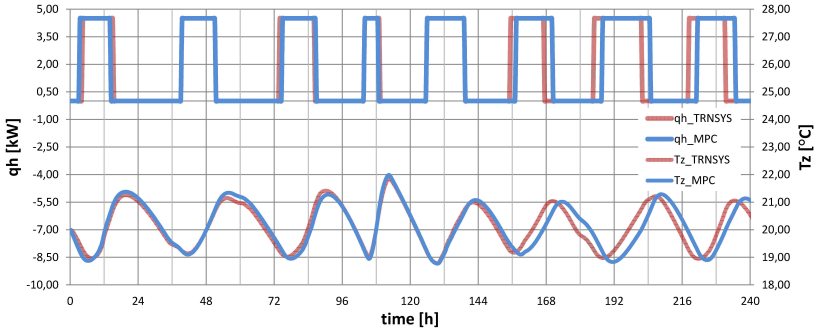

Figure 2.10 – Heat pump control simulation results for light building structure

2R2C model is improved due to the synchronization. It can be expected that other house cases may show a similar improvement due to synchronization.

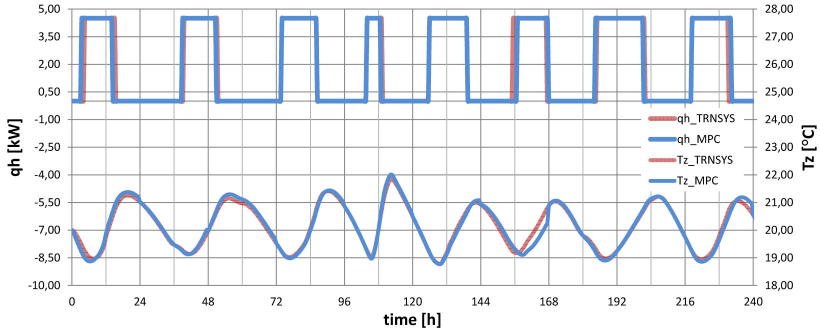

Figure 2.11 – Improved heat pump planning due to synchronization every 24 hours

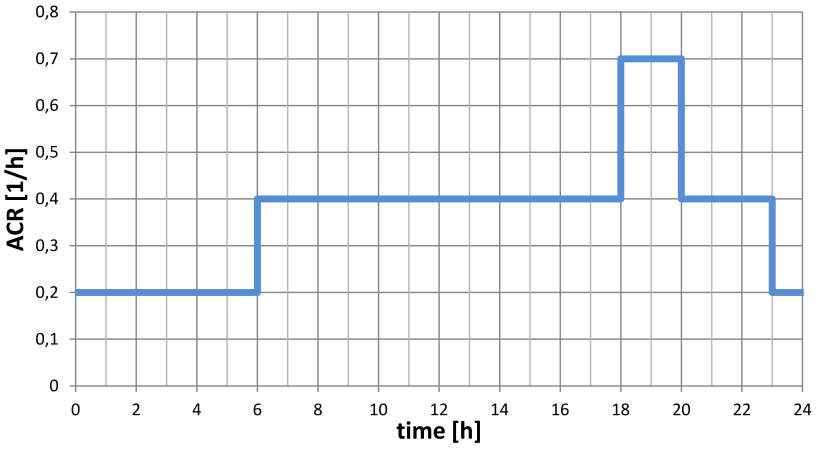

Figure 2.12 – Daily air change rate schedule

2.8.1 Heat pump control including ventilation air flows

The results thus far are restricted to heat loss and solar gain through the building envelope and heat gains from an interior floor heating system. The parameters of the 2R2C model which is proposed in this chapter are directly related to these heat flows. As shown in Figure 2.2, other types of heat loss and gain like ventilation air flows and internal gains from people and electrical appliances, have a direct influence on the zone temperature. This is why these heat flows are part of the heat balance equation for the zone temperature. In this equation, heat loss and heat gain cancel each other out. To validate the accuracy of the 2R2C model, it is therefore most interesting to investigate the most extreme case, i.e. either the highest possible heat loss or heat gain applicable at the zone temperature. The most extreme case is the case where the house is ventilated by a forced ventilation system using outside air to refresh the interior air. In Figure 2.12 a daily ventilation schedule is shown in terms of the air change rate (ACR) of the entire interior volume per hour. The associated heat loss is calculated from (2.6). In this equation, $V_{air,i}$ is the interior air volume, p is the ambient air pressure, Rs the specific gas constant of air and $c_{p,air}$ the specific heat of air.

$$q_{vent} = ACR \cdot V_{air,i} \cdot \frac{p}{Ta \cdot Rs} \cdot c_{p,air} \cdot (T_a - T_z) \tag{2.6}$$

For the heavy house structure case ($V_{air,i} = 323m^3$), the results of the control simulations with TRNSYS and the 2R2C model are shown in Figure 2.13. When the ventilation ACR increases sharply around 6.00 and 18.00 hrs each day, the TRNSYS results for the zone temperature show a kink at those hours. This is not seen on the 2R2C model. This is obvious, because the TRNSYS model computes the temperature change of the air volume separate from the surrounding building structure, while the 2R2C model computes this with only one large thermal mass

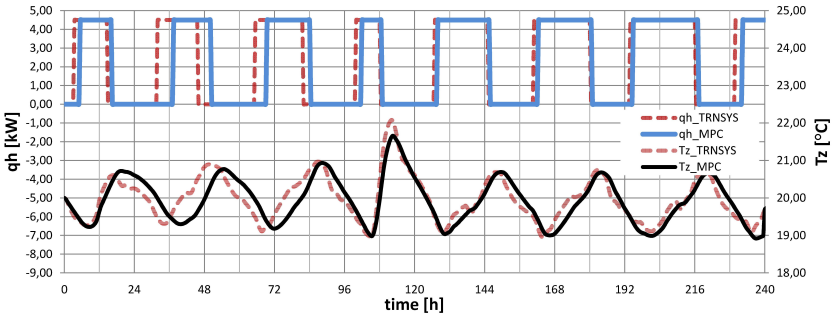

Figure 2.13 – Heat pump control simulation results for heavy building structure, including ventilation

for the interior structure including the interior air. The 2R2C model could be extended with a separate zone air node with a very low capacitance, but this would create numerical instability with a simulation time period of 30 minutes. In TRNSYS, this problem is bypassed by subdividing each time period into much smaller increments which are solved first. However, when this is used in model predictive control of many houses, this increases complexity of the algorithm and computational time significantly. Hence, it is investigated if the present method can also be used with sufficient accuracy also for this extreme case with ventilation heat loss.
In Figure 2.14, improved 2R2C simulation control results are shown due to synchronization with the TRNSYS results every 6 hours. In this case, the zone temperatures and the heat pump control of the 2R2C model, match the TRNSYS results sufficiently close. For the light house structure case, the non-synchronized results of the 2R2C model are closer to the TRNSYS results. This is because the zone capacitance of the 2R2C model is much smaller than in the heavy house case. In general the conclusion is justified that the 2R2C model presented in this chapter can be used with sufficient accuracy for model predictive control for heavy and light house structures. However, the accuracy of the 2R2C model increases with decreasing weight of the internal house structure.

2.9 Conclusions

In this Chapter, various possible predictive models for Dutch low energy houses based on thermal network representations are investigated. A model parameter estimation procedure is based on data from detailed TRNSYS simulations. A 3R3C grey box model gives the best correlation between model predictions and the TRNSYS data. However, a 2R2C model with thermal mass terms for the interior zone and the floor shows almost the same correlation but has the advantage that the thermal capacitance and resistance parameters more closely match physical calculations, so the model then is more white box than grey box. This makes it possible to quickly determine model parameters for simulation purposes when

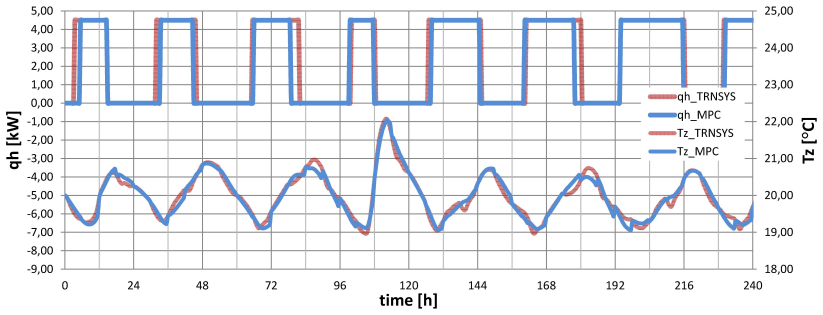

Figure 2.14 – Improved heat pump planning due to synchronization every 6 hours including ventilation

different types of houses are concerned. Although the estimation procedure is applied successfully to all types of Dutch reference houses, the work should be extended to more recent developments like houses with better thermal insulation properties and houses with different heating systems. Also, the performance of the models for cooling of the houses in the summer is not tested. Another part of future work is to test the prediction accuracy of the models for every week of the year as it is found that parameter values following from the estimation method vary slightly when different periods of data are used.

Furthermore, it has been shown theoretically that the 2R2C model can be used for Smart Grid control simulations. A practical demonstration on the fitness of the model for control algorithms is part of future validation work. In practice, the model and its parameters will probably cause some inaccuracies of the predictions. The main causes for this are partly the model itself, partly that no house is built perfectly the same. However, unpredictability of the situation around the house (e.g. orientation, shadows from trees for the incident solar energy, wind vulnerability) and unpredictability of occupant behavior or errors in weather forecasts may cause more significant prediction errors. If required, a stochastic parameter estimation from real data may be applied, although this leads to significantly more complex estimation algorithms as shown in [100]. A different approach may be more straightforward and may lead to better results: in this chapter, the parameter estimation of the model is deliberately separated from occupancy related events and ventilation air flows. When real data is used in practice, this separation is not possible. This is why a white box model has the advantage that thermal properties of the house can be pre-calculated from design data. When real data is used, the occupancy related thermal events can be learned with a black box model from the prediction errors of the white box model. For this purpose, a neural network model or linear parametric model is proposed as part of future work involving experimental data of houses.

	1R1C	2R2C_f	2R2C_Cf	2R2C_m	3R3C_f	3R3C_w	6R4C	2R2C_physical	unit
MAR_240	1.20	0.22	0.40	1.15	0.24	0.25	0.46	2.3	K^{-1}
MAR_1344	2.67	1.02	1.74	1.79	0.64	1.18	1.59	4.7	K^{-1}
MAPE_240	1.45	0.37	0.43	1.71	0.30	0.32	0.26	7	%
MAPE_1344	3.98	1.87	3.34	2.08	1.09	2.47	2.96	12	%
Re	9.582	10.591	10.686	10.435	10.701	10.570	11.227	11.8	K/kW
Cz	25.484	7.686	10.505	16.271	8.792	7.560	2.573	8.5	kWh/K
Rf		0.996	2.104		1.066	0.988	2.079	1.4	K/kW
Cf		9.087	3.6		7.704	9.070	7.716	3.6	kWh/K
Rm				3.442	6.594		0.320		K/kW
Cm				200	146.6		5.547		kWh/K
Rw						0.158	0.501		K/kW
Cw						1.690	1		kWh/K
Rfm							3.945		k/kW
Aw	12.429	8.914	8.074	11.439	9.657	7.989	7.291	10.2	m^2
Awall						19.020	13.158		m^2

Table 2.2 – estimated terraced house model parameters

		corner			semi-detached			detached		
parameter	unit	EST	PHYS	RE	EST	PHYS	RE	EST	PHYS	RE
Re	K/kW	8.23	9.9	-0.17	8.67	9.0	-0.04	7.17	6.4	0.13
Cz	kWh/K	16.74	12.9	0.30	20.34	18.0	0.13	22.48	21.1	0.07
Rf	K/kW	2.81	1.4	0.99	1.69	1.1	0.52	1.66	1.0	0.66
Cf	kWh/K	3.6	3.6	-	4.6	4.6	-	5.1	5.1	-
Aw	m^2	8.91	10.4	-0.14	5.00	5.5	-0.08	8.74	9.5	-0.08

Table 2.3 – estimated and physical model parameters of the corner, semi-detached and detached house, EST=estimation, PHYS=physical parameters, RE=relative error

		terraced			corner			semi-detached			detached		
parameter	unit	EST	PHYS	RE	EST	PHYS	RE	EST	PHYS	RE	EST	PHYS	RE
Re	K/kW	11.53	13.3	-0.13	9.09	9.9	-0.08	9.47	9.0	0.05	7.89	6.4	0.23
Cz	kWh/K	4.65	4.5	0.03	5.02	4.9	0.02	4.21	5.9	-0.29	4.60	6.0	-0.23
Rf	K/kW	3.32	1.4	1.37	3.15	1.4	1.25	2.79	1.1	1.54	2.39	1.0	1.39
Cf	kWh/K	3.6	3.6	-	3.6	3.6	-	4.6	4.6	-	5.1	5.1	-
Aw	m^2	8.05	10.2	-0.21	8.42	10.4	-0.19	4.20	5.5	-0.23	7.74	9.5	-0.19

Table 2.4 – estimated and physical model parameters of the houses with lower thermal mass, EST=estimation, PHYS=physical parameters, RE=relative error

Chapter 3

Models for aggregated demand profiles

Abstract - In this chapter, a model for generating heating and cooling demand profiles of houses and districts is developed based on the models introduced in Chapter 2. Also, a model for household and district domestic hot water energy demand is developed and results are shown of simulations with a model for the electrical demand of households.

3.1 Introduction

As cases, which are investigated in Chapters 5 and 6 are lacking district heating and cooling demand data, profiles are generated by model simulations. In this chapter, a simulation method is developed for this, based on the model developed in Chapter 2. Besides that, for domestic hot water consumption, a statistical profiling method is developed for individual households and for districts. Furthermore, a model developed by others is applied to generate aggregated domestic electrical demand profiles.

3.1.1 General introduction of the Meppel case

Throughout Chapters 3 to 7, various cases are considered which originate from a project called Meppelenergie (Meppel-energy) [106]. Meppel is a city in the North-Eastern part of the Netherlands. In 2014, construction began of a new urban district called Nieuwveenselanden. Besides more stringent requirements on house thermal insulation than the national building requirements at that time, a heating and cooling supply system was envisioned which is almost 100% renewable. This energy concept is shown in Figure 3.1 and is given the name "Meppel

[†]Major parts of this chapter have been published in [RvL:6] and [RvL:11].

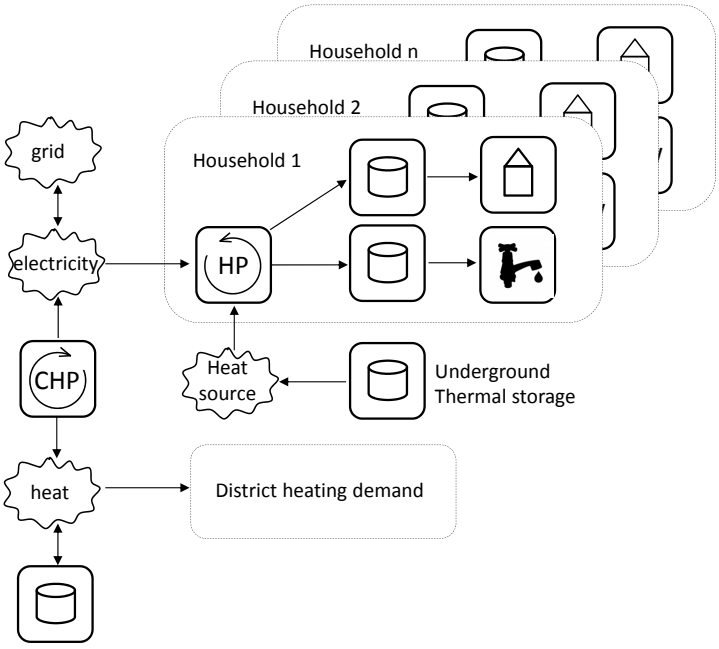

Figure 3.1 – Meppel energy concept

energy concept" throughout this thesis. It consists of a central biogas CHP (Combined Heat and Power unit), backup boilers (not drawn), High Temperature (HT) water storage, a district heating network, heat pumps (HP) in a number of houses and aquifer underground thermal storage as source for the heat pumps and for the cooling of all the houses (not drawn). The CHP generates electric and thermal energy from biogas which comes from a nearby waste water treatment plant. The thermal energy of the CHP is used for the district heating system and the electricity is used to supply heat pumps placed at houses with no connection to the district heating, or is exported to the external grid. The district heating utility does not have a permit to supply electricity for household consumption to the households. Instead, this is supplied by the licensed grid operator. Therefore, the electricity to the heat pumps is transported over a separate installation cable. This cable, the connection at the houses and the heat pumps are owned by the district heating utility. In this way, the district heating utility sells thermal energy to all households. In Chapter 6 the implications of this legislative construction are discussed in relation with alternative renewable energy concepts.

The Meppel energy system is a combination of two common types of local renewable energy systems: district heating based on biogas co-generation and heat pumps combined with underground thermal storage. In the Netherlands, Germany and Denmark there are numerous regional areas where biogas from waste water treatment plants is used as a source for co-generation of heat and power

which is distributed to local consumers through a district heating network and a local electricity grid which has a connection to the larger grid. A large scale example of this is in Apeldoorn Zuidbroek [45] where 2500 houses are heated in this way.
All houses receive cooling during the summer months from the underground aquifer thermal storage. An aquifer is an underground groundwater reservoir at a depth of around 60-120 meters. The temperature of the water is approximately 15°C, which is suitable as source energy for heat pump evaporators during the heating season. During the summer, the groundwater is used to cool the houses, which also regenerates the reservoir temperature after the heat pumps have cooled the reservoir down during the heating season. In recent years, this type of storage is commonly applied for new larger buildings and urban areas in North Western Europe. The increasing use of heat pumps in new building projects combined with suitable soil conditions and existence of large underground aquifers almost anywhere in the Netherlands, result in increasing applications of this type of storage. In the original concept, another source for regeneration during the summer months is provided by an effluent water stream from the municipal waste water treatment plant.
The Meppel project received support of the Dutch government within the program TKI-Switch2Smartgrids to develop a smart grid control for the energy concept. Development of the smart grid control system is the joined task of a project group formed by University of Twente, University of Delft, the district heating utility Rendo, the Meppel city council and system integration company i-NRG. The main task for the University of Twente is to develop smart grid control algorithms for the central CHP and heat pumps. Results of this task are given in Chapter 7.
Due to an economic recession in the Dutch housing market until the year 2015 and deteriorating financial position of institutional building corporations, the construction planning of the district changed. Smaller building phases were defined and the original plan for houses with heat pumps was withdrawn from the project because these houses were larger and more expensive and the market for them deteriorated. As a result, at the time of writing this thesis, approximately 150 houses are built and occupied (in stead of 300 houses as originally planned), all connected to a district heating system with heat produced by natural gas boilers. New transition directions of this temporary energy system towards an approximately 100% renewable energy system are investigated in Chapters 5 and 6.

3.2 Related work

Patterns for the aggregated heating and cooling demand of multiple households are either based on measured data or simulation models. Suitable methods based on measured data are treated in [27] and [44]. As measurement data is often lacking, simulation methods are used. In [154], [65] deterministic modeling approaches are given. In Chapter 2, a modeling approach based on a general thermal network model of the Meppel houses is given. This method is also adopted in this

chapter, whereby we give only the used parameters and results.

3.3 Model for heating and cooling demand of households and districts

3.3.1 Space heating and cooling model

The approach to determine a representative heating and cooling demand profile is as follows:

1. Develop a realistic simulation model of an average house. The process for this is illustrated in Chapter 2 in which for control purposes, a 2R2C model is concluded as sufficiently accurate. However, to generate an aggregated profile of the daily and hourly demand, the simpler 1R1C model is sufficiently accurate. Note that in the related work discussed, often a static degree-day model is used. Based on specifications of the houses built in Meppel, parameters for the model are given in Table 3.1. Besides that, we developed schedules for occupancy (internal gains) and ventilation flows. The general schematic of the model is shown in Chapter 2.
2. Determine heating and cooling demand of the house by simulation with representative climate data.
3. Determine average domestic hot water demand (see Section 3.3.2 for details).

For the 1R1C model, the model equations are formulated slightly different than in Chapter 2 because there is now also an interest in the cooling demand. Hence, the so called sol-air temperature T_{sa} is included, i.e. the surface temperature of the exterior brick wall. During the cooling season and daylight hours, this temperature is higher than the ambient air temperature due to solar absorption and thus causes part of the building cooling load.

$$\begin{aligned} C_z \cdot \frac{dT_z}{dt} &= \frac{T_{sa} - T_z}{R_{za}} + \frac{T_a - T_z}{R_{win}} + q_{h,c} + A_w \cdot q_s + \\ &\quad q_{int} + q_{vent} \\ T_{sa} &= \frac{T_z + R''_{za}\left[\alpha q_s + U''_{wall} T_a\right]}{1 + U''_{wall} R''_{za}} \\ q_{vent} &= \phi_v \cdot \rho_{air} \cdot c_{p,air} \cdot (T_a - T_z) \end{aligned} \tag{3.1}$$

The used parameters and variables are listed in Table 3.1. For the variables, this table mentions whether these are calculated during the simulation or given as input. The input variables q_{int} and ϕ_v are defined as time schedules.
Solar gains into the house are calculated based on mathematical relations and correlations given in [55] and [46], to translate horizontal solar irradiation into radiation on vertical building planes. In order to determine the space heating and cooling demand, a proportional control of the heating/cooling input $q_{h,c}$ is

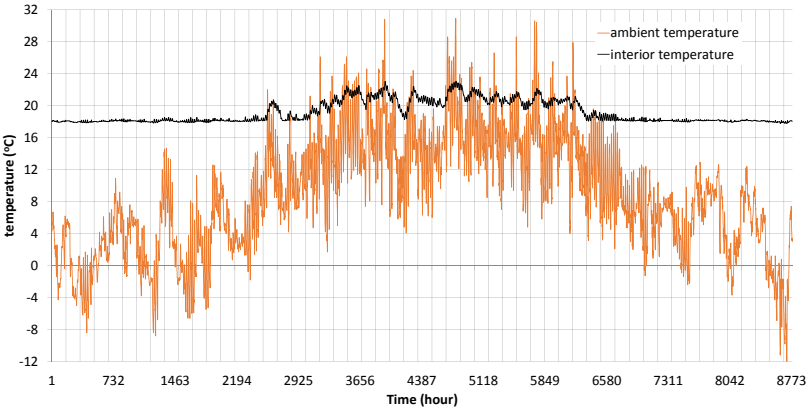

Figure 3.2 – controlled interior temperature in relation to ambient temperature

integrated into the simulation as a function of the error between the interior temperature and set-point temperatures. The purpose of the control is to keep the interior temperature within a narrow band around an average set-point of 18^oC for the whole house in case of heating and between a set-point of 20 and 24^oC in case of cooling. In [134] it is concluded from experimental data that a house can be divided in three zones (bathroom, bedrooms/attic and other rooms, e.g. living room and kitchen). For each zone there are different thermal comfort constraints. The living room and bathroom usually have a higher temperature (e.g. 20-21^oC), but sleeping rooms on the first floor and the attic are usually cooler (16-18^oC) during the heating season. Hence for heating, the average temperature of the house is assumed at 18^oC. However, due to better insulation of houses built today, temperature differences between zones are likely to decrease, leading to higher average house temperatures during the heating season. To which extend this is true is interesting for future work. The resulting temperature of the house for a complete year is shown in Figure 3.2.

To compensate for houses with a different orientation than South to North, the solar radiation which is used during simulations is multiplied with a single random number per house between 0.5 and 1. To compensate for the fact that the thermal demand for a group of houses is not perfectly simultaneous, the demand of each house is multiplied with a single random number between 0.8 and 1.2. In this way a large number of slightly different profiles, each representing one house can be generated and summed to obtain the overall heat demand of a group of households. This method is appropriate if the houses in the district have approximately similar building properties and most people living in the district have a regular, working life. If this is not the case, then an alternative method is to generate a number of individual household thermal demand profiles, using different house parameters and schedules during the simulation for the interior temperature set-points, the ventilation heat loss and the internal gains. The individual profiles are

then summed to obtain an aggregated profile.

3.3.2 Domestic hot water demand model of households and districts

The heating demand of a house includes demand for domestic hot water. Based on [135] and [24] this portion of the demand has a daily pattern which we approximate with suitable mathematical functions, for which we choose a set of Gaussian distribution functions of the following general form:

$$\begin{aligned} \dot{Q}_{dhw,h} &= \phi_i \cdot \rho_w \cdot c_w \cdot (T_{hw} - T_{cw}) \\ \phi_i &= \sum_j \frac{f_j}{\sigma_j \sqrt{2\pi}} \cdot e^{-\frac{1}{2}\left(\frac{i-\mu_j}{\sigma_j}\right)^2} , \end{aligned} \tag{3.2}$$

in which ϕ_i is a flow demand (e.g. in liters/hour at hour time i ($i \in 1,\dots 24$)), ρ_w and c_w the specific density and specific heat of water, T_{hw} and T_{cw} the hot water and cold water supply temperature to the household. The equation for ϕ_i is the sum of j Gaussian distribution functions, each with different average μ_j, standard deviation σ_j and scaling factor f_j. The parameters can be determined from simulated or measured data. However, in our case this is a somewhat arbitrary process as this data is not existing for the Meppel project.
The method is applied based on the results given in [24] (see Figure 3.3). As approximately three demand peaks per day are observed from this data, it is a logic choice that $j \in \{1,\dots,3\}$. The profile is then characterized by nine parameters, i.e. three values for parameters μ_j, σ_j and f_j which are determined by RMSE (Root Mean Square Error) optimization. The obtained parameters result in a calculated profile which is also shown in Figure 3.3 as an overlay (green line) to the results (aggregated district heating domestic hot water demand) shown in [24].
Defining a domestic hot water thermal demand profile for an average household is now a matter of scaling Equation 3.2. Based on [105] and [62] we estimate a yearly demand for domestic hot water per person of 3.2 GJ. Furthermore, based on information from the project, the average number of persons per household is 3.5. From this, a daily average demand is calculated per household and for each day of the year by applying Equation (3.3), which takes a variation of daily demand due to holidays into account (see [82]). A slightly varying hourly profile is obtained by multiplying the hourly values of the obtained profile with random numbers between 0.8 and 1.2. The domestic hot water profile is then multiplied by the number of households.

$$Q_{dhw,i} = nQ_{dhw,av} + n(1-p)Q_{dhw,av}\cos\Big(\frac{2\pi}{365}[i - day\_shift]\Big) \quad ; \quad i \in \{1,\dots,365\}\,, \tag{3.3}$$

in which n is the number of households, p is the fraction of households not on holiday during the holiday season, and day_shift the number of days that the

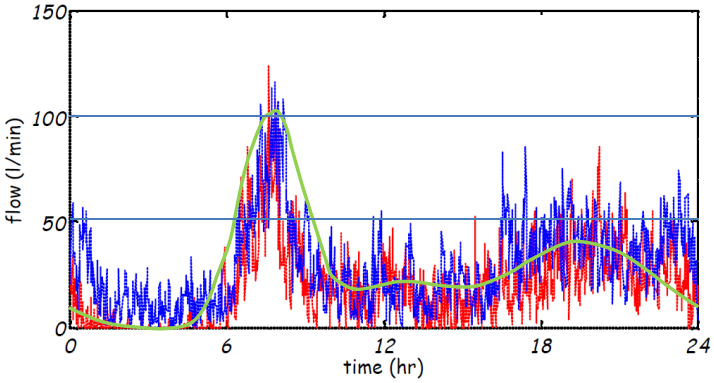

Figure 3.3 – Resulting domestic hot water profile (green line) calculated by (3.2) overlaid on literature results (blue=measurement, red=simulation, both taken from [24])

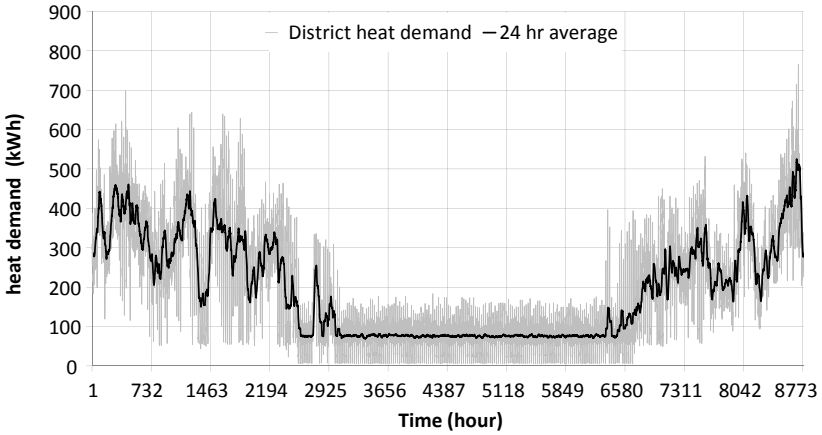

Figure 3.4 – aggregated district heating demand D_h

minimum of the cosine function (peak day of the holiday season with the least domestic hot water demand) is shifted forward from the first of July.
The domestic hot water demand profile is then added to the space heating demand profile which results in an aggregated heating demand profile D_h for the district. The total profile is shown in Figure 3.4. The district cooling demand profile D_c is shown in Figure 3.5.

Note that the developed method to generate an aggregated hot water consumption profile with a set of Gaussian probability functions has a wider range of application:

1. Generate realistic, individual household hot water consumption profiles. The

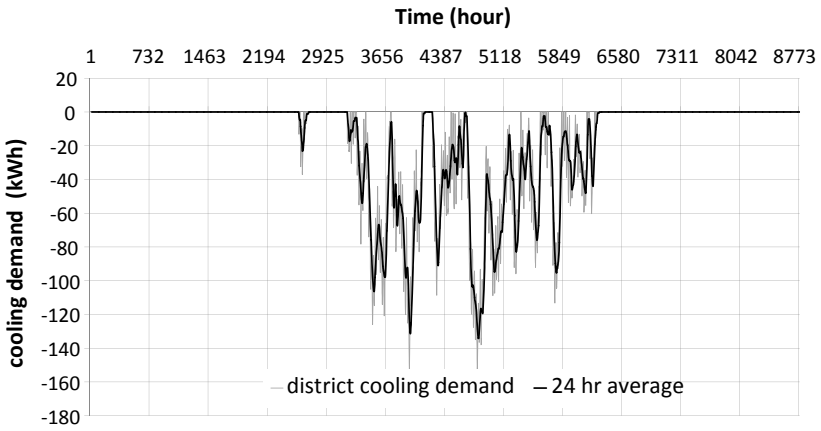

Figure 3.5 – aggregated district cooling demand D_c

values for parameters μ_j, σ_j and f_j may vary between households, or may be related to the day of the week. The values may also be slightly randomized to generate different daily profiles per household for each day. By redefining the discrete time variable i, profiles can be calculated with an hourly time scale, but also with a different time scale, e.g. 15 minutes.

2. Generate household and aggregated district electrical demand profiles. We notice from profile studies that such patterns have a similar shape as domestic hot water patterns. However, in this thesis we use a method which is verified with real data (see Section 3.4).
3. Generate household and aggregated district space heating demand profiles. Such profiles also have a similar shape. In that case, the parameters μ_j, σ_j are dominated by behavioral aspects, i.e. the time when heating is required. Parameter f_j is dominated by heat loss, i.e. the temperature difference between the interior and the ambient, but is also influenced by solar gains. It is possible that suitable functions which express these relations can be found, but this is part of future work.

3.4 Dynamic household electrical energy demand profile

To generate realistic data for the electric demand of households, a simulation method is used. For this we use an open source profile generator tool validated with real data of a group of Dutch households (see [74]). Within the tool, the following is chosen according to the population composition of the Meppel district:

- Power consumption of household electrical appliances such as: water kettle, washing machine, dishwasher, microwave, induction cooking, fridge, vacuum cleaner, etc.
- Occupancy related settings.

- Number of household types (estimated from project information): 18 single worker, 18 single retired, 20 dual worker, 20 dual with single worker, 20 dual retired, 36 family with dual worker, 68 family with single worker.

The profile generator outputs the hourly electricity consumption of each household excluding time shiftable devices such as a washing machine and dishwasher. For these appliances, a standard device profile is given as output next to starting times based on a random distribution. To include this consumption into the total electricity demand profile of all the households, a distribution function for the starting times is first determined. Then a total consumption profile for all the time shiftable devices is added to the total electricity demand profile. For the first week of the year, the resulting aggregated electricity profile of the Meppel district D_e is shown in Figure 3.6.
The average yearly consumption per household is 2882 kWh. This is similar to the present country average for two person households. The profile shape shows similar peaks as the standard network profile shown in [116].

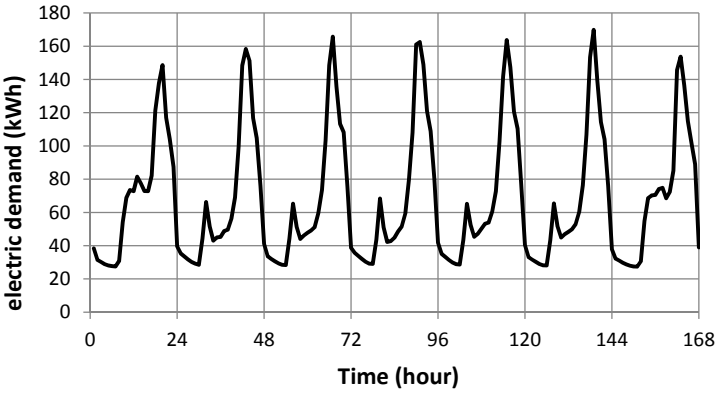

Figure 3.6 – aggregated household electric energy demand D_e

3.5 Conclusions

To generate dynamic demand profiles for space heating and cooling, a method for single household demand and for aggregated demand of a district is developed based on simulations with a thermal network model of a house, given in Chapter 2, and by applying randomization. For domestic hot water consumption, a suitable approximation method is developed using a set of Gaussian distribution functions which can be used to generate individual household profiles or aggregated profiles for a district. This method can also be used to generate household electrical demand profiles, but for this, a different method from literature is adopted. With these methods, aggregated demand data for the cases discussed in Chapters 5 and

6 can be generated. As future work, the method shown in this chapter should be validated with measured data from district heating systems in order to determine adequate calibration factors. Also, for the purpose of proper thermal demand profiling, it is interesting to compare the average interior temperature during the heating season of modern, well insulated houses with the average interior temperatures of less insulated houses.

parameter	unit	value	signification
R_{za}	K/kW	47.0	thermal resistance of insulated walls
$R^{"}_{za}$	m^2K/kW	5000	area specific thermal resistance
R_{win}	K/kW	47.5	thermal resistance of windows
α	-	0.7	brick wall solar absorptance
$U^{"}_{wall}$	kW/m^2K	0.005	exterior wall surface heat transfer coefficient
C_z	kWh/K	10.51	capacitance of the zone
A_w	m^2	12.5	effective window area on South side of the building
ρ_{air}	kg/m^3	1.25	air specific density
$c_{p,air}$	kJ/kg.K	1.005	air specific heat
variable	unit	type	signification
T_z	° C	calculated	interior (zone) thermal mass temperature
T_a	° C	input	outdoor (ambient) temperature
T_{sa}	° C	calculated	sol-air temperature of the building exterior wall surface
q_s	kW	input	solar energy on building planes with windows
$q_{h,c}$	kW	calculated	space heating or cooling demand
q_{int}	kW	input	thermal gains by occupants and appliances
q_{vent}	kW	calculated	heat loss by ventilation air flow
ϕ_v	m^3/s	input	ventilation air flow

Table 3.1 – model parameters and variables

Chapter 4

Models for energy storage with validations

Abstract - In this chapter, a generalized modeling approach for charging and discharging a thermal or electrical energy storage is developed. For both types of storage, results of validation experiments and a case application are discussed. Last, the possibility of thermal storage in the building structure and its suitability for smart control is investigated. The chapter ends with conclusions and future work.

4.1 Introduction

This chapter has the goal to develop predictive models for thermal and electrical energy storage. Like the building model, storage models are used as part of model predictive control during the first step (planning) within the Triana smart grid control method. To control the charging and discharging of a storage, algorithms used for smart energy control need actual information on the state of charge of the storage in order to predict the amount of charging or discharging which is possible in the near future.
As most smart control algorithms have to be executed on embedded systems and use either control heuristics or linear programming based approaches, also the predictive model should be simple but still sufficiently accurate. Describing charging and discharging processes for thermal storage systems is rather complex. Therefore the goal of this chapter is to develop and validate a relatively simple but sufficiently accurate model for storage, charging and discharging of a domestic hot water storage. Furthermore, application of the model for both a thermal and electrical storage is investigated.
Houses with a heat pump often have a domestic hot water storage facility. Additional storage capacity for space heating can be provided by the inert concrete

[†]Major parts of this chapter have been published in [RvL:9], [RvL:4] and [RvL:3].

floor heating system, which we will name Floor Heating Thermal Energy Storage (FHTES) throughout the chapter. The application and economics of such a storage system within the control of an electrical smart grid is investigated in [168] and [122] which demonstrates that investments for strengthening the electricity grid can be avoided by applying FHTES for demand side control. However, FHTES has immediate effects on thermal comfort of residents and also on energy loss of the building and therefore costs for the residents, which are not yet investigated.

4.2 Related work

In this section, related work for a thermal energy storage and electrical energy storage is investigated.

Thermal storage
The behavior of a thermal storage during standstill, charging and discharging is studied by numerous authors. One of most important aspects of a thermal storage is thermal stratification, as this leads to maximum exergy utilization [147]. An overview of research into thermal stratification is reported by [68], while [56] reports on the influence of heat loss on thermal stratification.
Predictive modeling for the temperature distribution within a thermal storage in relation to inlet and outlet flows is a well investigated area. This concerns mainly one-dimensional models, e.g. the lumped capacitance multi-node approximation [86] which is implemented in simulation software like TRNSYS. Good results are obtained by approximating the thermal storage with at least 15 nodes or uniform temperature layers. An even more detailed approach of temperature distribution and flow patterns within the storage is possible with a two-dimensional, finite volume model which includes natural and mixed convection boundary conditions [125]. The one and two-dimensional approaches are computationally expensive mainly because of the small time intervals, (e.g. seconds to minutes) required for simulation. For smart control of the storage and heat pump, such a detailed knowledge of the temperature distribution is not required. Also, time intervals used in smart control are in general much larger, e.g. 15 minutes to 1 hour. In [67] a lumped capacitance single node model of a thermal storage is used for model predictions as part of a smart control system. This model essentially describes energy content of the storage and is also introduced by others [91], [70]. This model is straightforward to apply for model predictions as part of smart control, however the relation between heat pump performance and lower temperatures within the bottom part of a thermally stratified storage is lost. Hence, prediction of electricity consumption in time, one of the most important goals of the predictions, is less accurate.
A grey-box model with a system identification method is proposed by [43]. The model is the same one-dimensional multi-node approximation discussed earlier but in this case, 5 nodes are proposed together with a parameter identification

method based on the Markov-chain Monte-Carlo method. Although the results of this method are reasonable, we foresee two problems in our applications: (1) such identification algorithms are difficult to apply within low cost embedded device controllers with limited available memory and computational power, (2) even with only 5 nodes, evaluation of the model prediction involves for accuracy reasons, time intervals in the order of minutes rather than 15 minutes to 1 hour.
An iterative model which approximates the storage into two layers, one hot layer at the top and one mixed layer with an average temperature below, is reported in [21]. This approach is promising and is partly the basis for the present chapter. Our model predicts without iterations both the storage state of charge and heat pump electric consumption of a future charging cycle in a one step calculation, based on available data of the inlet/outlet flows.

Electrical storage
Predictive models for electrical energy storage which describe the state of charge and relevant storage conditions (cell voltage) are investigated by numerous authors.
For electric batteries, various models are developed for different fields of interest. The ideal battery model assumes constant voltage during discharging and the capacity of the battery is not influenced by the discharge current. However, real batteries behave differently: voltage drops during discharging and the capacity is lower when higher loads are applied, which is called the rate capacity effect. For design purposes, electrochemical [115] and electric-circuit models [121] are used. Also, stochastic models, (e.g. Markov chain models [95]) are used for on-line probability evaluation of multiple battery states which is computationally intensive to combine in smart energy control algorithms that use mathematical optimization. Lastly, analytical models such as the Kinetic Battery model (KiBam) [102] and the diffusion model describe the rate capacity effect. Jongerden et al. [80] prove that the KiBam model is a first order approximation of the diffusion model and demonstrate with experimental data the accuracy of the KiBam model for energy critical embedded system applications.
The voltage drop during the discharging of batteries (see Figure 4.11) is in fact similar to the temperature drop during the discharging of a thermal storage (see Figure 4.5), where voltage is the equivalent of outlet temperature and current is the equivalent of outlet water flow rate. Van Leeuwen et al. [RvL:4] demonstrate the accuracy of a relatively simple model to predict actual state of charge, the electric power consumption profile and duration of a future charging cycle from a given state of charge for a thermal storage. It is interesting to investigate the application of the same model for electric storage.
The simple model is based on energy conservation. The rate capacity effect results in less energy discharged than was charged and occurs more pronounced when a battery is discharged with high loads. The principle of energy conservation is not violated as part of the energy is lost by production of heat. Van Leeuwen et al. [RvL:4] demonstrate that a similar effect also occurs in case of a thermal storage. In that case, the loss of useful energy output is not caused by heat production but

by mixing of hot and cold water. To account for this effect, a minimum state of charge related to the minimum useable outlet temperature can be defined which is rate dependent. For a thermal storage, a constant minimum state of charge is applicable for a practical range of discharging rates. In this chapter, the application of this principle on batteries is investigated.
The rate capacity effect also includes recovering the voltage state in case of varying loads or when the load is suddenly released. This mechanism is called KiBam effect in this chapter and is equivalent to recovery of the temperature stratification in a thermal storage which is seen when the storage is discharged with very high flow rates and the discharging is suddenly stopped at a certain state of charge. The recovery mechanism of an electric battery can be interpreted as a form of energy conservation. The capacity of the battery is partly recovered to what would be expected from the simple energy conservation relation.

Storage in the building structure
Thermal storage within the building structure is investigated in the last part of this chapter. This type of storage is part of power to heat integrating for which heat pumps are used. Heat pumps are increasingly applied in the Netherlands to heat houses and utility buildings such as hospitals, offices and malls. A heat pump requires a low temperature heat source for which ambient air, underground water aquifers or underground vertical heat exchanger poles are used [36]. An example of a Dutch housing project with heat pumps is given in [182].
Demand Side Flexibility (DSF) offered by Heating, Ventilation, Cooling and Air Condition (HVAC) systems is investigated with practical measurements in an office building for spring and summer periods in [3]. Although an office in theory offers more possibilities for DSF strategies than a house due to a larger structure and an often larger cooling load which approximately coincides with solar PV generation, the paper demonstrates that air based cooling and air conditioning systems offer only a limited energy storage capability in relation to thermal comfort limits.
Floor Heating Thermal Energy Storage (FHTES) is investigated also in relation to cooling offices by lowering floor temperatures during night hours (see [57], [93], [133], [144] and [149]). Another purpose that is investigated is to lower the peak heating power for residential buildings [11]. More close to the present application is a study on measured performance of heating and cooling systems using FHTES in apartments [15].
Besides effects on thermal comfort, FHTES also influences energy loss of the building and therefore energy costs paid by the residents. In [151] the ecocost approach was applied to investigate a novel house heating/cooling system with individual room temperature control for the Meppel project. In [164] the contribution of a control strategy for power balancing and FHTES is investigated. Thermal tolerance is introduced as a measure for effects on thermal comfort due to FHTES. In [176] optimal heat pump control in case of floor heating in relation with varying electricity prices is investigated. Thermal tolerance is introduced as a measure for effects of thermal discomfort. Instead of using thermal tolerance, the approach proposed in

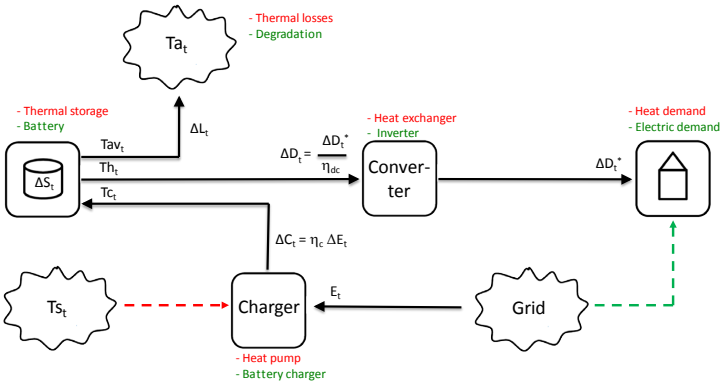

Figure 4.1 – Schematic representation of the energy charging and discharging model. Thermal storage processes are indicated in red, electric storage processes in green.

this chapter is to develop measures from governing standards on thermal comfort, as outlined in Section 4.7.
Most of the mathematical work within the cited papers is applicable for general use. However, effects on thermal comfort, energy loss and energy costs are not investigated yet in a way corresponding with thermal comfort standards. Therefore this chapter investigates how thermal comfort is influenced by Floor Heating and from this, constraints and guidelines are deduced for control algorithms.

4.3 Model for water tank thermal storage

4.3.1 General storage characteristics

A general energy flow representation of energy storage is shown for a thermal storage (red) and electric battery (green) in Figure 4.1. In case of a thermal storage, the charger may be an electric heat pump which uses electric energy (E_t) to transform thermal energy from a low temperature source (T_s) to a higher temperature (T_c). From the storage, water with a high temperature (T_h) is directly supplied to the demand, while cold water (T_c) enters the storage. The storage looses a small energy fraction (L_t) due to the temperature difference between the average storage temperature (T_{av}) and ambient temperature (T_a). Pipe losses cause a minor difference between thermal energy supplied by the storage (D_t) and the real demand (D_t^*).
The size of an electric battery is typically 2-10 kWh. As indicated in Figure 4.1 the battery charger transforms alternating current electric energy (E_t) into direct current energy (C_t). During charging, measured voltage and current signals are sent to the smart controller. For discharging, the inverter transforms direct current energy (D_t) from the storage into alternating current energy towards the demand (D_t^*). Output power of the inverter is controlled by the smart controller. The de-

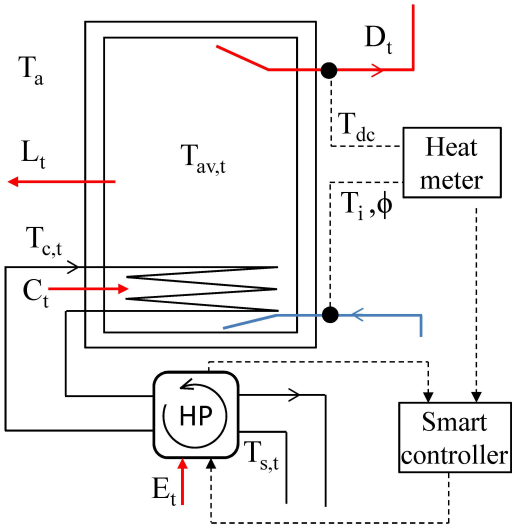

Figure 4.2 – schematic picture of the thermal storage

mand can be supplied by the battery, but also by the grid, depending on loads and energy prices which is a decision made by the smart controller. Efficiencies of the charger and inverter are signified as η_c and η_{dc}, respectively. A small fraction of the stored energy is lost (L_t) by transformation into heat and the capacity of the battery decreases in time due to degradation (aging).

A common storage configuration for domestic hot water supply is shown in Figure 4.2. Cold water flows in at the bottom, hot water is drawn from the top of the storage. A heat pump or solar collector generates heat which is transferred by a coil heat exchanger within the bottom region of the storage tank.

The size of a thermal storage is typically 200 liters, which is sufficient for daily hot water consumption of households up to 5 persons. The storage may not be the only hot water system within a house. Hot water for kitchen use, e.g. to wash dishes, may be supplied by a separate 10-15 liters electric hot water storage. The model derived in this section may also be applicable for this type of storage. It is interesting to incorporate a thermal storage in a smart energy control system due to the relatively high power demand, i.e. typically 2500 W for charging periods ranging from 30 minutes (small storages) to 2 hours (large storages). Figure 4.2 also shows the connection of the storage to a heat meter and smart controller. The heat meter determines the supplied energy and volume of hot water. The smart controller determines the actual state of charge and decides when to start the heat pump (HP) for charging, based on optimization objectives. We discuss this topic further in Section 4.6.

The thermal storage supplies the daily demand for domestic hot water for a single household. The demand pattern can be learned over time, e.g. specified as hot

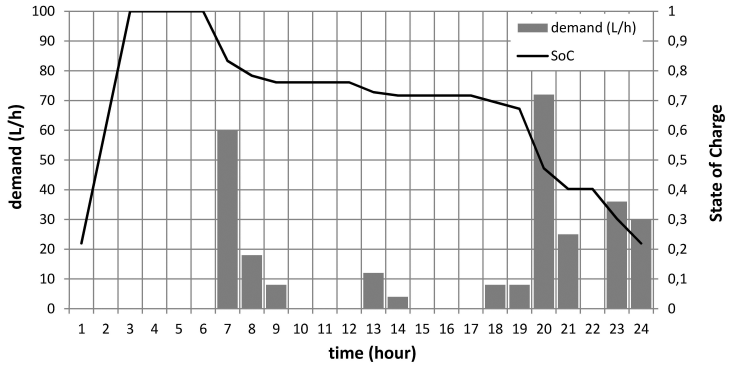

Figure 4.3 – typical daily hot water demand pattern of a household

water usage per time interval. For a single house, the uncertainty on the demand pattern is large if it is evaluated for small time intervals, but the uncertainty is smaller if demand is evaluated for larger time intervals, e.g. as total demand per hour. Figure 4.3 shows a typical daily demand pattern of a 4 person household with an annual domestic hot water energy demand of 9 GJ/y.

The demand pattern is given in liters/hour of $40°C$. The thermal storage has a size of 200 liters and is charged to $60°C$. The State of Charge (SoC) of the storage which is explained in Section 4.3.3 is charged to 100% early in the night and drops to nearly 21% at the end of the day due to the discharge of hot water. The daily SoC pattern shows that for the evaluation of the SoC, a resolution of one hour for the demand prediction is sufficient in this case.

Another aspect to take into account is the comfort of domestic hot water supply. Measures for comfort are the water temperature and the availability in time of warm water. People's expectations of comfort may vary throughout the day. For the control system, information about warm water demand and expected comfort is important in order to decide which amount of water of a certain temperature should be at least available within the thermal storage at certain moments during the day. The predictive model for charging and discharging the storage should be able to provide this information.

A similar approach but different demand pattern may apply for domestic electric energy storage in batteries. Lead acid (Pb-acid) batteries are most commonly used for stationary, domestic storage. Other types, i.e. lithium ion (Li-ion), Nickel-Cadmium (Ni-Cd) or Nickel-Metal hydride (Ni-Mh) are also used but are better suitable for non-stationary applications, e.g. electric vehicles and personal electronic devices. Model predictions and experimental data in this thesis are limited to Pb-acid battery types.

4.3.2 General model formulation

A general and widely applicable model for the energy supply from a thermal storage or electric battery is based on energy conservation which states:

$$\Delta S_t = C_t - D_t - L_t \,, \tag{4.1}$$

in which the term ΔS_t signifies the change of stored energy, C_t the charged energy, D_t the demand and L_t the energy loss, all within a time interval Δt, which is the interval $(t-1, t)$. In the following, the terms in Equation (4.1) are discussed.

4.3.3 Discharging experiments and model formulation

If the storage (see Figure 4.2) is ideally stratified, the entire volume of hot water with a uniform temperature moves upwards, perfectly separated from a growing volume of cold water from the bottom. However, the incoming cold water flow induces some mixing of cold and hot water. The result is that less water with a high temperature can be drawn from the tank than in the perfect stratified case. Lab experiments are carried out to investigate this behavior. The experiments involve charging and discharging cycles for two commercially available, combined heat pump and thermal storage units. One is a 200 liter combination with a ground water source heat pump from Alpha-Innotec, (see Figure 4.4). The other is a 50 liter combination with an air source heat pump from Inventum which is used to verify the experienced phenomena.

To investigate the stratification, we carried out a test where we withdraw hot water at specified constant flow rates, without heating up the storage. For three different flow rates, the results (discharge temperature (T_{dc})) are given in Figure 4.5. In case of perfect stratification, the entire volume of the storage should flow from the outlet with the high temperature and then drop instantaneous to the low temperature. If so, the storage should supply hot water with a constant high temperature for 2400, 1200 and 800 seconds for the respective flow rates of 5, 10 and 15 l/min, which is determined by dividing the storage volume with the flow rate in liters/sec. However, Figure 4.5 shows that already at 2150, 1050 and 650 seconds, the outlet water temperature has dropped below the minimum use temperature of 40 °C, which demonstrates the effects of mixing of cold and hot water within the thermal storage during discharging.

The purpose of a model for the storage is to determine:

- the present SoC of the thermal storage,
- the amount of useful energy ($T \geq 40°C$) that the storage is still able to supply.

Assuming that energy supply from the storage equals energy demand, the supplied energy D_t in time interval Δt is calculated with Equation 4.2.

$$D_t = \Delta t \cdot \phi_t \cdot \rho \cdot c_p \cdot (T_{dc,t} - T_{i,t}) \,, \tag{4.2}$$

in which ϕ_t is the water flow, ρ is the water density, c_p is the water specific heat, $T_{dc,t}$ is the outlet temperature and $T_{i,t}$ is the inlet temperature. In this chapter, ρ

Figure 4.4 – Alpha-Innotec heat pump storage combination used for testing

and c_p are assumed constant although they vary slightly with temperature. When a heat meter is connected to the thermal storage, the outlet and inlet temperature and the flow are registered. This data is used to learn the demand over time. The heat meter calculates the supplied energy by applying Equation (4.2). A smart grid algorithm may use this information to determine the actual SoC of the thermal storage, which is calculated by:

$$SoC_t = \frac{S_t}{S_{max}}, 0 \leq SoC_t \leq 1. \tag{4.3}$$

The stored energy S_t and the maximum charged energy are determined by:

$$S_t = S_{t-1} + \Delta S_t \tag{4.4}$$

$$S_{max} = V \cdot \rho \cdot c_p \cdot (T_{max} - T_i), \tag{4.5}$$

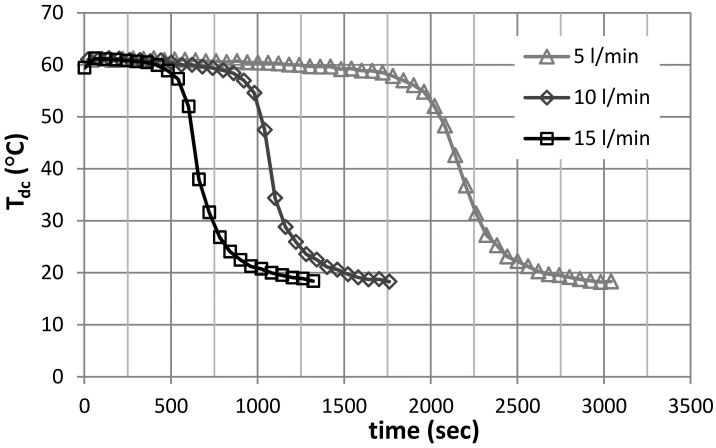

Figure 4.5 – Outlet water temperature at constant flow rates. (Relative accuracy Flow (2%), Absolute accuracy Temperature $\pm 0.2^o$C)

in which V is the water volume in the storage, T_{max} is the maximum, uniform temperature of the storage, which is determined by the storage thermostat settings. T_i is the inlet cold water temperature which is assumed to be constant. In practice, a certain volume of the inlet cold water may warm up to room temperature conditions due to stand-still heat transfer in the inlet pipes. Furthermore, the cold water temperature also varies with the seasons.
The amount of useful energy that can be supplied by the storage is determined by a minimum SoC value. In Figure 4.6 the minimum SoC is determined from the intersection with a supply temperature of $40°C$.

In Figure 4.7, the minimum SoC of this system is shown as a function of flow rate. Assuming negligible mixing effects (which is equivalent with a minimum SoC of zero) for a flow rate close to zero, the minimum SoC appears to increase approximately linear with the flow rate. In practice, flow rates are not constant but may vary per draw between 5 and 15 l/min. It is convenient to use a single value for the minimum SoC, e.g. the worst case which is around 0.18. Together with the calculation of the stored energy from Equation (4.4), the minimum SoC value determines the amount of useful energy that the storage is still able to supply.

4.3.4 Charging experiments and model formulation

During charging, heat is transferred from the coil at the bottom of the storage to the water in the storage by the principle of natural convection. In a fully discharged state, the entire water volume in the storage is cold and during charging the temperature increases gradually. The heat pump efficiency decreases with increasing water temperature during the charging process. The heat pump's refrigerant flows through the coil heat exchanger where it condensates at constant

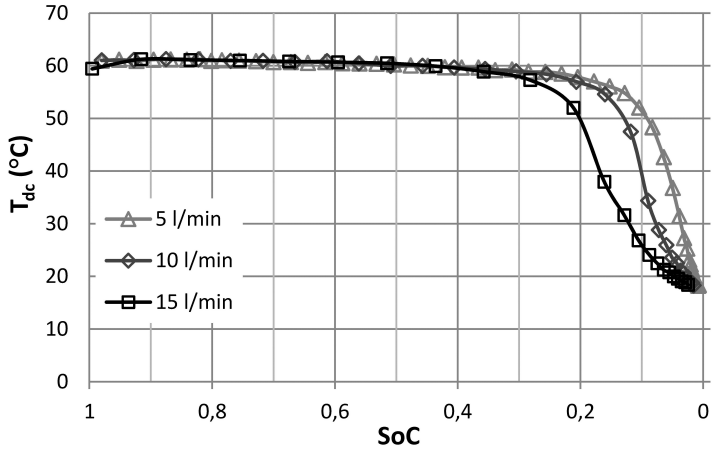

Figure 4.6 – relation between storage State of Charge and discharge temperature

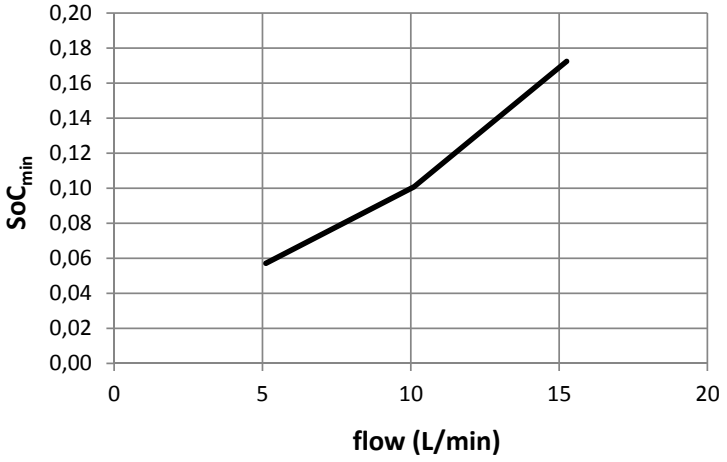

Figure 4.7 – minimum State of Charge as a function of constant flow rate

temperature. The coil is usually made of thin-walled copper, aluminum or stainless steel with an approximately negligible conduction resistance.
Based on supplier heat pump characteristics [13] and validation measurements, the amount of charged energy by the heat pump C_t is approximately linear with the source temperature $T_{s,t}$. The electric energy E_t used by the heat pump during Δt is approximately linear with the condenser temperature $T_{c,t}$, Equation (4.6).

$$\begin{aligned} C_t &= a \cdot T_{s,t} + b \\ E_t &= c \cdot T_{c,t} + d \,, \end{aligned} \tag{4.6}$$

in which a, b, c, d are constants which are determined from supplier data. For the 200 liter installation, these constants are given in Table 4.1. It is common practice for domestic heat pumps to measure the condenser and source temperature for safety reasons. Hence, a smart control system should be connected to the heat pump to obtain this data. The source temperature may vary in time but this depends on the heat source, e.g. ambient air varies much more than ground water.

Neglecting the coil conductive resistance, the coil temperature approximately

Parameter	Value	Unit
a	0.172	kW/K
b	-42.2	kW
c	0.04	kW/K
d	-10.2	kW
$h \cdot A$	1.191	kW/K

Table 4.1 – heat pump and coil model parameters

equals the condenser temperature. The heat transfer from the coil to the surrounding water in the storage is given by:

$$C_t = h \cdot A \cdot (T_{c,t} - T_{w,t}), \tag{4.7}$$

in which h is the coil heat transfer coefficient, A the coil outside area and $T_{w,t}$ the surrounding water temperature within the storage. The product $h \cdot A$ is approximately constant for a complete charging cycle, can be obtained from supplier data and is given in Table 4.1. When the surrounding water temperature is known, combining Equations (4.6) and (4.7) yields the condenser temperature $T_{c,t}$ which determines the electric energy consumption by the heat pump E_t. It remains to find a suitable prediction of the water temperature within the thermal storage around the coil. For this we introduce the simplification of the state of a thermal storage shown in Figure 4.8. According to the discharge temperatures shown in Figure 4.5, the water volume within the storage can be approximated with three zones: a hot zone at the top, a cold zone at the bottom and a small transition zone between the hot and cold zone. We approximate the temperatures of each zone in Figure 4.5 with T_{max} for the hot zone, T_i (inlet temperature) for the cold zone and a linear distribution for the transition zone. Further, we simplify these zones with two layers: a hot layer with volume $V_{h,t}$ and temperature T_{max} and mixed layer with volume $V - V_{h,t}$ and average temperature $T_{w,t}$.

We assume that the storage is not discharged beyond the minimum SoC. In Figure 4.9 the decrease of the SoC in dependance of the total discharged volume from the storage is shown. It indicates a linear decrease down to the minimum SoC level. For the slope, we get:

$$\frac{\Delta SoC}{\Delta V} = \frac{1}{V}. \tag{4.8}$$

For a given SoC_t ($SoC_{min} \leq SoC_t \leq 1$), the volume of hot water $V_{h,t}$ at the top of the storage can be calculated by substituting for $\Delta SoC = SoC_t - SoC_{min}$ and for

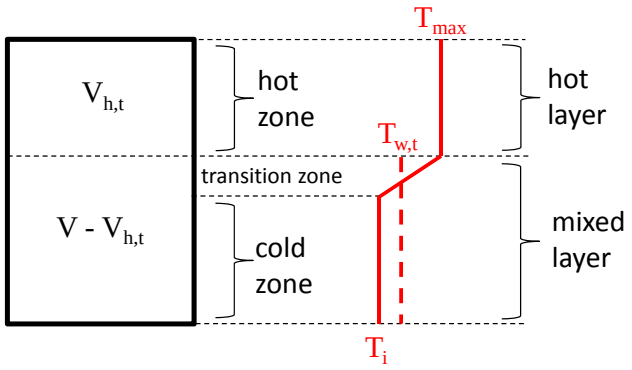

Figure 4.8 – simplified thermal storage representation

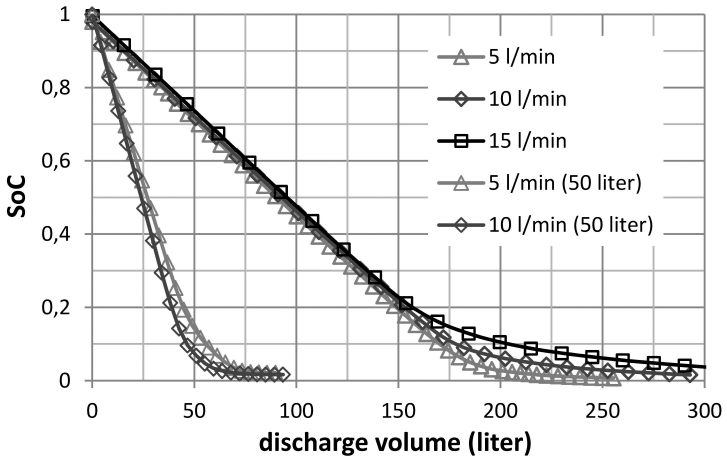

Figure 4.9 – State of Charge as a function of discharged volume

$\Delta V = V_{h,t}$ in Equation (4.8).

The average temperature $T_{w,t}$ of the mixed layer is calculated with the following equation for the stored energy S_t:

$$S_t = \rho \cdot c_p \cdot [V_{h,t} \cdot (T_{max} - T_i) + (V - V_{h,t}) \cdot (T_{w,t} - T_i)] \,. \tag{4.9}$$

Figure 4.10 shows the measured electric power used by the heat pump during charging from an empty to a full state of the storage. During charging, the water temperature is measured at two locations, at a quarter of the storage height and at the top. These temperatures also increase approximately linear and differ only a few degrees during charging, so we conclude that during charging from an empty state, the storage temperature is increased isothermal. Hence, the used electric power increases approximately linear with the water temperature

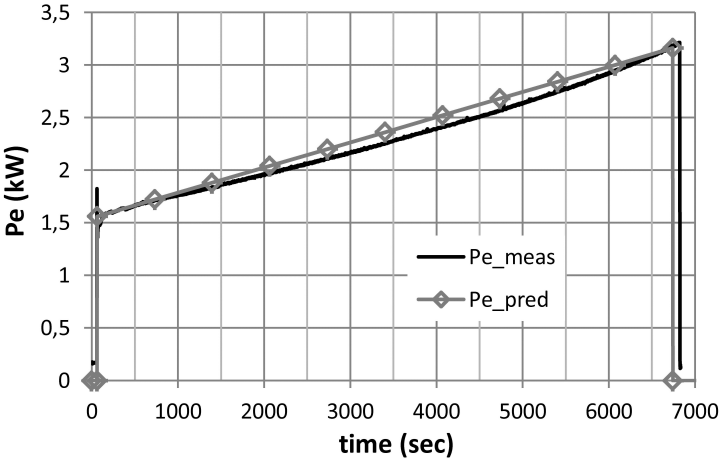

Figure 4.10 – Measured electric power during charging

within the storage. It follows that when the charging process starts from an arbitrary SoC state, the average water temperature of the water volume that needs a temperature increase determines the duration and the amount of electric energy.

The total required thermal charging energy needed if the buffer has to be fully charged starting at time interval t is calculated by:

$$C_{tot,t} = (1 - SoC_t) \cdot S_{max},\ for SoC_{min} \le SoC_t \le 1\,. \tag{4.10}$$

The duration of the charging process τ_t is calculated by:

$$\tau_t = \frac{C_{tot,t}}{C_t}\,, \tag{4.11}$$

in which ΔC_t is calculated with Equation (4.6). Note, that we assume here that C_t does not change over time. The electric power consumption P_{e,t^*} of a future charging cycle in which t^* is a time interval within the charging cycle, from a given SoC_t to fully charged conditions, is predicted as a linear function in time and given by Equation (4.12). This function starts at a value P_{e,t_i^*} and ends with $P_{e,t_i^*+\tau}$. These values are calculated with E_t, from Equation (4.6). Note, that t_i^* is some time in the future when charging is initiated, which is a control variable for the smart control system.

$$P_{e,t^*} = P_{e,t_i^*} + \frac{P_{e,t_i^*+\tau} - P_{e,t_i^*}}{\tau} \cdot t^* \qquad 0 \le t^* \le \tau \tag{4.12}$$

The total electric energy consumption of the future charging cycle is calculated by:

$$E_{tot,\tau} = \frac{\tau}{2} \cdot (P_{e,t_i^*} + P_{e,t_i^*+\tau})\,. \tag{4.13}$$

Using the parameters given in Table 4.1 the values shown in Table 4.2 are calculated for the charging cycle of Figure 4.10. In this figure, the resulting prediction profile is also shown for comparison and this demonstrates the excellent accuracy of the approach.

Result	Measured	Predicted	Unit
τ	6763	6677	sec
P_{e,t_i^*}	1.45	1.56	kW
$P_{e,t_i^*+\tau}$	3.21	3.16	kW
$E_{tot,\tau}$	15564	15759	kJ

Table 4.2 – Comparison between prediction and measurements of electric energy consumption

4.3.5 Energy loss from the thermal storage

When the storage is charged and discharged daily, energy losses from the storage to the surrounding air are insignificant due to good insulation of modern thermal storage tanks. However, when the storage is not discharged for many days and placed in a relatively cold environment, losses may be more significant. The heat loss ΔL_t is calculated by the general heat transfer relation:

$$\Delta L_t = UA \cdot (T_{av,t} - T_{a,t}) \,, \tag{4.14}$$

in which UA is the storage heat loss coefficient, $T_{av,t}$ the average storage temperature and $T_{a,t}$ the ambient air temperature which may be assumed constant in time, depending on the situation. Assuming constant water density and specific heat, $T_{av,t}$ is calculated by:

$$T_{av,t} = \frac{V_{h,t} \cdot T_{max} + (V - V_{h,t}) \cdot T_{w,t}}{V} \,. \tag{4.15}$$

4.3.6 Summary of prediction model

Summarizing, the model prediction involves the following calculation order:

1. Initialize the charged energy S_{t-1} from the previous time interval.
2. Calculate the hot layer volume $V_{h,t}$ with Equation (4.8) (substitute as explained underneath the equation).
3. Calculate the mixed layer water temperature $T_{w,t}$ with Equation (4.9).
4. Calculate (when applicable) the charging energy C_t with the first equation of (4.6) and then the condensing temperature $T_{c,t}$ with Equation (4.7).
5. Calculate (when applicable) the electrical energy consumption of the heat pump E_t with the second equation of (4.6).

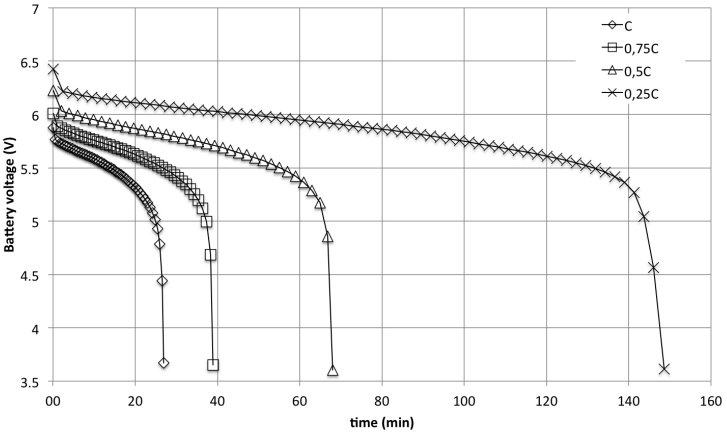

Figure 4.11 – Battery voltage during constant current discharge.

6. Calculate the charged energy for the present time interval S_t with Equations (4.1) and (4.4), in which the demand D_t (when applicable) is calculated with Equation (4.2).
7. Calculate duration τ of future charging cycle with Equation (4.11)
8. Calculate the minimum and maximum electric power of a future charging cycle P_{e,t_i^*} and $P_{e,t_i^*+\tau}$ with Equation (4.6)
9. Calculate the total electric energy consumption during a future charging cycle E_{tot} with Equation (4.13).

4.4 Application of the model to electrical energy storage

As introduced in Section 4.3.1, the model can be applied for thermal storage but also for electrical storage. To demonstrate the similarity between temperature (thermal storage) and voltage (electrical storage), heat flow and electric current, Figure 4.11 shows the discharge voltage of a 4Ah capacity, lead acid battery in time for various constant currents. Hereby C is the battery capacity in Ah divided by the discharge current in A, so C refers to a discharge current of 4A.
In [RvL:3] the model for thermal storage is reformulated for electric battery storage and validated with measurements. An extension of the model to include the rate capacity and capacity restoration effects experienced in batteries is developed in [73]. Further validations of this model are part of future work.

4.5 Validation experiments

This Section discusses Validation of the model for thermal storage. Validation of a similar model for electrical energy storage (without the extension mentioned in Section 4.4) is reported in [RvL:3].

Validation of the thermal model is performed by discharging the storage with constant flow ϕ starting at SoC=1 to a certain end value of the state of charge, SoC_{end}, followed by charging to SoC=1. The used values for ϕ and SoC_{end} are given in Table 4.3.

During discharging, flow and temperature are measured of the inlet and outlet

Experiment	ϕ (l/min)	SoC_{end}
1	5	0.6
2	10	0.6
3	15	0.6
4	10	0.4
5	10	0.2

Table 4.3 – Validation experiment settings

water. During charging, the electric energy consumption is measured. The validation compares predictions (see Section 4.3.6) of the model for the duration τ, the minimum and maximum electric power P_{e,t_i^*} and $P_{e,t_i^*+\tau}$ and the total electric energy consumption E_{tot} (which characterize the future charging cycle) with the measured charging cycle.

4.5.1 Results and discussion

The validation results are shown in Table 4.6 (last page of this chapter). The measured duration τ_{meas}, measured minimum and maximum electric power consumption P_{e,t_i^*} and $P_{e,t_i^*+\tau}$ and measured total electric energy consumption $E_{tot,meas}$ are listed for each experiment. The error of the predictions is given as a percentage of the measured values. For the predictions, the average water temperature of the cold and mixed water layer $T_{w,pred}$ calculated from Equation (4.9) is shown, from which the electric power at the start of the charging cycle is predicted.

For a future charging cycle, accurate prediction of the total electric consumption and duration are the most important aspects for smart energy control purposes. Table 4.6 indicates an excellent prediction accuracy of the total electric consumption, as in most cases the percentage error is smaller than 1%. Although the prediction of duration seems less accurate in some cases, the maximum error of 9.1% is only a difference of 4.5 minutes. Smart energy control algorithms usually evaluate predictions in time intervals of 15 minutes, hence this maximum error is acceptable.

For the prediction of the energy consumption profile, the maximum error (8.7%) is 280 W, which appears at the end of the charging cycle. This error is mainly due to differences in the same order of magnitude between supplier data of electric power consumption which is used for the model and actual measurements of electric power consumption. We verified that if the constants c,d in Equation 4.6 are based partly on supplier data and partly on the measured power consumption at the end of charging, the prediction profile is more accurate. This information could

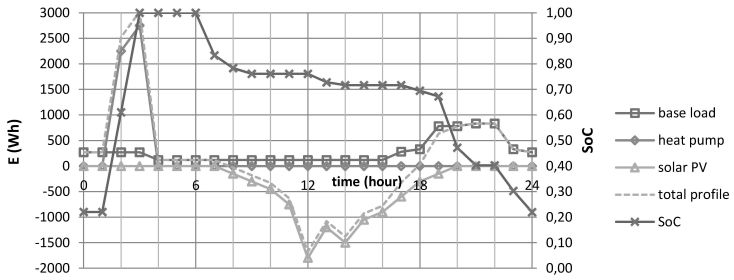

Figure 4.12 – Reference electricity consumption and solar PV generation profile

be made available to the control system by a connected smart electricity meter. It also has to be taken into account that the errors are in the same order of magnitude as the propagated measurement errors of the used sensors. Therefore we conclude that the predictive model is very well capable to accurately predict the duration, the power consumption and the power consumption profile for future charging cycles of the thermal storage.

4.6 Case application

In this section, an application of the model developed in the previous sections for thermal and electrical storage is investigated. The used case focuses on increasing the self consumption of domestic solar PV electricity. Figure 4.12 shows a reference profile of a day in the spring season. The figure shows the electric power consumption and solar PV generation without smart control for a four person household. The yearly sum of daily base loads totals 2600 kWh/y and includes electricity consumption of lights, dishwasher, washing machine, washing dryer, television, computer and small electronic devices. The base load is considered non-flexible in this case. The heat pump which charges the thermal storage is a flexible device which can be controlled by a smart controller (see also Figure 4.2. The profiles show that solar PV energy generation during the day is mostly exported to the grid, as the occupants are mostly out of the house during the day and come home around 17.00 hours. Financially, this may be unfavorable, depending on the feed-in tariff. Besides the mentioned energy flows, the charging energy of the heat pump and the SoC of the thermal storage are shown. The total profile illustrates the load on the power grid, ranging from a feed-in peak of -1380 Wh during the day to a demand peak of 3020 Wh during the night, mainly due to the heat pump consumption for charging the thermal storage.

We extend the given scenario with an electric battery which is able to charge when there is a surplus of electricity generation and to discharge when there is insufficient generation. We call this "variant 1" and the results are given in Figure

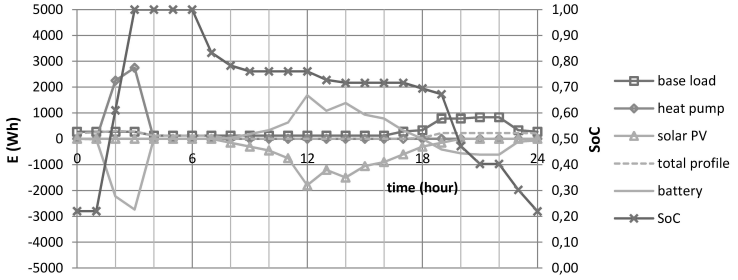

Figure 4.13 – Variant 1: electricity profile with optimized electric battery storage

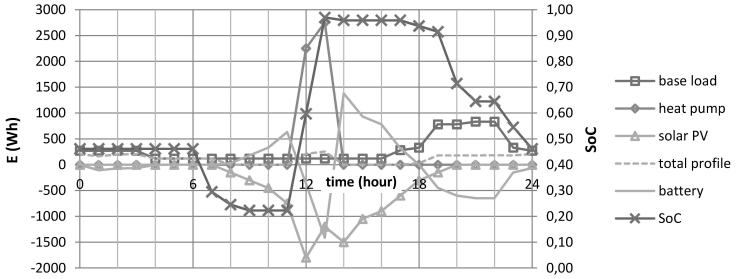

Figure 4.14 – Variant 2: electricity profile with optimized heat pump control and electric battery storage

4.13. The hourly amounts of charged and discharged energy are determined by an optimization algorithm which minimizes peaks of the total profile with charging and discharging of the battery as control variables. The objective also contains a penalty on battery size. The required battery capacity for this profile is calculated at 7.34 kWh. Using the battery reduces the electricity consumption peak to 293 Wh during the night.

The latter scenario is extended to include smart control of the heat pump. We call this "variant 2" and the results are given in Figure 4.14. The control algorithm minimizes the peak of the total profile and does this in a way that a minimal capacity of the battery is used. The thermal storage and heat pump charging model developed in this chapter are included in the control algorithm to predict SoC and electricity consumption of the heat pump. As result, the required battery capacity is decreased to 4.58 kWh and the electricity consumption peak is now 256 Wh which occurs during daytime hours.
The results of variant 2 show several positive effects:

- Decreased battery capacity resulting into significant lower investments compared to variant 1.
- Lower electricity peak values compared to variant 1.

- Shift of electricity shortage towards daytime hours, allowing e.g. more local consumption of other renewable energy generated in the district.

The main purpose of the case study is to show the significance of a model for prediction of energy for charging the thermal storage. A more elaborate case study involving different households, more days throughout the year and comparisons with conventional storage control is required to get thorough insights in the effects of smart control. Also, there may be undesired side effects such as shortened life cycle of the battery due to the applied "greedy" algorithm for charging and discharging the battery. More elegant methods for optimal control of battery charging and discharging are for instance reported in [183] and [81].

4.7 Thermal storage in the building structure

When a house is equipped with a heat pump for heating, some storage capacity also can be provided by the structure of the house itself, i.e. within the concrete floor heating system. However, this has effects on thermal comfort and could result in more energy losses. Therefore, in this section we consider the questions: what are the effects on thermal comfort if energy is stored in the floor heating system, what are the energy losses and what are the related financial consequences? Section 4.7.1 describes the theoretical background of a model used for this analysis. Section 4.8 describes a case study, followed by the results and a discussion.

4.7.1 Theoretical background

As shown in Chapter 2, the thermal network approach can be used as a convenient way to model the dynamic heating or cooling demand of buildings. However, the intended use for the models in Chapter 2 is to generate demand profiles and to control appliances. To study the influence of floor heating thermal storage, the internal part of the model should be extended to include thermal comfort parameters. Therefore we first discuss theory on thermal comfort in order to develop a suitable model.

Theory on thermal comfort

A well known model to evaluate thermal comfort is the model developed by Fanger [76] and [19]. Thermal comfort is evaluated by means of the PMV (Predicted Mean Vote) and PPD (Percentage of People Dissatisfied). PMV calculations involve determination of the operative temperature, clo-factor (signifying the clothing worn by people in a room), met-factor (signifying activity level of people in a room), moisture level and air speed. The PMV is expressed in values between -3 and +3 in which 0 is neutral, negative means too cold, positive means too warm. Within the PMV calculation, the operative temperature is the only objective parameter which can be determined by calculations. In the evaluation following, the operational temperature is also the only value that is influenced by the control methods. The

other parameters of the PMV calculation are assumed to be not influenced. The operative temperature evaluates the influence of radiation from surfaces and air temperature. For relatively low air velocities applicable for home situations, the operative temperature of a zone is calculated by (see [19]):

$$T_{op} = \frac{T_{air} + T_{rad}}{2}, \tag{4.16}$$

in which T_{air} is the zone air temperature and T_{rad} is the mean radiation temperature of the interior surfaces surrounding a person. It is impractical to calculate T_{rad} for each person as this also depends on the place where the person is situated in a room. Hence an average for a zone is proposed in [18]:

$$T_{rad}^4 \cdot \sum_{i=1}^{6} A_i = \sum_{i=1}^{6} \left[A_i \cdot T_i^4 \right]. \tag{4.17}$$

In this equation, the living room zone contains six surface areas A_i, each with a surface temperature T_i. Guidelines for the operative temperatures including adaptivity to outdoor temperatures are defined as (see [76]):

- If $T_a < 15^oC$ then $20^oC < T_{op} < 24^oC$
- If $T_a > 15^oC$ then $22^oC < T_{op} < 26^oC$.

A heated or cooled floor has an effect on the mean radiant temperature and therefore on the operative temperature. However, according to [76], a warm or cold floor also directly influences the thermal comfort of people. Limits on the floor temperature T_f can be calculated from the PPD (Percentage People Dissatisfied) equation shown in [76] which yields the following requirement: $19,2^oC < T_f < 28^oC$.
According to [76], there is also a constraint on the time gradient of the operative temperature. Periodic variations should be limited to 1^oC which is combined with a maximum rate of change of less than 2^oC/hour.
Limits on radiant temperature asymmetry (surface temperature differences) pointed out in [76] are quite large and are therefore assumed to be irrelevant for floor heating systems.
For domestic applications, the following is noted:

1. ISO standard 7730 [76] is developed and validated mainly for people working in offices and schools. People may evaluate thermal comfort different in a home situation, as people are more at rest while being at home. Besides that, older aged people tend to appreciate higher operative temperatures than younger people. This is one of the causes for differences in energy demand between households.
2. The minimum allowable floor temperature may not be reached during the heating season, as the floor heating will have to compromise heat loss of the house. So the minimum floor temperature is the floor temperature which is necessary to maintain a comfortable operative temperature of the zone.
3. The minimum allowable floor temperature limits the cooling capacity of the floor cooling system during the summer season.

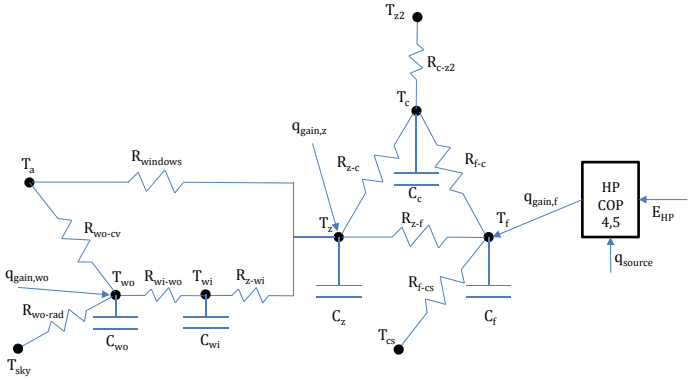

Figure 4.15 – Thermal network model of a living room

Model for studying comfort aspects of floor heating

As a consequence, the internal part of the model should contain at least the dominating surface temperatures experienced by inhabitants in order to determine the operative temperature. Figure 4.15 shows a schematic of the thermal network of a living room. Nomenclature of the parameters involved is listed in Table 4.4 and the heat balance equations of the thermal network are given in Equation (4.18). The operative temperature is calculated by applying Equations (4.16) and (4.17). The latter equation contains the following surface temperatures: zone, ceiling, floor and inner wall. The air temperature in Equation (4.16) is assumed to be the average of the zone, ceiling and inner wall temperatures.

$$
\begin{aligned}
C_z \frac{dT_z}{dt} &= \frac{T_c - T_z}{R_{z-c}} + \frac{T_a - T_z}{R_{win}} + \frac{T_{wi} - T_z}{R_{z-w}} + \frac{T_f - T_z}{R_{z-f}} + q_{gain,z} \\
C_f \frac{dT_f}{dt} &= \frac{T_z - T_f}{R_{z-f}} + \frac{T_{cs} - T_f}{R_{f-cs}} + \frac{T_c - T_f}{R_{f-c}} + q_{gain,f} \\
C_{wi} \frac{dT_{wi}}{dt} &= \frac{T_z - T_{wi}}{R_{z-wi}} + \frac{T_{wo} - T_{wi}}{R_{wi-wo}} \\
C_c \frac{dT_c}{dt} &= \frac{T_z - T_c}{R_{z-c}} + \frac{T_{z2} - T_c}{R_{c-z2}} + \frac{T_f - T_c}{R_{f-c}} \\
C_{wo} \frac{dT_{wo}}{dt} &= \frac{T_{wi} - T_{wo}}{R_{wi-wo}} + \frac{T_a - T_{wo}}{R_{wo-cv}} + \frac{T_{sky} - T_{wo}}{R_{wo-rad}} + q_{gain,wo}
\end{aligned}
\tag{4.18}
$$

The concrete floor, the zone including internal separation walls, inner and outer parts of envelope walls and ceiling are modeled as temperature nodes with a thermal capacitance. Solar gains are defined at the outer wall node and the zone node by window transmittance. Heat loss due to ventilation and infiltration is defined at the zone node, as well as heat gains by appliances and the presence of people. Heating input from the heat pump is defined at the floor node. Finally, parameters are calculated for a typical Dutch low energy house as defined in [10].

Nomenclature	
T	Temperature
R	thermal Resistance
E	electric Energy
q	thermal Energy
HP	Heat Pump
Subscripts	
z	zone
f	floor
c	ceiling
z2	zone on first floor above living room
cs	creeping space
wi	interior wall of envelope wall
wo	exterior wall of envelope wall
rad	radiation
cv	convection
a	ambient or outdoor

Table 4.4 – Model parameters

For the weather data, hourly recordings of a local weather station are used which contain ambient temperature and global transmittance, i.e. total solar radiation on the horizontal plane. This is used as input data for the model. Solar radiation on building planes is calculated using equations given by Duffie in [46] and cloud correlations defined by Erbs [55]. Transmitted solar radiation through the windows is assumed to be absorbed by the floor for 25% and by the zone for 75%, which is a simplification of reality. The house is oriented with its front area to the south which is ideal for passive solar gains and there are no obstacles which could cast shadows on the house surfaces. In practice, this may not always be the case, especially not in mid-winter when the angle of the sun is quite low.
The simulation model based on the above, which is used in the next section, includes Proportional Integral (PI) control of the heating/cooling input to the floor with the error between the zone temperature and its set point as controlled variable.

4.8 Case description

In this section, a case study using the model given in the previous section is discussed. First some further details are described for the living room thermal model are given and the scenarios for the case study are defined.
The model parameters for the thermal resistances and capacitances of the concrete floor, the ceiling and the walls are calculated by applying specific building physics formulas, deriving the required constants from Dutch building details (see [29], [34] and [177]), which are commonly applied for the construction of low energy

houses in the Netherlands. The floor is a hollow channel concrete type. On top of the floor, the floor heating tubes are laid on a grid mat filled up with a concrete casting. Specific density of the total floor is typically 514 kg/m^2. The ceiling has the same structure as the floor. The envelope wall consists of a concrete inner wall, insulation material, air gap and brick outer wall.
For the heat pump, a constant COP of 4.5 is assumed at all times.
The weather data of a relatively cold week in February 2012 from station Hoogeveen is used because a cold period has the largest effects on radiant surface temperatures. Simulation results are shown for the second week which runs from hour 168 to 336, i.e. midnight of the first until the seventh day of that week.

The following control scenarios are investigated:

1. Control 1: Constant temperature set point of 20^oC.
2. Control 2: Varying temperature set point: 19.5^oC at night, 20.5^oC during daytime. Control 2 is scheduled in such a way that operative temperatures are within thermal comfort limits during daytime hours and total energy demand is comparable to control 1.
3. Control 3: Same as scenario 2 but with additional short term heat storage for district power balancing. This is done by additional heat input to the floor.

Besides these three control scenarios, the following energy price schemes are investigated:

1. Conventional: conventional power grid fixed prices with lower night time energy rates. Peak rate hours are: 7 AM until 11 PM.
2. Alternative: district power grid based on renewable PV-generation. Lower rates apply during hours with sunshine and higher rates during other hours. Peak rate hours are: 6 PM until 9 AM.

4.8.1 Discussion of results

The heating input by the heat pump for Control 1 is calculated by simulation and shown in Figure 4.16 together with the global transmission ($G_{t,h}$ i.e. horizontal plane solar radiation) and the operative temperature of the living room. The influence of solar absorption by the interior of the living room can be observed in hours of less or even no required heating input. However, besides this positive effect, this reduces the possibilities for Floor Heating Thermal Energy Storage (FHTES) by the heat pump, as is deduced from the operative temperature. As explained in section 4.7.1, operative temperature variation during a period of e.g. one day should be less than 1^oC, so the allowable range for this case is $20-21^oC$. On the first day, 21.3^oC is reached due to solar absorption. As this is just outside the allowable range and energy can be saved by using the absorbed solar energy, there is no need to use the heat pump on that day. However, as solar energy decreases during the remainder of the week, longer periods of heating energy are

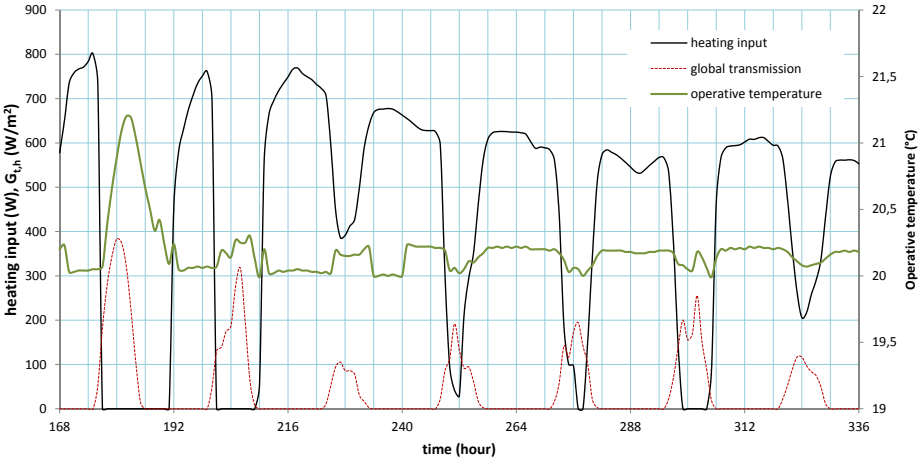

Figure 4.16 – Floor heating input and operative temperature for control 1

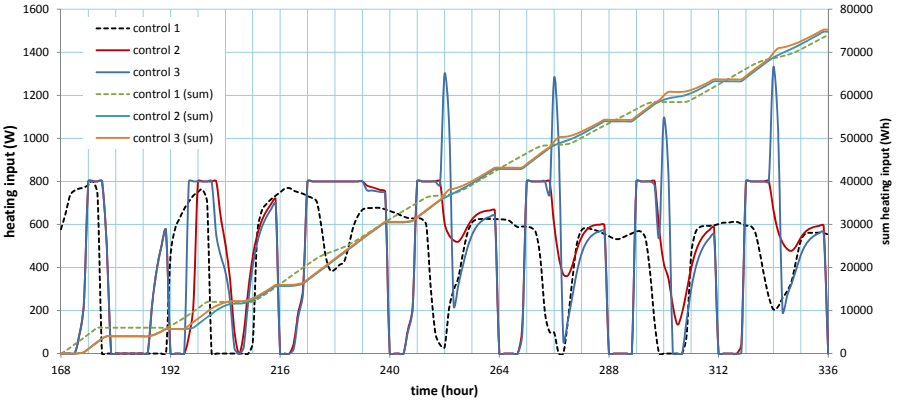

Figure 4.17 – Heating input and sum of heating input to floor heating system

required and operative temperatures are more stable, enabling more possibilities for FHTES by a heat pump.

In Figure 4.17 we show the heating input by the heat pump for the three control scenarios. Also, the cumulative heating input is shown for the three control scenarios, which starts at zero on the first day of the week and increases towards a maximum value at the end of the last day of the week. In Figure 4.18, the resulting operative temperatures for the three control scenarios is shown.
To study heat loss, Control 3 is basically the same as Control 2 but with small additional two hour storage periods taking place at the indicated circles in Figure 4.18. As is observed from Figure 4.17, the heating input of Control 3 is shifted in time

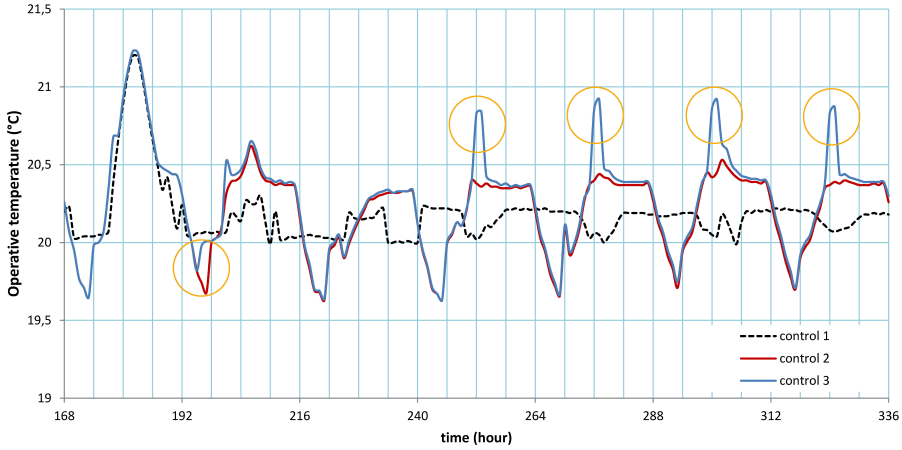

Figure 4.18 – Operative temperatures for all control scenarios

compared to Control 2. A simple way to accomplish this in a smart grid is that a central controller asks a home controller to temporarily raise the temperature set point. The total stored energy in the floor during each short term storage period (Control 3) is 1600 Wh. Observe from Figure 4.17 that the total energy demand for the whole week is almost not influenced by these storage periods. The additional energy loss is calculated at 479 Wh, i.e. 6% of the total heat input (8.000 Wh). This is rather small because of (a) good insulation of the house and (b) stored heat is transferred slowly to the interior and results in a period of less heating input, as can be observed from the larger drop in the heating input of Control 3 after each storage period, compared to Control 2.

The effects of the storage periods on the operative temperature can be deduced from Figure 4.18 by comparing Control 3 with Control 2. The last four peaks almost reach to 21^oC, which is just within the allowable range. The operative temperature seems to increase quite fast, but still less than 0.5^oC/h, well below the requirements set out in Section 4.7.1.

The short term storage period of Control 3 is significant for district power balancing. For the living room, the average heating requirement during the investigated week is calculated at 475 W. With the heat pump COP assumed to be at 4.5 it is using on average 106 W electric energy for the living room. The short term storage period of Control 3 involves 800 W thermal or 178 W electrical energy. This is 168% of the average electric energy demand. Hence it is concluded that the possibility for short term periods of thermal storage within floor heating systems can make a significant contribution to district power balancing.

To study energy costs for the residents, the simulated energy input for the three

	energy price scheme	
control	conventional	alternative
1	100	112
2	119	100
3	-	100

Table 4.5 – energy cost index per control scenario

control methods is translated into total required electric energy which is multiplied by energy price rates. A peak rate of €0.30/kWh and low rate of €0.20/kWh including taxes and network costs are assumed as reference according to present Dutch consumer electricity tariffs.

Energy costs for the investigated week are related to the costs for Control 1 with the conventional price scheme. These costs are given as index a value of 100 (see Table 4.5). As observed from this table, the costs are higher for Control 2 than for Control 1 in case of a conventional price scheme, because energy demand for Control 2 is shifted towards daytime hours and during those hours the peak rate applies.
However, in case of an alternative price scheme, the costs for Control 2 is lower than for Control 1 because the energy demand for Control 2 is shifted towards daytime hours and during those hours the low rate applies.

Control 3 has almost the same temperature control as control 2 but with some additional heat storage periods during daytime hours. The purpose of these storage periods is to increase consumption of solar PV energy. If besides the alternative price scheme, an energy price is offered at €0.19/kWh during the short periods of additional heat storage, then the costs are similar as the costs for Control 2.
As a general rule for the energy price during smart storage periods, the standard rate should be reduced with the percentage energy loss (i.e. 6% in this case) caused by storage to offer a cost neutral proposition for the residents.

4.9 Conclusions

In this chapter, predictive models are developed for a domestic hot water thermal storage which is charged by a heat pump and for an electric energy storage. The models are derived from energy balance equations combined with insights from experimental data. The models involve a set of relatively simple algebraic equations which are easy to incorporate in smart energy control algorithms. For the thermal storage the required inputs are: recordings of measured inlet and outlet water temperature and water flow, which can be performed by low cost heat meters in practice. For the electrical energy storage, the required inputs are (dis)charging voltage and currents. Outputs of the model are: the electric consumption profile and the total electric energy consumption of a future charging cycle from the present state of charge to fully charged conditions.

The accuracy of the model is validated by comparing results of model predictions with experimental findings. The accuracy of the predicted time needed for and the total energy consumption of the charging cycle is excellent, while the prediction accuracy of the electric power profile is within the range of the measurement errors. Hence, the model can be applied for simulation or control purposes of similar domestic hot water and electrical energy storage configurations, although the relations introduced for the charging power consumption, may be different for different types of heat pumps, batteries and chargers and different heat pump control systems. However, changing these relations is a relatively simple task which only involves analysis of the heat pump or battery charger characteristics, either from supplier data or by executing a few discharging and charging cycle experiments.
Application of the model is investigated with a case of increased self consumption of local solar PV energy. The developed predictive model is relatively easy to implement into an optimization control algorithm which minimizes peak electricity consumption of a household and electric battery capacity. The results of this application show a decreased battery capacity, lower electricity peak values and a shift of hours of electricity shortage from nighttime to daytime hours, which is favorable for local consumption of renewable energy generation in a district with solar PV panels.
The last part of this chapter investigates Floor Heating Thermal Energy Storage (FHTES) by a renewable energy supply system. To explore the limits, simulation results with a white box model of a living room show that the amount of energy that can be stored in a floor heating system depends on the house and floor heating structure, the degree of insulation, the weather and temperature settings by the residents. The investigation shows theoretically that a floor heating system is able to offer significant flexibility. However, the effects that are demonstrated, especially the effects on experienced thermal comfort should be evaluated in practice as the theoretical investigation was limited to effects on the operative temperature. As future work, it is interesting to determine and compare effects on the Predicted Mean Vote (PMV) by detailed building simulations, measurements and interviewing people.
With simulations, three types of temperature control are investigated. A constant day/night temperature set point (Control 1) shows that heating demand mostly occurs at night hours. A lower set point during night hours (Control 2) shifts heating demand towards day hours. Control 2 has the advantage that the heat pump can be used more flexible during the night for generating domestic hot water. If additional to Control 2, short storage periods during daytime hours are introduced (Control 3), it is found that operative temperatures remain within allowable comfort limits. It is concluded from this that a house with a floor heating system provides substantial storage capacity which can be used to maintain power balance within a district energy supply system. Energy losses due to storing energy in the floor appears to be small, at least for low energy houses. Further research is required to compare these effects for houses with different insulation properties. A fair energy cost policy should take the energy losses into account, e.g. by

offering a discount energy storage rate to residents during the charging periods. More practical experience with this method of compensation for residents has to be gained in practice.

Experiment	τ_{meas} (sec)	% error τ	P_{e,t_i^*} (kW)	$P_{e,t_i^*+\tau}$ (kW)	MAX % error ΔP_e	$T_{w,pred}$ $^\circ C$	$E_{tot,meas}$ (kJ)	% error E_{tot}
1	2911	-7.2	2.17	3.20	6.2	31.2	14872	0.3
2	2637	2.5	2.10	3.22	5.6	29.9	14465	3.1
3	2973	-9.1	2.16	3.22	5.4	31.6	15018	-0.7
4	4050	-1.6	1.86	3.22	8.7	27.6	22352	0.1
5	5229	1.1	1.85	3.23	5.2	25.4	29662	0.1

Table 4.6 – Validation results

Chapter 5

Case I: Modeling district heating co-generation capacity

Abstract - In this chapter, the best possible size for a co-generation unit and a boiler are determined together with their operational hours with information of the Meppel project case. A migration strategy is developed which starts with a simple system concept supported by boilers to a larger system which includes a CHP. Sustainability in terms of CO_2 emission savings of the energy concept is compared with other possible energy concepts.

5.1 Introduction

In this chapter a possible scenario is investigated for the transition of the Meppel case district heating system (refer to Section 3.1) from a preliminary system (System 1) with natural gas boilers and a refrigeration chiller up to a system with co-generation and a natural cooling source, e.g. underground aquifer (System 2). It has to be determined for System 1 which size of the generators (boiler and CHP) results in the most profitable situation. A schematic representation of the energy system is shown in Figure 5.1. As fuel supply, biogas is locally available but the decision to invest in a supply pipeline is postponed until the district has reached sufficient scale. At this moment, all heat generators use natural gas and a contribution to renewable energy is realized by purchasing certified green energy (green-gas).
The first goal of this chapter is to determine the required heating and cooling generator capacities. The second goal is to determine the most economic heat converter (boiler or CHP) in relation to the number of houses and the influence of houses with a heat pump on the business case of System 1. The third goal is to investigate the sustainability performance.
The remainder of this chapter is structured as follows: Section 5.2 defines the

[†]Major parts of this chapter have been published in [RvL:11].

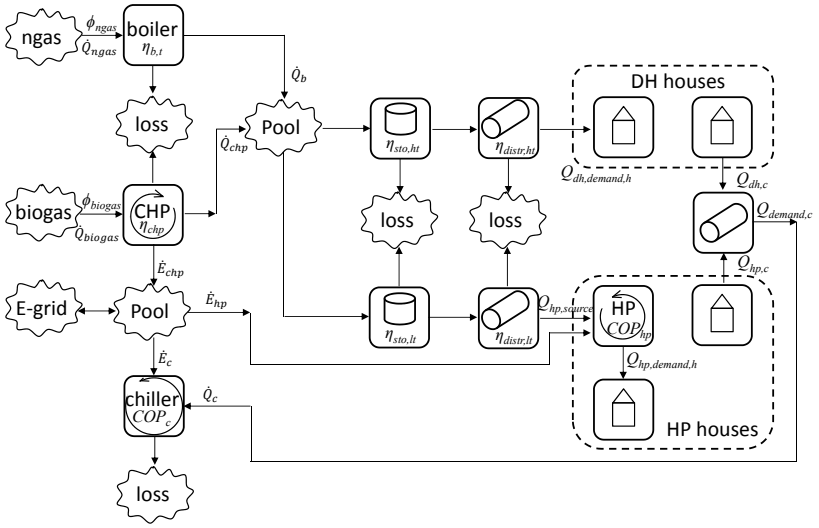

Figure 5.1 – schematic overview of the energy system

energy model, equations and case related parameters, Section 5.3 presents the results and finally, in Section 5.4 conclusions are drawn.

5.2 Energy model and equations

5.2.1 District Heating system energy model

A schematic of the district heating system (DH system) is shown in Figure 5.1. Left are the converters, starting with the boiler at the top with a natural gas input (ngas). Below the co-generator (CHP) with biogas input. Drawn at the bottom is a chiller which generates cooling energy for the district with electrical energy input. In the middle is the distribution system with at the top, the district heating system (DH). Second is the heat pump thermal source distribution system which is connected to the heating pool of the district heating system, which is a temporary solution. Third is the cooling distribution system which provides cooling for houses which have a heat pump but also for houses which are connected to the district heating system. Next to the system elements are variables which signify converter efficiencies, energy sources, energy demands and energy flows. These are explained in more detail in Table 5.4 at the end of this chapter.

Efficiency of the thermal storage is determined by the size, the wall insulation and the average temperature difference between water within the storage and outside air. For the model it is assumed that the size of the storage is sufficient to store and supply thermal energy within a daily cycle. As a rule of thumb, 125 liter/household storage capacity is estimated for a DH system with maximum storage temperature of 90 °C. Hence, capacity or size of the storage is not a variable

within the model.
The DH system is conceived as a utility which buys energy (biogas, natural gas, electricity) from the upstream market, converts it to electricity and heat, and sells heat to the downstream market, i.e. the households. The electricity is used by circulation pumps and by heat pumps. Surplus electricity produced by the CHP and not used by the local energy system, is sold to the grid. The first emphasis is on the primary choice between either a DH system with only natural gas boilers or with a biogas CHP and some supporting natural gas boilers.
Besides differences in capital and operational costs of the generators, we have to take cost differences of the downstream system (i.e. storage and network assets) into account caused by the type of converter being applied. For the considered situation, the network assets are not influenced, but for the CHP, a larger HT storage is needed. When only boilers are applied it is easy to adjust the generated thermal power instantly within a large range due to cascading and power modulation. With a CHP the thermal modulation range is not as large and running a CHP at reduced load involves a loss of electrical generation efficiency. Besides that, for best efficiency and lifetime performance, a CHP should run with a more or less constant speed when it runs and should not constantly follow the actual demand of the network. Therefore, for the CHP case, we calculate with increased HT storage capital costs.
Aggregated heating and cooling demand profiles are already explained in Chapter 3. The hourly patterns obtained from that model are summed for each day to yield daily demand profiles. For the CHP, an additional peak boiler is added to provide sufficient heating capacity during extremely cold days which occur infrequently. The peak boiler capacity is calculated from the coldest day during the last five years. For cooling, the generator size is determined directly from the warmest day during the last five years.
Energy tariffs (natural gas, electricity) are assumed to be only related to total yearly amounts, although on the electricity spot market and day ahead market, prices vary dynamically. But these variations are small and often fixed electricity prices are contracted for longer periods. In this way, the complexity and the number of required iterations for the optimization problem to find the number of houses for break even profit is significantly reduced.

The yearly heat balance for the CHP and boiler production (i.e. the capacities Q_{chp} and Q_b multiplied with their yearly operational hours $t_{op,chp}$ and $t_{op,b}$) and demand of the district heating system ($Q_{dh,demand,h}$) and source energy for the heat pumps ($Q_{hp,source}$) is:

$$\left[\frac{Q_{dh,demand,h}}{\eta_{distr}\cdot\eta_{sto,ht}}+Q_{hp,source}\right]\cdot\frac{10^6}{3600}=\dot{Q}_{chp}\cdot t_{op,chp}+\dot{Q}_b\cdot t_{op,b}\,. \tag{5.1}$$

When the CHP and the boilers together generate the required heat, the CHP has priority and the boilers have a supportive function. Hence, an additional expression is required which relates the operational hours of the CHP to the size

of the CHP. This expression is developed in Section 5.2.3.
The total yearly heat demand of the DH system ($Q_{dh,demand,h}$) is determined from an aggregated, hourly demand profile, for which the method outlined in Chapter 3 is used. n is used as variable for the number of connected houses to the district heating system. The heat demand of houses with a heat pump ($Q_{hp,demand,h}$) is determined in the same way. We use m as variable for the number of houses with a heat pump.
The source heat demand of the heat pumps is related to the household demand by:

$$Q_{hp,source} = Q_{hp,demand,h} \cdot \left[1 - \frac{1}{COP_{hp}}\right]. \tag{5.2}$$

The CHP heat generation rate $\dot{Q}_{chp}$ is related to CHP electric power rate $\dot{E}_{chp}$ as follows:

$$\dot{Q}_{chp} = \dot{E}_{chp} \cdot \frac{\eta_{chp,th}}{\eta_{chp,e}}. \tag{5.3}$$

The biogas and natural gas (ngas) flows (ϕ) are related to the CHP electric and boiler thermal power rate $\dot{Q}_b$ respectively as follows:

$$\phi_{biogas} = \frac{\dot{E}_{chp} \cdot 3600}{\eta_{chp,e} \cdot LHV_{biogas} \cdot 1000} \tag{5.4}$$

$$\phi_{ngas} = \frac{\dot{Q}_b \cdot 3600}{\eta_{b,th} \cdot LHV_{ngas} \cdot 1000}. \tag{5.5}$$

The total yearly electric energy demand including generation of cooling energy is as follows:

$$\begin{aligned} E_{demand} = \Big(&Q_{hp,demand,h} \cdot \left[\frac{1}{COP_{hp}} + f_{netw,p}\right] + \\ &f_{netw,p} \cdot Q_{dh,demand,h} + Q_{demand,c} \cdot \left[f_{netw,p} + \frac{1}{COP_c}\right]\Big) \cdot \frac{10^6}{3600}, \end{aligned} \tag{5.6}$$

in which $f_{netw,p}$ is an estimated average percentage which discounts the required electric energy for the network pumps as a percentage of the thermal energy transmitted through the piping network. The amount of energy needed for the pumps has to be estimated from network fluid friction calculations and frequency controlled pump characteristics. As a simplification, a value of 5% is used for the calculations.

5.2.2 Optimization model

The financial aspects of the energy concept shown in Figure 5.1 is analyzed with an equation in which profit terms are considered related to selling energy to houses (heating and cooling) and to the network (only in case of surplus CHP electricity). Cost terms that are taken into account are: the input energy costs (fuel and

electricity bought from the network) and the true capital and operational costs of specific energy generators (boilers, CHP, heat pumps and related storage facilities). Excluded are infrastructural costs of the downstream network because in practice, all infrastructural investments are payed for by home owners through connection fees, so these are not carried by the utility. However, there are also financial reservations to be made for reinvestments in the infrastructure and in that case, there is a difference between the DH system and heat pumps as the infrastructure for the heat pumps is relatively cheaper. This difference is accounted for in the fixed part of the heat tariff and is translated into additional income in the case of heat pumps. This is explained further in section 5.2.4.
The net yearly profit (P_{net}) is the objective for a maximization and is expressed as:

$$\begin{aligned} P_{net} = \quad & B_{E,grid,sell} + B_{Q,dh,h} + B_{Q,hp,h} + B_{Q,dh,c} + B_{Q,hp,c} \\ & - C_{E,grid,buy} - C_{biogas} - C_{ngas} - \sum_{j \in J} \left\{ C_{cap,j} + C_{op,j} \right\}, \\ & J = \{chp, b, hp, sto_{chp}, sto_{hp}\}, \end{aligned} \tag{5.7}$$

in which B signifies Benefit with respect to the following indices: electricity sold to the grid (E,grid,sell), heat sold to district heating customers (Q,dh,h), heat sold to customers with a heat pump (Q,hp,h), cooling sold to houses connected to the district heating (Q,dh,c) or houses with a heat pump (Q,hp,c). The following Costs (C) are substracted: electricity bought from the grid (E,grid,buy), biogas consumption (biogas), natural gas consumption (ngas), capital costs (CAPEX) of equipment within a set J (cap,j) and operational costs (OPEX) of this equipment (op,j). The terms are summarized in Table 5.5 on the last pages of this chapter.
Electricity generated by the CHP is partly also consumed by the electric equipment of the DH network (pumps, heat pumps, chiller). In general, an objective of Smart Grid control is to balance power generation and consumption as much as possible. Thus, in our case, the objective is to match the daily CHP operating times closely with the operating times of electric and thermal consumers. The smaller the CHP, the longer it will have to run daily and the higher the chance of matching its generation power with consumption. Using this basic principle, a simple algorithm is implemented which calculates the fraction of CHP operating time matching operational times of electrical demand by the heat pumps, chiller and network pumps. This is combined with an algorithm that determines the electricity costs including energy tax and profit for buying energy from the grid and feeding into the grid. To avoid long explanations which defer from the main goal of this chapter, these algorithms are left out of the thesis.

Capital costs for equipment such as the CHP, boiler, heat pumps and storage are determined by investments in relation to size or capacity. For this we define the Invested capital per unit size I (€per unit size) which is calculated by power functions. Combined with the capacity this determines the investment INV (€). Suitable power function coefficients for I are obtained from cost engineering handbooks, field experts and company quotations. To shorten the discussion in this chapter, the coefficients are not further detailed in this chapter but for a similar

approach, coefficients are given in Chapter 6.
Capital costs are expressed as net present value and are determined by initial investments, the interest rate r which is assumed the same for all equipment, and equipment life time LT as follows:

$$C_{cap,j} = INV_j \frac{r}{1 - \frac{1}{(1+r)^{LT_j}}} \quad j \in J\,. \tag{5.8}$$

Operational costs for each equipment are assumed to be a fixed percentage of the initial investment.

5.2.3 Relation between CHP size and operational time

In case a CHP is included in the system, it can be supported by boilers, depending on the CHP size and heat demand. A suitable size relation between CHP and boiler size is determined from the balance at the coldest day:

$$\dot{Q}_{max} = \dot{Q}_{chp} + \dot{Q}_b \tag{5.9}$$

This implies that on the coldest day, both heat generators will run continuously for 24 hours to generate the required thermal energy. Hence, the following relation between the heat demand and required peak thermal power applies for the coldest day:

$$\dot{Q}_{max} = \left(\frac{Q^{max}_{dh,demand,h}}{\eta_{distr} \cdot \eta_{sto,ht}} + Q_{hp,source} \right) \cdot \frac{10^6}{3600 \cdot 24}\,. \tag{5.10}$$

Let Q_{demand} be a data array in which the daily heat demand is sorted from days with the largest to the smallest heat demand. Note that $Q^{max}_{dh,demand,h}$ from Equation (5.10) is the first entry in this array. In Figure 5.2 the array is shown as descending curve, next to a shaded area which signifies the heat demand coverage by a CHP with a capacity which is just enough to generate the heat demand which is indicated with a dot. The shaded area on the left side of the dot shows the amount of heat generated by this CHP per day when it operates 24 hours per day on full capacity. The shaded area on the right side of the dot shows the amount of heat generated by the CHP but for these days, the CHP does not need its full production capacity. The remaining area above the shaded area on the left side of the dot is covered by natural gas boilers.

Let $\dot{Q}_i$ be a certain maximum CHP generation capacity such that on day i (see Figure 5.2 in which i signifies the x-axis), 24 hours operating time with this capacity results in exactly the heat demand of that day, i.e. $Q_{demand,i}$. For the entire shaded area shown in Figure 5.2, the following equations determine the yearly operating time $t_{op,chp}$ (hours/year) if it is always operated at its maximum CHP generation capacity $\dot{Q}_i$ (kW):

$$t_{op,chp} = \left(i + \sum_{j=i}^{365} \frac{Q_{demand,j}}{Q_{demand,i}} \right) \cdot 24\,. \tag{5.11}$$

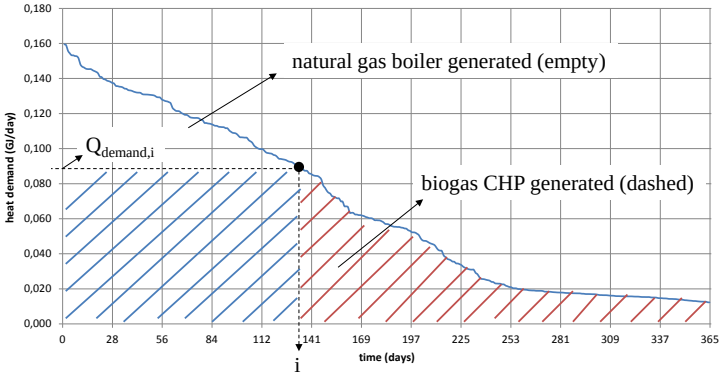

Figure 5.2 – Sorted heat demand and indicated areas at a certain hour point i

$\dot{Q}_i$ can be a CHP of choice with a thermal capacity (kW) between 0 and $\dot{Q}_{max}$. With Equation (5.11), it is possible to calculate the full power operational time in hours/year for any chosen CHP capacity within these boundaries. As a result, Figure 5.3 shows the relation between CHP size $\dot{Q}_{chp}$ and full power operation hours per year, $t_{op,chp}$. The relation appears to be approximately linear for CHP sizes between 30% and 100% of the maximum required thermal power on the coldest day.

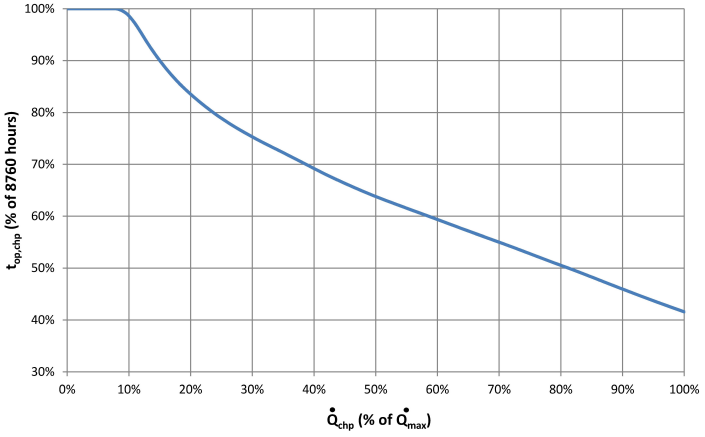

Figure 5.3 – Relation between operational time and CHP size

5.2.4 Case related energy financial parameters

Benefit and cost rate of electricity

In the Meppel case, the utility company Meppel Energy buys electric energy from the grid and in case of a CHP it will also feed in surplus electricity into the grid. Contractual buying and selling prices of energy are usually based on the expected amount of energy drawn from and fed into the grid within a certain time period. Following Dutch CHP practice, we assume the buying and selling prices are equal for energy transported to and from the grid over the period of one year.
In general the price of energy drops when the amount of energy being bought increases. For very large amounts (i.e. above 500.000 kWh/year) electricity prices are close to the spot market or day ahead market price of electricity, which is currently around 5.5 €ct/kWh. In case of CHP generation with various electricity consumers, if the amount of sold (surplus) energy exceeds the amount of bought energy, network utilities are often reluctant to pay any compensation, or spot market prices at most. Based on this, specific energy price equations are developed for the Dutch situation and implemented into the model. The details of these equations are outside the scope of the present chapter.

Benefits for supplying heat

Infrastructural investments are payed off by the residents with a one time connection fee. This fee is usually part of the building price of a house. Besides the connection fee, residents are charged for the consumed heat according to the following equation, based on the Dutch heat law, effective from January 2014 which defines the maximum possible Benefit as (see [39]): $B_{Q,h} = 209,92 + 19.86 \cdot Q_{demand,h}$ (excl. VAT).

Financial reservations have to be made for reinvestments in the required infrastructure. For this there is a difference between houses connected to the DH system and houses with heat pumps:

- In the case of houses connected to the DH system, the yearly costs of reservations for infrastructural reinvestments are estimated from a net connection fee per household of €7300 with a 50 year depreciation period at: €146.00 /(year.household). This leaves as Benefit for the profit model, (see (5.8)): $B_{Q,dh,h} = 63.00 + 19.86 \cdot Q_{demand,dh,h}$
- In case of houses with a heat pump, lower reservations (€3250 per household with a 50 year depreciation period) are estimated for infrastructural reinvestments due to the use of non-insulated pipes and a generation building is not required for heat pumps, this leads to €65.00 /(year.household) and leaves as Benefit: $B_{Q,hp,h} = 145.00 + 19.86 \cdot Q_{demand,hp,h}$.

Benefits for supplying cooling

Originally the Meppel project was planned for a larger starting scale, including the use of the aquifer for cooling energy and as source energy for the heat pumps. Cooling of the houses provides part of the required energy to balance temperature of the aquifers and is therefore offered for free to the residents. Meppel energy wants to keep its promise of free cooling to the residents and therefore the Benefit for cooling is zero, $B_{Q,c} = 0$.

Costs of biogas for the CHP and natural gas for the boilers

Cost relations for natural gas from the national grid, specific relations for biogas and applicable energy taxes are developed and implemented as algorithms into the optimization model, but not explained in more detail in this thesis.

5.3 Case results

5.3.1 Maximum required generation capacities

For the two building phases (phase 1: 40 DH houses; phase 2: 160 DH houses, 16 HP houses), the maximum required generation capacities are shown in Table 5.1.

	heat generation $\dot{Q}_{max}$ (kW)	cooling generation $\dot{Q}_c$ (kW)
phase 1	87	74
phase 2	373	322

Table 5.1 – Maximum required generation capacities

5.3.2 Best possible CHP size and operating times

The best possible size of the CHP and the accompanying boiler size are determined by maximizing the net profit objective, Equation (5.8) with $\dot{Q}_{chp}$ as variable. For the two building phases, the best possible sizes are shown in Table 5.2.
We find as result rather small CHP capacities as optimum. A possible cause lies

(n,m)	CHP size $\dot{E}_{chp}$ (kW)	$t_{op,chp}$ (hour/year)	boiler size $\dot{Q}_b$ (kW)	$t_{op,b}$ (hour/year)
(40,0)	6	8659	78	3077
(160,16)	100	6140	228	2033

Table 5.2 – Best possible CHP and boiler capacities for building phase 1 and 2

in the small scale of the district for which relatively small CHP units are required but these have relatively high investment costs (compared to large CHP units

for larger districts). Also, in case the CHP produces electricity for the grid, the financial benefits are small compared to importing grid electricity. In our analysis, we did not include possible subsidies for the biogas to power conversion. In the Netherlands, such subsidies exist an could result in a more positive business case and larger CHP capacity as optimum.
In Table 5.3, values for the objective are shown, which indicates that the profit is always negative (although less negative for the case with a CHP). Care should be

(n,m)	profit without CHP (€/year)	profit with CHP (€/year)
(40,0)	-6,911	-2,571
(160,16)	-20,807	-12,380

Table 5.3 – Objective values for building phase 1 and 2

taken in the interpretation of the profit values as they are influenced by assumptions explained in Section 5.2. Because we lack detailed insight in the Meppel energy business case, we may have exaggerated certain investment costs. On the other hand, practical experience indicates problematic profitability of small-scale DH systems, which support our results. In the Meppel case, there is more pressure on profitability because the houses have a lower heating demand (and thus lower revenue per household) than usual and there are generation costs involved for cooling while on the other hand, cooling is offered free of charge. If a fee for cooling is introduced based on break even costs-benefits, we get €64.00 /year and €70.00 /year per household for phase 1 and 2 respectively. To place this in perspective of what households would normally pay if they generate the required cooling with home based air conditioning equipment, the average cooling demand of 6 GJ/year requires 555 kWh electric energy per household which would costs each household €127.00 /year only for electricity. Hence the calculated fees are reasonable propositions to the residents.

Next, we consider the influence of houses with heat pumps on the profit. By maximizing the objective with $\dot{Q}_{chp}$ and the number of houses with a heat pump (m) as variables, it is found that independent of the size of the district heating system, no houses with a heat pump is always optimal. So in all cases, houses with heat pumps have a negative influence on profit. There are two reasons for this. First, in System 1, the source heat for the heat pumps is generated by the CHP and boilers, with fuel costs as a consequence. Second, individual heat pumps for each house are relatively expensive in comparison with district heating connections. Heat pumps require more investments and maintenance and also have a shorter life time. Clearly, the compensation offered by a higher revenue is not sufficient for an equally profitable operation of heat pumps compared to houses connected to the DH system.

Next, we consider the situation that the number of houses connected to the dis-

trict heating system expands, and investigate if now the operation will become profitable. The answer is that this depends mostly on (a) the applied interest rate r and (b) the household heating demand. If $r = 4\%$ then operation breaks even at 490 houses. The corresponding best possible generation capacities and operating times are: $\dot{E}_{chp} = 426$ kW, $t_{op,chp} = 5293$ hours/year, $\dot{Q}_b = 448$ kW and $t_{op,b} = 1340$ hours/year. For $r = 2\%$ the break even point is 277 houses.

5.3.3 CHP migration steps

From the start of the house building project, the number of houses in the district increases gradually. Ideally, the CHP and boiler sizes also gradually increase ir order to reach the best possible profitability. However, it is relatively easy and cheap to install additional boiler capacity, but more complex and costly to replace or add CHP units. In general, a gradual expansion of CHP capacity is possible in two ways: either by leasing CHP units for a period of time, or by investing in a somewhat larger CHP unit which is close to being optimal for a small number of houses at the beginning of the project as well as for a much larger number of houses after some years. Because the Dutch tax scheme offers substantial tax reductions for CHP investments, the investment scenario is selected as the most appropriate. Therefore, the relation between CHP size and profit is investigated in four steps from building phase 1 to phase 2, to estimate the proper CHP sizes. The result is shown in Figure 5.4.

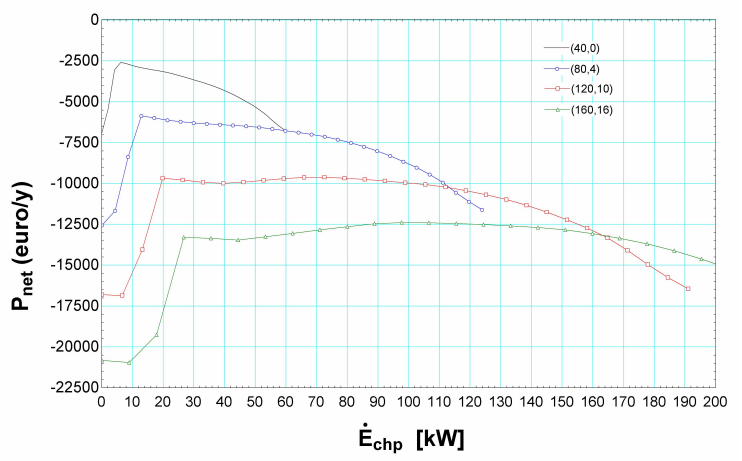

Figure 5.4 – CHP optimum for possible migration steps

For each line in the Figure, the corresponding number of houses with a district heating connection (n) and houses with a heat pump (m) are mentioned as couple (n,m). Around the optimum of each line, the relation between profit and CHP size appears to be rather flat. This gives some flexibility to choose the CHP size according to the migration steps for the district. As the house building project

is scheduled to reach 130 houses within two years, it is not interesting to invest in very small CHP units which are only optimal for a small number of houses. On the other hand, for 130 houses, the net profit is more or less equal for CHP units between 20 and 120 kW. The eventual scale of the housing project and for this energy concept is 350 houses, which will take in total seven years to reach. Considering these building plans, it is most appropriate to choose a CHP unit which will give the best possible profit during the building phase but also for the remaining service life of the CHP unit. Based on Figure 5.4, we estimate a CHP capacity between 80 and 160 kW as best possible choice.

5.3.4 Comparison on sustainability

Sustainability of the Meppel energy concept is investigated by comparing fossil fuel requirements for building phase 2 (176 houses of which 160 houses are connected to the district heating system and 16 houses have a heat pump). We consider five cases:

1. Case 1: System 1 with optimal sized CHP on biogas supported by a boiler on natural gas. The Sankey or energy flow diagram for this case is shown in Figure 5.5. The total natural gas input is 1648 GJ/y and the total biogas inputis 6177 GJ/y. If the CHP runs on natural gas, the total natural gas input is 7825 GJ/y.
2. Case 2: System 1 without a CHP. In this case the boiler delivers 4860 GJ/y with an equal natural gas input. The required electricity for heat pumps, cooling and network pumps and energy delivered to the region total 2222 GJ/y. This requires 4938 GJ/y of natural gas input at a grid based electrical power plant, taking Dutch national fuel efficiency of 45% into account. Hence, the total natural gas input is 9798 GJ/y.
3. Case 3: Dutch conventional house heating by individual home fitted natural gas boilers. In this case for heating, 4318 GJ/y natural gas is required. The required electricity for cooling and comparable electricity supplied to the region in total is 1816 GJ/y. If a grid based electrical power plant is used, 4036 GJ/y natural gas input is required. In that case, the natural gas input is in total 8354 GJ/y.
4. Case 4: as an alternative for Case 3, the 1816 GJ/y electricity is generated by home installed solar PV, which amounts to 2866 kWh/y per household. The total natural gas input for heating is 4318 GJ/y.
5. Case 5: similar as Case 4 but now houses with a lower heat demand are considered, i.e. houses according to Passive House (PH) building standards.

The resulting natural gas input is shown in Figure 5.6. Case 1 shows the best sustainability results. However, if natural gas is used for the CHP, the concept is only 6% more sustainable than Case 3, which has conventional house heating with natural gas boilers. Case 2 shows that the DH system without a CHP actually has

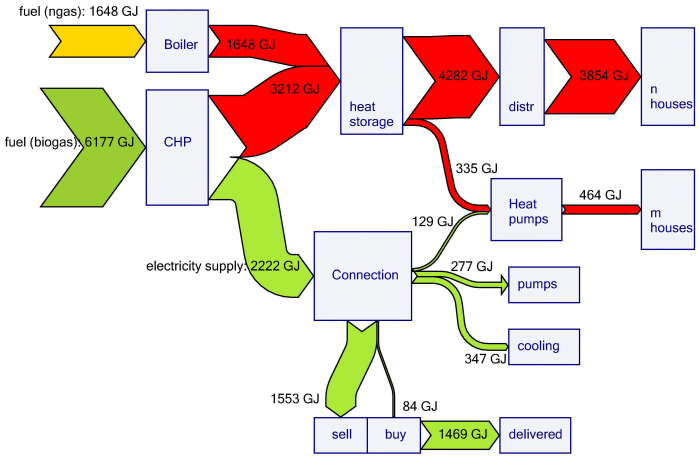

Figure 5.5 – Sankey diagram system 1, building phase 2

the worst performance on sustainability.
Case 4 with home PV installations is interesting as improved sustainability is combined with less infrastructural investments than in Case 1 and is hence easier to implement in an unsure house building market. Case 4 also stimulates another objective, namely to invest into more energy efficient houses, in order to further reduce natural gas consumption, which is shown in Case 5. This case can be further extended by replacing natural gas boilers with heat pumps. The district then contains houses with a low heating demand (e.g. Passive Houses), solar PV and heat pumps which are connected to a ground source or aquifer either collectively or individually. The use of natural gas is then eliminated totally. However, a drawback of such a concept is the imbalance between periods of major PV electricity generation and periods with the highest heating demand. Further comparisons of these concepts including financial aspects and loads on the electricity network are part of the analysis in Chapter 6.

Last, we investigate the number of houses and optimal capacity of the CHP when all the available biogas of the municipality is used, which is 9200 GJ/y. For this, we maximize the profit objective stated in Equation (5.8) in which we fix the biogas consumption and define the number of houses and CHP capacity as variables. As optimum we find 232 houses connected to the district heating system and a CHP capacity of: $\dot{E}_{chp}$ = 159 kW. The required natural gas input for boilers is in that case 1775 GJ/y. The net profit (or loss in this case) is calculated at -€5,711/y. When a cooling fee of €50.00/y is asked from each household, the net profit is positive at €5,899/y.

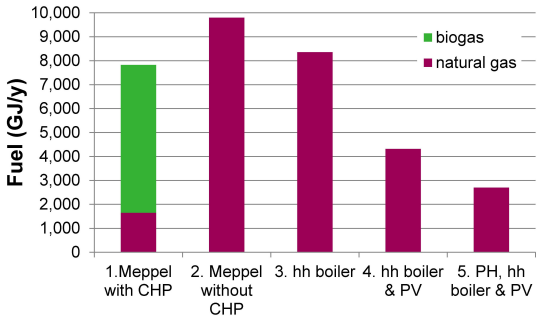

Figure 5.6 – case related fuel input comparison

5.4 Conclusions

In this chapter, optimal heat and power generation sizes are determined for the new urban district Nieuwveenslanden situated in Meppel for two building phases starting at 40 houses and expanding towards 176 houses. Besides optimal CHP and boiler sizes, corresponding profits and sustainability are determined for the network based on fossil fuel requirements. Profits appear to be negative on a first sight, however more than 50% improvement is possible if a CHP is used for heat and power generation compared to operation with only boilers. With an interest rate of 4% on invested capital, profits are positive when more than 490 houses are connected, with 2% this is reduced to 277 houses. If households are charged a modest fee for cooling, the energy concept with a CHP is profitable from the start. Based on maximizing profit and considering the scheduled number of houses for the building project, a CHP unit within the range of 80 to 160 kW electrical capacity is proposed as best possible choice for the building project.
Sustainability of the energy concept is compared with the Dutch reference, i.e. houses heated by individual natural gas boilers. If a CHP on biogas is applied, the Meppel energy concept performs much better on sustainability than this reference. However, if the CHP runs on natural gas, the performance is only 6% better. It should be mentioned that a scenario based on the Dutch reference combined with home solar PV is another possible route towards improved sustainability but involves less infrastructural investments, see also Chapter 6. However, the Meppel district heating system concept with a CHP on biogas still performs better on sustainability than this alternative route.
For the Meppel DH system, houses with a heat pump have a negative influence on the profitability. This is because the source heat for the heat pump is generated by the CHP and boilers of the district heating system and because the heat pumps of the households are more expensive to operate than the district heating system. It is interesting to further investigate the results if source heat and cooling are generated by an underground aquifer. In that case a better profitability is expected. This investigation is part of Chapter 6.

term	signification
$\eta_{chp,e}$, $\eta_{chp,t}$	CHP electric and thermal efficiency
$\eta_{b,t}$	boiler thermal efficiency
$\eta_{sto,ht}$	High Temperature (HT) thermal storage average efficiency
$\eta_{sto,lt}$	Low Temperature (LT) thermal storage average efficiency
η_{distr}	DH distribution network average efficiency
COP_{hp}	heat pump (HP) Coefficient Of Performance (COP)
COP_c	refrigeration chiller COP
$f_{netw,p}$	fraction of required electric pump energy for network pumps related to transmitted thermal energy of the network
ϕ_{biogas}, ϕ_{ngas}	biogas supply to CHP, natural gas supply to boilers ($m^3/hour$)
LHV	Lower Heating Value (MJ/m^3)
$\dot{Q}_{biogas}$ or $\dot{Q}_{ngas}$	fuel related thermal energy input (kW)
$Q_{dh,demand,h}$	total DH heating demand of (n) connected houses (GJ)
$Q_{hp,demand,h}$	total heating energy demand of (m) houses with a heat pump (GJ)
$Q_{hp,source}$	total low temperature source heat for the heat pumps (GJ)
Q_{dhw}, Q_{sh}	domestic hot water demand and space heating demand (GJ)
$Q_{demand,c}$, $Q_{dh,c}$, $Q_{hp,c}$	cooling energy demand, for DH network houses, for houses with heat pumps (GJ)
$\dot{E}_{chp}$	CHP electric rated power (kW)
$\dot{Q}_{chp}$	CHP thermal rated power (kW)
$\dot{Q}_b$	boiler thermal rated power (kW)
$t_{op,chp}$ and $t_{op,b}$	full load operational hours of the CHP and boiler ($hours/y$)
$\dot{E}_c$, $\dot{Q}_c$	refrigeration chiller electric rated power and cooling rate (kW)

Table 5.4 – Nomenclature energy system

term	signification (unit: €/year)
$B_{E,grid,sell}$	benefit made on electricity sold to the grid
$B_{Q,dh,h}$	benefit made on heat sold through the DH network
$B_{Q,hp,h}$	benefit made on heat sold to houses fitted with a heat pump
$B_{Q,dh,c}$	benefit made on cooling sold through the DH network
$B_{Q,hp,c}$	benefit made on cooling sold to houses fitted with a heat pump
$C_{E,grid,buy}$	costs of electricity bought from the grid
C_{biogas}	costs of biogas supply to the DH system
C_{ngas}	costs of natural gas supply to the DH system
$C_{cap,j}$	capital costs of investments and required future reinvestments into specific equipment type j
$C_{op,j}$	operational costs (operator, maintenance, insurrance, etc) of specific equipment type j
$chp, b, hp, sto_{chp}, sto_{hp}$	specific equipment: CHP, boiler, heat pump, storage related to the CHP, storage related to the heat pumps

Table 5.5 – Nomenclature profit function

Chapter 6

Case II: Modeling integrated urban energy systems

Abstract - The purpose of this chapter is to develop a model to analyze options for 100% renewable urban districts which self-consume locally generated renewable energy as much as possible and import (or export) energy from (or to) external grids as little as possible. Energy scheduling algorithms are developed to prioritize energy generation and storage of local renewable energy. The model is applied in a Dutch case study in which three renewable energy system concepts are evaluated against the case reference. Optimal capacities are determined for minimal operational costs including a penalty on carbon dioxide production. Attractiveness of these concepts is discussed in relation to costs, environmental concerns and applicability within the Dutch context of the energy transition.

6.1 Introduction

This chapter investigates options to integrate renewable energy within the Meppel case, which is introduced in Section 3.1, in such a way that the generated renewable energy is deployed by the district as much as possible. The analysis and results presented in this chapter are to some extend relevant for many new and existing urban districts in the Netherlands, either having a collective or individual heating system.
For the Meppel energy system and for future scenarios of the expanding district, the aim is to investigate possible routes towards integration of renewable energy. The first route is to shift to biofuel in stead of natural gas by replacing the boilers with a wood boiler or biogas fired co-generator. To cover the electric energy demand, besides biogas co-generation, local solar PV generation and a regional wind turbine can be used. The second route (all electric) is to eliminate the use of

[†]Major parts of this chapter have been published in [RvL:6].

fuels entirely and to replace the boilers with heat pumps. As supply options for the resulting large electricity demand, local solar PV and regional wind energy are investigated, and as a separate case, a combination with biogas co-generation. Hereby, integration of renewable energy for the cooling demand of the houses is also taken into account. Renewable cooling sources that are investigated are: an underground aquifer used in the heat pump scenario, and a nearby sand excavation lake used in the biofuel scenario.
The investigation is based on model simulations as there is no relevant data yet from the district heating system. The simulation methods discussed in Chapters 2 and 3 are used to generate hourly household and aggregated electrical, heating and cooling demand. To analyze energy flows on an hourly basis, a specific algorithm framework is developed for hourly scheduling of energy flows based on demand, renewable generation and the charge states of thermal and electric storage facilities. Generation capacities are determined by mathematical optimization and together with the hourly energy flows and yearly balances, these are used for cost calculations and for environmental considerations.
The chapter is structured as follows. Section 6.2 summarizes related work into models for integration of renewable energy and for determining optimal configuration of energy systems. Section 6.3 introduces the modeling framework to determine the optimal size of generators and storage facilities, operational costs and environmental impact. Section 6.4 discusses case related results. Finally, conclusions are presented in Section 6.8.

6.2 Related work

Determination of optimal generation capacities of renewable generators for (district) heating systems is a recent investigation area. For larger area and district energy supply studies, the software "Energyplan" is suitable to analyze system capacities and energy flows [54]. For a case application see [130]. In Energyplan it is possible to configure renewable generators which are applicable for local, urban districts and to use fixed scheduling methods for least costs or least CO_2 production. However, the control of thermal and electrical generation and storage energy flows as part of a local energy system, determines the resulting capacities but also to which extend the generated renewable energy is effectively used for the local consumption, which is our main goal. We have no detailed insight of the scheduling methods of Energyplan for this purpose, which is why we develop our own model for this. Besides that, some of our future work involves renewable energy systems which contain a new type of seasonal thermal storage (Ecovat, see [49]) for which control of different temperature layers is important in relation to the thermal energy generation and demand. This new type of storage is not yet part of Energyplan.
In Chapter 5, a method is developed to determine optimal capacities of a biogas CHP and thermal storage in relation to the size of the district. The present chapter has a much wider scope and aims to integrate different renewable energy gener-

ators in order to analyze different concepts. The optimal capacities of renewable energy generators for a specific project, depend on often contradicting objectives, and many of the relations between capacity and costs are non-linear. Hence, this is a particularly difficult problem for mathematical optimization. In [41] genetic algorithms are used to find optimal capacities of heat pumps for a Swiss district heating system. In [136] a non linear programming model is used to design district heating networks which are minimized with respect to total energy consumption and operational costs. In [143], optimal size of a residential micro CHP and storage in Japan is determined by applying a mixed integer nonlinear programming model. Finally, an example of a similar scheduling approach as the one presented in this chapter is given in [137] for a case study which involves solar PV integration with power to heat and thermal storage for a district heating system in Italy. They use Multi-Objective Evolutionary Algorithms with a Pareto front to determine optimal capacities of solar PV generation with electrical and thermal storage. The present chapter aims at the development of an energy priority scheduling approach and a thorough discussion of the case results in terms of energy flow behavior and the achievable economic and environmental results.

6.3 Methods

6.3.1 Energy system model

Following more recent developments in the Meppel district heating project, it is assumed that 200 houses are connected to a district heating and cooling system and a local electricity grid which is connected to the larger grid. As defined in Chapter 5, the case reference energy system contains collective boilers with natural gas as fuel for heating, a small thermal storage to guarantee continuous temperature supply of hot water and electric cooling compressors for the supply of cold water. For the case reference, all household electrical demand is supplied by the larger grid which contains a mixture of generation sources.

To integrate renewable energy, the Meppel district heating utility company will replace the natural gas boilers of the case reference system with a boiler which burns locally available wood chips (biofuel). As discussed in Chapter 5, a biogas co-generator may also be used as there is local biogas available for which a supply pipeline is considered. For the cooling demand, various renewable options are available. Often used in the Netherlands are natural sources with sufficient low temperatures of 8-12^oC. Most commonly used are underground aquifers. Close to the Meppel project is a deep lake formed by sand excavations. This lake can be used as cooling source and as source for heat pumps. Aquifer and lake source cooling have the advantage of low electric energy consumption as they only require pumping energy. The main disadvantage is that initially, the investment is much higher than for compression cooling (see [187] and [128]).
Another possible way to integrate renewable energy into the district heating sup-

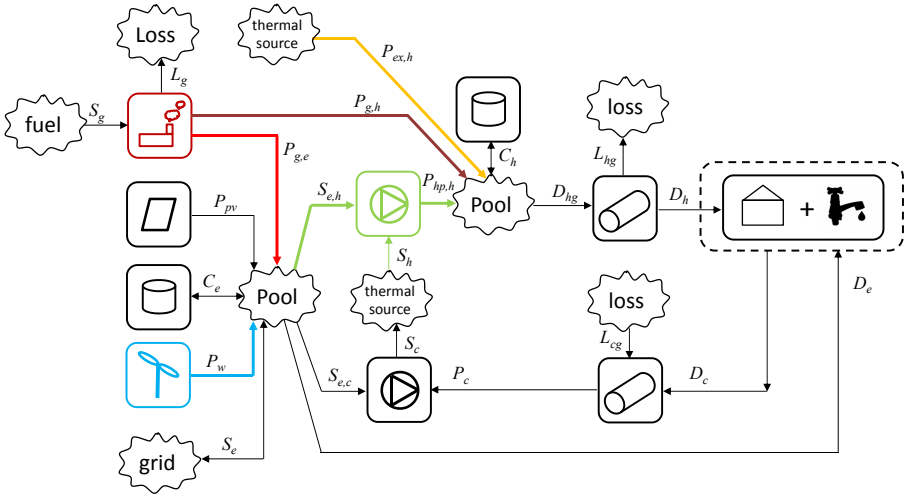

Figure 6.1 – global demand-supply scheme of modeling framework

ply is power to heat. Local or regional renewable electricity is transformed into heat by using heat pumps. As source for renewable electricity a large Photo Voltaic (PV) facility and regional wind turbine are considered. The wind turbine may compensate the production drop of solar PV energy in the winter period. It is investigated whether biofuel co-generation on a smaller scale may be valuable as a supplement to the power to heat option or not.
A global schematic which represents all these possible options is shown in Figure 6.1 for which the terms are explained in Table 6.1. The scheme does not include all possible renewable energy options, whereby the most important of these is solar thermal energy, either as a decentral or central system. A decentral installation, consisting of rooftop solar collectors and household scale storage is difficult to integrate within a district heating system and involves substantial additional costs, but offers only fuel or electricity savings, depending on the district heating generation concept. A central solar thermal system (collector field and large scale storage) is often not a feasible economical option in the Netherlands due to the required land space and associated property costs. This is the main reason why solar thermal energy was rejected by the Meppel district heating utility in an early stage of the project.
The scheme contains an "external" heat supply, which is in our case a natural gas boiler which is used to supply the residual heat demand which cannot be supplied by the configured renewable sources.

In the following subsections a modeling framework is developed for the scheme shown in Figure 6.1. The main purpose of the framework is to investigate the costs of energy supply and also the system component capacities which determine the equipment investment costs. For this type of analysis, an hourly time scale

Term	Signification	Group
S	energy from Source	
P	Produced energy by converter	
D	energy supplied to Demand	supply chain elements
C	energy Charged to/from storage	
L	Loss of energy	
h	heating	
c	cooling	energy functions
e	electricity	
g	generator (boiler/co-generator)	
cc	compression cooler	
pv	photo voltaic modules	converters
w	local wind turbines	
hp	heat pumps	
ex	external heating	
hg	heating grid	pipes or
cg	cooling grid	networks

Table 6.1 – energy model terms

seems to be sufficiently accurate, and is also convenient as this is also the time scale of weather data from weather stations around the world, from which heat demand and renewable energy generation is calculated. A limitation of the modeling framework is that the peak transport in the electric and thermal network in practice may be higher than the hourly average values given in the model. Hence, the modeling framework should not be used for final dimensioning of the electrical network (cables, transformers, power switches etc.) or the thermal network (pipe diameters, pumps, valves etc.).

6.3.2 Demand profiles (D_h, D_c, D_e)

In Chapter 3 a method is developed to generate hourly, aggregated demand patterns for heating (D_h), cooling (D_c) and electrical energy demand (D_e). Also, the demand patterns are shown for the district of 200 houses which are used in this chapter.

6.3.3 Solar PV and wind turbine generation (P_{pv}, P_w)

To calculate solar PV electricity production, the same relations are used as mentioned in Section 3.3 to translate global solar irradiation into radiation on the plane of the PV panels, which are assumed to be placed due South with a 40 degrees tilting angle. Hourly PV production in kWh/m^2 unit is calculated by multiplying the solar radiation on the PV panel with a constant state-of-industry efficiency of 16% for a PV system including PV module efficiency, inverter effi-

ciency and minor cable losses. For simplicity, the influence of module temperature on the electricity production is neglected. Solar PV is financially and juridically part of the local urban energy system as in most cases, home installations are payed for by the home owners or by the local energy utility.

Because larger wind turbines produce significantly more energy than required for 200 houses, wind turbines are financially and juridically assumed not to be part of the local urban energy system. In our model, wind energy is treated as a special form of grid electricity import. Priority is given to wind energy when it is available and an excess of wind energy is not stored in the electrical storage. The amount of available wind energy is determined by the production of a single wind turbine, for which we assume a state-of-industry 1.5 MW wind turbine with 80 meters axle height and 70 meters rotor diameter. The generation profile is determined in three steps:
(1) Application of the wind profile power law to calculate average hourly wind speed at axle height from the wind speed data at 10 meters height given by the same weather data as used for the solar PV production and thermal demand of the houses.
(2) Calculation of the possible wind turbine power production by the following kinetic energy relation:

$$P_w^* = C_p \cdot \frac{1}{2} \cdot \rho \cdot v^3 \cdot A \,, \tag{6.1}$$

in which C_p is the power coefficient which is estimated at 0.45 from supplier power curves, ρ the air specific density assumed to be constant at 1.25 kg/m^3. v is the air velocity at axle height and A the through-flow area of the rotor.
(3) Application of the following rules to determine the power production:

- if $v < 3$ then $P_w = 0$
- if $P_w^* > 1500$ and $v < 25$ then $P_w = 1500$
- if $v > 25$ then $P_w = 0$

The wind turbine produces a yearly amount of electrical energy equivalent to the yearly demand of 1000 households. Hence, for 200 houses, one fifth of the energy produced by the wind turbine is available when grid imports are required. Although the basic tariff for wind energy is somewhat higher than the basic tariff for "grey" electricity, there are no CO_2 costs involved for wind energy. Therefore, the total costs per unit (basic tariff plus CO_2 costs) are approximately equal to "grey" energy from the grid.

6.3.4 biofuel boiler and CHP generation ($P_{g,h}$, $P_{g,e}$)

For the biofuel boiler or CHP, we assume that the hourly production can be controlled in 10 equal increments between 0 and maximum power. To calculate the fuel requirement, a constant thermal efficiency of 0.95 and 0.62 for the boiler and CHP respectively are taken. The CHP electrical efficiency is assumed at 0.33 for

all control steps. Not that this is a simplification of the reality, and that efficiency of industry-standard CHP-installations usually drops for lower operation modes.

6.3.5 Heat pump and cooling generation ($P_{hp,h}$, P_c)

For the heat pump a constant Coefficient Of Performance (COP) of 3.8 is determined from thermodynamic heat pump cycle calculations with an evaporator temperature of 5 degrees and condenser temperature of 65 degrees Celsius and compressor efficiency of 88%. Pumping energy for the thermal source is included in the COP. For the generation of cooling energy, the COP of a lake source or aquifer is project-dependent. For both options the COP is estimated at 20. Practical performance of these options is reported in [187] and [128].

6.3.6 Thermal and electric storage (C_h, C_e)

A storage may have several functions within an urban energy system:

- Increase self-consumption: bridge the mismatch between production and consumption hours of energy produced locally by renewable energy generators like solar PV and wind turbines.
- Enable smaller generation capacities.
- Increase profitability: store (electric) energy at times of low energy prices, sell (electric or thermal) energy for higher prices.

The present analysis is limited to storage of energy with a daily charge and discharge pattern. Energy losses from the storage are assumed negligible but are included as part of future work.

6.3.7 Electricity grid import and export (S_e)

This chapter has a focus on self-consumption of locally generated renewable energy. The reasons for this are:

- In comparison to "grey" energy from the main grid, renewable energy is in general still more expensive to generate but has a lower market value when it is being exported to the main grid, i.e. it is financially often more attractive to self-consume the generated energy. However, the present situation for Dutch households is that by law an equivalent unit price is received for exports and levied for imports of electricity as long as the yearly exports don't exceed the imports. A yearly export surplus is multiplied with a much lower unit price and is therefore a less attractive situation.
- A capacity optimization on minimum energy costs which includes low prices for imports of "grey" energy from the main grid will lead to much less renewable energy generation and hence, counteract a greener energy supply.

- Self consumption within a neighborhood reduces energy transport losses on a larger scale.

- Many people like the idea to produce and consume their own energy.

To steer the optimization towards self-consumption, a higher constant price for grid imports is assumed and lower constant price for grid exports, which is realistic from the viewpoint of a utility who buys and sells electricity on the market. The values are based on present day average spot market price levels. Within the model, we did not introduce a pricing penalty on electricity peaks. However, the costs of transformers and cables within the model has a relation with the peak electricity values and these costs will increase with higher electricity peaks

6.3.8 Optimization model

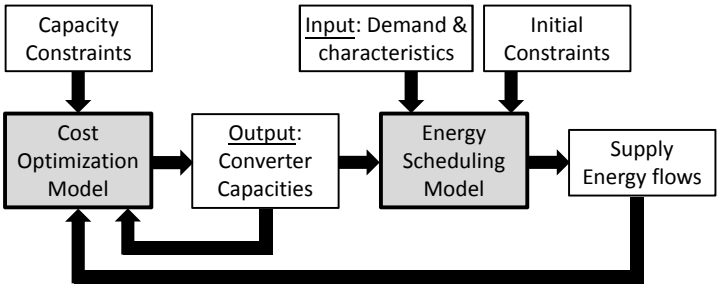

Figure 6.2 – General framework of the optimization model

It is common practice in the design of heating and cooling equipment to determine capacities based on the maximum heating and cooling demand. However, if the demand is supplied by a combination of different generators and partly by a storage, the determination of such capacities is no longer straightforward and simulations are a proper tool to determine the capacities. With multiple supply sources, the capacity of each generator should be related to the objective, which is in general a cost minimization. An iterative optimization model is developed for which the general framework is shown in Figure 6.2. Initial capacities are input to an energy scheduling model which is explained in Section 6.3.9 and which has hourly demand as input and supply energy flows as output. The supply energy flows are translated by the cost optimization model into operational expenditures. Through multiple iterations with a suitable solving method, generator capacities can be determined in relation to a predefined objective. The following objective for

the optimization is proposed:

$$\begin{aligned} &\text{Minimize } \sum_{j \in J} C_{j,capex} + C_{j,opex} + C_{import,grid} + \\ &\qquad C_{CO2,grid} + C_{CO2,ngas} - B_{export,grid} \\ &\text{variables: } X_j \\ &\text{subject to:} \\ &\qquad X_{min,j} \leq X_j \leq X_{max,j} \end{aligned} \tag{6.2}$$

in which:

- X_j signifies the capacity X of equipment j within a group of appliances J.
- J={biofuel CHP, biofuel boiler, heat pump, refrigerator, heat pump/natural cooling source, solar PV, thermal storage, electrical storage, grid connection, external heat}, i.e. J represents a set which constitutes energy converters, storage facilities and capacity dependent grid connection equipment.
- A wind turbine is not part of set J. The model calculates as last step the required electricity import from the grid. Within this import, wind energy has priority before import of "grey" electricity from the grid.
- Yearly capital expenditures (CAPEX) of the configured options from set J, consisting of the depreciation of investments, which is related to capacity by the following equation:

$$C_{j,capex} = \frac{X_j \cdot Y_{min,j}}{LifeTime_j} \cdot \left(\frac{X_j}{X_{min}} \right)^{-a} \tag{6.3}$$

  in which Y_{min} signifies the Investment Cost Per Unit Size or Capacity and X_{min} signifies the Capacity of equipment within set J, both for the smallest considered unit. The parameter a is a power law factor which is determined from various project related references on equipment investments. Values for these parameters are given in Table 6.3 at the end of this chapter. In this table, Y_{max} and X_{max} signify investment cost per unit size and capacity of the largest considered unit. $LifeTime$ signifies the service life of equipment within set J.

- Yearly operational expenditures (OPEX), consisting of two parts: (1) yearly maintenance costs expressed as fixed percentage of investments, (2) yearly costs of energy supply, e.g. fuel costs for which we write:

$$C_{fuel} = \sum_{t}^{\tau} C_{ngas,t} + C_{biogas,t} + C_{biomass,t}\,, \tag{6.4}$$

  in which the following signification is used: $ngas$ is natural gas consumption (external heat in the model), $biogas$ is biogas consumption of the CHP and $biomass$ is biomass consumption by the boiler. For the summation, τ is the set of hours per year. For cost parameters, we refer to Table 6.2 and 6.3.

- Costs (C) and benefits (B) of grid imports and exports, evaluated with a similar expression as Equation (6.4). The applied costs per unit energy are specified in Table 6.2. For simplicity reasons, yearly totals of the grid import and export are multiplied by fixed prices. In reality, dynamic electricity market prices could apply, e.g. varying hourly average prices, but this depends on the case circumstances. The used tariffs are given in Table 6.2.
- A penalty for CO_2 production applicable only for combustion of natural gas and imports of "grey" electricity. To steer the optimization more towards self-consumption, there is no CO_2 benefit within the objective for exporting renewable electricity to the grid. We introduce an artificial high price as the present average European trading price for CO_2 emissions of approximately 7 €/ton is by far not high enough to play a decisive role during the optimization. In [84] the effects of CO_2 trading prices on reducing emissions worldwide are investigated. To be an effective instrument for the world climate targets, a price in the range of 40-50 €/ton is concluded as a tipping point for large scale integration of green electricity production and storage. However, for heat generation within urban energy systems, we find with the model that 60 €/ton is the minimum CO_2 price level for which systems based on renewable energy are starting to be feasible as outcome of the optimization. The Dutch energy tax for household energy consumption can also be interpreted as a CO_2 tax. Presently, the energy tax is €0.25/m^3 natural gas and €0.10/kWh electricity. For natural gas combustion into heat, a ratio of 52 kg CO_2/GJ or 0.187 kg CO_2/kWh$_{th}$ is accounted for. For grid electricity, the ratio is deduced from [37] which states that the Dutch energy production sector emitted 53 MTon CO_2 in 2015 and according to [48] the production was 97 TWh in 2015. This leads to 0.558 kg CO_2/kWh$_e$. When the Dutch energy tax for households is interpreted as CO_2 tax, the present price is calculated at a minimum of €134/ton. Part of future work is to further investigate the relation between renewable energy system capacities and the price of CO_2 emissions.

equipment/process	fuel type	cost (€/kWh)
biofuel CHP	biogas	0.045
external heat supply	natural gas	0.028
biofuel boiler	wood chips	0.023
wind energy	-	0.11
grid imports	-	0.07
grid exports	-	-0.04

Table 6.2 – energy price parameters

The optimization problem is non-linear and convex. The convexity is dominated by the decrease of unit price with size, i.e. $f_j(\alpha x) \leq \alpha f_j(x)$ which applies to all

CAPEX and OPEX terms related to the use of equipment in set J. Excel's built in non-linear solver is used to solve this problem. The process involves some art to manually determine size constraint boundaries and then to apply local optimization with a randomized algorithm to increase the probability of finding a good solution. The process is time consuming but in this way, solutions can be found for all investigations considered in this chapter.
Note that the results depend on the CAPEX and OPEX parameters given in Tables 6.2 and 6.3. Although these parameters are the result of an investigation into cost information from projects across Europe, quotation information is subject to interpretation. Besides that, prices change in time and prices differ between countries, projects and suppliers. The given parameters are also limited within a certain size range, applicable for urban districts ranging in size from only a few houses up to approximately 2000 houses. Hence, Table 6.2 and 6.3 should be applied with great care or altered according to more recent or specific insights.

6.3.9 Energy scheduling model

In this section a model is developed for the global system shown in Figure 6.1, in the form of algorithms which express the scheduling order and the magnitude of energy generation and storage.
The main algorithm is given in Algorithm 6.1 and is listed together with the sub-algorithms at the end of this chapter.
For nomenclature of energy flow variables used in the algorithms, refer to Table 6.1. In the algorithms, E is electrical energy balance, T is thermal energy balance, t is the present time interval, and τ is the total evaluated time (8760 hours). The main algorithm contains 6 steps which are evaluated in consecutive order for each time step. Numbers used as index terms within the algorithms refer to these steps. As an overview, the steps contain the following evaluations:

1. In the first step, the electrical energy balance is calculated, taking solar PV generation and the demand into account. It is then verified whether it is the best decision to charge or discharge the electrical storage and to what amount, refer to Algorithm 6.2. For this, the heat demand and the possibility to use electrical energy for the heat pump is taken into account through control variable $CE_{1,t}$ (value: 0 or 1). In case of surplus renewable electricity production, priority is given to heat production, $CE_{1,t} = 1$ (if possible and required) or to electrical storage, $CE_{1,t} = 0$.
2. In the second step, the heat pump production from the surplus renewable electricity production is calculated when applicable, refer to Algorithm 6.3.
3. The third step involves a more complicated consideration for charging or discharging the thermal storage, depending on storage status and thermal demand. Also, the storage or demand can be charged or supplied by either a biofuel boiler or CHP. In case of a CHP, a heat pump may consume the generated electricity and become a co-producer of heat. Heat production of

the CHP is split into two parts: a part which generates heat for charging the thermal storage, $PT_{g,h,t}$, and a part which generates heat for the heat grid demand, $PHG_{g,h,t}$. The possible heat production of a heat pump, $P_{hp,3,t}$ is during this step limited by the total generated electrical energy by the CHP, but the CHP may produce more heat and electricity when required, refer to Algorithm 6.5. The decision to charge or discharge the thermal storage is expressed by control variable $CT_{3,t}$ (value: 0 or 1) which is determined by Algorithm 6.4. The decision is determined by the thermal storage state (Q_{t-1}), a safe minimum thermal storage state which is related to the seasonal heat demand (Q_{min}) and the maximum storage state (Q_{max}). Once the heat generation of the biofuel generators and heat pump are determined, the charging or discharging energy of the thermal storage is calculated by Algorithm 6.6.

4. In the fourth step, the thermal and electrical energy balances are calculated to determine if charging of the electrical storage is possible and to what amount, refer to Algorithm 6.7.
5. The fifth step evaluates the remaining heat grid demand and determines the possibility and amount of heat production by the heat pump, for which electricity from the grid is imported in case the electricity energy balance is negative (shortage), refer to Algorithm 6.8 in which the required import from or export to the electricity grid is calculated. In this algorithm, priority is given to wind energy and if this is insufficient, then additionally, "grey" electricity is imported.
6. In the sixth step the remaining heat demand is calculated. To balance this, generation by the external heat supply is calculated in Algorithm 6.9.

The following assumptions and principles for the generators and storage facilities are taken into account:

- The electrical storage is charged and discharged in complete cycles as much as possible in order to improve lifetime of batteries.
- The thermal storage is only charged by the biofuel CHP or boiler and not by the heat pump (due to lower temperature of heat production from a heat pump) or by the external heat supply.
- There is a maximum charge and discharge rate for all storage facilities which is determined by the maximum generation and storage capacities.
- To avoid unnecessary charging and thermal losses during periods with low heat demand, the maximum state of charge of the thermal storage is related to the longer term average heat demand around the present time interval. In practice this can be achieved with a storage which contains multiple heat exchangers and which is thermally stratified.
- The heat pump and external heat supply have an infinite number of operational states between zero and maximum heat production and follow the demand without any time delay.

- The biofuel generators are scheduled in a limited number of discrete production steps. An operational state is maintained for at least two hours, i.e. to increase efficiency and lifetime.

6.4 Results

Four renewable energy system concepts are considered:

1. Bio-heat: biofuel boiler, solar PV, wind energy, thermal and electrical storage, natural cooling source.
2. All-electric: heat pump, solar PV, wind energy, aquifer thermal source and electrical storage.
3. Mixed: biofuel CHP, heat pump, solar PV, wind energy, aquifer thermal source, thermal and electrical storage.
4. Near autonomous: the same as the Mixed concept but optimized for minimal exchange of grid electricity.

In the following, we discuss the results for these concepts.

6.4.1 Equipment size

For the reference case, the peak capacity of the boiler is determined by the peak heat demand. For the four renewable energy system concepts, generation capacities are determined by optimization and the results are shown in Table 6.4 at the end of this chapter.

6.4.2 Sensitivity analysis

The influence of varying the capacity values on the objective that is found as best possible solution is shown in Figure 6.3 for Concept 3 (other concepts show similar results). This figure shows five lines of which four lines show a single capacity variation (see horizontal axis for the variation percentage) of the heat pump, the CHP, solar PV area and the thermal storage size. The fifth line concerns simultaneous variation of these capacities. The vertical axis shows the percentage increase of the objective function, relative to the objective value shown in Table 6.4.

Observe that a relatively large variation of the capacities (25%) results in a relatively small increase of the objective function. Also, the relation appears to be non-linear. Besides that, variation of the thermal storage size has a minor influence.

6.4.3 Energy flows

The total yearly electrical and thermal production and consumption are shown in Tables 6.5 and 6.7 (shown on the last pages of this chapter). Besides that, the

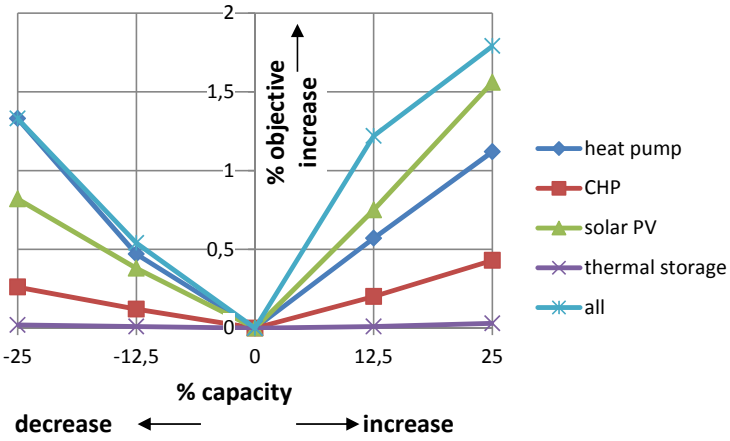

Figure 6.3 – Capacity variation sensitivity for concept 3

yearly grid import and export totals together with the highest occuring hourly peak values are shown in Table 6.6. The electrical demand of the case reference is slightly higher than for the other concepts because the reference requires more electrical energy for cooling due to a lower Coefficient of Performance for cooling. In the following we discuss for Concept 1 to 3 the achieved percentage self-consumption and percentage renewable energy used to supply the heat demand. Results of Concept 4 are further discussed in Section 6.4.4.

For Concept 1, 74% self-consumption of solar PV energy is achieved and 36% of the total electrical demand is imported from the grid. The heat demand is for 78% supplied by biofuel and the remaining part (22%) by the natural gas boiler (external heat).

For Concept 2, 73% self-consumption of solar PV energy is achieved and 44% of the total electrical demand is imported from the grid. The heat demand is for 73% supplied by the heat pump and the remaining part (27%) by the natural gas boiler.

For Concept 3, 88% self-consumption of solar PV and CHP electrical energy is achieved and 22% of the total electrical demand is imported from the grid. The heat demand is for 34% supplied by the CHP, for 50% by the heat pump and the remaining part (16%) by the natural gas boiler.

To evaluate hourly energy flows, results for two test weeks are shown in Figure 6.4. The first diagram shows electrical energy flows and the second diagram the thermal energy flows for the first week. The left axis scales the hourly energy flow values and the right axis the storage charge state. The test weeks consist of (a) a summer week with abundant sunshine and (b) the coldest week in the winter. To avoid a lengthy discussion of the concepts, the results are only shown for Concept 2 to demonstrate the interaction between electrical and thermal energy generation and demand.

During the summer week, a daily pattern of storage of excess solar PV energy is visible. The electrical demand, consisting of household demand and demand by

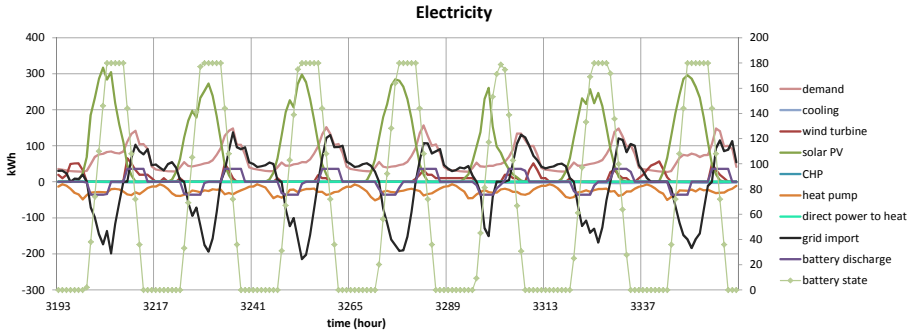

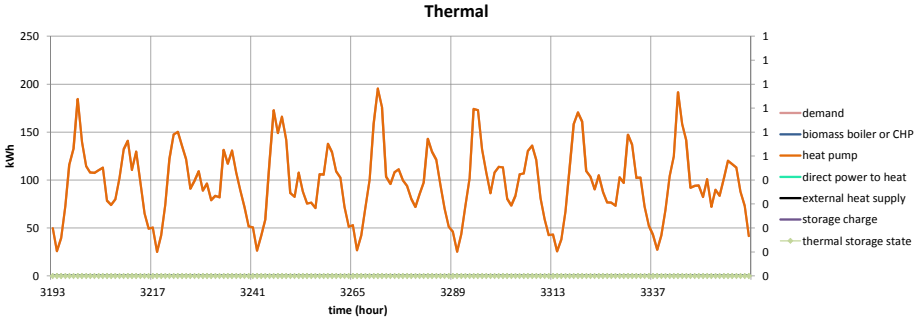

(a) power to heat, summer

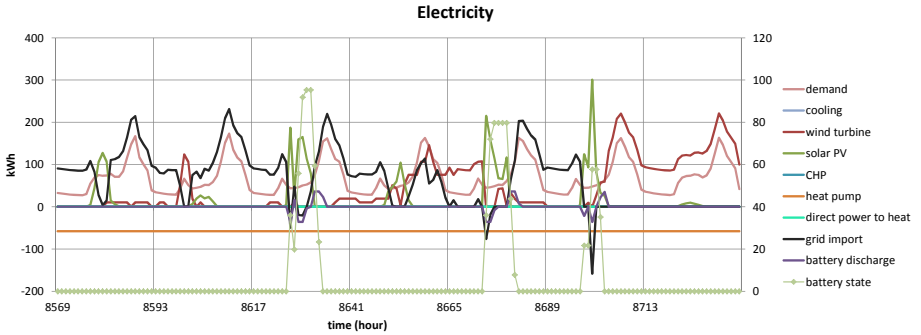

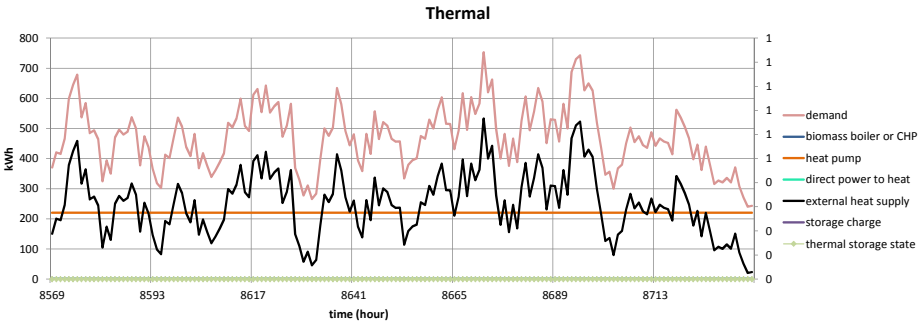

(b) power to heat, winter

Figure 6.4 – Energy flows concept 2

the heat pump is mainly supplied by solar PV, electrical storage, wind energy and some imports from the grid. The thermal demand is supplied entirely by the heat pump. We further observe a minor contribution of wind energy during this period. The electricity flows during the winter week are entirely different. During that week, there is a lack of solar energy but this is compensated by a much larger contribution of wind energy. Hence, there are only a few moments of electricity exports, while large amounts of electricity are imported from the grid. The heat pump is running continuously with additional support of the natural gas boiler (named external heat in the figure). We further observe that wind energy supplies the entire electrical demand on some days, but on some days has only a minor contribution. However, on the latter days there is also insufficient solar energy. Based on these results we may conclude that on some days, wind and solar energy compensate each other, meaning that on days with a lot of solar energy, there appears to be little wind energy and vice-versa. However, the results also show that on some days both sources are insufficient.

6.4.4 Reaching near energy autonomy

Concept 3 generates electricity by the CHP during periods of insufficient solar PV and wind energy generation. Hence, the concept provides a possibility to reach near energy autonomy, which is defined as: zero consumption of natural gas and zero imports of "grey" electricity from the grid. To find the best possible capacities for such a system, a different optimization objective is required which steers more rigorously towards zero CO_2 production and low grid energy exchanges. Simply increasing the penalty on CO_2 production appears to be insufficient and leads to high storage costs and large feed-in electricity peaks of renewable energy to the grid, which increases grid dependency. A penalty multiplication factor of 10 is introduced for the CAPEX and OPEX of the grid connection equipment and a factor of 100 for the CO_2 costs. Besides that, the energy model is extended with a method to directly dissipate surplus electrical energy into heat. This method is named "direct power to heat" and implemented in the main algorithm after step 2. As result, the yearly electrical and thermal production totals are shown in Tables 6.5, 6.6 and 6.7. From the very small yearly natural gas consumption and grid import, we may conclude that this concept is indeed nearly energy autonomous. The resulting generation capacities are shown in Table 6.4. The objective function in the last column is in this case not the objective used during the optimization, while this has little practical use due to the high penalties. Hence, the same objective is shown as for the other three renewable energy concepts to enable direct comparison.

Hourly energy flows for the summer and winter week are shown in Figure 6.5. The interaction between electrical and thermal energy generation, energy storage and energy supply is very dynamic. During the summer week, the high solar PV generation leads to interactions with electrical storage, with the heat pump and also results in direct power to heat scheduling. Combined with some moments

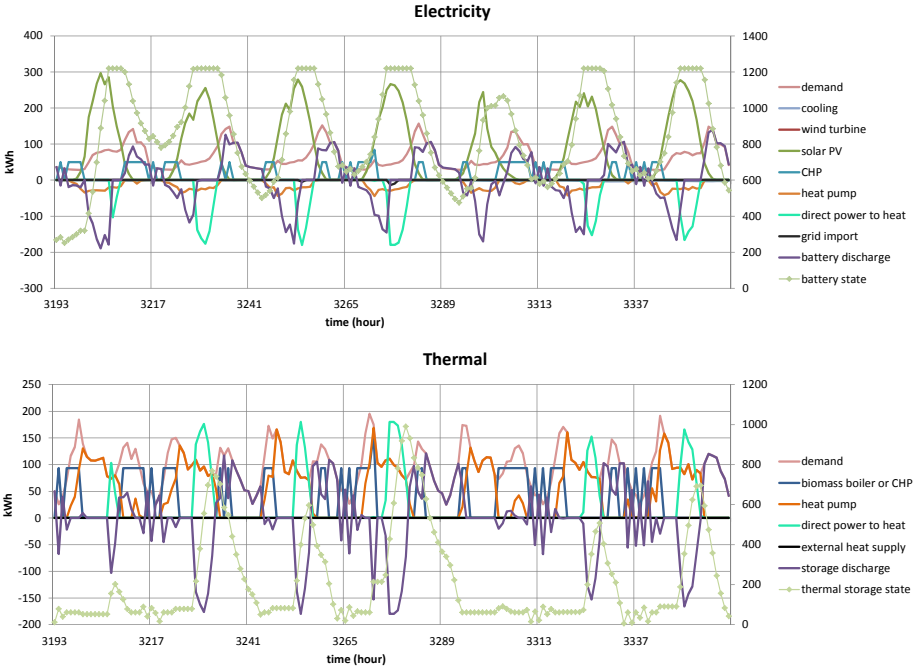

(a) near autonomous, summer

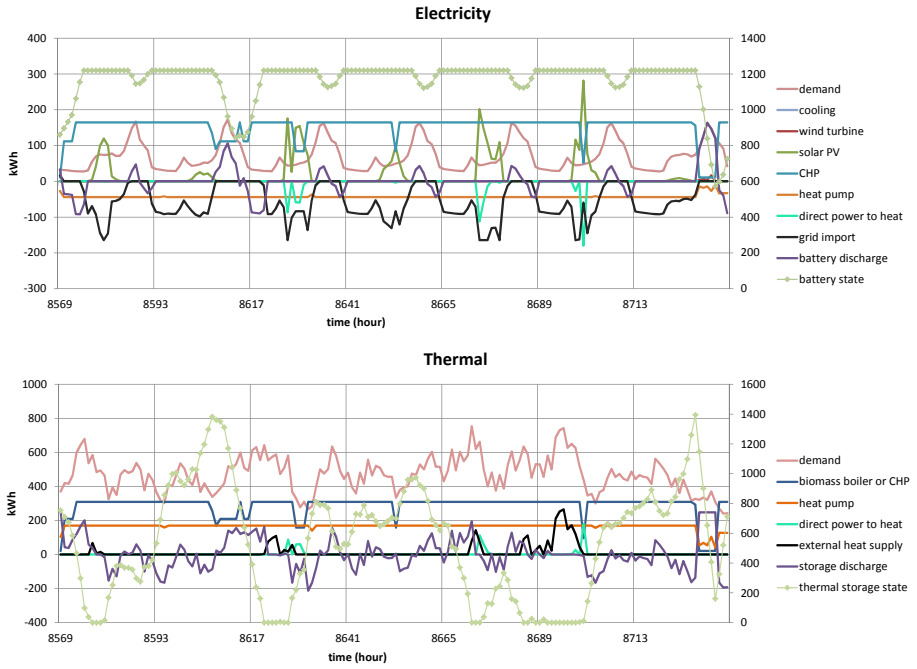

(b) near autonomous, winter

Figure 6.5 – Energy flows near autonomous concept

when the CHP produces electricity, there is no electricity exchange with the grid during this week. The winter week shows an almost constant operation of the CHP and of the heat pump, while the natural gas boiler is only required for a few hours. However, the system is producing too much electrical energy and is mostly exporting electrical energy to the grid during that week. Hence, the direct power to heat option could have been implemented in a smarter way, e.g. by including a forecast of the thermal demand, such that a higher thermal storage state of charge is maintained which would avoid any natural gas consumption and also limits electricity exports.
The use of the electrical and thermal storage capacity is significant and large storage capacities are found as result, i.e. 1220 kWh electrical and 1410 kWh thermal capacity. This is equivalent to a battery of 6.1 kWh per house and 7.1 kWh or 95 liters (domestic water tank) thermal storage per house. Energy losses due to electrical and thermal storage are more significant for these larger storage sizes and therefore we will include these losses as part of future work.

6.4.5 Economical and environmental analysis

The optimization objective (see Equation (6.2)) is used to verify the economically most attractive concept in relation to the environmental performance. In Figure 6.6, the costs which are included in the objective are shown for the case reference and for the four renewable concepts. Note that the CO_2 costs are introduced in the objective with an artificial high price of 60 €/ton.
The costs for the case reference are dominated by fuel costs and electricity im-

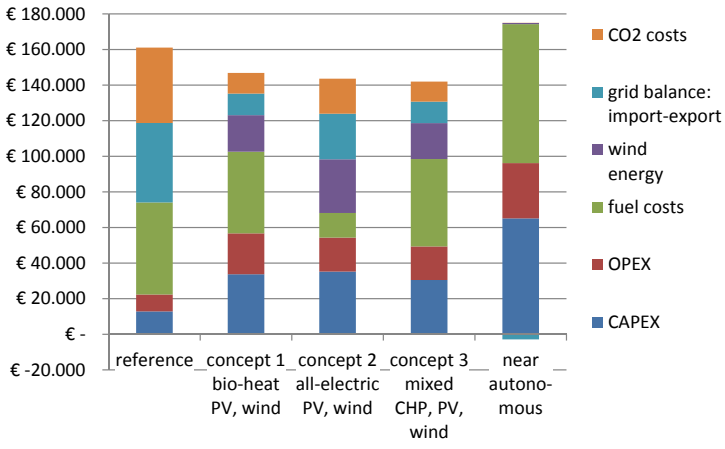

Figure 6.6 – Comparison between concepts

ports, as the accompanying CAPEX and OPEX are low. The renewable energy concepts show much higher CAPEX and OPEX, with the highest costs for the near autonomous concept. The high costs for this concept are dominated by expensive

biogas for the CHP and high investment costs for the batteries. However, this may change in the future: subsidies may be given on the biogas and new battery technologies presently in different levels of technology readiness may become much cheaper. When we consider as special variants, a decrease of 50% for the costs of batteries (Variant 1), an equal price per kWh for the consumed biogas as the present price of natural gas (Variant 2), and a combination of both (Variant 3), the following results are obtained:

1. Variant 1: 159,264 €/y, which approximately equals the yearly costs of the case reference.
2. Variant 2: 140,206 €/y, which approximately equals the yearly costs of Concept 1 and 2.
3. Variant 3: 129,263 €/y, which is lower than the costs of all other concepts. However, the costs of Concept 3 should also be updated with the same biogas price reduction. In that case, the costs of Concept 3 are: 125,370 €/y. From this we conclude that if in the future, the price of batteries reduces by more than 50% and the price of biogas per kWh equals the price of natural gas, near autonomous energy concepts are financially attractive.

For Concepts 1 to 3, wind energy is an important source to supply the electrical demand. However, Concept 4 requires almost no electricity imports and hence also no wind energy. From this we conclude that a CHP is a better alternative than wind energy to reach near energy autonomy.
Concept 2 has the largest electricity costs while Concept 3 has the largest fuel costs due to the high price of biogas. However, the biogas price we used for Concepts 3 and 4 is below the present day market price, otherwise a biogas CHP would not come out as feasible. Hence, feasibility of Concepts 3 and 4 on the short term is questionable but this depends on possible subsidies for the biogas.
Concept 1 depends on the market price of wood chips. At present this price is more or less stable but when more urban energy projects decide to implement a biomass boiler, the availability of wood chips may decrease and the price may increase.
We should also compare the concepts without the artificial high price of CO_2. We then conclude that Concept 2 is presently the most attractive renewable concept while the costs are only slightly higher than the case reference. However, the concept depends more than the other concepts on grid electricity imports and natural gas consumption to support the heat production. Hence, Concept 2 performs less on CO_2 emissions than the other concepts. Concept 2 reduces emissions by approximately 53% compared to the case reference, but Concept 1 and 3 reduce emissions by 73%.
For the coming 5 to 10 years, the following influences are important for Concept 2:

- natural gas prices in the Netherlands are expected to rise due to recent policies in favor of stimulating the energy transition away from natural gas consumption. It could be an option to connect the energy system of Concept 2 with a biogas network to eliminate the natural gas consumption entirely, and

- due to recent large scale offshore wind energy implementation plans, the percentage green energy of the electricity grid is expected to rise the coming years. This will result in lower CO_2 production for Concept 2 in the future.

Note that not all costs and benefits are part of the objective function. Other costs include: a building for the central generation and storage equipment, the district heating network, household connections and energy consumption meters, organizational costs, insurances. Benefits include: heat sales revenues and electricity sales revenues. Hence, the cost comparison we present should not be used directly as a business case evaluation of the concepts.

6.5 Application within a collective or individual heating system

At present, the most common way of heating houses in the Netherlands is by individual natural gas boilers. This is why further development of individual directions receives much attention. Individual alternatives for Concepts 1 to 3 are:

- Individual Concept (IC) 1: household wood pellet boiler, rooftop solar PV, household scale thermal and electrical storage.
- Individual Concept (IC) 2: household heat pump with ground thermal source, rooftop solar PV, household scale thermal and electrical storage.
- Individual Concept (IC) 3: biogas micro CHP/boiler combination, household air source heat pump, household scale thermal and electrical storage.

As a wood pellet boiler emits harmful particles through its flue gasses, IC 1 should only be applied within less densely populated areas. However, IC 2 and IC 3 can be applied within densely populated areas without such problems.
Large scale application of IC 2 may become problematic for existing power grids. Due to other types of electrification, such as electric vehicles, IC 2 results in a large increase of electrical demand and high demand peaks which could lead to costly grid strengthening measures in low voltage power grids. For a large part this can be solved by local renewable energy generation, electrical storage and smart control, which is demonstrated in [123].
The individual biogas route or IC 3 is attractive from the side of the existing infrastructure and continuation of using household boilers. However, it requires large scale production of green-gas. Biogas can be upgraded or in a further future, power to gas techniques may be applied. At this moment, such technology is insufficiently mature in terms of the technology readiness level and the economy of scale. Hence, green-gas still has a relatively high cost at present in comparison with the other options.
The comparison between the collective and individual energy system approach is interesting in many ways. Within the collective approach, a district heating system which interacts with the power system through power to heat, but which

also contains different heat generators and methods of energy storage, provides an interesting platform for the integration of renewable energy. On the other hand, within the individual approach, interactions between a "greener" power system and a future "greener" gas network may provide a similar platform for the integration [146]. It is well known that the choice for a certain infrastructure dominates further developments and possibilities for many decades. To make a choice between an individual or collective system, we should at least consider:

- local possibilities and chances to integrate renewable energy. Some renewable options like waste heat simply require a collective heating system,
- the involved costs, i.e. the costs of new district heating infrastructure versus the costs of individual supply systems. Today, individual natural gas boilers have a very low cost, while individual renewable heat options (e.g. heat pumps and a suitable source system) are much more costly. At this stage, a collective system may be a more economical choice, and
- effects on local economy and jobs. Individual heat converters are connected to larger systems, i.e. the national gas and power grid. Collective heating systems usually operate on a local or regional scale. The development and operation of district heating systems therefore offers more opportunities for local or regional job creation which is an attractive outlook in today's society. The same can be said about house renovations with the purpose to improve energy efficiency. There are many houses to renovate and the process is labor intensive which creates jobs for a relatively long period of time. Combining house renovations, district heating and integration of renewable energy creates local jobs which is one of the successes of the Danish energy transition and a cornerstone of the fourth generation district heating concept [97]. This may also be an attractive perspective for many regions in the Netherlands.

Further investigation into these considerations is part of future work and for instance part of the WIEfm-project [181].

6.6 Governance aspects

Important governance aspects which are already discussed in the previous sections are supportive tax and subsidy schemes to create more attractive business cases for renewable energy systems. However, for the Meppel case, another important aspect is the regulation of permits for utilities. For the electricity sector, the country is divided into several regions and for each region there is only one utility with a permit to operate and maintain the low voltage electricity grid. In Meppel, the low voltage grid utility is a different company than the utility who operates the district heating network. This appears to be an obstacle for the integration of renewable energy as the district heating utility is not responsible for the supply of household electricity and is therefore also not rewarded for the integration of renewable energy for which interactions between the heat and power grid are beneficial, as this chapter demonstrates. The renewable energy concepts presented

in this paper produce significant amounts of renewable electricity for which it is assumed that the utility is able to sell this to the households for an interesting price. To achieve this, specific solutions are required, such as:

- both utilities (district heating operator and power grid operator) participate or at least agree on beneficial tariffs for the import and export of electricity between the district heating and the low voltage power system, or
- a local, private Energy Service Company (ESCO) takes over the ownership and operation of the district heating and the low voltage power grid. This possibility is offered by the Dutch government, provided that all households are within the same postal code and all citizens within that district agree. This solution enables a local exchange market for generation and supply of renewable electricity and heat, with prices that are independent from the larger power grid.

With one of these solutions, it is possible to implement a renewable energy concept of choice from the concepts discussed in this chapter in such a way that the proposed business case may actually be positive. In the coming years we expect that more public and private partnerships are established in the Netherlands which gain experience with these solutions.

6.7 Alternative routes

The case study to this point focused on achieving a CO_2 neutral collective energy system by integration of large shares of renewable energy. However, the current practice in the Netherlands often shows different levels of ambitions and different routes as an alternative, which are also important to consider for the Meppel case. We discuss the following alternatives:

Alternative 1
The case reference is extended with a natural gas co-generation unit. This saves CO_2 emissions due to lower electricity grid imports. However, if in the future the share of renewable energy within the power grid increases to 50% (presently 15%), the positive effect of co-generation on CO_2 emissions vanishes.
Using the energy model presented in this chapter with the optimization objective discussed in Section 6.3.8, the following capacities are determined for the CHP: 180 kW thermal and 96 kW electrical output. The resulting costs are shown in Figure 6.7, (Alt. 1). Compared with the case reference, the CAPEX, OPEX and fuel costs increase, but grid imports and CO_2 costs decrease to a larger extend. Economically, this variant is at present the most attractive option, although the difference with the case reference is small when CO_2 costs are neglected.

The following alternatives have the upcoming Near Zero Energy Building (NZEB) standard as starting point. From 1995, building standards in the Netherlands gradually include more restrictive limits for building heat losses. Towards 2020,

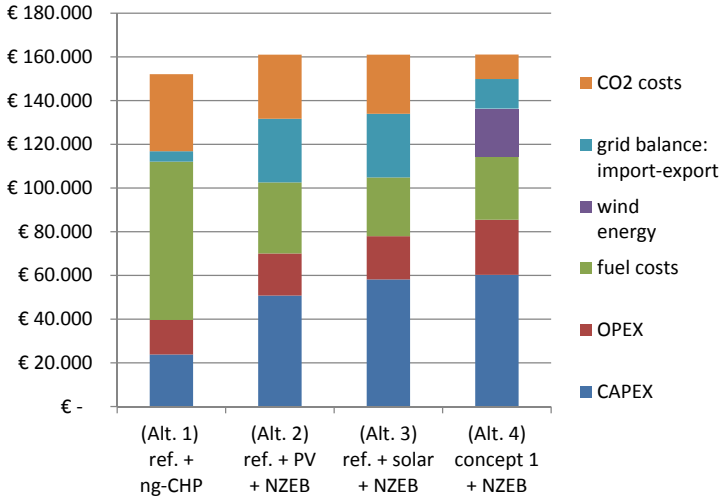

Figure 6.7 – Costs (optimization objective) for alternative variants

the limits are further reduced to the level of the European NZEB standard. The 200 houses of the Meppel case reference, are built according to the 2012 and 2014 building standard and thus have an EPC (Energy Performance Coefficient) of 0.8 and 0.6. On average, the requirement for space heating per house is calculated at 28 GJ/y. In case of NZEB this should be approximately reduced to 50% of that value, i.e. 14 GJ/y. This is accomplished by the following measures:

- higher insulation properties of walls, windows and doors,
- improved airtight construction details of the house, and
- heat recovery equipment for ventilation and shower water.

These measures involve additional investments. If a new house is built today, we estimate additional investments in the order of €15,000 per house in order to build the house according to the NZEB standard. However, from 2020 the NZEB standard is mandatory and we expect additional investments to be lower due to economy of scale effects. As we do not know the future investment required for building a NZEB house, we decided to determine for the following alternatives which additional investment is allowed in order to reach the same yearly costs as the case reference. To calculate this, the investments are depreciated within 50 years and operational costs associated with the measures mentioned above are calculated as fixed percentage (0.5%) of the investment.

Alternative 2
The case reference is now built with NZEB houses and solar PV is installed to generate electrical energy. The size of the PV-system is determined at 1780 m^2 by the optimization procedure introduced in Section 6.3.8. To reach the same yearly

costs as the case reference, €6,525 per house is allowed as investment to achieve the NZEB standard. Compared to the case reference, CAPEX and OPEX increase significantly, but fuel costs, grid imports and CO_2 costs decrease, see Alt. 2 in Figure 6.7.

Alternative 3
Besides Alternative 2, a solar thermal collector and thermal storage are installed for each house. The solar thermal collector partly supplies the demand for domestic hot water which reduces the heating demand and thus reduces fuel costs. The costs for the solar thermal installation are included in the costs of the energy system. To reach the same yearly costs as the case reference, €4,680 per house is allowed as investment to achieve the NZEB standard. Compared to Alternative 2, the CAPEX and OPEX further increase due to the solar thermal installation costs. However, fuel costs and CO_2 costs decrease, see Alt. 3 in Figure 6.7.

Alternative 4
NZEB houses are now combined with Concept 1 (bio-heat + solar PV + wind energy). The following capacities are determined by the optimization procedure introduced in Section 6.3.8: biofuel boiler: 136 kW thermal output, solar PV: 1404 m^2, thermal storage: 135 kWh, electrical storage: 50 kWh. To reach the same yearly costs as the case reference, €8,410 per house is allowed as investment to achieve the NZEB standard. Alt. 4 in Figure 6.7 shows that compared to Concept 1, this alternative has higher CAPEX and OPEX costs. However, the fuel costs are decreased, which also reduces the vulnerability of Concept 2 for biomass price fluctuations.

6.8 Conclusions

In this chapter, a model for capacity optimization of renewable urban energy systems is developed. Demand data is generated by simulations for a case study involving 200 houses which are part of a new urban district in Meppel, the Netherlands. The following renewable energy concepts to replace the case reference (central natural gas boilers for heating, an electric refrigerator for cooling and "grey" electricity for the electrical demand) are investigated:

1. Bio-heat: central biomass boiler, solar PV, regional wind energy, supported by thermal and electrical storage, cooling by lake or ground source with high COP,
2. All-electric: central heat pump, ground source, solar PV, regional wind energy, supported by thermal and electrical storage, cooling by ground source with high COP,
3. Combined: central biogas CHP, central heat pump, solar PV, regional wind energy, supported by thermal and electrical storage, cooling by ground source with high COP, and

4. Near autonomous: the same as Concept 3 but with more renewable energy generation and storage to reach energy autonomy.

Generation and storage capacities are determined for each concept based on optimization with a general formulated objective.
Results depend on the CO_2 price level for which €60/ton is assumed. Although the present market value of CO_2 emissions is only €7/ton, much higher prices levels are needed for feasible renewable energy systems. However, if Dutch energy taxes for households are interpreted as CO_2 tax, the evaluated CO_2 price level is still moderate. As part of future work we will investigate in more detail the influence of CO_2 emission prices on the system capacities.
A cost comparison and environmental comparison on CO_2 emissions between the renewable concepts and the case reference shows that although the case reference is financially more attractive at present, it is environmentally the least attractive. The renewable concepts show a change in the dominating cost factor, from high fuel costs (case reference) towards high CAPEX and OPEX costs (renewable concepts). The all-electric concept (Concept 2) is financially the most attractive of the renewable concepts, but the bio-heat and combined concept perform better on CO_2 emissions. The combined concept (Concept 3) can be extended to a near autonomous concept (Concept 4), thereby requiring almost no natural gas consumption or energy imports from the grid, resulting in almost no CO_2 emissions. For this concept much larger electric and thermal storage sizes are found. Part of future work is to include energy losses due to the intense use of the electrical and thermal storage. The near autonomous concept is at this stage financially less attractive, mainly due to the high price of biogas and higher investment costs. In the future, cheaper batteries and subsidies on biogas may have the result that Concept 4 is one of the most attractive concepts.
The energy flows of the all-electric concept show relatively high grid peak imports and exports which cannot be avoided by energy storage alone. Hence, this concept could benefit from smart grid control of the heat pump, direct injection of power to heat into a thermal storage and smart charging of the electrical storage. Further flexibility for this is offered by the thermal capacity of the houses, thermal storage, electrical storage and possibly some household electrical devices. In the next chapter we develop a smart control method in order to balance electricity production by a single CHP and demand of a large group of domestic heat pumps. Triana, a smart grid control method developed at the University of Twente, may be applied for the control cases of this paper, for examples see [169], [109] and [22], but also the results presented in Chapter 8. As part of future work, we intend to develop an urban energy analysis tool which includes energy priority algorithms and methods of smart control in order to investigate effects of smart control on system capacities and energy flows. As proposed in the related work section of this chapter, the next step of future work is to verify the results of this paper with Energyplan, using the least cost and least CO_2 scheduling methods of Energyplan. Furthermore, the complexity of governance aspects is addressed for situations like the Meppel case. There are two different utilities, one with a permit to operate the

electricity grid and the other with a permit to operate the district heating network. This appears to be an obstacle for a positive business case for one of the renewable energy concepts presented in this paper. One solution is to establish a joint venture between the two utilities, another is to establish a citizen involved local Energy Service Company who takes over the ownership of both local networks and creates a local energy exchange market.

Finally, this chapter investigates the influence of a further reduction of the heat demand through the Near Zero Energy Building (NZEB) standard. As such houses are not yet mandatory, we investigate the required additional investment for NZEB houses compared with the houses that have been built so far in Meppel. As result, investments are determined in a range between €4,680 and €8,410 per house for three alternatives in order to reach the same yearly costs as the case reference. In the near future (from 2020), when houses according to the NZEB standard are mandatory, such investments may be realistic due to economy of scale effects.

equipment	unit	Y_{min} €/unit	Y_{max} €/unit	X_{min} unit	X_{max} unit	a	Life Time years	maintenance %
biofuel CHP	kW_e	2000	1400	50	1000	0.125	15	4
external heat supply	kW_{th}	60	40	50	1000	0.132	15	4
biofuel boiler	kW_{th}	1200	800	50	1000	0.129	30	4
solar PV	kW_p	1600	900	10	1000	0.125	25	1
heat pump/refrigerator	kW_{th}	500	360	50	500	0.148	20	4
heat pump/cooling source	kW_{th}	1200	750	5	3,333	0.065	50	2
thermal storage	kWh	70	40	10	2500	0.096	50	1
electrical storage	kWh	300	150	10	2000	0.145	10	2
grid connection cables & transformers	kW	140	26	100	1000	0.780	25	3

Table 6.3 – CAPEX, lifetime and maintenance parameters

concept	external heat supply kW	heat pump kW	biofuel boiler CHP thermal kW	CHP electric kW	solar PV m^2	thermal storage kWh	electric storage kWh	objective function €/y
reference	752							161,073
1	511		241		1570	250	200	146,861
2	532	500			2140	0	180	143,613
3	501	161	90	48	1400	150	0	141,982
4	265	169	309	164	2004	1410	1220	172,134

Table 6.4 – Production unit capacities for the case reference and 3 renewable energy concepts

concept	household electric demand	cooling electric demand	wind turbine production	solar PV production	direct power to heat	CHP electric production	heat pump consumption
reference	-576,449	-61,519					
1	-576,449	-7,690	186,618	351,110			
2	-576,449	-7,690	274,345	345,004			-360,222
3	-576,449	-7,690	183,643	225,704		283,039	-251,986
4	-576,449	-7,690	5,647	323,039	-47,658	571,720	-195,416

Table 6.5 – Yearly total electrical production (positive) and consumption (negative) (kWh/y)

concept	grid import (kWh/y)	grid export (kWh/y)	peak import (kW)	peak export (kW)
reference	637,968		212	0
1	211,821	-67,511	173	-173
2	420,264	-95,342	231	-231
3	209,861	-66,123	167	-167
4	2,182	-75,314	142	-164

Table 6.6 – Electrical imports and exports

concept	heat grid demand	biofuel boiler or CHP production	heat pump production	direct power to heat	external heat production
reference	-1,867,817				1,867,817
1	-1,867,817	1,464,052			403,641
2	-1,867,817		1,368,845		498,973
3	-1,867,817	531,771	957,546		378,452
4	-1,867,817	1,074,140	742,582	47,658	3,080

Table 6.7 – Yearly total thermal production (positive) and consumption (negative) (kWh/y)

Algorithm 6.1: Main algorithm: energy scheduling order

Input: D_{hg}, D_c, D_e ... the aggregated demand
Input: P_w, P_{pv} ... the aggregated non-scheduled renewable electricity production
Input: Q_i, E_i ... the initial thermal and electrical storage state of charge

foreach $t \in \tau$ **do**
  begin Step 1
    $E_{1,t} = P_{pv,t} - D_{e,t} - S_{e,c,t}$
    $C_{e,1,t} =$ **function**(Echarge1)
  end
  begin Step 2
    $E_{2,t} = E_{1,t} + C_{e,1,t}$
    $P_{hp,2,t} =$ **function**(HeatPump2)
    $T_{2,t} = -D_{hg,t} + P_{hp,2,t}$
  end
  begin Step 3
    $E_{3,t} = E_{2,t} - \frac{P_{hp,2,t}}{COP_h}$
    $PT_{g,h,t} =$ **function**(TSproduction3)
    $P_{hp,3,1,t} =$ **MIN**$\left(-T_{2,t}; PT_{g,h,t} \cdot \frac{eta_{e,chp}}{eta_{t,chp}} \cdot COP_h; P_{hp,max} - P_{hp,2,t}\right)$
    $T_{3,1,t} = T_{2,t} + P_{hp,3,1,t}$
    $\left[PHG_{g,h,t}; P_{hp,3,2,t}\right] =$ **Procedure**(BioFuel3)
    $P_{g,h,t} = PT_{g,h,t} + PHG_{g,h,t}$
    $P_{g,e,t} = P_{g,h,t} \cdot \frac{eta_{e,chp}}{eta_{t,chp}}$
    $P_{hp,3,t} = P_{hp,3,1,t} + P_{hp,3,2,t}$
    $T_{3,2,t} = T_{2,t} + P_{g,h,t} + P_{hp,3,t}$
    $C_{h,t} =$ **function**(TScharge3)
    $Q_t = Q_{t-1} + C_{h,t}$
  end
  begin Step 4
    $T_{4,t} = T_{2,t} + P_{g,h,t} + P_{hp,3,t} + C_{h,t}$
    $E_{4,t} = E_{3,t} + P_{g,e,t} + \frac{P_{hp,3,t}}{COP_h}$
    $C_{e,4,t} =$ **function**(Echarge4)
    $E_t = E_{t-1} + C_{e,1,t} + C_{e,4,t}$
  end
  begin Step 5
    $E_{5,t} = E_{4,t} + C_{e,4,t}$
    $P_{hp,5,t} =$ **function**(HeatPump5)
    $P_{hp,t} = P_{hp,2,t} + P_{hp,3,t} + P_{hp,5,t}$
    $S_{e,t} = -E_{5,t} - \frac{P_{hp,5,t}}{COP_h}$
  end
  begin Step 6
    $T_{6,t} = T_{3,t} + P_{hp,5,t}$
    $P_{ex,h,t} =$ **function**(ExHeat6)
  end
end

Algorithm 6.2: function Echarge1

Input: $E_{1,t}$ ... electrical energy pool balance
Input: $D_{h,t}$ ... heat demand
Input: Ce_{max},E_{max} ... maximum charge rate and capacity
Input: E_{t-1} ... previous time step charge state

if $E_{1,t} > 0$ **then**
  if $E_{1,t} \cdot COP_{hp} \geq D_{h,t} \wedge (E_{t-1} \leq 0.1 \cdot E_{max} \vee E_{t-1} \leq E_{max})$ **then** $CE_{1,t} = 1$
  else $CE_{1,t} = 0$
else
  $CE_{1,t} = 0$
end
if $E_{1,t} > 0 \wedge CE_{1,t} = 1$ **then**
  $Ce_{1,t} = -\text{MIN}\left(Ce_{max}; E_{1,t}; E_{max} - E_{t-1}\right)$
else if $E_{1,t} < 0 \wedge CE_{1,t} = 0$ **then**
  $Ce_{1,t} = \text{MIN}\left(E_{t-1}; Ce_{max}; -E_{1,t}\right)$
else
  $Ce_{1,t} = 0$
end

Algorithm 6.3: function HeatPump2

Input: $E_{2,t}$ ... electrical energy pool balance
Input: Php_{max} ... heat pump maximum capacity
Input: $D_{hg,t}$ ... heat grid demand

if $E_{2,t} > 0$ **then**
  $Php_{2,t} = \text{MIN}\left(D_{hg}; P_{hp,max}; E_{2,t} \cdot COP_h\right)$
else
  $Php_{2,t} = 0$
end

Algorithm 6.4: function TSproduction3

Input: $C_{h,max}$ ... maximum charging heat transfer to thermal storage
Input: Q_{max} ... thermal storage maximum charge state
Input: Q_{min} ... thermal storage minimum charge state
Input: Q_{t-1} ... previous time step thermal storage charge state
Input: $CT_{3,t-1}$ ... previous time step thermal storage charge control variable

if $Q_{t-1} \leq Q_{min} \vee \left(CT_{3,t-1} = 1 \wedge Q_{t-1} < 0.9 \cdot Q_{max}\right)$ **then**
  $CT_{3,t} = 1$
else
  $CT_{3,t} = 0$
end
$PT_{g,h,t} = CT_{3,t} \cdot \textbf{MIN}\left(C_{h,max}; Q_{max} - Q_{t-1}\right)$

Algorithm 6.5: Procedure BioFuel3

Input: $E_{3,t}; T_{3,1}$ ... electric and thermal energy pool balance
Input: $P_{hp,h,max}; P_{g,h,max}$ ... maximum thermal capacity of heat pump and biofuel generator
Input: $P_{hp,2,t}; P_{hp,3,1,t}$ ... heat pump production of previous steps

if $P_{hp,h,max} = 0$ **then**
  $P_{hg,g,t} = \text{MIN}\left(P_{g,h,max} - PT_{g,t}; -T_{3,1}\right)$
  $P_{hp,3,2,t} = 0$
else if $-T_{3,1} \geq P_{g,h,max} - PT_{g,t} + P_{hp,h,max} - P_{hp,2,t} - P_{hp,3,1,t}$ **then**
  $P_{hg,g,t} = P_{g,h,max} - PT_{g,t}$
  $P_{hp,3,2,t} = P_{hg,g,t} \cdot \frac{eta_{e,chp}}{eta_{t,chp}} \cdot COP_h$
else if $\frac{-T_{3,1}}{1+\frac{eta_{e,chp}}{eta_{t,chp}} \cdot COP_h} \geq P_{hp,h,max} - P_{hp,2,t} - P_{hp,3,1,t}$ **then**
  $P_{hg,g,t} = \text{MIN}\left(-T_{3,1} - (P_{hp,h,max} - P_{hp,2,t} - P_{hp,3,1,t}); P_{g,h,max} - PT_{g,t}\right)$
  $P_{hp,3,2,t} = P_{hp,h,max} - P_{hp,2,t} - P_{hp,3,1,t}$
else if $E_{3,t} \geq 0$ **then**
  $P_{hg,g,t} = \text{MIN}\left(P_{g,h,max} - PT_{g,t}; \frac{-T_{3,1}}{1+\frac{eta_{e,chp}}{eta_{t,chp}} \cdot COP_h}\right)$
  $P_{hp,3,2,t} = P_{hg,g,t} \cdot \frac{eta_{e,chp}}{eta_{t,chp}} \cdot COP_h$
else
  $P_{hg,g,t} = \text{MIN}\left(-T_{3,1}; P_{g,h,max} - PT_{g,t}; -E_{3,t} \cdot \frac{eta_{t,chp}}{eta_{e,chp}} - \frac{T_{3,1}}{(1+\frac{eta_{e,chp}}{eta_{t,chp}} \cdot COP_h)}\right)$
  $P_{hp,3,2,t} = P_{hp,h,max} - P_{hp,2,t} - P_{hp,3,1,t}$
end

Algorithm 6.6: function TScharge3

Input: $T_{3,2,t}$ ... thermal pool balance
Input: $Q_{max}; C_{h,max}$ ... thermal storage maximum capacity and charge rate
Input: Q_{t-1} ... thermal storage state of previous time step

if $T_{3,2,t} \geq 0$ **then**
  $C_{h,t}$ = -MIN$\left(T_{3,2,t}; Q_{max} - Q_{t-1}; C_{h,max}\right)$
else
  $C_{h,t} = \text{MIN}\left(-T_{3,2,t}; Q_{t-1}; C_{h,max}\right)$
end

Algorithm 6.7: function Echarge4

Input: $E_{4,t}$ ... electrical energy pool balance
Input: $E_{max}; C_{e,max}$ ... electrical storage maximum capacity and charge rate
Input: $C_{e,1,t}; E_{t-1}$ ... previous step charge rate and previous time step storage state

if $E_{4,t} \leq 0$ **then**
  $C_{e,4,t} = 0$
else if $C_{e,1,t} \geq 0$ **then**
  $C_{e,4,t} = \text{-MIN}\left(E_{4,t}; C_{e,max}; E_{max} - E_{t,1}\right)$
else
  $C_{e,4,t} = \text{-MIN}\left(E_{4,t}; C_{e,max} + C_{e,1,t}; E_{max} - E_{t,1}\right)$
end

Algorithm 6.8: function HeatPump5

Input: $T_{4,t}$ ... thermal energy pool balance
Input: Php_{max} ... heat pump maximum capacity
Input: $P_{hp,2,t}; P_{hp,3,t}$ ... previous step heat pump production

if $T_{4,t} < 0$ **then**
  $P_{hp,5,t} = \text{MIN}\left(-T_{4,t}; P_{hp,max} - P_{hp,2,t} - P_{hp,3,t}\right)$
else
  $P_{hp,5,t} = 0$
end

Algorithm 6.9: function ExHeat6

Input: $T_{6,t}$ ... thermal energy pool balance

if $T_{6,t} < 0$ **then**
  $P_{ex,h,t} = -T_{6,t}$
else
  $P_{ex,h,t} = 0$
end

Chapter 7

Case III: Smart control of a central CHP and group of heat pumps

Abstract - In this chapter, simulated results are shown and discussed of model predictive control of a group of heat pumps powered by a single co-generation unit. The control algorithms are based on a common MILP (Mixed Integer Linear Program) problem formulation and two specific solution methods are developed to reduce computational effort: time-scale MILP and a heuristic solution method based on the earliest deadline first algorithm. The results obtained by applying these solution methods within the Meppel project are discussed and it is concluded which method is favorable.

7.1 Introduction

As introduced in Chapter 1, heat pumps powered by renewable electric energy are a possible way to realize the transition towards integration of renewable energy in the building environment [79], [152]. However, in Chapter 6 we have shown that this can also lead to large peaks within the power system which could not be solved by the algorithmic control introduced in that chapter. Therefore, this chapter investigates a particular case for a group of domestic heat pumps for which we develop a smart grid control method which enables optimal planning of the heat pumps. The case is part of the Meppel project which is introduced in Section 3.1. In the Meppel case, the entire district heating and cooling system, including the heat pumps which will be placed at a number of houses, are owned by a single utility company. To power the heat pumps there will be a dedicated electricity power supply line to the heat pumps. As a consequence, the utility has the possibility to control the operation of each heat pump from a central level.
In this chapter, the following results are shown for model predictive control of a central CHP and group of heat pumps:

[†]Major parts of this chapter have been published in [RvL:8], [RvL:2] and [RvL:1].

- methods for model predictive control for planning the operation of a single CHP and group of heat pumps in a district,
- case results of minimizing the peak electricity consumption of a group of heat pumps,
- case results of achieved (simulated) thermal comfort within the households, and
- a comparison of model predictive control results with conventional feedback control of individual heat pumps.

The chapter is structured as follows. Section 7.2 discusses related work for model predictive control and heat pump planning in smart micro grids. In Section 7.3, models are formulated for prediction of space heating and domestic hot water demand and input data for the Meppel case is described. Section 7.4 formulates the general control and optimization problem. Section 7.5 shows results on the achievable aggregated energy consumption profile of the heat pumps. Also, the resulting thermal comfort of the households is shown. The earliest deadline first method and results are shown in Section 7.6.2. Finally, conclusions are given in Section 7.7.

7.2 Related work

A heat pump is an electric appliance with a low temperature thermal input and a higher temperature thermal output which is used for space heating or domestic hot water [108], [71]. Model predictive control (MPC) of heat pumps in the building environment is a relatively recent research area. MPC can be applied for building climate control to minimize energy consumption, or for power balancing of smart micro grids. Early work on MPC is performed by Madsen et al [100]. Recent research which include experimental results are carried out by [124], [157] and [138]. [66] investigates the use of MPC for the control of a domestic heat pump in relation to minimizing energy costs for heating a house, for which Nordic spot market electricity prices are taken as input data. [42] demonstrates how a domestic heat pump can be controlled by MPC such that self consumption of PV-generated electricity is increased.
These examples of related work on MPC consider climate control of single buildings in relation to minimizing costs or energy consumption. Based on this work, the conclusion is justified that MPC is a promising control method which outperforms conventional feedback control methods when the control system has more objectives than only room temperature control. Our main interest, however, is not on the optimal control of a single building or a single heat pump, but on controlling many heat pumps for houses within a district. The main goal of this chapter is to demonstrate the quality of reaching multiple objectives for a smart micro grid with MPC controlled heat pumps, such as minimizing peak loads on the electric network and maintaining thermal comfort in the houses and adequate charge

states of domestic hot water storage facilities.

Planning of electric devices in micro grids is a recent research area. To obtain flexibility within a smart grid, it is required that (a) devices are controllable and (b) the use of the device can be shifted in time without unacceptable consequences for the customer. Such devices in a household environment are: energy storage, (dish)washing machines, dryers, fridges and heat pumps. [28] developed specific planning algorithms for smart micro grids, while [22] and [113] investigate various case applications like the planning of a group of fridges in relation to varying electricity price schemes, due to renewable energy production by solar PV. Claessen et al. [38] compare two smart grid control approaches: Triana and Intelligator. The Triana approach contains three steps to control devices: prediction on device level, planning based on price signals from the aggregator and real time control by the device controller. The Intelligator approach is based on the Powermatcher concept [89] which uses a multi-agent electricity market. Device agents send bids to a central auctioneer agent. The price signal from the auctioneer clears the market with the purpose to adjust the bids in such a way that the market equilibrium is steered towards the optimization objective. Claessen et al. demonstrate that both approaches are able to reach certain objectives but also demonstrates the improvement which is possible when predictions (Triana) are part of the approach.
In practice, the concept of dynamic pricing may lead to the problem that all devices jump to time intervals with the lowest price, thus increasing demand peaks in these time intervals. This is improved by differentiated dynamic pricing [114]. A new control concept called profile steering is recently introduced in [61]. [85] applies this concept for controlling a group of EV chargers, while [74] applies this concept to islanded operation of an electricity network, demonstrating positive effects on power quality within the entire network. Profile steering involves a planning phase based on predictions of consumption where each house is asked to plan devices such that the house profile is as flat as possible. The aggregator then sums these profiles and compares the result with a desired grid profile. The deviations between the sum of the planned house profiles and the desired grid profile are used as steering signals during an iterative phase.

In the Meppel case it is possible to simplify the control method and let a central controller directly determine the planning of the heat pumps based on heat demand predictions for each household. As part of this project and thesis work, a model predictive control method is developed for which we developed a solution strategy called time-scale MILP (Mixed Integer Linear Program) in [RvL:2] which enables efficient solving of large scale central optimization problems. In this strategy, the planning step considers planning of the heat pumps from 2 up to 24 hours ahead, whereas the real time control step considers planning of the heat pumps for the actual time up to a few time steps ahead. The central controller has to solve one large optimization problem every time step of 15 minutes with a time window of 24 hours ahead. However, the time scale MILP method reduces the size

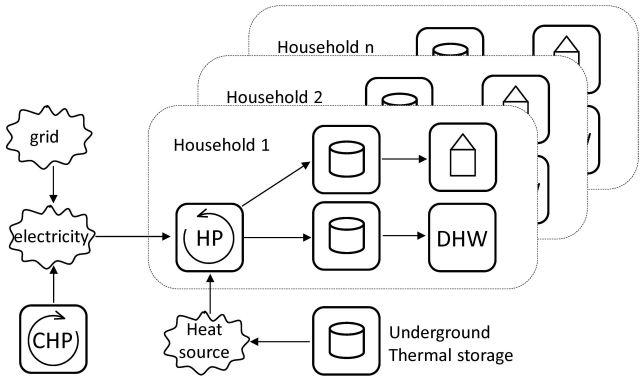

Figure 7.1 – scheme of the energy system

of the problem by considering larger time steps for moments further in time. In this way, the planning gets more rough, the further it looks into the future, which reduces computational effort.
In this chapter, we first demonstrate that the obtained control behavior involves frequent switching of the heat pumps and the central CHP. If constraints on switching would be introduced, computational time to find optimal solutions would increase, which is undesired. Hence, we developed another solution strategy based on an earliest deadline first heuristic algorithm in [RvL:1]. For this strategy, much better control performance and further reduced computational effort in comparison with time scale MILP is demonstrated.

7.3 Methods

7.3.1 Model of the energy system

In Figure 7.1, a schematic overview of the energy system is given, showing a range of houses (labeled 1 to n). Each house has a heat pump (HP) which is connected to two types of thermal buffers: (a) a floor heating system and (b) a hot water storage for domestic hot water (DHW). The ability of the floor heating to store thermal energy and possible consequences on thermal comfort and costs is demonstrated in Chapter 4. The energy inputs to the heat pumps are: (a) low temperature source energy from an underground thermal storage and (b) electric energy from a bio-gas Combined Heat and Power system (CHP), which due to the constant bio-gas flow runs continuously. The CHP is also connected to the main electricity grid. Heat produced by the CHP (not shown in Figure 7.1), is distributed to a district heating network which involves many more houses than the number of houses with a heat pump.
The energy system is configured in such a way that the average electric production of the CHP equals the average required electric input by all heat pumps on the coldest possible day. Furthermore, there are only two energy prices, arranged by a

contract with the grid operator. A low price for selling electricity from the CHP to the grid and a high price for buying electricity from the grid. Hence, the objectives for the heat pump control are:

- maintain thermal comfort for space heating within each house,
- maintain sufficient state of charge of the hot water buffer to cover DHW demand of each house, and
- use electricity of the CHP as much as possible locally for the heat pumps and avoid buying electricity from the grid. This objective can be reached when the electric demand is flattened towards the average demand. Also, investments and losses in electricity cables throughout the district and transformers at the energy house are minimal when the peak electric demand is as low as possible. Therefore, the control objective is formulated as: minimize peaks of the aggregated heat pump electricity demand.

Following the area plan of the Meppel building project at the time of writing, 104 houses with a heat pump are studied. The investigation involves simulations based on specific models which are discussed in the following subsections.

7.3.2 Household space heating demand model and simulation case description

For the model of space heating demand in relation to ambient conditions, we use the 2R2C thermal network model with floor heating; for details (model scheme, equations and parameters for different type of houses) see Chapter 2.
The simulation study involves a separate model for each of the 104 houses. The possible types of occupancy (families, couples, etc.) are based on case data of the project. The following 3 types of occupancy and distribution over 104 households are defined: young family (52%), elder couple (15%) and young couple (33%). The house orientation, indicated by the facing direction of the front facade, and the distribution of occupant types over the different house types, is as follows, whereby the relation between occupant type and house orientation is assumed to be random:

- 41 terraced houses with their front plane orientation distributed as follows: 20-North/4-East/7-South/10-West, and distributed as follows over the occupant types: 12-young family/2-elder couple/27-young couple.
- 20 corner houses: 10-North/2-East/4-South/4-West. Households and occupant type: 18-young family/0-elder couple/2-young couple.
- 26 semi detached houses: 0-North/10-East/4-South/12-West. Households and occupant type: 16-young family/6-elder couple/4-young couple.
- 17 detached houses: 0-North/8-East/8-South/1-West. Households and occupant type: 8-young family/8-elder couple/1-young couple.

7.3.3 Occupancy related thermal losses or gains

For each type of occupancy, hourly schedules are defined for working days and days of the weekend for relevant thermal events. The schedules are related to common behavioral patterns of working people. For each occupancy type, basic, simplified schedules are defined and to create multiple profiles, randomization is performed on some of the time points at which thermal events occur. In the following, we show the basic profile only for the type "young family", for which further in the chapter we also discuss results. An energy related schedule for a working weekday is shown in Figure 7.2. IT shows relative to a defined maximum, the following thermal events:

- Occupancy: thermal gains by occupants present in the house. Schedules consist of a number of time points at which the number of occupants which are present in the house are defined. Based on [108] the thermal gain by people is on average 40 W per person during sleeping hours and 110 W per person during day and evening hours. Figure 7.2 shows the number of occupants present in the house.
- Ventilation rates: typically, ventilation schedules depend on: (a) the time of the day, (b) the number of occupants present in the house, (c) cooking events which require higher ventilation rates, (d) shower or bath events in the bathroom which require higher ventilation rates. The ventilation system has 4 states for the ventilation rate: (1) cooking, (2) high, (3) medium, (4) low. This relates to typical existing Dutch house ventilation systems. Figure 7.2 shows ventilation rates for each hour.
- Appliance thermal gains: Four appliance classes are defined: (1) computers and television, (2) lighting, (3) fridge and freezer, (4) background appliances like pumps, fans and standby electronic equipment. The total yearly electricity consumption of the schedule in Figure 7.2 is approximately equivalent to Dutch average consumption figures published by [107].
- DHW (Domestic Hot Water) demand: for a single household this is determined by several events at certain timepoints each day. In total, 6 possible events are defined, each with a specific amount of required water of 40°C: (1) shower, (2) bath, (3) hand cleaning, (4) small dish wash, (5) large dish wash and (6) body washing. Figure 7.2 shows the water amounts for a number of events. The amount of water per event and the time points are slightly randomized.

In the same way, schedules are worked out for other occupancy types, both for working days and weekend days.

7.3.4 Heat pump model

The heat pump performance is approximated as a constant relation between electric input and thermal output of the heat pump for two operational modes: space

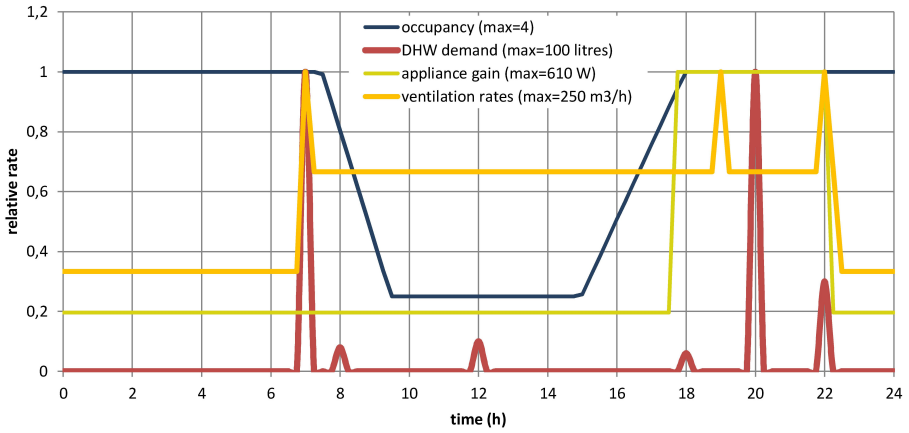

Figure 7.2 – Example weekday thermal event schedule

heating mode with an output temperature of 35°C and thermal storage mode with an output temperature of 65°C. Hence, the heat pump has 3 operational states: (1) off, (2) space heating, (3) thermal storage. A summary of the used parameters is given in Table 7.1 which is based on average supplier data [14].

state	unit	input	output
off	kW	0.0	0.0
space heating	kW	1.3	6.0
thermal storage	kW	1.8	5.0

Table 7.1 – heat pump energy specification

7.4 Control algorithms

In [RvL:2] a general approach for off-line and on-line heat pump central control problems is introduced and corresponding algorithms are explained in detail. In this chapter, we concern an off-line problem, where the weather and occupancy related data are known beforehand as forecasts. Within the simulations we furthermore assume that the real behavior follows the model predictions, thereby avoiding two separate simulation environments which should run in parallel: one for the predictions, another one for the real behavior. The optimization process is explained in more detail in [58]. For the simulation, script files in the Python programming language contain the house model, the variation of model parameters for the house types, the occupant related schedules, the weather and solar calculation module, and algorithms for the reference control and the optimized control. These files are called from the Triana smart grid simulator, developed at the University of Twente and written in the C++ programming language. MILP

instances for the optimized control case are solved by the CPLEX solver package. For the reference control, the differential equations of the thermal model are solved in discrete time steps. The problem formulations for the optimized control and reference control are explained in the following subsections.

7.4.1 Optimized control

Planning of the heat pumps is determined in two steps: a prediction step and a planning step. The Triana method also contains a third step: real time control, but for this type of off-line problem with perfect predictions, this step is not relevant. Note that, if an on-line control problem is studied, the real time control step involves a comparison between measurements in real time and predictions for the short term, resulting in adjustment of the short term heat pump control planning (the next time intervals) to reduce possible deviations.
For the optimization problem of the heat pump control, the objective (minimize total peak electric demand) is formulated as follows:

$$\begin{aligned} &\text{Minimize } \max_{t\in T} \sum_{OP} \sum_{c=1}^{n} E_{op} \cdot X_{c,op,t} \\ &X_{c,op,t} \in \{0,1\}\ ,\ c \in \{1,..,n\}\ ,\ op \in OP\ , \end{aligned} \tag{7.1}$$

in which E_{op} is the electric demand of a heat pump converter, $OP = \{sh, dhw\}$ denotes the set of operational modes of the heat pump, in this case space heating (sh) or domestic hot water (dhw), and $X_{c,op,t}$ is the control state of each heat pump converter (c) in time interval $t \in T$.
Each heat pump in each time period t, for each mode op is either "on" ($X_{c,op,t} = 1$) or "off" ($X_{c,op,t} = 0$). However, two operational modes for one heat pump cannot be "on" at the same time, that is $\sum_{op} X_{c,op,t} \leq 1$. For this we introduce additional control variables.
Let $x_{c,t}$ be the control variable for space heating during the prediction phase, $y_{c,t}$ be the control variable for space heating during the planning phase and $z_{c,t}$ be the control variable for DHW during the planning phase.
The first stage heat pump planning $x_{c,t}$ for space heating follows from the prediction phase in which we optimize for a given heat pump converter $c \in \{1,..,n\}$:

$$\begin{aligned} &\text{Minimize } \sum_{t} X_{c,sh,t} \\ &0 \leq X_{c,sh,t} \leq 1 \end{aligned}$$

subject to the following constraints:

- $Tz_t \geq T_{pref,t}$ for all $t \in T$ where Tz_t is the interior zone temperature of a house and $T_{pref,t}$ is the setpoint for the zone temperature, which may be a different time schedule for each house.
- Pe-calculation of heat loss for each house by simulation with a 2R2C model in which parameters and schedules for thermal gains and ventilation heat losses are pre-determined (either learned or assumed).

- Pre-calculation of solar gains for each house.

The output of the prediction phase is a first stage planning of the heat pumps in order to exactly match the space heating demand of each house. Note that DHW is neglected during this phase.
During the second phase of the calculation, i.e. the planning phase, the first stage planning of the space heating converters is re-calculated but now the optimization includes an artificial buffering capacity which signifies a certain possibility to exceed the temperature of each house's interior zone. The state of charge of this artificial buffer is also stored in the database and signifies a certain priority, i.e. houses with a low state of charge of the artificial buffer receive a higher priority when heat pumps are planned to minimize peaks than houses with a higher state of charge. In the second phase, calculation of the planning also includes the DHW demand prediction and the State of Charge of the DHW thermal buffer for which a similar prioritization rule is applied. Equation (7.1) is now subject to the following constraints:

- $0 \leq \sum_{i=1}^{t}(y_{c,i} - x_{c,i}) \leq \frac{SH_{max}}{q_{hp,sh}\Delta t}$ in which $y_{c,i}$ signifies the re-planned control states of each converter for space heating and $q_{hp,sh}$ the thermal output of the heat pump for space heating: $q_{hp,sh} = X_{c,sh,t} \cdot \text{output}_{c,sh}$ in which $\text{output}_{c,sh}$ is the thermal output of the heat pump specified in Table 7.1. Furthermore, Δt signifies the incremental length of the time interval t and SH_{max} the maximum capacity of the artificial space heating buffer. This capacity is deduced from the results shown in [RvL:9].
- $0 \leq SoC_t \leq DHW_{max}$ in which SoC_t signifies the State of Charge of the DHW buffer and DHW_{max} the maximum capacity of the DHW buffer, i.e. determined by the water volume and fully charged average temperature.
- $SoC_{t+1} = SoC_t + z_{c,t} \cdot q_{hp,dhw} - D_{t,dhw}$ which yields the control states of the heat pump converters $z_{c,t}$ for the DHW operation mode. $q_{hp,dwh}$ signifies the heat pump thermal output and $D_{t,dhw}$ the DHW demand during time period t. Heat loss of the heat buffer is not modeled, but could be incorporated in $D_{t,dhw}$. Operation of the heat pump for DHW has priority over space heating: $y_{c,t} = 0$ if $z_{c,t} = 1$.

For further details of the MILP optimization approach, see [RvL:2] and [58].

7.4.2 Reference control

The reference control is based on a simple set of feedback control rules which results in approximately the same behavior as individual feedback control of each heat pump. At each time interval, the following is evaluated for each house:

- For space heating, the operative temperature Tz_t is compared with $T_{pref,t}$ which is the minimum allowed temperature defined in schedules. If the interior zone temperature falls below this value, the heat pump is switched

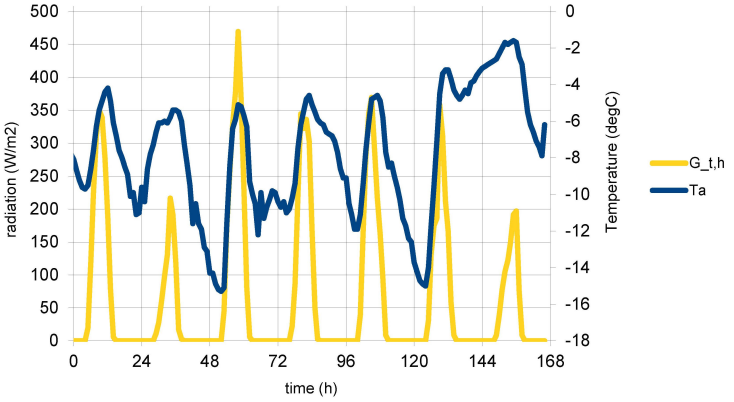

Figure 7.3 – input weather data

on. If it is above this value plus a positive deadband value, the heat pump is switched off (on/off control with deadband).

- For DHW, the State of Charge of the buffer SoC_t is compared with a minimum allowed value. If the SoC falls below this value, the heat pump is switched on. If it is above a value close to the maximum SoC, the heat pump is switched off.
- Operation of the heat pump for DHW has priority over space heating: $y_{c,t} = 0$ if $z_{c,t} = 1$.

7.5 Case study results

7.5.1 Results for a cold week

To discuss the quality of the obtained results, the coldest week of the year 2012 (weather data of station Hoogeveen) is investigated first, as this week has the highest average heat demand and therefore the longest peak load duration. The input weather data, i.e. the ambient temperature (Ta) and global horizontal solar radiation ($G_{t,h}$) are shown in Figure 7.3.

In Figure 7.4 the electrical energy demand is shown for the reference control (ref_control) and optimized control. Furthermore, curves of the sorted values from high to low (ref_control_s and optimized_s) are given in this figure. These sorted curves demonstrate the quality of the peak minimization achieved by the optimized control. The peak for the reference control is 162 kW. This is the peak electric consumption when all heat pumps have their own on/off controlled thermostats. The peak for the optimized control is 108 kW. The average electricity power for the shown period is 74 kW. Compared to this average, the maximum peak of the reference control is 119% higher and of the optimized control only 46% higher.

Figure 7.5 shows an example of the indoor temperature T_z and the floor heating

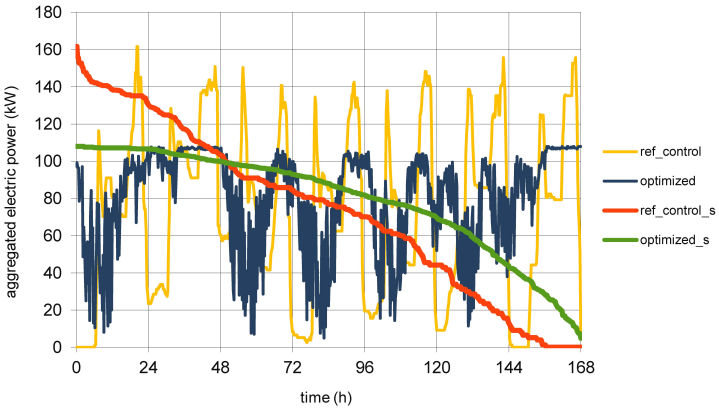

Figure 7.4 – aggregated electrical energy demand

temperatures T_f for the reference and optimized control. The example concerns a detached house occupied by a young family. Other households show similar results. Tz_setpoint relates to the desired setpoint temperature which is set at 18°C during the night and 20°C during the day. Tz_ref_control relates to the indoor temperature in case of reference control. Tz relates to the optimized control. Notice that the reference control is not able to keep the indoor temperatures at the desired daytime setpoints. This is due to the sharp contrast between daylight hours with a relatively high amount of solar gains and nighttime hours with low ambient temperatures. The reference control has no knowledge of the upcoming heat loss during the night. When it reacts, the floor heating system gives a slow response due to its inertia, which is seen on the Tf_ref_control line.
In contrast, the optimized control is based on weather forecasts and controls the indoor temperatures such that the desired temperatures are reached exactly at the first moment when they are needed, i.e. each morning around 07.00. The average floor heating temperature and average indoor temperature during this week are thus higher than for the reference control. On some days, the indoor temperatures reach 22°C, which is due to solar gains. The optimized control evaluates the setpoint temperatures as the minimum allowed temperatures and has no upper limits on the indoor temperature during the heating season. However, the way the objective is formulated also minimizes heat loss of each house which leads automatically to the constraint that indoor temperatures should be as low as possible.

Figure 7.5 also shows the indoor temperatures which are calculated as result of the prediction step (Tz_pred). The result of the planning step (Tz) is only slightly different which is caused by the relatively small size of the space heating buffer, which corresponds to 12 time periods of 15 minutes continuous charging with the heat pump output for space heating. This equals a storage capacity of $12 \cdot \frac{15}{60} \cdot 6.0 = 18$ kWh. When this buffer is larger (e.g. 24 time periods instead of 12 time periods) the result is that the electrical energy demand is pushed more

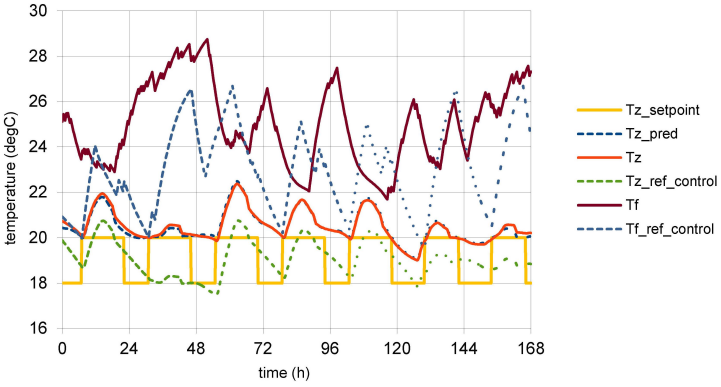

Figure 7.5 – example indoor and floor heating temperatures

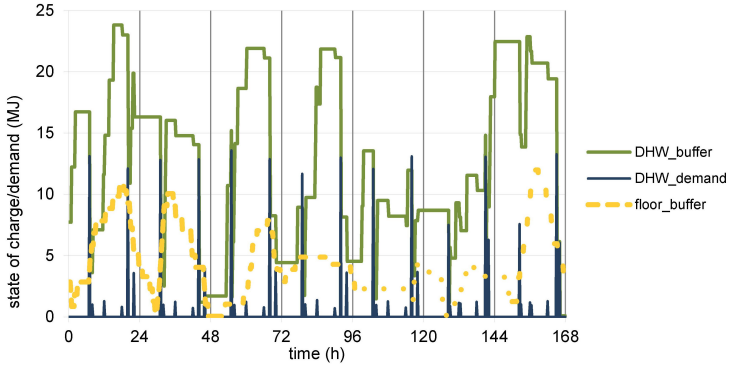

Figure 7.6 – floor heating and DHW buffer state of charge

towards the average for the whole week, but the real indoor temperatures differ more from the first stage control which is the result of the prediction step.
In Figure 7.6 the state of charge (SoC) of the artificial buffer (floor_buffer, dimensionless) for space heating and DHW buffer (DHW_buffer, MJ) with the DHW demand (DHW_demand, MJ) for the example household are shown. The space heating SoC has a relation with the floor heating temperature and operative zone temperature shown in Figure 7.5. In general, the SoC increases when the zone temperatures are higher than the setpoint and decreases when the zone temperatures approach the setpoint values.
Figure 7.6 also shows the relation between the SoC of the DHW buffer and the DHW demand. The SoC increases due to heat input from the heat pump. Corresponding operational states of the heat pump are shown in Figure 7.7. In this case, the DHW buffer is large enough to supply the largest short time demand peaks, i.e. for filling a bath. The states of the heat pump are indicated as 0 (off) or 1 (on). For improved visibility, the heat pump state for space heating (right vertical

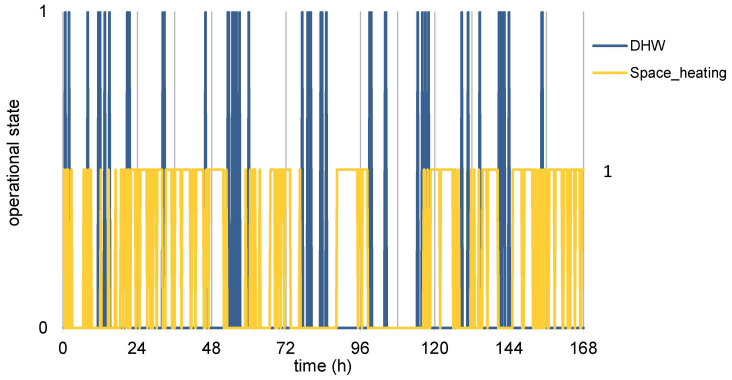

Figure 7.7 – heat pump operational states

axis) is scaled different and drawn with a thicker line than for DHW (left vertical axis) in Figure 7.7. Note that the heat pump only operates for one function each time interval (SH or DHW) but that this is not so clear in the figure due to the thickness of the lines.

7.5.2 Broader analyses of results

Heat pump on/off switching behavior
As Figure 7.7 shows, the heat pump switches on and off frequently. Although this is just one of 104 heat pumps, the other heat pumps show similar behavior, which is undesirable for the service life of the heat pumps. Therefore at first, two possibilities to reduce the amount of switching are considered:

1. To constrain the minimum running time within the heat pump control, e.g. half an hour. Another constraint can be to charge the domestic hot water storage until it is fully charged. Both methods will have some effect but this will also limit the amount of feasible solutions considerably, and therefore increase the time to solve the optimization problem.
2. To increase the time interval of the simulation from 15 minutes to 30 minutes. This has a number of possible effects: (1) the number of heat pump on/off switches should reduce with 50% as theoretical maximum, (2) the number of variables are decreased and so the time to solve the optimization problem decreases. However, (3) the performance for temperature control of the interior and DHW bufer may decrease because control decisions are now taken for larger time intervals which could lead to undershooting or overshooting behavior.

When the latter method is applied, the load duration curves are similar to the results which are shown in Figure 7.4. The interior temperatures have a minor difference, which is shown in Figure 7.8. In this Figure, the subscripts _15 and _30

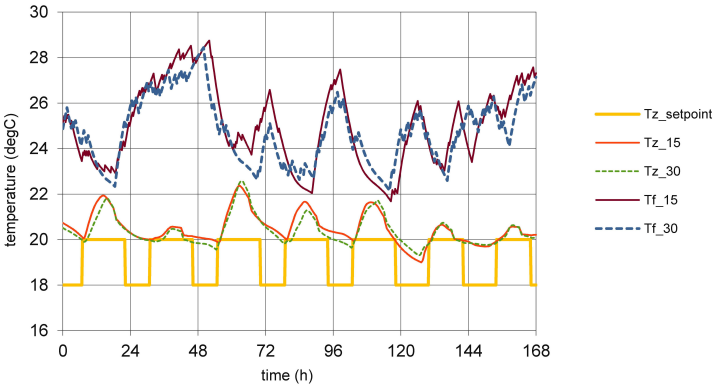

Figure 7.8 – Temperature response for 15 and 30 minute time intervals

indicate a 15 minute and 30 minute time interval during simulation respectively. The advantage of the 30 minute time interval is shown in Figure 7.9, which shows the amount of on/off switches in relation to the amount of uninterrupted running time intervals of the heat pump. For the investigated week, the total amount of switches reduces from 92 to 53. A further reduction can be expected when an additional charging constraint is included for the domestic hot water storage, as most of the heat pump switches are related to short charging periods of this storage.

By comparison, the reference control switches only 11 times. This is an advantage for the service life of the heat pump, but Figure 7.5 demonstrates drawbacks on the experienced comfort. The on/off thermostats programmed for reference control of the space heating and the domestic hot water storage, cause too much cooling down of the house and of the hot water storage, which results in long periods of heating demand afterwards. This is observed from the high number of intervals of uninterrupted operation of the heat pump in case of the reference control in Figure 7.9. For the reference control the longest period is 65 time intervals of 15 minutes or 16.25 hours, for the optimized control this is 19 time intervals of 30 minutes or 9.5 hours. In practice, when a PID controller is used to control the space heating demand, and the set-point temperature would rather ramp up and down in stead of abruptly changing from 18 to 20 degrees and back, the temperature control performance would probably be much better than the on/off reference control. However, in that case more expensive frequency controlled heat pumps are required for proportional heat production. This should also result in more steady operation of the heat pumps and could be another way to reach the same objective: reduction of the aggregated peak electrical loads compared to the reference control.

Results for periods with less heat demand

As shown in Figure 7.4 and discussed on Section 7.5.1, the peak electrical load

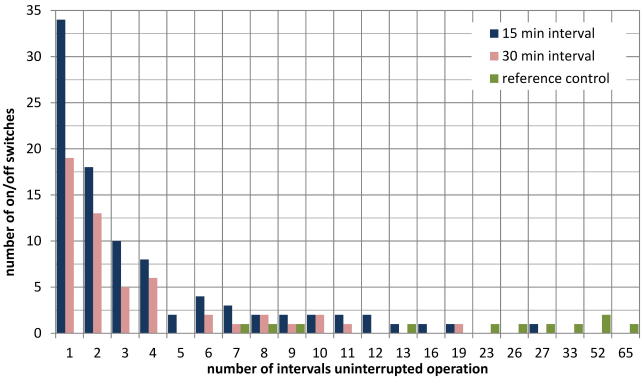

Figure 7.9 – Amount of heat pump on/off switches related to uninterrupted operation time intervals

is reduced significantly for the optimized control. It is interesting to verify if a similar result is found for periods with less heat demand. In Figure 7.10, weather data of a different week for the same location and climatic year is shown. The aggregated electrical energy demand for the optimized and reference control is shown in Figure 7.11. The indoor temperatures (floor heating temperature Tf and interior zone temperature Tz) for the same detached house are shown in Figure 7.12.

During this week, the domestic hot water demand dominates the aggregated electrical energy demand, while the space heating demand is largely concentrated on one day (between hours 72 and 96). Due to approximately 80% simultaneity in the operation of the heat pumps for domestic hot water, the reference control shows a high peak electrical demand of 145 kW. The optimized control reduces this to 45 kW, see Figure 7.11.

Figure 7.12 indicates that the interior zone temperatures are approximately similar for the reference and optimized control. The slightly increasing temperatures above the set-points which is seen on the last two days are due to relatively high solar gains. The short term up and down movement of the floor heating temperatures from 0 up to 84 hours indicates frequent on/off switching of the heat pump. Also in this case, the heat pump switching is more frequent for the optimized control than for the reference control. The total amount of switches for this week is 32 for the optimized control and 10 for the reference control. However, the longest period of uninterrupted heat pump operation is 3 hours for the optimized control and 10.25 hours for the reference control, which increases the chance for simultaneity and hence explains the high peak electrical load of the reference control. This also has a relation with the schedules shown in Figure 7.2. As young families and young couples dominate the district's population and the applied schedules for domestic hot water demand and interior temperature set-points of these occupancy types are approximately similar, the chance for simultaneity is high. A commonly used hot water storage contains a single temperature sensor. Within the storage,

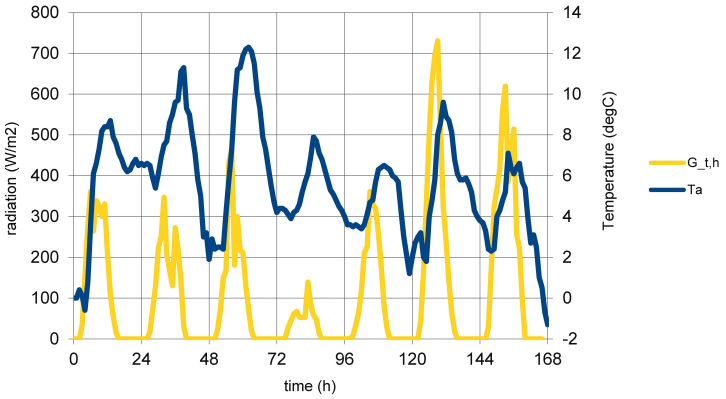

Figure 7.10 – Input weather data for a week with less heat demand

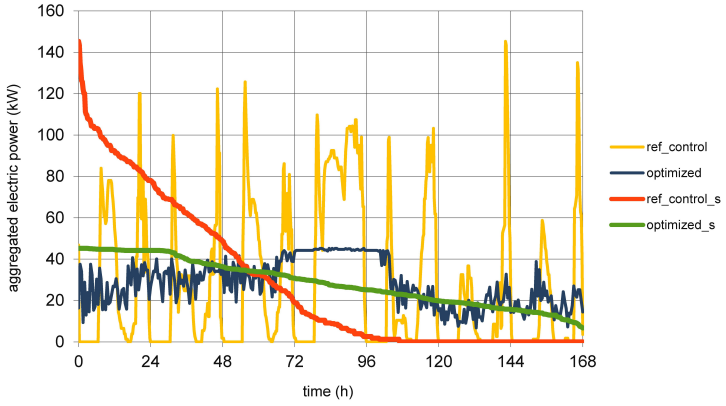

Figure 7.11 – Aggregated electrical energy demand for a week with less heat demand

a good degree of temperature stratification of hot and cold water layers is present. In that case, a PID controller would not perform much better than the simple on/off reference control.

Quality of the control

The main objective for the optimization is to minimize peak electricity consumption. Besides this objective, there are some hard constraints on the thermal comfort, i.e. a minimum temperature, maximum size of the flexible space heating storage and minimum hot water storage state of charge. Besides that, a 30 minute time interval is introduced during optimization to avoid excessive on/off switching of the heat pumps. Hence, the definition of what is in this case really "optimum" for the control is not so obvious. As the results show, the peak electricity decreases

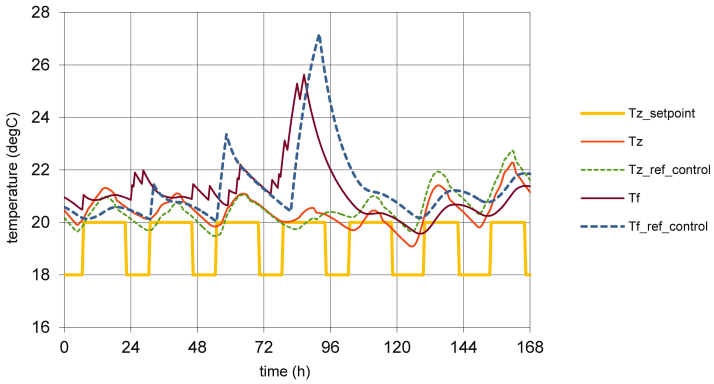

Figure 7.12 – Indoor temperatures for a week with less heat demand

significantly as the result of the optimized control, but there is a trade off between the quality of this objective, reaching comfort temperatures in the house which are close to the set-points and limiting the amount of heat pump on/off switches. Another drawback is the amount of operational state changes of the co-generation unit which produces the electricity. Notice from Figures 7.4 and 7.11 that especially the first (colder) period involves many changes of the electrical demand in time and hence, many operational state changes of the co-generator. For the second (warmer) period, the electrical demand is flatter and a few state changes of the co-generator are sufficient during that period. Besides the heat pump control, the co-generator should also be controlled in such a way that it runs in the same operational state for as many time intervals as possible. With the planning results, a control planning for the co-generator can be determined with a separate algorithm, e.g. a moving average algorithm. However, due to the drawbacks discovered for both the heat pump and co-generator control, it was decided to develop a different, integrated control method for both type of coupled generators. This method is explained in the following sections.

7.6 Earliest deadline first control method

7.6.1 Related work

The previous sections evaluated smart control at the aggregated level: the aggregator decides which device will be switched on or off in time. However, this external control may be overruled by an internal control layer, e.g. a feedback controller of a heat pump in case the planning leads to violations of certain operational margins which may happen in case the prediction and thus the planning contains errors. The main advantage of directly controlling heat pumps from the aggregated level is that the home or device controllers may be simple or non-smart. The intelligence is on the aggregated level. The result is that each house needs to transfer

information about state of charge of a thermal storage, room temperature and status of the heat pump to the aggregator. The aggregator is then able to learn demand profiles from this information and to plan the heat pumps based on model predictive control principles. However, this type of information is privacy sensitive. Another disadvantage of this type of control is a reduced scalability towards large groups of heat pumps. Similar to the method introduced in this chapter (called time-scale MILP), other researchers have also developed alternative methods, e.g. a clustering method to reduce complexity for large numbers of heat pumps and increase scalability [120]. Another aspect to take into account is that direct control by the aggregator may not work so well if there is a lot of uncertainty to take into account. However, the demand for space heating or domestic hot water consumption is relatively predictable, with a low level of uncertainty.
To improve the control behavior of the heat pumps and co-generator, an interesting question remains if a method can be developed other than defining more hard constraints on the heat pump operation cycles, which could limit the solution space considerably. In [58] a mathematical proof is given that minimizing peaks, which is typically the objective for the heat pump scheduling problem, is an NP-hard problem which requires heuristics to solve. In that paper, Fink and Hurink develop an algorithm within a dynamic programming framework. The solution method presented in this section uses a different approach and is based on the mathematical concept of earliest deadline first (EDF). A very readable introduction of EDF with appli-cation of EDF in real time task scheduling for embedded systems is given in [78]. This paper demonstrates the computational advantage of EDF which is also shown in the present section. A similar framework to EDF called color power algorithm is introduced in [12]. Suitability of this method for real time DSM is demonstrated with a simulation of 100 electronic devices. However, in our case a prediction and planning horizon is required due to the time delays of the thermal systems involved. As the planning horizon can be limited, EDF is suitable for (near) real time control. Another advantage compared to other optimization methods used on the aggregator level, is that predictions can now be made by the houses and only their priority is communicated towards the aggregator level. This relieves the privacy issues involved but on the other hand requires smartness on the device level.

7.6.2 Control method

For simplification, a discrete time model for the considered problem is considered, meaning that the planning period is split into T time intervals of the same length. Furthermore, let $C = \{1, .., n\}$ be the set of houses with a heat pump converter c. In this section, the index t denotes a time interval and h denotes a house or a heat pump.

CHP model

The CHP can operate in a few modes. In every mode, the CHP consumes some amount of gas and produces some amount of electricity and heat. However, in this chapter, only the electricity output is studied. For every time interval, the algorithm (refer to [RvL:1] for details) chooses one mode in which the CHP will operate. The approach is summarized in the following.

The following objectives are imposed on the CHP control.

- The CHP should not switch the operation mode too often.
- Heat pumps should only consume the electricity generated by the CHP.
- The overproduction of electricity should be minimal.

Note that the electricity output generated by the CHP cannot be exactly equal to the aggregated demand of all heat pumps. Besides many technical reasons which are not considered in the model, there is also the following mathematical one. For illustrative purposes, assume that the CHP generates 11 kW and the electricity consumption of one heat pump is 2 kW. In this setting, we can either turn 5 heat pumps on and export 1 kW, or turn 6 heat pumps on and import 1 kW. However, it is impossible to consume exactly the generated electricity. As in the case study, exporting electricity is more preferable than importing, the goal is to control the CHP and all heat pumps so that electricity is not imported and the export of electricity is smaller than the electricity demand of one heat pump. However, the control rules can be easily adopted if importing electricity is more preferable than exporting.
The CHP control has two parts. The first part determines the amount of electricity produced by the CHP and the second one chooses which heat pumps will consume electricity in the next time interval. In the second part, all heat pumps are sorted by their deadlines and the electricity is consumed in this ordering until the CHP output is reached.

Heat pump control

As stated in the previous sections, each heat pump has only three modes: heating the house, heating DHW and off. Furthermore, to increase the efficiency of heating and the lifetime of the heat pump, the following constrains are set on the Earliest deadline control of all heat pumps.

- The hot water buffer should be completely heated up every time a heat pump is turned on to the hot water mode.
- A heat pump should not switch the operation mode too often. Therefore, a heat pump has to be turned off for at least m time intervals whenever it is switched off and similarly, it has to heat the house for at least m time intervals whenever it is switched into the house heating mode. In the presented

simulations, we consider two values of m: 4 and 8. These two simulations are abbreviated by EDF4 and EDF8.

In order to mathematically describe the control model of a house with heat pump c, let $x_{c,t,SH}$ and $x_{c,t,DHW}$ be the binary variable which denotes whether the heat pump c in a house is heating the house (Space Heating, SH) or DHW in time interval t, respectively. Since the heat pump cannot heat the house and DHW in the same interval, we require $x_{c,t,SH} + x_{c,t,CHP} \leq 1$ in every time interval t and house h. The amount of energy injected into the space heating and DHW of the house is given by $H_{c,SH} \cdot x_{c,t,SH}$ and $H_{c,DHW} \cdot x_{c,t,DHW}$ where $H_{c,SH}$ and $H_{c,DHW}$ is the heat output in space heating and DHW mode, respectively. The consumed electricity of heat pump c is given by $E_{c,SH} \cdot x_{c,t,SH} + E_{c,DHW} \cdot x_{c,t,DHW}$ where $E_{c,SH}$ and $E_{c,DHW}$ is the electricity consumption in space heating and DHW mode, respectively.
The earliest deadline algorithm has to decide operation modes of the CHP and all heat pumps for the coming time interval which is denoded by t_1. This decision has two phases. First, an energy plan is computed by all house controllers and sent to the central controller. Second, these energy plans from all houses are used to determine operation modes of the CHP and all heat pumps by the central controller. For this the central controller needs from each house controller, the following information:

- the possible electricity consumption of the heat pump in time interval t_1,
- the latest time interval $t_{d,c}$ (called deadline) when the heat pump needs to be turned on, and
- the lower bound $l_{c,t}$ and the upper bound $u_{c,t}$ for the total electricity consumption up to the time interval t. These two bounds follow from the fact that heating the house and the DHW can be shifted in time. So, the upper (lower) bound is the maximal (minimal) amount of electricity that the heat pump can consume during the first t time intervals when the heat pump heats up as early (late) as possible.

Both heating modes of the heat pump have some scheduling freedom which determines the energy plan. A given heat pump can consume electricity at time interval t_1 unless the heat pump was turned off less than m time intervals ago, or both the house and the DHW buffer are fully heated up. Furthermore, note that the deadline $t_{d,c}$ in the energy plan is not the earlier time of the deadlines of the two heat pump modes because e.g. when these two deadlines are the same then the heat pump cannot fulfill both demands at once.
There are various ways to calculate an energy plan. Classical dynamic programming is applied in this case. In order to determine the amount of electricity produced by the CHP, the aggregated lower $l_t = \sum_{c \in C} l_{c,t}$ and upper $u_t = \sum_{c \in C} u_{c,t}$ bounds are calculated. Using these bounds we can determine the production p_t for time intervals $t \in T$ such that:

- $l_t \leq \sum_{i \leq t} p_i \leq u_t$ to ensure that the production up to the time interval t is between the minimal and the maximal demands, and
- the number of time intervals $t \in T$ where the consecutive values p_t and p_{t+1} difference is minimal.

Note that, since the algorithm is on-line, only the production p_1 is determined for the coming time interval t_1. Let p_0 be the power generated in the time interval before t_1. In order to avoid frequent changes of the CHP mode, the production level p_1 is kept on the previous value p_0 unless this choice leads to underproduction or overproduction of electricity. In [RvL:1] a number of rules for this are explained depending on typical situations which may occur in practice. Also, further explanations and illustrations of possible control situations are given in [RvL:1].

7.6.3 Results

The control objectives for space heating are somewhat contradictory: the thermal comfort should be as close to the desired setpoints as possible, the energy consumption should be as low as possible and the number of times the heat pump switches on or off should be limited. We have shown in previous sections of this chapter that if the number of heat pump switches are not part of the control algorithm, optimal thermal comfort and minimal energy consumption is reached with a rather frequent switching of each heat pump. Therefore we implement an additional rule within the earliest deadline algorithm to keep the heat pump in space heating mode once it is turned on, for 4 up to 8 consecutive time periods. With this, we investigate:

- The number of times the heat pumps switch between on/off states compared to MILP-control. This is evaluated by counting the number of times the state of a heat pump changes (denoted by parameter SC_{hp}) and by determining the average number of consecutive time intervals a heat pump operates for the two similar weeks as investigated for the MILP-control ($\bar{OP}_{hp}$).
- The thermal comfort for each house. This is evaluated by summing for two categories (under and over temperature) the temperature difference between the achieved interior temperature and the set point interior temperature for each of the two weeks, divided by the total number of time intervals with under or over temperature respectively (ΔT^+ and ΔT^-).
- The number of times the CHP switches to different operation modes. This is evaluated by counting the number of state changes of the CHP (SC_{chp}) for each of the two weeks.
- Direct supply of the heat pumps by the CHP, implying that there is a minimal electricity flow to/from the grid. This is evaluated by summing the electricity flow to/from the grid, separated into under and over production and divided

by the total number of time intervals with under or over production respectively ($GRID^{+}_{chp}$ and $GRID^{-}_{chp}$). Furthermore, we determine the maximum flow for each of the two weeks ($MAX_{grid,chp}$).

Robustness of the heat pump control can be investigated by evaluating the obtained switching behavior of every heat pump in time. It can be seen, that there are no significant differences between the 104 heat pumps when it concerns the number of switches and the number of hours of continuous operation. The only significant difference is the moment when each heat pump starts and stops. Hence, the same example heat pump as used in the previous discussion on MILP-control is shown from the group of 104 heat pumps. In Figure 7.13 the control of this heat pump is shown for the coldest week in the winter and in 7.14 for the week in spring. In these figures, first the reference control is shown, second the control obtained from MILP-algorithms discussed in the previous sections and third, two cases of the control obtained from the EDF-algorithms, EDF4 and EDF8 which signify the number of time intervals the heat pump is forced to be on (off) once it is turned on (off). As expected, EDF8 results in higher fluctuation of the interior temperature, see Figure 7.15.
The results are summarized in Table 7.2. For both weeks EDF-control shows much less state changes of the heat pump (SC_{hp}) and longer time intervals of continuous operation ($\bar{OP}_{hp}$) compared with MILP-control. The two EDF controls also show some differences. EDF8 results in approximately the same number of state changes as the reference control. To compare the achieved thermal comfort, the room temperatures are shown in Figure 7.15. As discussed in previous sections, the room temperature obtained by reference control is sometimes lower than the set-point temperature, which is a violation of the minimum requirements. Hence, in Table 7.2 reference control has the largest values for ΔT^{-}. Notice also an equally good performance of MILP-control and EDF-control, which is promising as EDF is a much faster algorithm. Furthermore, notice that the values for ΔT^{+} are of less concern. These slightly higher temperatures above the set-points are caused by solar gains. During the heating season, slightly higher temperatures due to solar gains are usually not interpreted as comfort violations by inhabitants.

The control of the CHP is investigated for the same week in the winter and spring. Figure 7.16 shows for the week in winter, the results of the reference control, the MILP-control and the two cases of EDF-control. Figure 7.17 shows the same for the week in spring. Results are also summarized in Table 7.2. Both figures demonstrate that the objective of the MILP-control, i.e. to minimize the peak electricity demand, is reached very well by this control but without additional constraints this also results in a CHP control which changes the operational state of the CHP very often, resulting in the high values for SC_{chp} in Table 7.2. The EDF-control shows very stable CHP operation, i.e. low values for SC_{chp}. However, EDF-control produces some peaks on the fourth day, i.e. the day with the highest heating demand, where most of the heat pumps simply have to run simultaneously and the CHP has to produce the associated electrical energy demand. Note, that on that

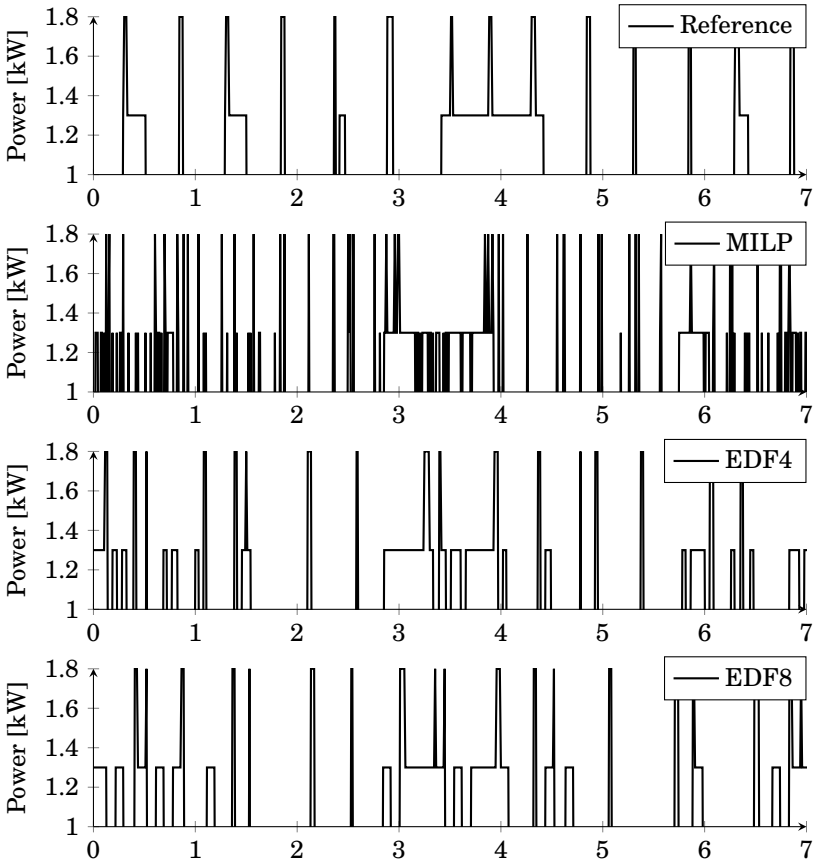

Figure 7.13 – Consumption of electricity by one heat pump in winter

day the reference control is not able to support adequate thermal comfort (refer to Figure 7.15) and MILP-control switches the heat pumps on and off the most frequent (refer to Figure 7.13).
Figure 7.17 shows for the EDF-control an interesting advantage of the EDF8 variant. In that week, on the fifth day there is suddenly the first space heating demand of that week. Before that day, the CHP produces constantly the electric demand for some of the heat pumps to produce thermal energy for domestic hot water. On the fifth day, the EDF8 variant produces a smaller peak than the EDF4 variant. So the advantage of increased constraints on buffer capacity and operational time of EDF8 is that this reduces required production peaks of the CHP and this may lead to a smaller size and lower costs of the CHP.

As explained in Section 7.6.2 EDF-control is programmed in such a way that the CHP is never producing insufficient amounts of electric energy for the aggregated demand of the heat pumps. Figure 7.18 shows that the CHP is always slightly

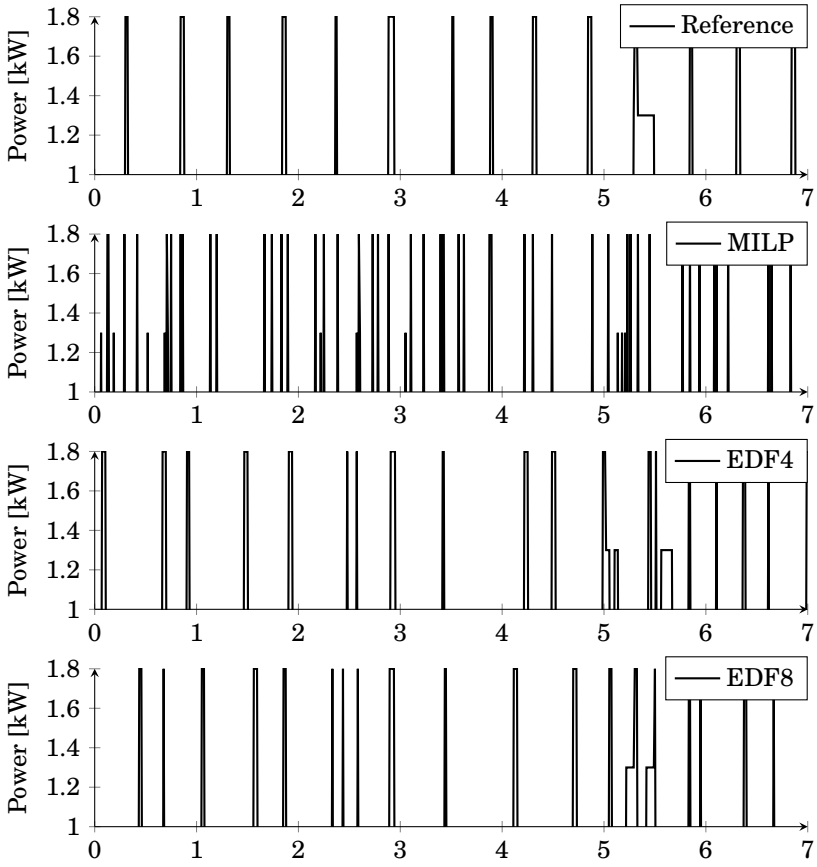

Figure 7.14 – Consumption of electricity by one heat pump in spring

overproducing, as is also seen in the value of $GRID^{-}_{chp}$ in Table 7.2. In some intervals in the winter, when heat demand is the highest, the CHP has significant overproduction for short periods of time, seen from the peaks in Figure 7.18 and the value in winter for $MAX_{grid,chp}$ in Table 7.2. This is caused by the chosen control steps of the CHP and the programmed bandwidth between minimal and maximal estimated demand. If a larger range of steps is programmed and the bandwidth is narrowed, the overproduction peak is decreased and could vanish entirely. This is a matter of tuning the algorithms in practice.

The presented simulations were run on a computer with the processor Intel(R) Core i7-6700 (TM) CPU @ 3.40GHz using only a single thread. The running time of one simulation consisting of 104 houses and 1920 time intervals is 63 seconds which is 315 μs per house and per time interval, whereby most of the running time is spent in the dynamic programming step to determine the energy plan of each house at every time interval. As a consequence, it is possible to embed

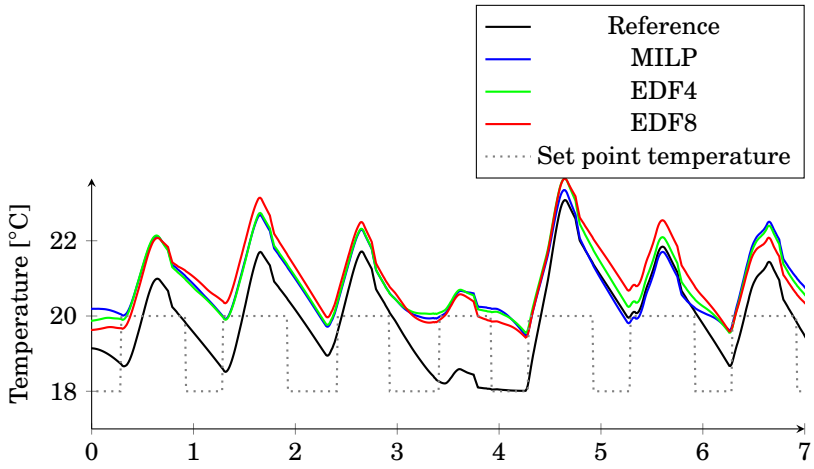

Figure 7.15 – Zone temperature in one house in winter

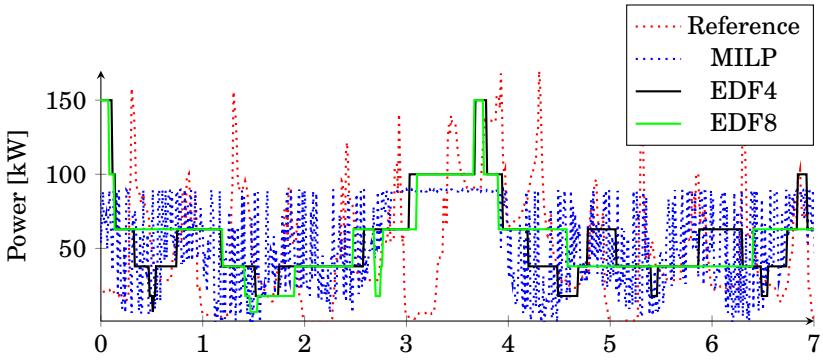

Figure 7.16 – Electricity produced by CHP in winter

the house controller such that it can run on a simple and cheap micro-controller. Furthermore, the amount of transmitted data between house controllers and the central controller is small. The energy plan sent from each house controller to the central one is made for a day (96 time intervals) ahead, so it consists of less than 200 numbers which can be transmitted in a single TCP/IP packet. The response from the central controller is a boolean for every house whether its heat pump is selected to run or not.

7.7 Conclusions

In this chapter, optimal control is investigated of a group of 104 heat pumps and a single Combined Heat and Power (CHP) unit, which is placed on the level of

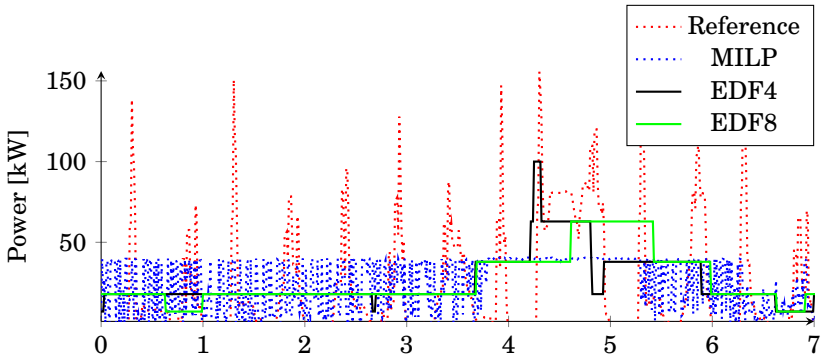

Figure 7.17 – Electricity produced by CHP in spring

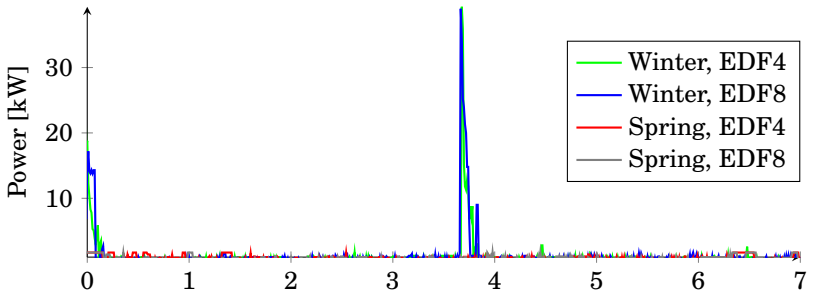

Figure 7.18 – Earliest deadline: Export of electricity

the aggregator. The heat pumps supply thermal energy for households for space heating and domestic hot water. Each house has floor heating for space heating and a thermal storage for domestic hot water. In the first part of the chapter, control of the heat pumps by Mixed Integer Linear Program (MILP) optimization and a faster algorithmic variant called time scale MILP is investigated. Compared to feedback (reference) control, the optimal control methods result in improved thermal comfort for the residents and a reduction of the aggregated electricity demand peaks of the heat pumps. However the obtained control schemes of the heat pumps and CHP result in too frequent on/off switching of these devices. Besides this, for privacy reasons, it is not desired to communicate household thermal comfort information towards a central controller. To overcome these problems, an alternative control method based on the mathematical concept of Earliest Deadline first (EDF) is investigated in the second part of the chapter. Unlike the control methods based on MILP where all calculations are performed on the aggregator level, each houses now has a smart controller which performs the model predictions of heat demand and communicates to the central CHP controller their priority which is done by specifying an upper and lower bound for the electricity demand up to a certain time interval. This relieves the previous encountered privacy issues considerably.

Control results are shown for a cold week in winter and a warmer week in spring. Results for one heat pump are shown as all heat pumps show similar behavior. The EDF-control method results in an equal thermal comfort for the households as MILP-control. However, the switching behavior of the EDF-heat pump control is much better than MILP-control, which has an advantage for the operational life of the heat pumps.

Similar to the heat pump control, the EDF-control of the CHP demonstrates a very steady behavior of the CHP with only a few changes in the operational state of the CHP per week, contrary to the MILP-control which results in many changes per day. The EDF-control also demonstrates peak reduction capabilities and the capability to choose if the CHP should always produce a bit less than, as close as possible to or more than the demand. This can be influenced by more sophisticated programming of the control states of the CHP, which is left for future work when this type of control is implemented in a real system. Also part of future work is to verify how the control behaves in practice and if a 15 minute time interval for the evaluation of deadlines is sufficient. Another approach is to modify the earliest deadline rules in such a way that the CHP and all heat pumps are controlled in real time.

Besides the advantages already mentioned, the EDF-control algorithm appears to be very fast and is therefore ultimately scalable to larger and more complex energy systems. In the Meppel case which is discussed in this chapter, the heating system is separated from the domestic electricity supply system. However, in the future the latter system may involve renewable energy from rooftop PV panels and smart control of flexible devices for each house, such as a battery charger/dis-charger and a washing machine. The EDF-control may be extended to include this type of control as well. In this way, depending on the application, EDF-control may be an alternative to well established smart grid control methods such as cost based or auction based control. Part of future work is to further investigate to which extend EDF-control is capable to control more complex energy systems containing multiple energy supply sources and large numbers of flexible devices.

parameter	SC_{hp}	$\bar{OP}_{hp}$	ΔT^{+}	ΔT^{-}	SC_{chp}	$GRID^{+}_{chp}$	$GRID^{-}_{chp}$	$MAX_{grid,chp}$
unit	-	intervals	^{o}C	^{o}C	-	kW	kW	kW
winter								
ref	38	14.6	1.18	-1.11	386	-	-	-
MILP	200	2.5	1.72	-0.09	634	-	-	-
EDF4	67	7.5	1.78	-0.10	30	0.99	0	39.3
EDF8	58	10.5	1.92	-0.14	18	1.17	0	39
spring								
ref	30	4.1	3.26	-0.24	297	-	-	-
MILP	112	1.1	3.34	-0.10	618	-	-	-
EDF4	42	3.4	3.30	-0.04	13	0.69	0	1.7
EDF8	40	3.3	3.40	-0.1	8	0.65	0	1.7

Table 7.2 – Results

Chapter 8

Case IV: Off-grid energy system for a neighborhood

Abstract - In this chapter, the possibility for off-grid operation for a neighborhood of 16 houses is investigated. This investigation is performed with a smart grid simulation model of the neighborhood which consists of modern, well-insulated terraced houses. Each house is equipped with roof-mounted photovoltaic (PV) panels and has a battery. The neighborhood has a district heating system to which the houses are connected. The system uses a bio-gas co-generator with thermal storage. The technical feasibility for near off-grid operation of this neighborhood is demonstrated and the role of smart control is investigated. The investigation also includes an estimation of system dimensions, e.g. for solar PV, CHP and storage capacities. For this, methods developed in Chapters 2, 3 and 6 are applied.

8.1 Introduction

As explained in Chapter 1, hours in which renewable energy is produced by solar or wind energy often do not match the hours in which the energy demand occurs. In [123] it is shown that electrical energy storage, controllable electric devices and smart grids are ways to improve the match between demand at one time and available energy from renewable sources at another time. A specific area of interest is the so-called smart controlled micro grid, which is a low-voltage power grid which matches supply and demand locally, without causing peak loads on the larger distribution grid. This chapter investigates the feasibility of such a smart controlled micro grid for a group of houses with the specific challenge to balance local energy supply with the demand of the houses as much as possible. The purpose of this control is to operate almost independently of the main grid, which is called soft-islanding. Such a system adds robustness to the larger grid

[†]Major parts of this chapter have been published in [RvL:7].

to reduce large power peaks caused by moments of peak feed-in or peak demand within the neighborhood. This chapter verifies the feasibility of such a system using the Triana Demand Side Management (DSM) methodology developed at the University of Twente [110].
The main contributions of this chapter are to demonstrate for an integrated, small scale urban energy system:

- the role of smart device planning to reach electricity grid independence,
- the relation between capacity sizing and smart control.

8.2 Related work

The possibility to control energy production and consumption of houses or neighborhoods as part of a smart grid is a recent research area [103]. Some researchers focus on demand side management strategies in order to minimize energy costs for residents, or shaving peak loads on the network, while others focus on power quality and stability aspects in case of true islanded operation of microgrids.

In [112], loads on the network are investigated in case of a peak shaving strategy and energy cost minimization strategy for residents. In [111], results are shown for short term islanded operation of a single house, using a micro CHP with electrical and thermal storage. In [91], a more complex residential energy system is investigated which contains solar PV, solar thermal, a CHP and a boiler as generators and thermal and electric storages. Demand side management with model predictive control aspects is used to minimize energy costs for residents. The simulated results indicate that up to 30% cost reduction for residents is achievable. However, the optimization objective of minimizing energy costs for residents, results into frequent exchange of energy to the grid at times of high feed-in prices and from the grid at times of low energy prices. To reach off-grid operation, the goal is rather to minimize exchanges with the grid.

In [141] a decentralized microgrid for a residential area containing solar PV, wind turbines and electric storage is investigated on the capability to function independent from the main grid. The investigation considers only the domestic electric energy demand. This is also the case in [99] where models for power generators are used in order to investigate power quality and loads within off-grid microgrids.

The research presented in this chapter combines both generation and demand for electric and thermal energy within a small microgrid consisting of 16 houses. In general, the purpose is to reach (near) autonomous operation or soft-islanding from the main electricity grid. However, the decentralized energy system still needs a grid connection and connection to a gas grid, preferably a local bio-gas grid. The main contribution compared to related work is the integration of thermal energy demand and generation, combined with model predictive control to fulfill both electrical and thermal demand.

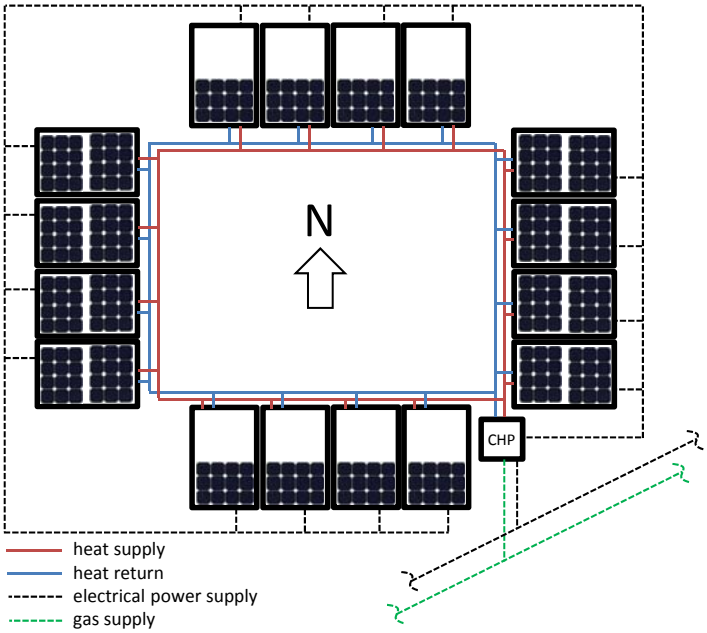

Figure 8.1 – Layout of the neighborhood and energy system

8.3 Methods

In this section we present an energy model of the neighborhood and determine preliminary the size of the CHP and thermal storage. Further, we present the methods used to determine the thermal and electrical load profiles of the neighborhood, and the optimization approach.

8.3.1 Model of the neighborhood

In Figure 8.1 a layout of the neighborhood is shown. Each block (16 blocks in total) represents a house, and gives the top view of the roof, including the placement of PV panels. The neighborhood comprises 8 corner houses and 8 terraced houses. The central CHP is shown together with its connections to the main gas and electricity grid. Via this CHP, each house is connected to the district heating and electrical micro grid.
The controller aims to meet the thermal and electrical energy demands while also leveraging local resources such as a hot water storage tank, time-shiftable flexible loads and the CHP plant.
Energy flows within the neighborhood are modeled as shown in Figure 8.2. The domestic thermal demand is given in the lower right corner, the domestic electrical energy demand in the upper right corner and the energy supply system is given on the left side. The symbols used for the domestic electrical demand are (top

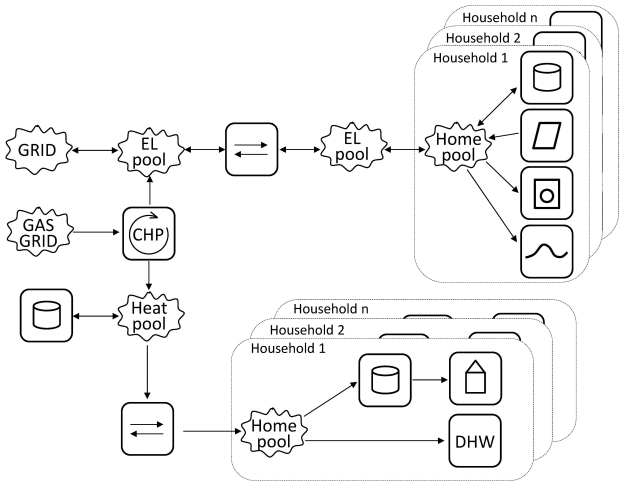

Figure 8.2 – Schematic representation of the neighborhood energy system.

to bottom): battery storage, PV panels, flexible devices (e.g. washing machine), uncontrollable demand.

8.3.2 Thermal loads

In this section, the methods used to obtain the aggregated, hourly thermal load profile and dimensions of the CHP and thermal storage are explained. Thermal load data is created with the methods explained in Chapter 2, using the 2R2C models for a corner and terraced house. Higher daytime and lower nighttime set-points for the interior temperature are used. Orientation of the houses in relation to solar gain calculation is taken into account. Besides that, small differences between the houses with respect to interior temperature, ventilation set points and occupancy related heat gains are taken into account. The domestic hot water demand profile is obtained by summation of manually defined household demand schedules, multiplied with a random number. The thermal load profile method is based on the method explained in more detail in Chapter 3. Each house has, on average, a thermal demand of approximately 28 GJ per year of which 18 GJ is for space heating and 10 GJ is for domestic hot water.

Preliminary sizing of the CHP and thermal storage

At the time of performing the smart grid simulations for the related paper [RvL:7] (discussed in Section 8.4), the capacity sizing method explained in Chapter 6 was not yet developed. A method is used, which is described in more detail below. The used parameters and variables are given in Table 8.1.

In general, the thermal demand can be generated by the CHP in mono operation (only the CHP), or in dual operation (with a supporting boiler). The storage size

Parameter	Signification	Unit
V	buffer capacity	m^3
D_t	aggregated thermal demand at time interval t	MJ
t	time interval, $t \in \tau = [0, \frac{15}{60}, \frac{30}{60}, .., 24]$	hour
$\bar{D}_\tau$	average demand per time interval	MJ
$\hat{D}_\tau$	peak demand per time interval	MJ
$Q_{chp,max}$	CHP maximum thermal production capacity per time interval	MJ
$Q_{chp,t}$	CHP thermal production at time interval t	MJ
$Q_{b,max}$	boiler maximum thermal production capacity per time interval	MJ
$Q_{b,t}$	boiler thermal production at time interval t	MJ
$E_{st,t}$	stored thermal energy in the thermal storage at time interval t	MJ
$E_{st,max}$	maximum capacity of the thermal storage	MJ
$E_{st,min}$	minimum capacity of the thermal storage	MJ
x_t	CHP control variable	-
z_t	boiler control variable	-
T_s	supply temperature from the storage	C
T_r	average return temperature to the storage	C
ρ	water specific density	kg/m^3
c_p	water specific heat	kJ/kg K

Table 8.1 – storage size optimization parameters and variables

depends on this choice and on the size of the CHP plant. For the smart control case, the CHP size is chosen for mono-operation without a supporting boiler.
The capacity of the CHP plant and the thermal storage size are determined for the day with the highest thermal demand. In Figure 8.3 the aggregated thermal load on this day with the highest demand is shown.

The average demand $\bar{D}_\tau$ (sum of demand divided by total number of time intervals) and the peak demand value $\hat{D}_\tau$ are determined from the demand data shown in Figure 8.3. The following equations govern the heat transfer between supply and demand.

For the control of the heat production, we have

$$Q_{chp,t} = x_t \cdot Q_{chp,max} \tag{8.1}$$

$$Q_{b,t} = z_t \cdot Q_{b,max}\,, \tag{8.2}$$

whereby for the balance of the heat production, demand and storage we have

$$E_{st,t} = E_{st,t-1} + Q_{chp,t} + Q_{b,t} - D_t\,, \tag{8.3}$$

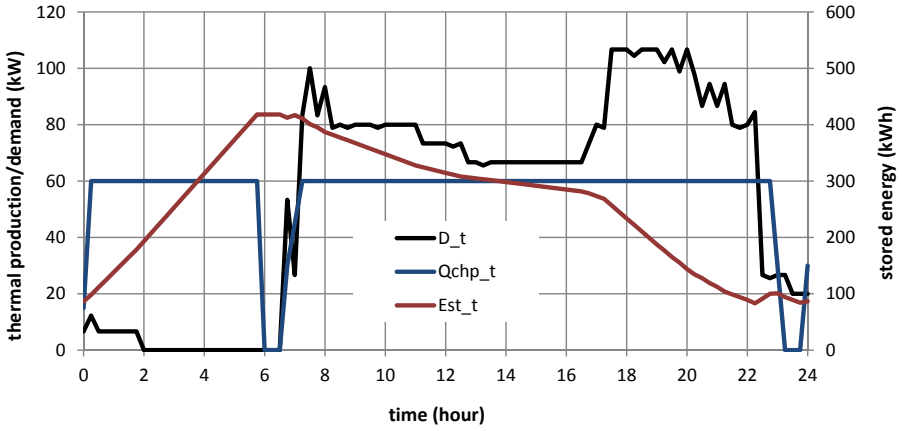

Figure 8.3 – Demand data and preliminary charging results

whereby for the constraints for the thermal storage are given by

$$\begin{aligned} E_{st,max} &= V \cdot \rho \cdot c_p \cdot (T_s - T_r) \\ E_{st,min} &= 0.2 \cdot E_{st,max} \\ E_{st,min} \leq E_{st,t} &\leq E_{st,max} \ \forall t \in \tau \,, \end{aligned} \tag{8.4}$$

in which the factor 0.2 is introduced as minimum charge level of the storage. Furthermore, the following relation between the boiler and CHP is introduced:

$$Q_{b,max} = \begin{cases} \hat{D}_\tau - Q_{chp,max} & \text{if } Q_{chp,max} < \bar{D}_\tau; \\ 0 & \text{if } Q_{chp,max} \geq \bar{D}_\tau, \end{cases}$$

where the optimal size of the thermal storage is determined by solving an optimization problem which has the following objective:

$$minimize \ \left\{ F1 \cdot \sum_\tau Q_{chp,t} + F2 \cdot \sum_\tau Q_{b,t} + F3 \cdot V \right\}, \tag{8.5}$$

where the factors F1 to F3 are cost factors which can be chosen as realistic values. However, we chose artificial scaling factors such that each term has more or less an equal weight within the objective.

The variables in the given problem are:

$$x_t, z_t, V \,;\, t \in \tau \,, \tag{8.6}$$

whereby these control variables are subject to the following constraints:

$$\begin{aligned} x_t &\in [0, \frac{1}{4}, ..., 1] \\ z_t &\in [0, \frac{1}{5}, ..., 1] \,, \end{aligned} \tag{8.7}$$

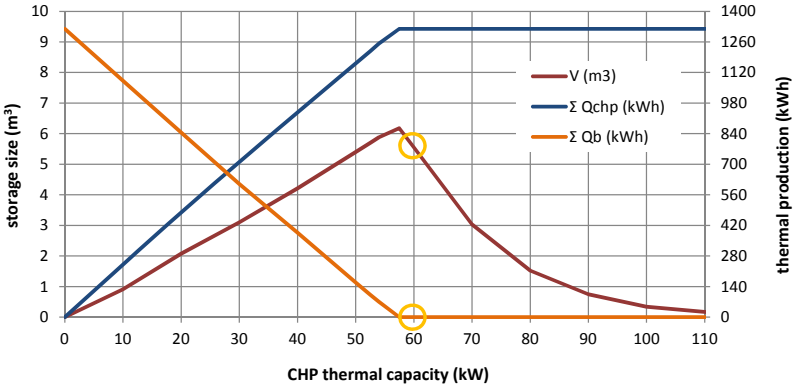

Figure 8.4 – Resulting capacity relations

indicating that the units have 4 and 5, respectively, operational states besides being off. The optimization is solved for a possible set of possible CHP thermal capacities ranging from 0 to 110 kW, using OpenSolver's linear branch and cut solver. For each pre-defined CHP size, the results include a planning for the CHP and the boiler and a storage size.

The resulting capacities are shown in Figure 8.4. The storage size is shown in m^3 water volume, scaled on the left vertical axis and the sum of the CHP and boiler thermal production is shown in kWh on the day with the highest demand, scaled on the right vertical axis. The horizontal axis signifies the thermal capacity of the CHP. The maximum storage size is determined at the point where the CHP thermal capacity equals the average demand $\bar{D}_\tau$, i.e. 56 kW. A smaller CHP size requires a supporting boiler and smaller storage size, a larger CHP requires a smaller storage size. Theoretically, the CHP is able to supply every demand without a thermal storage from the point where the CHP capacity equals the maximum demand $\hat{D}_\tau$, i.e. 107 kW. However, the graph shows still a small required storage size for that capacity due to the fact that the optimization is performed with as discrete control variable x_t which controls the CHP output in four steps rather than a continuous control variable.

Based on this analysis, the capacity of the CHP is chosen at 60 kW thermal and 30 kW electrical power based on conventional CHP efficiency values, in combination with a 5.55 m^3 storage tank, or 250 kWh thermal storage capacity, indicated with circles in Figure 8.4.

Besides the optimal storage size, the result of the optimization includes a planning for the CHP output and the stored energy for each time interval. It is interesting to verify if the electric production of the CHP matches the demand. The CHP planning for the coldest day is shown in Figure 8.3. The demand (D_t) and the CHP thermal production (Qchp_t) are scaled on the left, and the stored energy (Est_t) is scaled on the right vertical axis. Because the thermal capacity of the CHP is chosen close to the average thermal demand, the CHP operates almost continuously at

it's maximum capacity. On this day with the highest heating demand, the CHP produces in total 1320 kWh thermal energy and 660 kWh electrical energy, i.e. 41 kWh per house. This is much more than the daily electrical energy demand, which is given by 10.2 kWh, as is discussed in Section 8.3.3. To size the CHP also according to the electrical demand, other generation options may be investigated, e.g. support by a boiler or a heat pump. These options will diminish the electrical energy production to an amount which is closer to the real household demand during colder days.

8.3.3 Electrical loads

Uncontrollable devices

In the smart grid model, each house is given a unique static electricity consumption profile which represents the aggregated load of domestic devices such as lighting, electronics, ventilation, etc. The fixed load profile is artificially generated using the method discussed in Chapter 2 which is based on smart meter measurements obtained in the Dutch field test in Lochem (see [74]). Profiles are generated based on occupancy, activities and age of persons in a household and is given in the average power consumption for 15-minute time intervals. The resulting daily average electricity consumption per household is 7.6 kWh.
Electricity produced by the roof-mounted PV panels is calculated using weather data measurements of the year 2014 from the Twente measurement station [88]. This dataset provides the solar energy irradiation on a horizontal plane in hourly intervals. These values are linearly interpolated to match the 15-minute intervals used in the simulations. Calculations are then performed to estimate the direct and diffuse irradiation on a horizontal plane (see [158]), which are used to calculate the perpendicular irradiation on the PV panel. Based on the efficiency of the setup (PV panels and inverter), this solar energy is converted in the corresponding electricity production. The final chosen parameters are given in Section 8.3.5.

Controllable devices

Each house is assumed to own two time-shiftable devices: a dishwasher and a combined washing machine/dryer. The probability profile of startup times and delay times for each device in each house is assumed to follow the overall European profile. The actual energy use of each device is based on [74]. Combined with the static electricity profile for the base load, this results in a total electricity consumption of 10.2 kWh per household per day on average.

8.3.4 Optimization approach

Flexible Appliance Scheduling

To schedule the appliances, the profile steering methodology introduced in [61] is applied. The given implementation steers the energy use towards a desired profile,

i.e. the methodology attempts to minimize the difference between a desired profile and the realized profile. The methodology works hierarchically and in two phases. In the initial phase each appliance is requested by the controller to construct a schedule which results in a household load profile that is as flat as possible. Then the scheduled profiles are aggregated and the result is compared to the desired profile. In the second iterative phase, each appliance is then asked to construct a new, candidate schedule which best compensates for the deviations between the aggregated scheduled profile and the desired profile. In each iteration, the appliance with the best candidate schedule is picked. This appliance then updates its schedule to match the candidate schedule. The results presented in [61] show that, for a test case of 121 houses, the methodology significantly lowers the peak load and keeps voltages within legal bounds. To reach soft-islanding, the desired profile in this chapter is set to a zero profile, meaning that the objective is to minimize import and export of electricity.

Optimization Test Cases

Three different strategies are evaluated using the simulated electricity and heat demand data and applying optimization using ideal predictions of demand and weather forecasts to schedule the flexible devices.

i - Base Case (BASECASE) In the first case, no electricity storage system is implemented. The CHP is controlled only to meet the heating demand by maintaining a sufficient state-of-charge of the thermal storage. Additionally, the CHP is controlled such that it maintains a certain operational state as long as possible and can operate at a wide operational range. Practically, this can be achieved by parallel operation of several smaller CHPs, each having a more restricted operational range.

ii - Optimal Control (CON) In the second strategy, the controller decides on the start times of the time-shiftable devices and the operation of a thermal water tank. The optimization strategy of the controller is to flatten the energy profile for the community of houses such that there is zero or nearly zero energy withdrawn from the grid. To allow more freedom to adjust the CHP's electrical production according to the needs of profile steering, every operational state of the CHP is assumed to be possible between zero and maximum capacity.

iii - Optimal Control with Energy Storage (CON/BAT) In the final situation, control of domestic appliances is implemented, but additionally each house is given a battery storage system as a resource. In the overall control strategy, the accumulation of the batteries acts as a community resource and is used to further flatten the energy profile and minimize dependence on the electric grid. The possible CHP operational states are the same as for the CON strategy.

8.3.5 Sizing the system

Sizing of the solar PV and battery system is determined by preliminary calculations, which are explained in detail in [RvL:7]. As a result, the following values are used for the system:

- CHP with 60kW thermal/30kW electricity and 250kWh thermal storage connected to the CHP (CON and CON/BAT). Both are determined in Section 8.3.2. For the BASECASE, the storage capacity is chosen at 50 kWh.
- 15m^2 of PV panels per house
- 2kWh battery storage per household for case CON/BAT, and 0kWh for cases BASECASE and CON.

8.4 Results

In the paper [RvL:7], 5 different weeks are investigated to evaluate the seasonal effects on the system. In this chapter, two weeks from this paper are discussed, these are week 4 with a high heat demand and low PV generation and week 26 with a low heat demand and high PV generation.

Figure 8.5 shows the CHP power production and Figure 8.6 the power exchange with the larger grid for the two weeks, whereby negative values indicate energy exports to the grid. In the base case (BASECASE), operational changes of the CHP are driven by the constraints on meeting heating demand and charging the thermal storage. Both the control (CON) and control/battery storage (CON/BAT) strategies operate less often at extremes in CHP production when compared with BASECASE. This is because the systems efficiently utilize the larger thermal storage. The difference in the CON and CON/BAT profiles is the ability to shift electric loads to reduce peak loads compared to the base case. The additional benefit of battery storage in the CON/BAT case is that it is able to smoothen the demand profile even further, which is better for the operation of the CHP.
During the winter week, CHP production is driven primarily by heating demands for the community which results in overproduction of electricity. Observe that the CON and BAT/CON case show more variation of CHP operational states which is a consequence of the control algorithm implemented in the simulation. When for instance the earliest deadline control explained in Chapter 7 would be implemented, the CHP operation would be more constant. The BASE case shows that at some moments, grid imports are required, which is not seen in the CON and BAT/CON cases. In these two cases, the system is exporting electric energy at all times, with a flattened profile.
During the summer week, the CHP either operates with a much lower operational state (BASE case) or only for a portion of the day (CON and BAT/CON cases) because there is only a minimal heating demand. The combination with the PV system leads in the BASE case to much export of electricity, while in the morning

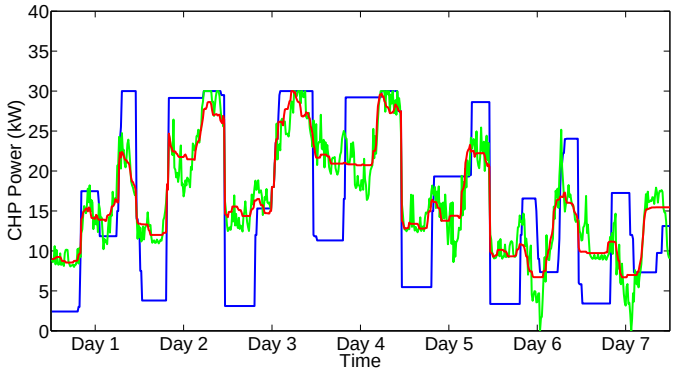

(a) Week 4

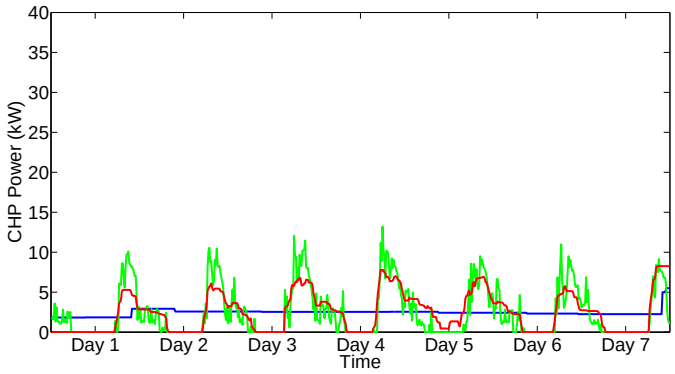

(b) Week 26

BASECASE CON CON/BAT

Figure 8.5 – CHP electric power production

hours, there is significant import of electricity from the grid. The CON case reduces these imports significantly, and the BAT/CON case removes them entirely and also diminishes the export peaks effectively.

The benefits of the CON and BAT/CON scheduling strategy are: (1) almost non-existing imports of grid electricity and (2) creation of predictable loads at the grid connection and in the BAT/CON case a flat profile. Thus, the interaction with the larger electricity grid can be realized in a predictable and consistent manner. However, the energy system has shown to be overproducing electricity during all the investigated test weeks. Therefore, a more careful sizing of the energy system with the method developed in Chapter 6 is investigated in the following section.

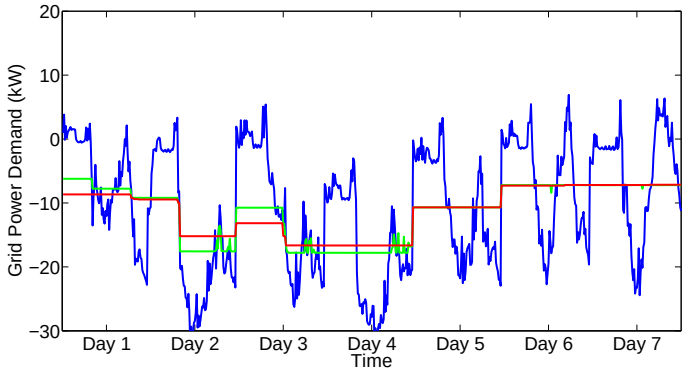

(a) Week 4

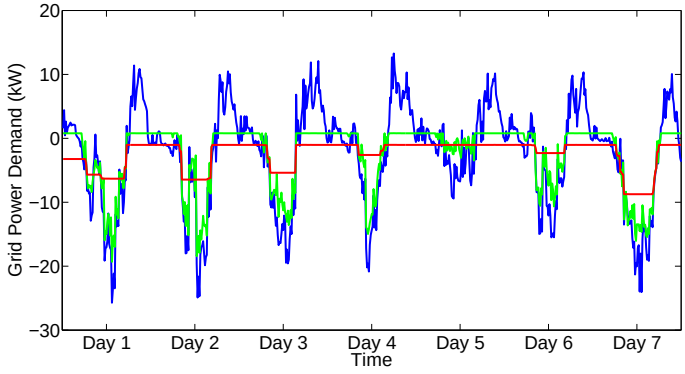

(b) Week 26

BASECASE CON CON/BAT

Figure 8.6 – Grid power demand

8.5 Evaluation of generation and storage sizes

Sizing the energy system for near off-grid operation the whole year appears to be complex. This is a consequence of the interaction of the thermal and electrical demand, control of the CHP for production of thermal and electrical energy, solar PV generation and control of the thermal and electrical storage. At this stage of development, the Triana smart grid simulator still depends on manual input of sizes of several assets. To determine optimal sizes in this way is very time consuming as it requires many simulations in which the size is changed manually for each simulation. This is why the capacity model developed in Chapter 6 and the algorithms shown on the last pages of that chapter are used to achieve a more appropriate set of capacities, which are possible in practice.
First, the market of micro-CHP units is investigated. Such units start from an

Figure 8.7 – common micro-CHP unit [35]

electrical output of 1kWe with electrical efficiency of approximately 20% (Stirling cycle) (average price level: €8000/kWe). Piston engines start from 5kWe with typical electrical efficiency of 28% (average price level: €4000/kWe), and suppliers include Dachs (Germany) or Honda (Japan). Istituto Motori-CNR in Italy reports on a research to improve the efficiency of a 10kWe piston engine shown in Figure 8.7, (see [35]).

Besides a CHP, a boiler is introduced as it is learned from the previous section that the CHP produces too much electricity in relation to the thermal production when there is only a CHP to supply the demand. The optimization objective is to minimize the yearly sum of the absolute values of the grid exports and imports. As result, the upper boundaries of the thermal and battery storage were found to be proper values. This is because the optimization does not consider costs. The thermal storage and electrical battery size are diminished manually after the optimization to lower the costs significantly while keeping the effects on the objective negligible. The following sizes are determined as (near) optimal in this case:

- CHP with 12.1 kW thermal/5.1 kW electricity
- 100kWh thermal storage connected to the CHP
- Boiler with 52 kW thermal capacity
- $8m^2$ of PV panels per house
- 4kWh battery storage per household

Comparing this with the results of Section 8.3.5 it appears that the earlier manual estimation based on rough calculation of the thermal and electrical demand led to a CHP, thermal storage and solar PV system which were too large. However, the thermal generation now also includes a boiler. The sum of CHP and boiler thermal capacity is 64 kW which is approximately similar as the thermal capacity of the CHP in the previous section. The battery system is larger than the system of the previous section. This may be due to the influence of smart control of flexible devices which is part of the analysis of the previous section, but is not part of the capacity model.
The yearly results of a simulation with the capacity model for the proposed system capacities are as follows:

- household electric demand: 44,524 kWh
- electricity production, CHP: 35,557 kWh, solar PV: 20,636 kWh
- grid import: 199 kWh, export without power to heat: 11,875 kWh, with power to heat: 4,385 kWh
- household thermal demand including network losses: 153,013 kWh
- CHP thermal production: 85,082 kWh, boiler thermal production: 67,881 kWh. These values are slightly lower in case of power to heat.

To conclude this evaluation, Figure 8.8 shows a particularly difficult week from the results of the algorithmic capacity model in which there is some import required from the electricity grid on the third and fourth day. CHP production is indicated with the blue line, boiler production with the black line (external heat). Evaluating the state of charge of the thermal storage and the production rate of the CHP, more production of the CHP could be possible on day three and four, which would result in a higher state of charge of the thermal storage and batteries during the difficult moments. The grid imports could then be avoided entirely. Such a control of the CHP is only possible if the control includes predictions of the upcoming electrical and thermal demand. Hence, if a smart CHP control is implemented, the energy system in theory, will not require any electrical energy from the main grid.
Also, with implementation of the power to heat (direct dissipation of electricity into the thermal storage) or an additional demand, e.g. an electric vehicle, the total grid exports could also be lower or even be non-existing. Note that the power to heat solution applied in the algorithmic capacity model, is used in a similar way (demand response) as smart control of flexible devices of the households in the previous section.
Although this is an artificial case and truly balancing such a small system in reality including prediction uncertainties is more difficult in practice, the case provides a clear demonstration of the capabilities of smart control to significantly reduce grid loads and the role it could play within future micro energy systems which may be nearly or entirely off-grid.

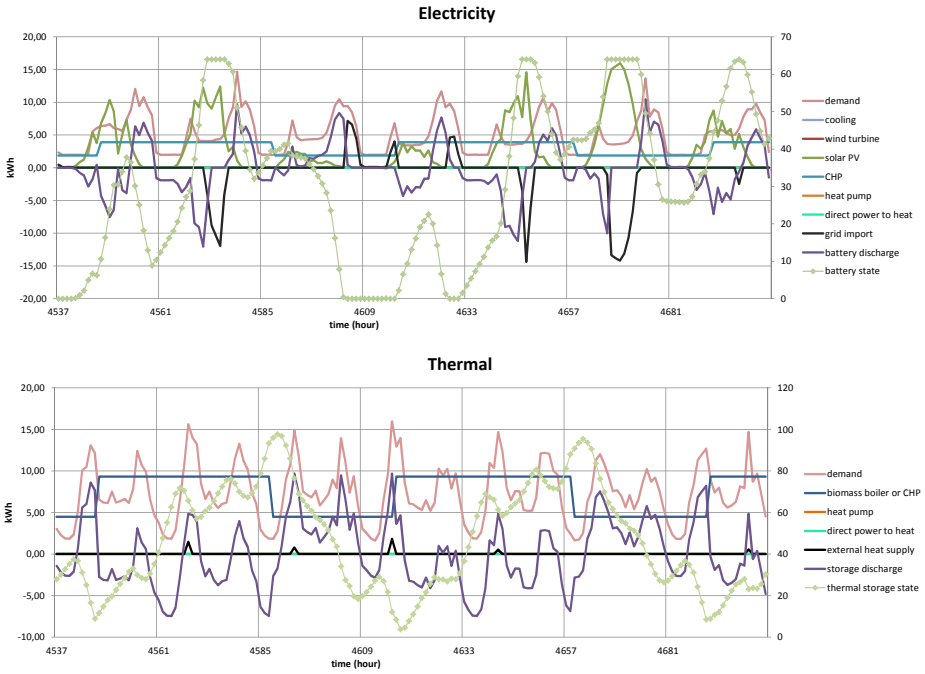

Figure 8.8 – Results capacity model for week 28

8.6 Conclusions

In this chapter, near off-grid operation of a neighborhood is investigated. Power balance is maintained using smart control of a CHP and flexible devices such as battery chargers and household devices such as washing machines. The thermal demand is supplied by a CHP entirely and the electric demand by the CHP and the solar PV system. Three cases are investigated: a base control without batteries and flexible devices (BASE), control of the flexible devices (CON) and control of flexible devices and batteries (BAT/CON). The BAT/CON control shows as expected the best performance to reduce grid imports and exports.

The simulations demonstrate the difficulty of sizing the energy system as the proposed energy system produces too much electricity during all weeks of the year. Therefore, in the second part of the chapter, sizing is investigated in more detail with the capacity model of Chapter 6. A boiler is added to the energy system to improve the balance between thermal and electrical energy generation. This leads to an energy system configuration that requires almost no grid imports and low grid exports. It is argued that the grid imports can be avoided entirely by implementation of the smart CHP and battery control discussed in the first part of the chapter.

If power to heat or an additional demand (e.g. electric vehicle) is introduced, the

electricity exports become negligible and the energy system is theoretically capable to go off-grid the whole year. However, in practice there are uncertainties which will make it more difficult to maintain this (theoretical) power balance. The case investigation demonstrates nicely the relation between the capabilities of smart control and optimal system capacities.

Chapter 9

Conclusions

Abstract - The integration of renewable energy in existing networks and specifically urban districts, introduces complex challenges for the energy system. Demand and supply patterns become more difficult to match and the emphasis is shifted from central towards regional and local investments in energy generation and storage technology. This leads to an increased importance of optimal capacity analysis and optimal energy control of such systems. This thesis is dedicated to the development of methods to deal with these aspects and demonstrates how smart control leads to better usage of renewable energy system assets.
Although the tools presented and investigated in this thesis can assist in developing and control smart urban energy systems, the realization of such systems involves much more than that. The required investments, sometimes negative public opinion e.g. about local wind turbines and legal issues about permissions to supply energy, prove to be more difficult obstacles than the technical issues investigated in this thesis. On the other hand, a number of initiatives like the Meppel project reported in this thesis are demonstrating that also today, it is possible to built more energy efficient houses and establish a 100% renewable, urban energy system.
This chapter is structured as follows. In Section 9.1 a summary is given, followed in Section 9.2 by answers in relation to the research questions formulated in Chapter 1. In Section 9.3 the scientific contributions of this thesis are summarized and in Section 9.4, recommendations for future work are given.

9.1 Summary

9.1.1 Modeling part

In Chapter 2, thermal network models are investigated with the purpose to use such models as white or grey box models to predict the thermal demand of houses within model predictive control methods. A model parameter estimation procedure is carried out based on data generated by simulations of detailed house models

with a single interior thermal zone made in TRNSYS. A model with two thermal resistances and two lumped thermal mass terms (2R2C) for the interior zone and the floor heating system appears to be sufficiently accurate and the parameters correspond to physical calculated values which allows this model to be used as white box model. As a consequence, it is possible to pre-calculate the model parameters from data on geometry and physical properties of houses. The estimation procedure and 2R2C model parameters (estimated and pre-calculated) are verified for light and heavy constructional variations of the most common types of Dutch reference houses. In general, the estimated and pre-calculated values of the model parameters agree well, except for the thermal resistance between the floor heating mass and the thermal zone mass.

In this thesis, thermal network representations of houses are used for two purposes: (1) to generate demand profiles of households and districts (refer to Chapter 3) and (2) for model predictions as part of smart heating control (refer to Chapter 7). It is demonstrated that the accuracy of the models is reasonable. However, influences such as the house orientation, the shadows cast by trees in relation to incident solar energy, air infiltration due to strong winds and last but not least occupant behavior and uncertainty margins of weather forecasts are likely to lead to more significant prediction errors than the errors resulting from the model approximation. Therefore, besides the thermal network model, an additional model is proposed for instance based on neural networks which is will learn its parameters from differences between measured values and model predictions.

By generating different profiles of different households and applying a randomization procedure, district heating and cooling demand profiles are generated. For domestic hot water consumption, an approximation method is developed using a set of Gaussian distribution functions which can be used to generate individual household profiles or aggregated profiles for a district. This method can also be used to generate household and district electrical demand profiles, but this application should be investigated further.

In Chapter 4, models for predicting the state of charge of a domestic hot water thermal storage charged by a heat pump and for an electrical battery are developed. The basic mathematical description for these models is similar. Energy balance equations are combined with physical insights from experimental data during charging and discharging. The models involve a set of relatively simple equations which are easy to evaluate by smart energy control algorithms without iterations. For the thermal storage the required inputs are: recordings of measured inlet and outlet water temperature and water flow, which can be performed by low cost heat meters in practice. For the electrical energy storage, the required inputs are (dis)charging voltage and currents. Possible outputs of the predictive model are: (a) the present state of charge and (b) for a future charging cycle, the electrical consumption profile.

Accuracy of the thermal storage model is validated by comparing results of model predictions with experimental findings. The accuracy of the predictions is within the range of the measurement errors. Hence the model can be applied for simulation or control purposes of the investigated type of domestic hot water storage.

Application of the thermal storage model is investigated with a case of increased self consumption of solar electric energy. It is verified that the model is relatively easy to integrate into an optimization control algorithm which in this case minimizes both peak electricity consumption of a household and the capacity of an electric battery.
However, the model for electric battery storage needs further development to include the rate capacity effect and restoration of capacity during discontinued discharging with high discharge rates, which is part of future work.
Also in Chapter 4, a model dedicated to Floor Heating Thermal Energy Storage is developed to study effects on operative temperature. Simulation results with this model show that the amount of energy that can be stored in a floor heating system depends on the house and floor heating structure, degree of insulation, weather conditions and temperature settings by the residents. The constraints are determined by current requirements on thermal comfort. Three types of temperature control are investigated. A constant day/night temperature set point (Control 1) shows that heating demand mostly occurs at night hours. A lower set point during night hours (Control 2) shifts heating demand towards day hours. For district power balancing, Control 2 has the advantage that the heat pump can be used more flexible during the night for generating domestic hot water. If additional to Control 2, short storage periods during daytime hours are introduced (Control 3), it is found that energy can be stored in the floor such that operative temperatures remain within allowable comfort limits. For low energy houses, energy loss due to the storage is small. However, a fair energy cost policy should take this loss into account, e.g. by offering lower energy tariffs during storage. It is concluded that a house with a concrete floor heating system provides substantial storage capacity (i.e. 2 hours charging with a heat pump operating at full capacity per day) which can be used by a smart grid controlled district energy supply system, while at the same time, acceptable levels of thermal comfort and energy costs for residents can be maintained.

9.1.2 Optimal capacity part

In Chapter 5, a specific model is developed to determine the mathematically optimal capacities of a co-generation and boiler unit for the Meppel district heating case. The model combines energy balance equations of the energy system with case specific size constraints and cost relations. With this model, capacities are determined and the corresponding financial profits and sustainability impact. Within the Meppel district heating case, cooling is offered free of charge to households which appears to result in overall negative profits of the system. Financially, co-generation appears to increase profitability by 50% compared to a system in which heat is only generated by boilers. When cooling is offered free of charge, the district heating system is profitable with co-generation when more than 277 houses are connected. However, if a modest fee is charged for the cooling, the project breaks even already at 40 connected houses.
A relevant question for the expanding district is how the optimal capacity of the

co-generation unit is related to the number of connected houses. With maximizing profit as objective, the optimization model shows that this relation is quite flat. Therefore, the capacity of the co-generation unit is less important than e.g. the costs of a suitable building for the installations, the pace in which the district's house building project develops and technical aspects like reliability and maintenance. Considering the rapid expansion of the district, a co-generation unit between 80-160 kWe is considered a near optimal choice for a large range of connected houses between 40-200 houses.
The sustainability of the energy concept is compared with the Dutch reference, where houses are heated by individual natural gas boilers. If the co-generator runs on bio-gas, the sustainability is much better than this reference. However, if the co-generator runs on natural gas, the performance is only 6% better.
Also the plan to include houses with an individual heat pump within the district heating system is investigated. In general, heat pumps appear to have a negative influence on the profitability. This is mainly because the source heat for the heat pumps is drawn from the district heating return and is then effectively generated by the co-generator or boilers. However, the number of houses is at this stage too small to justify investments in a joined underground source.

To extend the investigation on optimal capacities towards urban energy systems and more types of renewable energy generators, a more general model is developed in Chapter 6. The model is applied to a case involving 200 houses. The reference energy system for this case is a district heating system with natural gas boilers for heating, an electric refrigerator for cooling and "grey" electricity for the electrical demand. The following renewable energy concepts are investigated:

1. Bio-heat: central bio-mass boiler, solar PV, regional wind energy, supported by thermal and electrical storage, cooling by lake or ground source with high COP.
2. All-electric: central heat pump, ground source, solar PV, regional wind energy, supported by thermal and electrical storage, cooling by ground source with high COP.
3. Combined: central bio-gas CHP, central heat pump, solar PV, regional wind energy, supported by thermal and electrical storage, cooling by ground source with high COP.

With the model and hourly demand data, the mathematical optimal generation and storage capacities are determined for each concept. The model also gives insight into the energy flows as a result of the implemented priority algorithms. This reveals that the peak electricity flows and level of self consumption of renewable energy could be enhanced when control methods which include forecasts are implemented.
Financially, the case reference is at this stage the most attractive but environmentally, the least attractive. The renewable concepts show a change in the dominating cost factor, from fuel costs (case reference) towards CAPEX and OPEX (renewable

concepts). Of the renewable concepts, the all electric concept is financially the most attractive, but the bio-heat concepts have a better environmental performance. The energy flows of the all-electric concept show relatively high grid peak imports and exports which cannot be avoided by energy storage alone. Hence, this concept could benefit the most from smart grid control of the heat pump, and also by direct injection of power to heat into a thermal storage and smart charging of the electrical storage.
The Combined concept can be extended towards a 100% renewable energy system or near energy autonomy, which is defined as using zero natural gas and zero imports from the electricity grid. Simulations demonstrate the theoretical feasibility of this concept. However, this concept is financially only attractive when the biogas is subsidized towards an equal prices per kWh as natural gas and when batteries are more than 50% cheaper than they are today.
The influence of a further reduction of the heat demand through the Near Zero Energy Building (NZEB) standard is also investigated. As such houses are not yet mandatory, a determining variable at this stage is the required additional investment for NZEB houses compared with the houses built at this moment e.g. in Meppel. To reach the same costs as the case reference, additional investments into NZEB houses are estimated in a range from €4680 to €8410 per house. In general, NZEB houses decrease the differences between the renewable energy concepts with respect to the operational costs and environmental impact. The reduced heat demand of NZEB also reduces vulnerability to price fluctuations of e.g. biomass or biogas, but also reduces heat revenues for the district heating utility which is important to consider within future business cases.

9.1.3 Smart control part

The influence of smart control is further investigated in Chapter 7 for a group of 104 heat pumps powered by a single co-generation unit. Each heat pump supplies thermal energy for a household for space heating and domestic hot water. Each house has a concrete floor heating system for space heating and a thermal storage for domestic hot water. For control of the heat pumps, a Mixed Integer Linear Program (MILP) optimization and a faster algorithmic variant called time scale MILP is developed. Compared to feedback (reference) control, the optimal control methods result in improved thermal comfort for the residents and reduction of aggregated electricity demand peaks of the heat pumps. However, the obtained control schemes of the heat pumps and CHP result in very frequent on/off switching of these converters. Besides this, for privacy reasons, it is not desired to communicate household thermal comfort information towards a central controller. To overcome these problems, an alternative control method based on the mathematical concept of Earliest Deadline first (EDF) is investigated. Unlike the control methods based on MILP where the model predictions are performed on the central level, each house now has a smart controller which performs the model predictions of heat demand and communicates priority information to the central

CHP controller. This improves the privacy issues considerable. The MILP and EDF-control perform equal on reaching the objectives (i.e. minimize exchange of grid electricity and maintaining thermal comfort), but the problems with frequent on/off switching of the heat pumps and CHP are solved effectively only by the EDF-control. With the EDF-control it is also possible to choose if the CHP should always produce a bit less than the electrical demand, as close as possible to that demand or a bit more.
Besides the advantages already mentioned, the EDF-control algorithm appears to be very fast and the method is therefore scalable to larger and more complex energy systems. In the Meppel case which is discussed throughout this thesis, the heating system is separated from the domestic electricity supply system. However, in the future the latter system may involve renewable energy from rooftop PV panels and smart control of flexible devices for each house, such as a battery, EV and washing machine. The EDF-control may be extended to include this type of control as well. In this way, depending on the application, EDF-control may be an alternative for established smart grid control methods such as cost based or auction based control.
Last, near off-grid operation of a neighborhood of 16 houses is investigated in Chapter 8. Power balance is maintained using smart control for a central small scale CHP and flexible devices such as batteries and household devices such as washing machines. The thermal demand is supplied by the CHP entirely and the electric demand by the CHP and solar PV system. Three cases are investigated: a base control without batteries or flexible devices (BASE), control of the flexible devices (CON) and control of flexible devices and batteries (BAT/CON). The BAT/CON control shows as expected the best performance to reduce grid imports and exports. It is demonstrated that by careful capacity optimization and smart control, it is possible to develop an energy system that is theoretically capable to go off-grid for the whole year. However, in practice the control system has to deal with much more uncertainties which will make it more difficult to maintain the theoretical power balance around the whole year.

9.2 Conclusions

In this Section, answers are provided to the research questions mentioned in the introduction, Chapter 1. The central problem statement was formulated as follows:

How to determine urban energy system capacities with a high share of locally generated, renewable energy and how to control energy generation and storage in order to balance generation and demand in time?

First, the thesis shows that smart control is effective if: (a) the control is able to forecast demand and generation of renewable sources, at least a couple of hours ahead, and (b) the control objective is aimed at making use of renewable energy sources as much as possible while maintaining acceptable comfort for residents.

Also, it is demonstrated that smart control could lead to higher costs for residents than conventional control methods which should be avoided by dynamic energy tariffs. For predictions of household energy consumption, the thesis shows that there are methods available which avoid gathering privacy sensitive information from households on aggregated levels.
Second, the thesis shows that urban energy systems for which capacities of generators and storage facilities are carefully determined by a suitable model with realistic data, benefit from smart energy control. In general, the generation capacity (assets) is in that case utilized as much as possible leading to the lowest possible investments, power peaks are avoided leading to the lowest possible network costs, operation of generators can be optimized for prolonged life-time and last but not least, thermal comfort for residents can be improved.

The sub questions are answered as follows:

- *How to model heat demand of buildings such that we can use these models for predictions and to analyze the impact of smart control?*

  Different model approaches are investigated in Chapter 2 of this thesis and it is demonstrated that thermal network models are relatively easy to develop for this purpose. If a suitable model is selected, the parameters are also meaningful in relation to physical properties of the building. The accuracy of such models is investigated with data from more detailed building simulations. It is found that the accuracy is sufficient for the generation of demand data to investigate optimal capacities of urban energy systems. It is expected that the models are applicable for smart control purposes but for this purpose, it is important that an additional method is implemented which is capable of learning possible disturbances leading to inaccuracy of predictions, of which weather forecast errors and behavioral patterns of inhabitants are likely to be the most influential disturbances.

- *How much energy can be stored without significant cost and comfort consequences within the structure of a building?*

  It is demonstrated that a significant amount of energy, i.e. at least two hours of maximum heat pump operation can be stored within the structure (concrete floor heating) of a modern house without significant comfort consequences. However, there are minor cost consequences due to slightly increased thermal losses to the environment. Within a smart control context with smart meters, residents could be compensated for this with lower tariffs.

- *how to model the storage capacity and the charging and discharging process with sufficient accuracy?*

A general model for this is developed for the most common type of thermal storage and the most common type of electric batteries. The model translates observations from experimental data into relatively simple expressions. For electric batteries, the model is extended to include the rate capacity effect and capacity restoration due to intermittent fast discharging. Experimental validations show for the thermal storage, a good agreement between the model and measured data. However, more experiments are required to validate the model extension of the electric battery.

- *How to control a CHP and a large number of heat pumps within an individual or collective energy system in such a way that there are minimum peak electrical loads within the micro grid and there are minimum electricity flows between the micro grid and the larger electricity grid?*

- *How to develop the control such that it results in stable CHP or heat pump operation and delivers a high degree of thermal comfort to the inhabitants?*

A dedicated model predictive control method for a central CHP and group of heat pumps is developed. Three solving strategies are developed and compared of which the strategy which employs the earliest deadline first concept with dynamic programming gives the best performance on all relevant aspects: (a) thermal comfort of residents, (b) stable control of devices (heat pumps and CHP) and (c) reaching minimal grid power flow objectives. This is demonstrated with a case investigation, which involves perfect predictions, without disturbances. It is expected that the control algorithms will also perform well in the real world where disturbances are present, but this should be validated further.

- *How to develop the control such that it is computationally fast and does not require privacy sensitive information of inhabitants?*

Due to the difficulty of solving large scale optimization problems in case of central control, many researchers have abandoned the idea of a central smart control system entirely and have advanced into decentral control, using price steering mechanisms. However, the central control method developed in this thesis which applies the earliest deadline first algorithm and dynamic programming, appears to be computationally efficient and is scalable to much larger instances. In fact, the control idea is partly central but also contains decentral parts, i.e. the house controller performs the predictions. The difference is in the information exchange between the central and decentral layer: in our case priorities are communicated, in case of price or market based control, prices and bids are communicated. As such, the developed method may also be seen as a guided decentral approach. It is relevant to consider

which type of control system (priority or price based control) is most appropriate for a given situation. In this thesis, the priority based control system is only evaluated for the control of a single CHP and a group of heat pumps involving considerable flexibility offered by thermal storage. Whether the same control performs also adequate in case of other devices (e.g. washing machines, electric vehicles) and in cases where less flexibility is involved, is not evaluated and is an interesting scope for further research.

- *What are likely options for renewable energy integration for the thermal demand on the level of a single household, neighborhood and district and how do they compare on feasibility, costs and environmental impact?*

  Different options for the integration of renewable energy for the thermal and electrical demand of households are investigated. It is determined that at present, the bio-heat option (wood boiler) together with solar PV electricity and wind energy is the most cost effective way to reach sustainability targets. However, all electric solutions perform better on costs, but at present not on sustainability, mainly due to large grid power imports during the winter season. On the other hand, when the thermal demand of buildings decreases and the share of renewable energy within the grid increases, the all electric solution is the most attractive option for new districts. However, the all electric concept relies more on energy storage and smart control in order to keep grid infrastructural investments within affordable limits.

- *To what extend is self consumption of local renewable energy and (near) off-grid operation of a neighborhood possible?*

  First, it is already possible for houses and districts to generate sufficient energy by solar PV and heat pumps to cover the complete electrical and thermal demand on a yearly basis. This is called energy neutrality. However, without storage possibilities and smart control, only approximately 40% of the generated renewable energy is self-consumed. This also means that 60% of the energy is exported to the grid at one time, and imported at another time. As grid energy is still mostly supplied by fossil resources, efforts should be made to increase self-consumption of locally generated, renewable energy. The thesis demonstrates two cases of energy systems which reach almost 100% self-consumption of renewable energy. One is a district energy system for 200 houses with mixed resources: a central bio-gas CHP, central heat pump, solar PV, regional wind energy, supported by thermal and electrical storage and cooling by a ground cooling source which also supplies the thermal demand of the heat pump. Due to the larger operational scale and careful capacity modeling, maximum self-consumption is almost reached with simple priority control rules. Hence, adding some smart control features

with forecasting will improve control results. The other case involves a smaller group of 16 houses with much more dynamic demand profiles. In that case, near off-grid operation is possible with smart control of batteries and some household appliances. In both cases, self-consumption increases to nearly 100%.

9.3 Contributions

As a result of this thesis, the Triana smart grid control methodology developed at the University of Twente is extended with algorithms for the prediction of household thermal demand, thermal energy generation and thermal storage. For the scale of a larger district, algorithms for smart energy control are developed and implemented within the Triana simulator environment.
Through case investigations, this thesis demonstrates the feasibility of integration of renewable energy generation for the individual and collective approach and the importance of smart energy control. These results may help decision makers, either from governmental, institutional or from involved building or service companies how to approach the energy transition for the building environment.
The research has resulted into ten peer-reviewed publications, of which 4 journal publications and 6 with the author of this thesis as main author. The publications are listed in the appendix. Specific contributions reported in this thesis and in the publications are:

1. Models to determine the thermal demand of a house with a few parameters that agree well with physical parameters.
2. Models to determine the state of charge during charging and discharging of a thermal energy storage and an electrical battery storage.
3. A method to determine the relation between thermal storage in a floor heating structure, thermal comfort, energy loss and energy costs for residents.
4. Models and algorithms to determine optimal system dimensions for integration of renewable energy for the thermal and electrical demand of urban districts.
5. An algorithmic solution strategy for solving large scale energy control optimization problems.
6. A control strategy for neighborhoods and districts to enable near off-grid operation.

9.4 Recommendations

9.4.1 Modeling part

The thermal demand of houses with a floor heating system can be predicted with sufficient accuracy by relatively simple thermal network models. This makes such

models suitable for model predictive control purposes. However, more research is required into methods which enable a more accurate calculation of white box parameter values. For the model presented in this thesis, more research is required on the performance and accuracy of these models in real world experiments. During the last phase of the PhD research, experiments were carried out to measure temperatures and heat input of (a) a single office room on the university campus and (b) a household. At present, this research is still ongoing, but the first results indicate that the single office room appears to be very difficult to predict with sufficient accuracy. Dominating influences which are not part of the model are: air exchanges between the interior and exterior and with the main hall, movement of people in and out of the room and internal heat loads by computers. It is interesting to further investigate two possible ways to increase the accuracy of model predictions:

1. Stochastic parameter estimation from the measured data and re-formulation of the thermal network model such that it is in stochastic differential form, including a Kalman filter, as shown in [100].
2. Application of a neural network model and a machine learning algorithm to learn the impact of the mentioned influences in time and to determine corrections with this for the results predicted by the thermal network model.

This research is necessary to improve results of model predictions of single households and single office rooms, but may also be necessary for groups of houses, although inaccuracies in general are averaging out when a house contains more than one room or a building contains more than one office and there is only one heat generator for the building. The aim should be to develop model predictive control of heat pumps and district heating systems in such a way that the control is robust and self-correcting.

For the electric battery model, an extension is developed which models the rate capacity effect and capacity recovery effect. However, the performance of this model in relation to varying discharge currents and waiting times should be validated with more experiments and simulations in which results are compared with results from the Kinetic Battery Model (KiBam). It is also interesting to implement the models in a smart control system and perform practical validations with smart controlled batteries in household settings.

9.4.2 Optimal capacity part

The models presented in this thesis are not fully complete to study business cases of district heating systems for new districts with modern houses which have a low thermal demand. Specifically the use of heat pumps and the required number of houses for economically feasible operation of a collective, underground thermal source is an interesting topic to investigate further. The developed energy priority model should in that case be updated to include such systems. Also, verification

of the results of the energy model with a more established tool like Energyplan is recommended.
A deeper comparison on economical and sustainability aspects between individual and collective energy systems for groups of new built houses is required, specifically in relation to Near Zero Energy Building standards which will be mandatory from 2020. There are many situations thinkable where a collective or an individual approach is the best option. However, specific Dutch case investigations which clearly demonstrate the overall costs, sustainability and legal aspects of such districts and approaches are missing in the scientific field.
It would be ideal if the model developed and used in this thesis for optimal capacity analysis, is extended with a basic form of smart control including forecasts. In that case, the demand data should be structured per house or building and should be split into a base load and flexible load. With such an extended model, it is possible to include the capabilities of smart control in the determination of system capacities. It is believed that due to smart control, generation and storage capacities may reduce even further and thus lead to lower investments.

9.4.3 Smart control part

As the real world will include disturbances, the smart control method developed as part of this research should be validated in two steps. First, the control method should be tested in a simulation environment in which predictions are not perfect but a follow up simulation includes disturbances. Response of the control system to these disturbances should be verified and proper corrective procedures should be implemented when required. Second, the control method should be implemented in a practical setup, e.g. a group of houses or a specific experimental setup with a group of heat pumps, powered from a single electric energy source. In this experiment, the behavior and performance of such control systems should be validated, as well as social and economical aspects, e.g. how to compensate residents for heat loss associated with using the flexibility offered by their floor heating systems?
Also, the EDF-control method should be compared with other decentral smart grid control methods, e.g. price steering or auction based control methods. Recently, other researchers at the University of Twente developed a method called profile steering [169], which is also an alternative to compare with. Of particular interest is the validation of these methods in a real situation where not only predictions and planning of devices takes place, but also real-time control. If validation of the EDF-control method is positive then it should be investigated if this method is also capable to control more complex energy systems containing multiple energy supply sources and large numbers of flexible devices. Because the amount of computational overhead is limited, methods like EDF-control could be important on the way towards low-cost control solutions for urban areas in which 100% renewable resources are implemented.

Appendix A

TRNSYS house model

A.1 Introduction

In Chapter 2, parameters are determined for simplified thermal network models of a house. These models are used throughout the thesis for the generation of demand profiles and for model predictive control. In Chapter 1, Section 1.7, a schedule is shown which explains which models are used for which purpose in this thesis. The parameters are determined by a calibration process for which reliable data of the heating input and temperature response of the houses is required. To generate such data, TRNSYS models of houses are used. Details of the TRNSYS models are given in this appendix. In Section A.2 backgrounds are discussed on the energy performance of the house. In Section A.3 constructional data of the houses is given, followed by details of the TRNSYS models in Section A.4. In Section A.5 results are shown of a verification analysis in which the heating and cooling demand of the houses predicted by the TRNSYS models is compared with EPC calculations.

A.2 Type of houses and targeted energy performance

The thesis is dedicated to the Meppel housing project which is introduced in Chapter 3. The houses considered are built in the period 2013-2016 and their building permits were obtained in 2013. Hence, building details are based on the National building standard of 2013. As a consequence, the Energy Performance Coefficient (EPC) of the housing project is 0.6 which is a relative index used in the Netherlands to classify the energy performance of buildings and includes "building related" energy consumption (thermal and electrical) for heating, cooling, ventilation and lighting [30]. It is also possible to subtract generated energy e.g. by solar PV panels. Hence, it is possible to reach an EPC of 0.0 which is scheduled to be mandatory from 2020 or even to reach negative EPC values when the energy generation exceeds the energy demand. At present (2017) an EPC value of 0.4 is

mandatory.
Within the EPC calculation, the energy demand is expressed in terms of primary fuel energy. Hence, the EPC of a housing project depends on the specific energy supply system. The National reference for this is a home installation which uses natural gas for heating and electricity from the grid for which an equivalent fuel efficiency is defined. However, the heating supply system in Meppel is originally planned to include various renewable sources such as biogas and a Combined Heat and Power installation which produces heat for the district heating system and power for heat pumps in a number of houses. This supply system is analyzed in [64] and an equivalent heating supply efficiency of 2.925 is determined. The heating demand of the houses and this equivalent efficiency have a large influence in the EPC value. Hence, it is possible to compensate houses which are less energy efficient with an energy supply system that contains more renewable energy sources. At the time of writing the publications for this thesis for which results are shown in Chapter 2, constructional details of the houses were not fixed. Hence, the so called "RVO reference houses" are used for the modeling in TRNSYS [10]. It was clear that in order for the project to reach an EPC value of 0.6, the house details would be approximately similar to houses with an EPC value of 0.8 when equipped a reference energy supply system. For this, guidelines to reach an EPC value of 0.8 are published in [155]. These details have become out of date at the time of finalization of this thesis. However, it is possible to apply the methods shown in this appendix for newer houses with better EPC values by including other constructional details. Despite the update of the EPC standard, the reference house dimensional data is still used today.
EPC calculations are based on many rules which are explained in standard [30] and a large number of related standards for materials, constructional details and installation details. Specific software is available for EPC calculations in which details of the building and installations are defined as input.
In general, Dutch building methods are traditionally classified in relation to building material systems as:

- traditionally heavy: concrete or sandstone walls, hollow concrete floors, brick facade walls, wooden roof construction with sandwich panel roof covering with brick tiles,
- mixed heavy and light: hollow concrete walls and floors, cellular concrete or sandstone wall blocks, brick facade walls, wooden roof construction with sandwich panel roof covering with brick tiles, and
- light: wood skeleton construction, hollow concrete or wooden floors, cellular block or sandwich panel walls, facade carpentry, wooden roof construction with sandwich panel roof covering with brick tiles or roof panels.

Due to innovations, this classification is expanding with more building materials and systems. Houses in the Meppel project are built according to traditionally heavy standards. Constructional details are assumed to comply to SBR reference details [150]. Building materials and details are relevant for EPC calculations

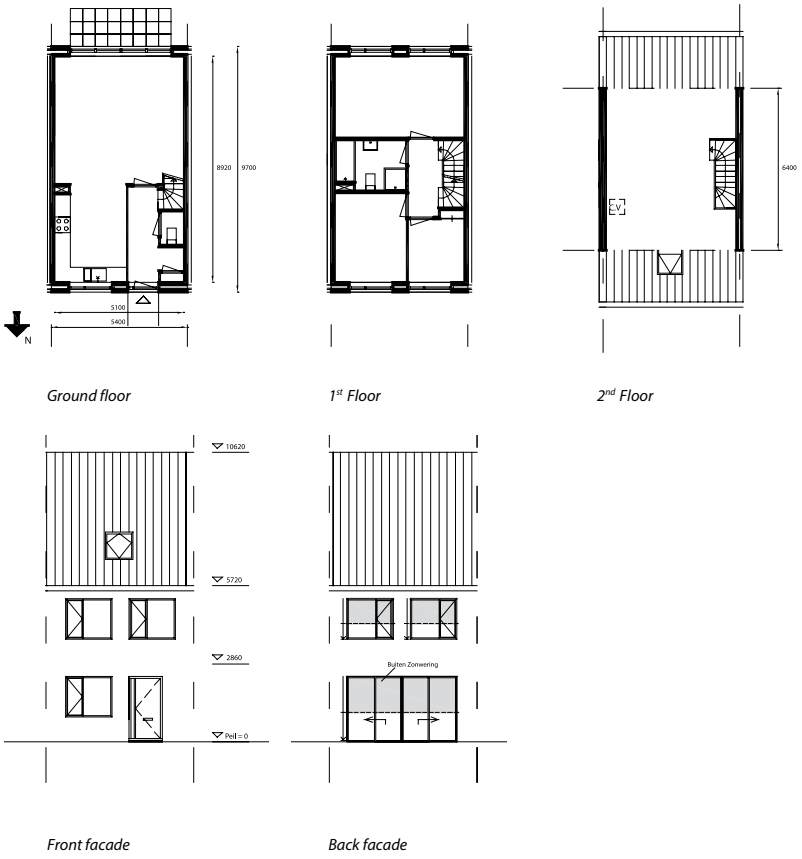

Figure A.1 – Floor plan terraced house

and heating demand simulations. The approach and assumptions are explained in more detail in Section A.3.

A.3 Main data of the modeled houses

Dimensional data of the reference houses are the result of an analysis of trends in the Dutch house building sector and together with data on building physics and installations listed in Table A.1. Floor plans of a terraced house and corner house are shown in Figures A.1 and A.2 respectively. Similar floor plans are used for the semi-detached and detached house. In table A.1, Rc signifies specific thermal resistance (for walls) and U signifies the heat loss coefficient (for windows). In the installation details, only the relevant details are shown which govern the building heat demand. Self steering window grates have a simple mechanism which responds to pressure differences between the exterior and the ambient

Figure A.2 – Floor plan corner house

and thereby avoids excessive air flows due to high wind pressure. The use of the alternative ventilation system is explained in Section A.5 in which TRNSYS model results are compared with EPC calculations.

Main geometric data					
Item	Unit	Terraced house	Corner house	Semi-detached house	Detached house
Internal house width	m	5.1	5.1	5.8	6.0
Internal house depth	m	8.9	8.9	9.0	10.2
Internal floor height	m	2.6	2.6	2.6	2.6
Useable interior floor surface	m^2	124.3	124.3	147.7	169.5
Heat loss surface	m^2	156.9	230.0	268.5	358.4
Building physics details					
Rc facade walls	m^2K/W	3.5	3.5	3.5	3.5
Rc roof	m^2K/W	4.0	4.0	4.0	4.0
Rc ground floor	m^2K/W	5.0	5.0	5.0	5.0
U windows	W/m^2K	1.8	1.8	1.8	1.8
U front door	W/m^2K	2.2	2.2	2.2	2.2
Installation details					
Heat generator		Heat pump			
Room heating system		Low temperature floor heating			
Ventilation supply		Self steering window grates			
Ventilation exhaust		Mechanical suction			
Alternative ventilation		Balanced ventilation with heat recovery			
Cooling supply		Electrical compression cooler			

Table A.1 – Main building data for heat loss calculations

A.4 TRNSYS modeling details

The scheme shown in Figure 2.1 (Chapter 2) is worked out into a simulation model in TRNSYS, version 16 [166]. The block model representation is shown in Figure A.3. The main four parts of the TRNSYS model that are indicated by the colored blocks part 1 to 4 are now discussed.

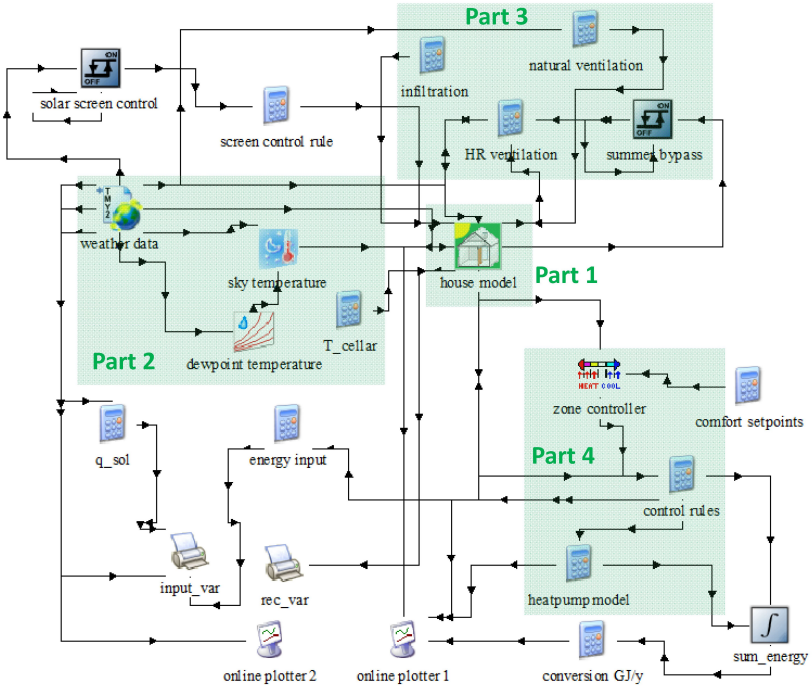

Figure A.3 – TRNSYS block model representation

A.4.1 TRNSYS house model

The house model is defined in TRNBuild type 56 and contains:

1. Geometric details (walls, wall angles, windows, doors, floors, roof) of the house structure, refer to Table A.2 in which this is shown in more detail for the terraced house. Each structure is defined with a certain layer type. Each layer type is defined with materials and thicknesses, for which standard materials from the TRNSYS library are used. For instance a "facade_wall" is defined in a heavy and light variety. The heavy version has a sandstone wall on the inside, then insulation, a small ventilation air gap and on the outside a brick wall. The light version has a wooden frame with gypsum board on the inside and brick strip panels on the outside with insulation

and small ventilation air gap in between. Floors are defined as channel type, hollow concrete structures. Active floors have a fluid tube layer on top, covered with a concrete layer. The ground floor has insulation on the bottom. All floors have a wooden floor covering on the top. All insulation material thicknesses of layers of category "external" are chosen such that the total Rc-value equals the values shown in Table A.1. "External" signifies a layer with one surface towards the exterior of the house."Boundary" signifies a layer for which at least one surface has a user defined temperature, for which the zone temperature is chosen. "Internal" signifies a layer which is part of the interior of the zone. For the wall structures, a view factor to the sky is defined as 0.5 for vertical walls, 1 for roof surfaces. Besides walls, a thermal bridge is defined as a loss area with heat transfer coefficient according to the guidelines given in [31], using the reference house EPC calculation details. For other house types than the terraced house, the definition is similar with the exception of the following differences:

- The corner house has one side wall to the East for which the layer type is "facade_wall" in stead of "wall". The side wall also has a small window.
- The semi-detached house is similar as the corner house but with somewhat larger areas of the structures.
- The detached house is similar as the semi-detached house but with somewhat larger areas of the structures and with the side wall to the West replaced with the layer type "wall".

2. Heating and cooling system details. For the thermal zone, two active floors for the floor heating system are defined, one for the ground floor, one for the first floor. The TRNBuild module determines the layout of the tubes within the floor based on a user defined number of fluid loops (four) and surface area. The supply temperature and mass flow to each floor are defined as input parameters, refer to Section A.4.4.
3. Ventilation system details. For the ventilation air flow, the air change rate and inlet temperature are defined as inputs, refer to Section A.4.3.
4. Infiltration details. For the infiltration air flow, the air change rate is defined as input, refer to Section A.4.3.
5. Internal heat gains by persons, appliances and lights. To determine heat gains by persons, a constant number of two persons out of a four person household is assumed to be in the house (122 W/person). For appliances, the consumption of a refrigerator, freezer, TV and computer are calculated at 495 kWh/y. For lights, 150 kWh/y is calculated based on energy saving light bulbs. Data is obtained from [107]. The use of a washing machine, wash dryer and cooking appliances (oven, induction cooker, magnetron) is assumed to be directly ventilated and therefore assumed not to contribute to internal heat gains. Hence, the total electricity consumption which is relevant for heat gains is 645 kWh/y. This is modeled as 74 W constant heat gains.

Structure	Layer	Area (m^2)	Orientation	Category
front facade	facade_wall	28.5	N	external
back facade	facade_wall	28.5	S	external
side wall left	wall	68.5	NA	boundary
side wall right	wall	68.5	NA	boundary
inner walls	wall	51.0	NA	internal
ground floor	active floor	46.2	NA	external
first floor	active floor	32.6	NA	boundary
attic floor	floor	32.6	NA	internal
front roof	roof	31.1	N	external
back roof	roof	31.1	S	external
front windows	window	8.0	N	external
back windows	window	14.8	S	external
front door	door	2.4	N	external
back door	door	2.4	S	external

Table A.2 – Main building data for heat loss calculations

An important choice is the number of thermal zones. In Dutch houses it is common practice that the temperature of only the living room (usually an open space with the kitchen on the ground floor) is controlled with a thermostat which controls the operation of the heating system. When the living room floor heating system receives thermal energy, the bedrooms and bathroom on the first floor simultaneously receive a portion of the generated heat, unless this floor is switched off by a valve which controls the water flow to the floor heating system. The assumption is made that rooms on the ground floor, first floor and attic are simultaneously heated. Hence, the house interior is modeled as a single thermal zone with a uniform temperature. This is a simplification of reality. In reality, there may be temperature differences between the ground floor, first floor and attic, which also leads to air exchange flows within the house, depending on closed or opened doors to rooms and window positions. A model with more thermal zones (e.g. in total three zones for the ground floor, first floor and attic) and air flows between the zones may be considered when the temperature of separate rooms or an entire floor is measured and controlled individually and is part of future work.

A.4.2 TRNSYS weather model

A weather data file in TMY2 format is used as input for the TRNSYS type 109 weather data calculator. The weather data is according to the reference Dutch climatic year [118] (appendix A1). The number of degree days is 2825 and 3516 for a reference temperature of 18^oC and 20^oC respectively.
Solar radiation on the building planes is calculated with the Perez model which is programmed into type 109. For details refer to [118], appendix E. The calculation of the sky temperature for thermal radiation from the house uses relative humidity and ambient temperature as input, for details refer to [104]. For details of the

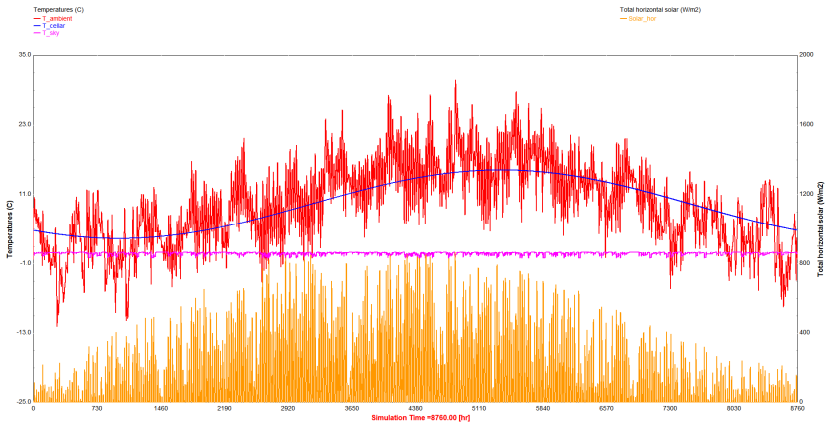

Figure A.4 – Weather data for Dutch climatic reference year

Dew Point calculation, refer to [18]. The sky temperature calculated by the model appears to be approximately constant at 1^oC.
Last, the cellar temperature (T_{cellar}) under the ground floor is calculated with Equation A.1, refer to [108].

$$T_{cellar} = \bar{T_a} - A_y e^{-x\sqrt{\frac{\pi}{\alpha N_{hour} \cdot 3600}}} cos\left(2\pi \frac{N_d}{N_{day}} - x\sqrt{\frac{\pi}{\alpha N_{hour} \cdot 3600}} - \phi\right), \qquad (A.1)$$

in which $\bar{T_a}$ is the annual average ambient air temperature, A_y is the annual ambient air temperature amplitude, x the depth measured from the earth surface (assumed at 0.5 m), α is the ground soil diffusivity factor (assumed at: $0.6 \cdot 10^-6$ m^2/s), N_{hour} is the number of hours in a year (8760 hours), N_d is the number of the day and ϕ is the phase angle which depends on the local climate and soil properties (assumed at 0.5). In Figure A.4 the ambient, cellar and sky temperature (red, blue and pink: scaled on left axis) and total radiation on the horizontal plane (light brown, scaled on right axis) is shown.

A.4.3 TRNSYS ventilation and infiltration model

For ventilation, the type of system is selected in the building model, refer to Section A.4.1. The following inputs are modeled:

1. HR ventilation block, i.e. a mechanical ventilation system with or without heat recovery (HR). The model computes the ventilation inlet air at time t ($T_{inlet,t}$) as follows:

$$T_{inlet,t} = \eta_{hr} \cdot Bypass_t \cdot (T_{z,t} - T_{a,t}) + T_{a,t}, \qquad (A.2)$$

in which η_{hr} is the heat recovery efficiency, $Bypass$ is a control binary (0 or 1) obtained from the calculation block "summer bypass" which outputs a value

0 (bypass of the heat recovery unit) if the zone temperature T_z is above 24^{o}C and the ambient temperature T_a is lower than T_z. Else, it outputs a value 1 (no bypass). The model is also used for a ventilation system without heat recovery. In that case $\eta_{hr} = 0$. The flow of the ventilation air is defined in the building model with a daily schedule for the air exchange rate as follows:

- nighttime from 8 pm to 6 am: 0.4 h^{-1}
- daytime from 6 am to 6 pm: 0.4 h^{-1}
- evening from 6 pm to 8 pm: 0.7 h^{-1}

The background for this schedule is the occupancy of the house with 4 persons and the mandatory ventilation flow of 7 $\frac{dm^3}{s}$ per person (refer to the Dutch building directive, [5]). The air change rate is determined by multiplying this rate with the number of persons and dividing through the net air volume of the rooms within the house.

2. Natural ventilation block, i.e. adjustable window openings at the front and back side of the building. The model calculates ventilation flow as output which depends (1) on wind pressure in relation to the orientation of the building and (2) on thermal stack effects due to the temperature difference between the interior and ambient air in relation to atmospheric pressure differences related to the height of the building. For governing equations, refer to [108], chapter 9.

For the infiltration, the air change rate can be determined in two ways:

1. Detailed calculation methods according to equations published in [108] and [173] to determine wind pressure and thermal stack effects. However, for these methods the leakage area of the building should be known or should be determined from blower door test results. Lacking such details, the following method is applied.
2. An estimation of constant infiltration air change rate according to the method outlined in standard NEN 8088-1 [174]. The specific infiltration flow rate $q_{v10;spec}$ is assumed at 0.5 $\frac{dm^3}{m^2 s}$. As an example, for the reference terraced house dimensions, using tables from NEN 8088-1, the infiltration flow $q_{ve;inf}$ is determined at 6.2 $\frac{dm^3}{s}$ or 22 $\frac{m^3}{h}$, which results in an air change rate of 0.07 h^{-1}. This is much lower than typical ventilation air change rates between 0.2 and 0.7 h^{-1} which is common for Dutch houses.
   The following rules are applied in relation to the type of ventilation system. For type D (heat recovery ventilation system), an infiltration air change rate of 0.07 h^{-1}. For type C: natural ventilation inlet, mechanical suction exhaust, zero infiltration air change rate is used. The reason for this is that the ventilation air inlet comes through the same window openings and cracks as the infiltration air. Hence, the infiltration air change rate is then only relevant when this rate is higher than the ventilation rate, which is not the case in newly built houses with a good level of air tightness.

A.4.4 TRNSYS heat pump and cooling model

Within the blocks "control rules" and "heat pump model" (refer to Figure A.3) the following is calculated. For the heat generator the same ground water source heat pump is assumed as shown in Chapter 4 (Alpha-Innotec), refer to Figure 4.4. The heat production and electric consumption of the heat pump are calculated with Equation 4.6 which shows a linear relation between the heat production and the ground water source temperature and linear relation between the electric consumption and the supply temperature. Coefficients are given in Table 4.1. If a constant ground water supply temperature of 12^oC is assumed, the heat production is $q_h = 6.82$ kW. The electric consumption P_e varies with the calculated supply temperature T_s. If $T_s = 30^oC$ then $Pe = 1.92$ kW.
Let ϕ_1, ϕ_2 be fixed and known mass flow rates to the ground floor and first floor heating system respectively. The house model outputs the return temperature from each floor as $T_{r,1}$ and $T_{r,2}$. The return temperature T_r towards the heat exchanger of the heat pump is calculated by:

$$(\phi_1 + \phi_2) \cdot T_r = \phi_1 \cdot T_{r,1} + \phi_2 \cdot T_{r,2} \,. \tag{A.3}$$

The supply temperature is calculated from the known supplied heat q_h:

$$q_h = (\phi_1 + \phi_2) \cdot c_p \cdot (T_s - Tr) \,, \tag{A.4}$$

in which c_p the specific heat of the floor heating water. Both floor heating sections (ground floor and first floor) receive the same supply temperature.
The model for cooling is the same as the model for heating. The ground water supply to the heat pump with a temperature of 12^oC is used as source for cooling. To be consistent with heating and for simplicity, a constant cooling production q_c of 2.5 kW is assumed for cooling. In the equations above for heating, q_h should be replaced with q_c to find the cooling supply temperature T_s to the floor cooling system. The flows ϕ_1 and ϕ_2 are assumed to be similar.
The block "control rules" has control variables (value 1 or 0) from the block "zone controller" as input and multiplies a control variable for heating with q_h and a control variable for cooling with q_c. The value of the control variables is determined by a deadband on/off controller which compares the interior zone temperature with setpoints for heating (20^oC) and cooling (24^oC).
To illustrate the results achieved by the heating and cooling system, refer to Figure A.5 which shows the interior temperature (red), supply (light blue) and return temperature (green), heating input (dark blue) and electric consumption (purple) of the heat pump for a cold month (January) and to Figure A.6 which shows the same but for cooling the house in a warm month (August), the cooling input has negative values and color cyan. Temperatures are scaled on the left vertical axis, thermal and electric energy on the right axis.
Figure A.6 shows that the cooling input is turned on if the interior temperature is above 24^oC. Sometimes the interior air reaches 26^oC. According to weather adaptive thermal comfort theory, the interior temperatures are within acceptable

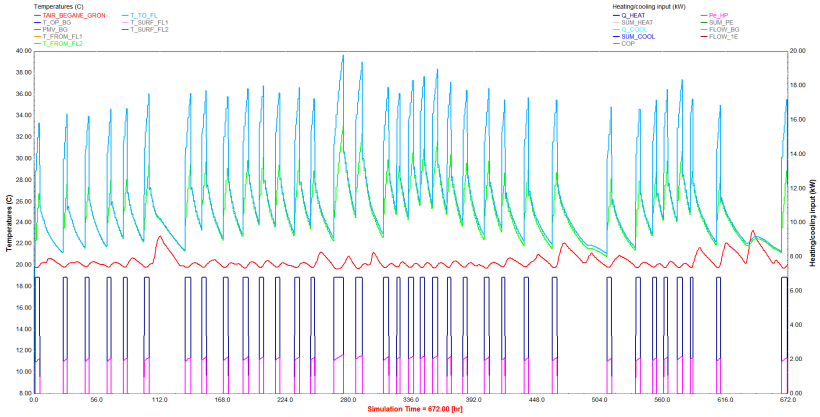

Figure A.5 – Temperature and heating input results January

Figure A.6 – Temperature and cooling input results August

comfort limits, although to be certain, the PMV (Predicted Mean Vote) should be checked. The floor cooling return temperature (green) shows that more cooling energy input is not possible, as this causes lower floor cooling temperatures than 18^oC at those moments which would be uncomfortable or could cause water condensation of the interior air.

A.5 Verification of heating and cooling demand

The performance of the TRNSYS model, specifically for the terraced and corner house is compared with results of EPC calculations for which the software Enorm is used [159]. The resulting heating and cooling demand of the houses (heavy and light construction variant) are shown in Table A.3 and A.4 respectively. Type C

signifies calculations with ventilation type C (window grate air inlet, mechanical suction exhaust), type D signifies a balanced mechanical ventilation (inlet and exhaust) with heat recovery efficiency of 0.8. Comparing the results, the following is observed:

- Heating demand. For the heavy construction, the largest difference between TRNSYS and EPC is 5.6%. For the light construction this is 7.5%. Both are in reasonably good agreement. The largest differences are found for ventilation type D.
- Cooling demand. For the heavy constructed terraced house, the TRNSYS values are almost twice as large as the EPC-values. However, for the similar corner house, TRNSYS values are 8% lower than the EPC-values. The large difference that is found for the terraced house is unexpected. A deeper investigation into the details and assumptions of EPC-cooling demand calculation is required to find the causes. For the light construction, a similar trend (higher cooling demand calculated by TRNSYS for the terraced house, lower for the corner house) is found, but the difference between EPC and TRNSYS is acceptable for the terraced house (11.6%) and reasonable for the corner house (19.7%).

This method of verification gives an indication that the TRNSYS model calculates the heating demand correctly. For the cooling demand, more investigation into details of the EPC-calculation is required to evaluate the differences with the TRNSYS model.

	Heavy construction		Light construction	
	Terraced	Corner	Terraced	Corner
EPC type C	23.23	32.02	23.03	30.56
TRNSYS type C	23.86	31.65	22.85	29.87
EPC type D	14.53	22.52	15.34	22.63
TRNSYS type D	15.28	21.26	14.98	20.94

Table A.3 – Heating demand results, values in GJ/y

	Heavy construction		Light construction	
	Terraced	Corner	Terraced	Corner
EPC type C	1.69	2.14	6.42	7.39
TRNSYS type C	3.22	1.97	6.93	6.14
EPC type D	2.96	3.11	7.51	8.54
TRNSYS type D	5.69	3.36	8.38	6.86

Table A.4 – Cooling demand results, values in GJ/y

References

[1] . *Energierapport: transitie naar duurzaam*. 2016. URL: https://www.rijksoverheid.nl/documenten/rapporten/2016/01/18/energierapport-transitie-naar-duurzaam.

[2] *Action plan sustainable energy. position paper*. Tech. rep. Netbeheer Nederland, 2013. URL: http://www.netbeheernederland.nl/publicaties/position-papers-factsheets/.

[3] KO Aduda, T Labeodan, W Zeiler and G Boxem. "Demand side flexibility coordination in office buildings: A framework and case study application". In: *Sustainable Cities and Society* 29 (2017), pp. 139–158.

[4] Dutch ministry of economic affairs. *Nationaal actieplan voor energie uit hernieuwbare bronnen*. 2009. URL: https://www.rijksoverheid.nl/binaries/rijksoverheid/documenten/rapporten/2010/06/23/rapport-nationaal-actieplan-voor-energie-uit-hernieuwbare-bronnen/10093332-1-bijlage.pdf.

[5] Dutch ministry of internal affairs. *Bouwbesluit 2012*. online. 2012. URL: https://www.onlinebouwbesluit.nl.

[6] IRENA International Renewable Energy Agency. *Renewable Energy Innovation Policy: Success Criteria and Strategies*. 2013. URL: https://www.irena.org/DocumentDownloads/Publications/Renewable_Energy_Innovation_Policy.pdf.

[7] RVO Netherlands Enterprise Agency. *Passief-renovatie Kroeven Roosendaal*. URL: http://www.rvo.nl/initiatieven/energiezuiniggebouwd/passief-renovatie-kroeven.

[8] RVO Netherlands Enterprise Agency. *Voorbeeldprojecten restwarmte*. 2013. URL: http://www.rvo.nl/sites/default/files/bijlagen/Voorbeeldprojecten%20Restwarmte.pdf.

[9] RVO Netherlands Enterprise Agency. *National policy wind energy (Dutch: Nationaal beleid windenergie)*. 2016. URL: http://www.rvo.nl/sites/default/files/Nationaalbeleidwindenergie2013-07-15.pdf.

[10] AgentschapNL. *Reference houses 2013 (in Dutch: Referentiewoningen nieuwbouw 2013)*. 2013. URL: http://www.rvo.nl/sites/default/files/2013/09/Referentiewoningen.pdf.

[11] M. Airaksinen and M. Vuolle. "Heating Energy and Peak-Power Demand in a Standard and Low Energy Building". In: *Energies* 6.1 (2013), pp. 235–250.

[12] Syed Muhammad Ali, Mohammad Naveed, Fahad Javed, Naveed Arshad and Jahangir Ikram. "DeLi2P: A user centric, scalable demand side management strategy for smart grids". In: *Smart Cities and Green ICT Systems (SMARTGREENS), 2015 International Conference on*. IEEE. 2015, pp. 1–9.

[13] Alpha-Innotec. *Brine/water heat pumps, WZS series - operating manual*. UK830501/200520.

[14] Alpha-Innotec. *Alpha-Innotec instruction and user manual WZS series brine/water heat pumps (in Dutch)*. 2014.

[15] A. Alvi and H.F. Qureshi. "Evaluation of Building Integrated Heating System in Terms of Thermal Comfort & Energy Efficiency". In: (2011).

[16] P.D. Andersen, M.J. Jimenez, H. Madsen and C. Rode. "Characterization of heat dynamics of an arctic low-energy house with floor heating". English. In: *Building Simulation* 7.6 (2014), pp. 595–614. ISSN: 1996-3599. DOI: 10.1007/s12273-014-0185-4. URL: http://dx.doi.org/10.1007/s12273-014-0185-4.

[17] ANSI-ASHRAE. *Standard 140-2014 – Standard Method of Test for the Evaluation of Building Energy Analysis Computer Programs*. American Society of Heating, Refrigerating, and Air-Conditioning Engineers, Atlanta, USA. 2014.

[18] ASHRAE. *ASHRAE Handbook-Fundamentals*. Atlanta: American Society of Heating, Refrigerating and Air-Conditioning Engineers (ASHRAE), 2009.

[19] ASHRAE. *ASHRAE standard 55-2010 Thermal environmental conditions for human occupancy*. ASHRAE, 2010.

[20] P. Bacher and H. Madsen. "Identifying suitable models for the heat dynamics of buildings". In: *Energy and Buildings* 43.7 (2011), pp. 1511–1522.

[21] Brecht Baeten, Frederik Rogiers, Dieter Patteeuw and Lieve Helsen. "Comparison of optimal control formulations for stratified sensible thermal energy storage in space heating applications". In: *The 13th International Conference on Energy Storage.* 2015.

[22] V. Bakker. "Triana: a control strategy for Smart Grids: Forecasting, planning & real-time control". PhD thesis. University of Twente, 2011. DOI: 10.3990/1.9789036533140.

[23] J. Benner, C. Leguijt and M. Koot. *Sustainable urban (re)development*. Ed. by CE Delft. 2010. URL: http://www.cedelft.eu/?go=home.downloadPub&id=1093&file=3142_defhoofdrapportLWMV.pdf&PHPSESSID=e51564b320e6621bd5f01f786f68785d.

[24] E.J.M. Blokker and K. Poortema. *Effect study domestic hot water (in Dutch: Effecten levering warm tapwater door derden)*. Tech. rep. KIWA, 2007.

[25] SER Dutch Social Economic Advisory Board. *Energy agreement for sustainable growth*. URL: https://www.ser.nl/~/media/files/internet/talen/engels/2013/energy-agreement-sustainable-growth-summary.ashx.

[26] SER Dutch Social Economic Advisory Board. *Energy agreement for sustainable growth*. 2013. URL: http://www.energieakkoordser.nl/doen/engels.aspx.

[27] B. Bøhm, Seung-kyu Ha, Won-tae Kim, T. Koljonen, Helge V. Larsen, M. Lucht, Sipilä Yong-soon Park, M. Wigbels and M. Wistbacka. *Simple models for operational optimisation*. Netherlands Agency for Energy and the Environment, 2002. ISBN: 90-5748-021-2.

[28] M. Bosman. "Planning in Smart Grids". PhD thesis. University of Twente, 2012. DOI: 10.3990/1.9789036533867.

[29] Bouwformatie. 2013.

[30] NEN commission energy performance of buildings. *NEN 7120+C2:2012/C5:2014 Energy performance of buildings - Determination method*. Tech. rep. NEN Netherlands Standardization Institute, 2011.

[31] NEN commission thermal properties of buildings. *NEN1068:2012+C2:2016 Thermal insulation of buildings - Calculation methods*. Tech. rep. NEN Netherlands Standardization Institute, 2016.

[32] C Buratti, E Moretti, E Belloni and F Cotana. "Unsteady simulation of energy performance and thermal comfort in non-residential buildings". In: *Building and Environment* 59 (2013), pp. 482–491.

[33] B. Burger. *Electricity production from solar and wind in Germany in 2014*. Ed. by Fraunhofer Institute for Solar Energy Systems. 2014. URL: https://www.ise.fraunhofer.de/en/downloads-englisch/pdf-files-englisch/data-nivc-/electricity-production-from-solar-and-wind-in-germany-2014.pdf.

[34] BUVA. *BUVA bouwdetails*. 2013.

[35] Pietro Capaldi. “A high efficiency 10kWe microcogenerator based on an Atkinson cycle internal combustion engine”. In: *Applied Thermal Engineering* 71.2 (2014). Special Issue: {MICROGEN} III: Promoting the transition to high efficiency distributed energy systems, pp. 913 –920. ISSN: 1359-4311. DOI: http://dx.doi.org/10.1016/j.applthermaleng.2014.02.035. URL: http://www.sciencedirect.com/science/article/pii/S1359431114001252.

[36] CBS. *Hernieuwbare energie in Nederland 2011*. Tech. rep. CBS.

[37] CBS. *Meer uitstoot broeikasgassen in 2015*. Ed. by CBS-Dutch bureau of statistics. 2016. URL: https://www.cbs.nl/nl-nl/nieuws/2016/36/meer-uitstoot-broeikasgassen-in-2015.

[38] F.N. Claessen, B. Claessens, M.P.F. Hommelberg, A. Molderink, V. Bakker and H.A. Toersche. “Comparative analysis of tertiary control systems for smart grids using the Flex Street model”. In: *Renewable energy* 69 (2014), pp. 260–270.

[39] Dutch Authority consumer and market. *Warmtewet 2014*. 2014. URL: https://www.acm.nl/nl/publicaties/publicatie/12481/Besluit-maximumprijs-levering-warmte-2014/.

[40] EREC European Renewable Energy Council. *Renewable Energy Technology Roadmap*. http://www.erec.org (visited May 30, 2015). 2008.

[41] Vinicio Curti, Daniel Favrat and Michael R von Spakovsky. “An environomic approach for the modeling and optimization of a district heating network based on centralized and decentralized heat pumps, cogeneration and/or gas furnace. Part II: Application”. In: *International Journal of Thermal Sciences* 39.7 (2000), pp. 731–741.

[42] Usman Ijaz Dar, Igor Sartori, Laurent Georges and Vojislav Novakovic. “Advanced control of heat pumps for improved flexibility of Net-ZEB towards the grid”. In: *Energy and Buildings* 69 (2014), pp. 74–84.

[43] Fjo De Ridder and Mathias Coomans. “Grey-box model and identification procedure for domestic thermal storage vessels”. In: *Applied Thermal Engineering* 67.1 (2014), pp. 147–158.

[44] Erik Dotzauer. “Simple model for prediction of loads in district-heating systems”. In: *Applied Energy* 73.3âĂŞ4 (2002), pp. 277 –284. ISSN: 0306-2619. DOI: http://dx.doi.org/10.1016/S0306-2619(02)00078-8. URL: http://www.sciencedirect.com/science/article/pii/S0306261902000788.

[45] L Dreijerink and J. Uitzinger. *Socio-economic evaluation report Apeldoorn*. Tech. rep. EU SORCER project. IVAM University of Amsterdam, 2013.

[46] J. A. Duffie and W. A. Beckman. *Solar engineering of thermal processes*. New York: Wiley, 1980.

[47] Generated here (Dutch: Hier opgewekt). *Local energy monitor (Dutch: lokale energie monitor) 2015*. 2015. URL: https://www.hieropgewekt.nl/sites/default/files/u20232/lokale_energie_monitor_2015_-_uitgave_januari_2016.pdf.

[48] ECN. *Nationale energie verkenning*. ECN-Dutch energy research centre. 2016. URL: http://www.pbl.nl/sites/default/files/cms/publicaties/pbl-2016-nationale-energieverkenning-2016.PDF.

[49] Ecovat. *Ecovat thermal storage system*. 2017. URL: http://www.ecovat.eu.

[50] EN-Natuurlijk. *Factsheet Apeldoorn-Zuidbroek*. 2016. URL: http://www.ennatuurlijk.nl/downloads/401/LR_Sheet_Zuidbroek_Ennatuurlijk_feb2016.pdf.

[51] EN-Natuurlijk. *Factsheet Paleiskwartier Den Bosch*. 2016. URL: http://www.ennatuurlijk.nl/downloads/406/LR_Sheet_Paleiskwartier_Ennatuurlijk_feb2016.pdf.

[52] EN-Natuurlijk. *Factsheet Polderwijk Zeewolde*. 2016. URL: http://www.ennatuurlijk.nl/downloads/402/LR_Sheet_Zeewolde_Ennatuurlijk_feb2016.pdf.

[53] US department of energy. *The smart grid: an Introduction*. URL: http://energy.gov/sites/prod/files/oeprod/DocumentsandMedia/DOE_SG_Book_Single_Pages(1).pdf.

[54] *Energyplan advanced energy system analysis computer model. advanced energy system analysis computer model*. University of Aalborg, 2016. URL: http://www.energyplan.eu/training/documentation/.

[55] D. G. Erbs, S. A. Klein and J. A. Duffie. "Estimation of the diffuse radiation fraction for hourly, daily and monthly-average global radiation". In: *Solar Energy* 28.4 (1982), pp. 293–302.

[56] Jianhua Fan and Simon Furbo. "Thermal stratification in a hot water tank established by heat loss from the tank". In: *Solar Energy* 86.11 (2012), pp. 3460–3469.

[57] Francesco Fellin and Klaus Sommer. "Study of a low energy office building with thermal slabs and ground coupled heat pump". In: *Dipartimento di Fisica Tecnica, UniversitÃă di Padova (Italia)* (2003).

[58] J. Fink and J. L. Hurink. "Minimizing costs is easier than minimizing peaks when supplying the heat demand of a group of houses". In: *European journal of operational research* 242.2 (2015), pp. 644–650. ISSN: 0377-2217.

[59] Solomie A. Gebrezgabher, Miranda P.M. Meuwissen, Bram A.M. Prins and Alfons G.J.M. Oude Lansink. “Economic analysis of anaerobic digestionŮA case of Green power biogas plant in The Netherlands”. In: *{NJAS} - Wageningen Journal of Life Sciences* 57.2 (2010), pp. 109 –115. ISSN: 1573-5214. DOI: http://dx.doi.org/10.1016/j.njas.2009.07.006. URL: http://www.sciencedirect.com/science/article/pii/S1573521409000049.

[60] M. Gehrels. *Warmteopwekking in de muziekwijk*. 2014. URL: http://www.biowkk.eu/wp-content/uploads/2014/12/1418830954Cogas-dhr.-Gehrels-141210_presentatie-Muziekwijk.pdf.

[61] Marco ET Gerards, Hermen A Toersche, Gerwin Hoogsteen, Thijs van der Klauw, Johann L Hurink and Gerard JM Smit. “Demand side management using profile steering”. In: *PowerTech, 2015 IEEE Eindhoven*. IEEE. 2015, pp. 1–6.

[62] P.J.J.G. Geudens. *Drinkwaterstatistieken 2015*. Tech. rep. VEWIN, 2015. URL: http://www.vewin.nl/SiteCollectionDocuments/Publicaties/Drinkwaterstatistieken_Vewin_2015.pdf.

[63] Willem Gilijamse. “Fuel saving options in heat supply systems”. 1993.

[64] J. Gout. *EMG verklaring Meppel Nieuwveense landen*. Ed. by DWA. 2014.

[65] Lei Haiyan and Pall Valdimarsson. “District heating modelling and simulation”. In: 2009. URL: https://pangea.stanford.edu/ERE/db/IGAstandard/record_detail.php?id=5524.

[66] R. Halvgaard, N.K. Poulsen, H. Madsen and J.B. Jorgensen. “Economic Model Predictive Control for building climate control in a Smart Grid”. In: *Proceedings of 2012 IEEE PES innovative Smart Grid Technologies (ISGT)* (2012).

[67] Rasmus Halvgaard, Peder Bacher, Bengt Perers, Elsa Andersen, Simon Furbo, John B Jørgensen, Niels K Poulsen and Henrik Madsen. “Model predictive control for a smart solar tank based on weather and consumption forecasts”. In: *Energy Procedia* 30 (2012), pp. 270–278.

[68] YM Han, RZ Wang and YJ Dai. “Thermal stratification within the water tank”. In: *Renewable and Sustainable Energy Reviews* 13.5 (2009), pp. 1014–1026.

[69] S. Hardeman. *De stroomversnelling, effecten voor productie en werkgelegenheid*. Ed. by EIB-Economisch Instituut voor de Bouw. http://www.eib.nl/pdf/de_stroomversnelling.pdf.

[70] Gregor P Henze, Clemens Felsmann and Gottfried Knabe. “Evaluation of optimal control for active and passive building thermal storage”. In: *International Journal of Thermal Sciences* 43.2 (2004), pp. 173–183.

[71] Arif Hepbasli and Yildiz Kalinci. “A review of heat pump water heating systems”. In: *Renewable and Sustainable Energy Reviews* 13.6 (2009), pp. 1211–1229.

[72] J.B. Holm-Nielsen, T. Al Seadi and P. Oleskowicz-Popiel. “The future of anaerobic digestion and biogas utilization”. In: *Bioresource Technology* 100.22 (2009). {OECD} Workshop: Livestock Waste Treatment Systems of the Future: A Challenge to Environmental Quality, Food Safety, and Sustainability, pp. 5478 –5484. ISSN: 0960-8524. DOI: http://dx.doi.org/10.1016/j.biortech.2008.12.046. URL: http://www.sciencedirect.com/science/article/pii/S0960852408011012.

[73] B. Homan, R.P. van Leeuwen, M.V. ten Kortenaar and G.J.M. Smit. “A comprehensive model for battery State of Charge prediction”. In: *accepted by IEEE Powertech 2017 conference*. 2017.

[74] G. Hoogsteen, A. Molderink, J. L. Hurink and G. J. M. Smit. “Generation of flexible domestic load profiles to evaluate Demand Side Management approaches”. In: *2016 IEEE International Energy Conference (ENERGYCON)*. 2016, pp. 1–6. DOI: 10.1109/ENERGYCON.2016.7513873.

[75] Xiaosong Hu, Yuan Zou and Yalian Yang. “Greener plug-in hybrid electric vehicles incorporating renewable energy and rapid system optimization”. In: *Energy* 111 (2016), pp. 971 –980. ISSN: 0360-5442. DOI: http://dx.doi.org/10.1016/j.energy.2016.06.037. URL: http://www.sciencedirect.com/science/article/pii/S0360544216308118.

[76] ISO. *NEN-EN-ISO 7730 Ergonomics of the thermal environment - Analytical determination and interpretation of thermal comfort using calculation of the PMV and PPD indices and local thermal comfort criteria (ISO 7730:2005,IDT)*. 2005.

[77] ISSO. *ISSO-kleintje Koellast, bepalingsmethode voor het koelvermogen in vertrekken en gebouwen*. 2010.

[78] Pierre G Jansen, Sape J Mullender, Paul JM Havinga and Hans Scholten. “Lightweight EDF scheduling with deadline inheritance”. In: *University of Twente* (2003).

[79] I. Janssen-Visschers and G. van der Lee. *Vision on electricity sector production and tax development (in Dutch: Visie op productie- en belastingontwikkelingen in de elektriciteitssector)*. Tech. rep. Tennet, 2013. URL: http://www.tennet.eu/nl/fileadmin/downloads/About_Tennet/Publications/Technical_Publications/Visie_Ontwikkelingen_Netbeheerdersoverleg.pdf.

[80] Marijn R Jongerden and Boudewijn R Haverkort. “Which battery model to use?” In: *Software, IET* 3.6 (2009), pp. 445–457.

[81] Marijn R Jongerden, Jannik Hüls, Boudewijn R Haverkort and Anne Remke. “Assessing the cost of energy independence”. In: *Energy Conference (ENERGYCON), 2016 IEEE International*. IEEE. 2016, pp. 1–6.

[82] Ulrike Jordan and Klaus Vajen. “Realistic domestic hot-water profiles in different time scales”. In: *Report for IEA-SHC Task* 26 (2001).

[83] H.G.J. Kamp. *Kamerbrief warmtevisie*. URL: https://www.rijksoverheid.nl/onderwerpen/energiebeleid/documenten/kamerstukken/2015/04/02/kamerbrief-warmtevisie.

[84] N. Kaufman, M. Obeiter and E. Krause. *Putting a Price on Carbon: Reducing Emissions*. Ed. by World resources institute. 2016. URL: https://www.wri.org/sites/default/files/Putting_a_Price_on_Carbon_Emissions.pdf.

[85] Thijs van der Klauw, Marco ET Gerards, Gerard JM Smit and Johann L Hurink. “Optimal scheduling of electrical vehicle charging under two types of steering signals”. In: *Innovative Smart Grid Technologies Conference Europe (ISGT-Europe), 2014 IEEE PES*. IEEE. 2014, pp. 1–6.

[86] Eberhard Markus Kleinbach, WA Beckman and SA Klein. “Performance study of one-dimensional models for stratified thermal storage tanks”. In: *Solar energy* 50.2 (1993), pp. 155–166.

[87] L. van Klink. *Toekomstscenario’s voor afvalverbranding in Nederland 2015 Ű 2022*. Ed. by Dutch ministry of energy. 2015. URL: file:///D:/Profiles/LeeuwenRP/Downloads/toekomstscenario-s-voor-afvalverbranding-in-nederland-2015-2022.pdf.

[88] KNMI. “weather records station Hoogeveen”. URL: http://www.knmi.nl.

[89] JK Kok, CJ Warmer and IG Kamphuis. “PowerMatcher: multiagent control in the electricity infrastructure”. In: *Proceedings of the fourth international joint conference on Autonomous agents and multiagent systems*. 2005, pp. 75–82.

[90] Rick Kramer, Jos Van Schijndel and Henk Schellen. “Simplified thermal and hygric building models: a literature review”. In: *Frontiers of Architectural Research* 1.4 (2012), pp. 318–325.

[91] Phillip Oliver Kriett and Matteo Salani. “Optimal control of a residential microgrid”. In: *Energy* 42.1 (2012), pp. 321–330.

[92] Corien Lambregtse. *Stroomversnelling Nederland 4,5 miljoen woningen naar Nul op de Meter*. Ed. by Taskforce Vergunningen. 2015. URL: http://stroomversnelling.nl/wp-content/uploads/2016/02/brochure_woningcorporaties.pdf.

[93] Beat Lehmann, Viktor Dorer and Markus Koschenz. “Application range of thermally activated building systems tabs”. In: *Energy and Buildings* 39.5 (2007), pp. 593–598.

[94] Hongwei Li and Svend Svendsen. “Energy and exergy analysis of low temperature district heating network”. In: *Energy* 45.1 (2012). The 24th International Conference on Efficiency, Cost, Optimization, Simulation and Environmental Impact of Energy, {ECOS} 2011, pp. 237 –246. ISSN: 0360-5442. DOI: http://dx.doi.org/10.1016/j.energy.2012.03.056. URL: http://www.sciencedirect.com/science/article/pii/S0360544212002599.

[95] Yue Li, Zheng Shen, Asok Ray and Christopher D Rahn. “Real-time estimation of lead-acid battery parameters: A dynamic data-driven approach”. In: *Journal of Power Sources* 268 (2014), pp. 758–764.

[96] Henrik Lund, Bernd Möller, Brian Vad Mathiesen and A Dyrelund. “The role of district heating in future renewable energy systems”. In: *Energy* 35.3 (2010), pp. 1381–1390.

[97] Henrik Lund, Sven Werner, Robin Wiltshire, Svend Svendsen, Jan Eric Thorsen, Frede Hvelplund and Brian Vad Mathiesen. “4th Generation District Heating (4GDH): Integrating smart thermal grids into future sustainable energy systems”. In: *Energy* 68 (2014), pp. 1 –11. ISSN: 0360-5442. DOI: http://dx.doi.org/10.1016/j.energy.2014.02.089. URL: http://www.sciencedirect.com/science/article/pii/S0360544214002369.

[98] John W Lund. “Direct utilization of geothermal energy”. In: *Energies* 3.8 (2010), pp. 1443–1471.

[99] Xiandong Ma, Yifei Wang and Jianrong Qin. “Generic model of a community-based microgrid integrating wind turbines, photovoltaics and CHP generations”. In: *Applied Energy* 112 (2013), pp. 1475–1482.

[100] H. Madsen and J. Holst. “Estimation of continuous-time models for the heat dynamics of a building”. In: *Energy and Buildings(1995) 67-79* (1995).

[101] Dasa Majcen. “Predicting energy consumption and savings in the housing stock: A performance gap analysis in the Netherlands”. In: *A+BE | Architecture and the Built Environment* 6.4 (2016), pp. 1–224. ISSN: 2214-7233. URL: http://journals.library.tudelft.nl/index.php/faculty-architecture/article/view/majcen.

[102] James F Manwell and Jon G McGowan. “Lead acid battery storage model for hybrid energy systems”. In: *Solar Energy* 50.5 (1993), pp. 399–405.

[103] Chris Marnay and Ryan Firestone. “Microgrids: An emerging paradigm for meeting building electricity and heat requirements efficiently and with appropriate energy quality”. In: *Lawrence Berkeley National Laboratory* (2007).

[104] M. Martin and P. Berdahl. “Characteristics of Infrared Sky Radiation in the United States”. In: *Solar Energy* 33.3/4 (1984), pp. 321–336.

[105] Marijke Menkveld. *Kentallen warmtevraag woningen*. Tech. rep. ECN - Dutch Energy Research Centre, 2009. URL: https://www.rvo.nl/sites/default/files/bijlagen/RapportKentallenwarmtevraagwoningenNEW.pdf.

[106] Meppelenergie. *Meppel energy (in Dutch: Meppel energie)*. ND. URL: http://www.meppelenergie.nl/nieuwveense-landen.

[107] Milieucentraal. *Insights into energy consumption (in Dutch: Inzicht in uw energierekening)*. http://www.milieucentraal.nl/, visited December 2014. ND. URL: http://www.milieucentraal.nl/.

[108] J.W. Mitchel and J.E. Braun. *Principles of Heating, Ventilation, and Air Conditioning in buildings*. New York: Wiley, 2013.

[109] A. Molderink. “On the tree step methodology for smart grids”. PhD thesis. University of Twente, 2011. DOI: 10.3990/1.9789036531702.

[110] A. Molderink, V. Bakker, M.G.C Bosman, J.L. Hurink and Gerard J.M. Smit. “Management and control of domestic smart grid technology”. In: *IEEE Transactions on Smart Grid* 1.2 (2010), pp. 109–119.

[111] Albert Molderink, Vincent Bakker, Johann L Hurink and Gerard JM Smit. “Islanded house operation using a micro CHP”. In: (2007).

[112] Albert Molderink, Vincent Bakker, Maurice GC Bosman, Johann L Hurink and Gerard JM Smit. “Domestic energy management methodology for optimizing efficiency in smart grids”. In: *PowerTech, 2009 IEEE Bucharest*. IEEE. 2009, pp. 1–7.

[113] Albert Molderink, Vincent Bakker, Maurice GC Bosman, Johann L Hurink and Gerard JM Smit. “A three-step methodology to improve domestic energy efficiency”. In: *Innovative Smart Grid Technologies (ISGT), 2010*. IEEE, 2010, pp. 1–8.

[114] Albert Molderink, Vincent Bakker, Johann L Hurink and Gerard JM Smit. “Comparing demand side management approaches”. In: *Innovative Smart Grid Technologies (ISGT Europe), 2012 3rd IEEE PES International Conference and Exhibition on*. IEEE. 2012, pp. 1–8.

[115] Scott J Moura, Nalin A Chaturvedi and Miroslav Krstić. “Adaptive Partial Differential Equation Observer for Battery State-of-Charge/State-of-Health Estimation Via an Electrochemical Model”. In: *Journal of Dynamic Systems, Measurement, and Control* 136.1 (2014), p. 011015.

[116] NEDU. *Electricity consumption profiles (in Dutch: verbruiksprofielen 2016)*. 2016. URL: http://www.nedu.nl/portfolio/verbruiksprofielen/.

[117] DB Nelson, MH Nehrir and C Wang. “Unit sizing and cost analysis of stand-alone hybrid wind/PV/fuel cell power generation systems”. In: *Renewable energy* 31.10 (2006), pp. 1641–1656.

[118] NEN. *NEN 5060 Climate Reference Year*. 2010.

[119] Joel Neymark, R Judkoff, G Knabe, H-T Le, M Dürig, A Glass and G Zweifel. “Applying the building energy simulation test (BESTEST) diagnostic method to verification of space conditioning equipment models used in whole-building energy simulation programs”. In: *Energy and Buildings* 34.9 (2002), pp. 917–931.

[120] Astrid Nieße and Michael Sonnenschein. “Using Grid Related Cluster Schedule Resemblance for Energy Rescheduling”. In: *SmartGreens* (2013), pp. 22–31.

[121] M Nikdel et al. “Various battery models for various simulation studies and applications”. In: *Renewable and Sustainable Energy Reviews* 32 (2014), pp. 477–485.

[122] S Nykamp, A Molderink, V Bakker, HA Toersche, JL Hurink and GJM Smit. “Integration of heat pumps in distribution grids: Economic motivation for grid control”. In: *3rd IEEE PES International Conference and Exhibition on Innovative Smart Grid Technologies (ISGT Europe)*. IEEE, pp. 1–8.

[123] Stefan Nykamp. “Integrating renewables in distribution grids - storage, regulation and the interaction of different stakeholders in future grids”. PhD thesis. University of Twente, 2013. DOI: 10.3990/1.9789036500579.

[124] Frauke Oldewurtel, Alessandra Parisio, Colin N Jones, Dimitrios Gyalistras, Markus Gwerder, Vanessa Stauch, Beat Lehmann and Manfred Morari. “Use of model predictive control and weather forecasts for energy efficient building climate control”. In: *Energy and Buildings* 45 (2012), pp. 15–27.

[125] Rejane De Césaro Oliveski, Arno Krenzinger and Horácio A Vielmo. “Comparison between models for the simulation of hot water storage tanks”. In: *Solar Energy* 75.2 (2003), pp. 121–134.

[126] PK Olsen, H Lambertsen, R Hummelshøj, B Bøhm, CH Christiansen, S Svendsen, CT Larsen and J Worm. “A new low-temperature district heating system for low-energy buildings”. In: *Proceedings of the 11th International Symposium on District Heating and Cooling, Iceland*. 2008.

[127] RVO Dutch enterprise organization. *Investeringssubsidie duurzame energie (ISDE)*. 2016. URL: http://www.rvo.nl/subsidies-regelingen/investeringssubsidie-duurzame-energie.

[128] RVO Dutch Enterprise Organization. *Lake Source Cooling Eesermeer*. 2013. URL: http://www.rvo.nl/subsidies-regelingen/projecten/lake-source-cooling-eesermeer.

[129] RVO Netherlands enterprise organization. *Saldering, zelflevering en tariefkorting*. 2016. URL: http://www.rvo.nl/onderwerpen/duurzaam-ondernemen/duurzame-energie-opwekken/duurzame-energie/saldering-en-zelflevering.

[130] Poul Alberg Østergaard and Henrik Lund. “A renewable energy system in Frederikshavn using low-temperature geothermal energy for district heating”. In: *Applied Energy* 88.2 (2011). The 5th Dubrovnik Conference on Sustainable Development of Energy, Water and Environment Systems, held in Dubrovnik September/October 2009, pp. 479 –487. ISSN: 0306-2619. DOI: http://dx.doi.org/10.1016/j.apenergy.2010.03.018. URL: http://www.sciencedirect.com/science/article/pii/S0306261910000826.

[131] R.K. Pachauri and L.A. Meyer. *Climate Change 2014: Synthesis Report. Contribution of Working Groups I, II and III to the Fifth Assessment Report of the Intergovernmental Panel on Climate Change*. Tech. rep. IPCC, Geneva, Switzerland, 2014.

[132] Verónica Palomares, Paula Serras, Irune Villaluenga, Karina B Hueso, Javier Carretero-González and Teófilo Rojo. “Na-ion batteries, recent advances and present challenges to become low cost energy storage systems”. In: *Energy & Environmental Science* 5.3 (2012), pp. 5884–5901.

[133] Georgi Krasimiroy Pavlov and Bjarne W Olesen. “Building thermal energy storage-concepts and applications”. In: (2011).

[134] Leen Peeters, Richard De Dear, Jan Hensen and William D'haeseleer. “Thermal comfort in residential buildings: Comfort values and scales for building energy simulation”. In: *Applied Energy* 86.5 (2009), pp. 772–780.

[135] E.J. Pieterse-Quirijns, H. Beverloo and E.J.M. Blokker. "Warmwaterverbruik utiliteitsbouw getoetst met metingen". In: *TVVL magazine* 09-2011 (2011).

[136] Marouf Pirouti. "Modelling and analysis of a district heating network". PhD thesis. Cardiff University, 2013.

[137] Matteo Prina, Marco Cozzini, Giulia Garegnani, David Moser, Ulrich Filippi Oberegger, Roberto Vaccaro and Wolfram Sparber. "Smart energy systems applied at urban level: the case of the municipality of Bressanone-Brixen". In: *International Journal of Sustainable Energy Planning and Management* 10.0 (2016), pp. 33–52. ISSN: 2246 - 2929. DOI: 10.5278/ijsepm.2016.10.4. URL: https://journals.aau.dk/index.php/sepm/article/view/1225.

[138] Samuel Prívara, Jan Široký, Lukáš Ferkl and Jiří Cigler. "Model predictive control of a building heating system: The first experience". In: *Energy and Buildings* 43.2 (2011), pp. 564–572.

[139] Danny Pudjianto, Predrag Djapic, Marko Aunedi, Chin Kim Gan, Goran Strbac, Sikai Huang and David Infield. "Smart control for minimizing distribution network reinforcement cost due to electrification". In: *Energy Policy* 52 (2013). Special Section: Transition Pathways to a Low Carbon Economy, pp. 76 –84. ISSN: 0301-4215. DOI: http://dx.doi.org/10.1016/j.enpol.2012.05.021. URL: http://www.sciencedirect.com/science/article/pii/S0301421512004338.

[140] Peter Quaak, Harrie Knoef and Hubert E Stassen. *Energy from biomass: a review of combustion and gasification technologies*. Vol. 23. World Bank Publications, 1999.

[141] Daniel Quiggin, Sarah Cornell, Michael Tierney and Richard Buswell. "A simulation and optimisation study: Towards a decentralised microgrid, using real world fluctuation data". In: *Energy* 41.1 (2012), pp. 549–559.

[142] T Agami Reddy. "Literature Review on Calibration of Building Energy Simulation Programs: Uses, Problems, Procedures, Uncertainty, and Tools." In: *ASHRAE transactions* 112.1 (2006).

[143] Hongbo Ren, Weijun Gao and Yingjun Ruan. "Optimal sizing for residential CHP system". In: *Applied Thermal Engineering* 28.5 (2008), pp. 514–523.

[144] D. O. Rijksen, C. J. Wisse and A. W. M. van Schijndel. "Reducing peak requirements for cooling by using thermally activated building systems". In: *Energy and Buildings* 42.3 (2010), pp. 298–304.

[145] Stephanie Ropenus and Henrik Klinge Jacobsen. *A Snapshot of the Danish Energy Transition: Objectives, Markets, Grid, Support Schemes and Acceptance. Study*. Agora Energiewende, 2015.

[146] J. Ros and K. Schure. *Vormgeving van de energietransitie*. Dutch. Ed. by Planbureau voor de leefomgeving (Dutch bureau for the environment). 2016. URL: http://www.pbl.nl/sites/default/files/cms/publicaties/pbl-2016-vormgeving-van-de-energietransitie-1749.pdf.

[147] Marc A Rosen. "The exergy of stratified thermal energy storages". In: *Solar energy* 71.3 (2001), pp. 173–185.

[148] E. Ryckebosch, M. Drouillon and H. Vervaeren. "Techniques for transformation of biogas to biomethane". In: *Biomass and Bioenergy* 35.5 (2011), pp. 1633 –1645. ISSN: 0961-9534. DOI: http://dx.doi.org/10.1016/j.biombioe.2011.02.033. URL: http://www.sciencedirect.com/science/article/pii/S0961953411001085.

[149] Dirk Saelens, Wout Parys and Ruben Baetens. "Energy and comfort performance of thermally activated building systems including occupant behavior". In: *Building and Environment* 46.4 (2011), pp. 835–848.

[150] SBR. *SBR reference building details*. 2017. URL: http://www.sbrcurnet.nl/producten/referentiedetails.

[151] A.E. Scheepens, Flipsen S.F.J., P. Vogiatzakis and J.C. Brezet. *An Ecocost-Value Ratio (EVR) approach to the design of a Product-Service System for environmentally sustainable residential heating energy use*. 2013.

[152] M.J.J. Scheepers, A.J. Seebregts, C.B. Hanschke and F.J.D. Nieuwenhout. *Influence of innovative technology on the future electricity infrastructure (in Dutch: Invloed van innovatieve technologie op de toekomstige elektriciteitsinfrastructuur)*. Tech. rep. ECN, 2007.

[153] B.L. Schepers and M.P.J. van Valkengoed. *Warmtenetten in Nederland - Overzicht van grootschalige en kleinschalige warmtenetten in Nederland*. Tech. rep. 09.3031.45. http://www.ce.nl/publicatie/warmtenetten_in_nederland/976. CE-Delft, 2009.

[154] Ken Sejling. "Modelling and prediction of load in district heating systems". PhD thesis. DTU, 1993. URL: http://www2.imm.dtu.dk/pubdb/views/edoc_download.php/6757/pdf/imm6757.pdf.

[155] SenterNovem. *Reference houses EPC 0.8 (in Dutch: Referentiewoningen nieuwbouw EPC 0.8)*. 2006-2011.

[156] Girish Kumar Singh. "Solar power generation by PV (photovoltaic) technology: a review". In: *Energy* 53 (2013), pp. 1–13.

[157] Jan Široký, Frauke Oldewurtel, Jiří Cigler and Samuel Prívara. "Experimental analysis of model predictive control for an energy efficient building heating system". In: *Applied Energy* 88.9 (2011), pp. 3079–3087.

[158] W.A.A. Slob W.H.; Monna. *Bepaling van directe en diffuse straling en van zonneschijnduur uit 10-minuutwaarden van de globale straling*. Tech. rep. TR-136. KNMI, 1991.

[159] DGMR Software. *Enorm software for EPC calculations*. 2017. URL: https://dgmrsoftware.nl/enorm.php.

[160] R. Sonderegger. "DIAGNOSTIC TESTS DETERMINING THE THERMAL RESPONSE OF A HOUSE". In: *ASHRAE Meeting, Atlanta, GA, January 29-February 2, 1978*. 1978.

[161] CBS Dutch bureau of Statistics. *Statistical energy balance Netherlands (in Dutch: StatLine Energiebalans Kerncijfers)*. URL: http://statline.cbs.nl/Statweb/publication/?DM=SLNL&PA=37281&D1=a&D2=0-1,4,7-12&D3=53,78,128,143,148,l&HDR=G1&STB=T,G2&VW=T.

[162] CBS Dutch bureau of statistics. *Compendium voor de leefomgeving*. 2016. URL: http://www.clo.nl/indicatoren/nl0053-energiebalans-nederland-tabel.

[163] Christian Struck. "Uncertainty propagation and sensitivity analysis techniques in building performance simulation to support conceptual building and system design". Thesis. Eindhoven University of Technology, the Netherlands, 2012.

[164] Fatemeh Tahersima, Jakob Stoustrup, Soroush Afkhami Meybodi and Henrik Rasmussen. "Contribution of domestic heating systems to smart grid control". In: *Decision and Control and European Control Conference (CDC-ECC), 2011 50th IEEE Conference on*. IEEE, pp. 3677–3681.

[165] TESS. *TRNSYS Transient System Simulation Tool*. http://www.trnsys.com/, visited December 2014. ND.

[166] TESS. *TRNSYS Transient System Simulation Tool*. http://www.trnsys.com/, visited December 2014. ND.

[167] Yuan Tian and Chang-Ying Zhao. "A review of solar collectors and thermal energy storage in solar thermal applications". In: *Applied Energy* 104 (2013), pp. 538–553.

[168] HA Toersche, V Bakker, A Molderink, S Nykamp, JL Hurink and GJM Smit. "Controlling the heating mode of heat pumps with the TRIANA three step methodology". In: *Innovative Smart Grid Technologies (ISGT), 2012 IEEE PES*. IEEE, pp. 1–7.

[169] Hermen A. Toersche. “Effective and efficient coordination of flexibility in smart grids”. PhD thesis. University of Twente. ISBN: 978-90-365-4197-8. DOI: 10.3990/1.9789036541978.

[170] UNFCCC. *Summary of the Kyoto protocol*. Ed. by UNFCCC. 2016. URL: http://bigpicture.unfccc.int/#content-the-paris-agreemen.

[171] Unicef. *The state of the world’s children, definitions*. 2012. URL: https://www.unicef.org/sowc2012/pdfs/SOWC-2012-DEFINITIONS.pdf.

[172] Miet Van Dael, Nathalie Márquez, Patrick Reumerman, Luc Pelkmans, Tom Kuppens and Steven Van Passel. “Development and techno-economic evaluation of a biorefinery based on biomass (waste) streams–case study in the Netherlands”. In: *Biofuels, Bioproducts and Biorefining* 8.5 (2014), pp. 635–644.

[173] Nathan Van Den Bossche. “Experimenteel onderzoek naar schattingsmethodes bij woningen”. Gent University, 2005. URL: http://lib.ugent.be/fulltxt/RUG01/000/895/774/RUG01-000895774_2010_0001_AC.pdf.

[174] NEN commission ventilation and air tightness of buildings. *NEN 8088-1+C1:2012 Ventilation and infiltration for buildings - Calculation method for the supply air temperature corrected ventilation and infiltration air volume rates for calculating energy performance - Part 1: Calculation method*. Tech. rep. NEN Dutch Standardization Institute, 2012.

[175] Geert Verbong and Frank Geels. “The ongoing energy transition: lessons from a socio-technical, multi-level analysis of the Dutch electricity system (1960–2004)”. In: *Energy policy* 35.2 (2007), pp. 1025–1037.

[176] Clara Verhelst, Filip Logist, Jan Van Impe and Lieve Helsen. “Study of the optimal control problem formulation for modulating air-to-water heat pumps connected to a residential floor heating system”. In: *Energy and Buildings* 45.0 (2012), pp. 43–53.

[177] VIEGA. *Technische handleiding Fonterra vloer- en wandverwarming*. 2009.

[178] H-J Wagner. “Introduction to wind energy systems”. In: *EPJ Web of Conferences*. Vol. 54. EDP Sciences. 2013, p. 01011.

[179] Wei Wang, Qingtao Luo, Bin Li, Xiaoliang Wei, Liyu Li and Zhenguo Yang. “Recent progress in redox flow battery research and development”. In: *Advanced Functional Materials* 23.8 (2013), pp. 970–986.

[180] Arthur Wellinger, Jerry D Murphy and David Baxter. *The biogas handbook: science, production and applications*. Elsevier, 2013.

[181] C. Wetter and J.B. de Wit. *Warmte in de Euregio*. 2016. URL: http://www.re2alko.de/wiefm/wp-content/uploads/2016/04/2016-02-10-niederländische-Broschüre-WiEfm-mit-Karte.pdf.

[182] H.J.L. Witte, A.J. van Gelder and P. Klep. "A very large distributed ground source heat pump project for domestic heating: Schoenmakershoek, Etten-Leur (the Netherlands)". In: *Proceedings Ecostock, the Tenth International Conference on Thermal Energy Storage. In Richard Stockton College, New Jersey*. 2006.

[183] Erik Ramsgaard Wognsen, Boudewijn R Haverkort, Marijn Jongerden, René Rydhof Hansen and Kim Guldstrand Larsen. "A score function for optimizing the cycle-life of battery-powered embedded systems". In: *International Conference on Formal Modeling and Analysis of Timed Systems*. Springer. 2015, pp. 305–320.

[184] J. Xu, R.Z. Wang and Y. Li. "A review of available technologies for seasonal thermal energy storage". In: *Solar Energy* (103 2014), pp. 610–638.

[185] Cheng Yan, Liandong Zhu and Yanxin Wang. "Photosynthetic {CO2} uptake by microalgae for biogas upgrading and simultaneously biogas slurry decontamination by using of microalgae photobioreactor under various light wavelengths, light intensities, and photoperiods". In: *Applied Energy* 178 (2016), pp. 9 –18. ISSN: 0306-2619. DOI: http://dx.doi.org/10.1016/j.apenergy.2016.06.012. URL: http://www.sciencedirect.com/science/article/pii/S0306261916307875.

[186] Liandong Zhu. "Biorefinery as a promising approach to promote microalgae industry: An innovative framework". In: *Renewable and Sustainable Energy Reviews* 41 (2015), pp. 1376 –1384. ISSN: 1364-0321. DOI: http://dx.doi.org/10.1016/j.rser.2014.09.040. URL: http://www.sciencedirect.com/science/article/pii/S1364032114008132.

[187] Bas de Zwart, Lucas van den Boogaard, Peter Heijboer, Jolt Oostra and Victor van Heekeren. *Handboek Geothermie in de Gebouwde Omgeving*. Tech. rep. 2012. URL: http://geothermie.nl/fileadmin/user_upload/documents/bestanden/Werkgroep_GO/Geothermie_in_de_Gebouwde_Omgeving.pdf.

Publications

[RvL:1] J. Fink and R. P. van Leeuwen. “Earliest Deadline Control of a Group of Heat Pumps with a Single Energy Source”. In: *Energies* 9.7 (2016), p. 552. ISSN: 1996-1073. DOI: 10.3390/en9070552. URL: http://www.mdpi.com/1996-1073/9/7/552.

In this paper, we develop and investigate the optimal control of a group of 104 heat pumps and a central Combined Heat and Power unit (CHP). The heat pumps supply space heating and domestic hot water to households. Each house has a buffer for domestic hot water and a floor heating system for space heating. Electricity for the heat pumps is generated by a central CHP unit, which also provides thermal energy to a district heating system. The paper reviews recent smart grid control approaches for central and distributed levels. An online algorithm is described based on the earliest deadline first theory that can be used on the aggregator level to control the CHP and to give signals to the heat pump controllers if they should start or should wait. The central controller requires only a limited amount of privacy-insensitive information from the heat pump controllers about their deadlines, which the heat pump controllers calculate for themselves by model predictions. In this way, a robust heat pump and CHP control is obtained, which is able to minimize energy demand and results in the desired thermal comfort for the households. The simulations demonstrate fast computation times due to minor computational and communication overheads.

[RvL:2] J. Fink, R. P. van Leeuwen, J. L. Hurink and G. J. M. Smit. “Linear programming control of a group of heat pumps”. In: *Energy, sustainability and society* 5.33 (2015). ISSN: 2192-0567.

For a new district in the Dutch city Meppel, a hybrid energy concept is developed based on bio-gas co-generation. The generated electricity is used to power domestic heat pumps which supply thermal energy for domestic hot water and space heating demand of households. In this paper, we investigate direct control of the heat pumps by the utility and how the large-scale optimization problem that is created can be reduced significantly. Two different linear programming control methods (global MILP and time scale MILP) are presented. The latter solves large-scale optimization problems in considerably less computational time. For

simulation purposes, data of household thermal demand is obtained from prediction models developed for this research. The control methods are compared with a reference control method resembling PI on/off control of each heat pump. The reference control results in a dynamic electricity consumption with many peak loads on the network, which indicates a high level of simultaneous running heat pumps at those times. Both methods of mix integer linear programming (MILP) control of the heat pumps lead to a much improved, almost flat electricity consumption profile. Both optimization control methods are equally able to minimize the maximum peak consumption of electric power by the heat pumps, but the time scale MILP method requires much less computational effort. Future work is dedicated on further development of optimized control of the heat pumps and the central CHP.

[RvL:3] B. Homan, R. P. van Leeuwen, G. J. M. Smit, L. Zhu and J. B. de Wit. "Validation of a predictive model for smart control of electrical energy storage". In: *2016 IEEE International Energy Conference (ENERGYCON), Leuven, Belgium*. Leuven, Belgium: IEEE Power Electronics Society, 2016.

The purpose of this paper is to investigate the applicability of a relatively simple model which is based on energy conservation for model predictions as part of smart control of thermal and electric storage. The paper reviews commonly used predictive models. Model predictions of charging and discharging cycles are compared with experimental data of a domestic hot water thermal storage and lead acid batteries.

[RvL:4] R. P. van Leeuwen, I. Gebhardt, J. B. de Wit and G. J. M. Smit. "A Predictive Model for Smart Control of a Domestic Heat Pump and Thermal Storage". In: *Proceedings of the 5th International Conference on Smart Cities and Green ICT Systems - Volume 1: SMARTGREENS,* 2016, pp. 136–145. ISBN: 978-989-758-184-7. DOI: 10.5220/0005762201360145.

[RvL:5] R.P. van Leeuwen, J.B. de Wit and G.J.M. Smit. "Review of urban energy transition in the Netherlands and the role of smart energy management". In: *submitted to Journal Energy Conversion and Management, special issue for the 4th Sustainable Thermal Energy Management International Conference (SusTEM2017), status: conditionally accepted after minor revisions*. 2017.

[RvL:6] R.P. van Leeuwen, J.B. de Wit and G.J.M. Smit. "Energy scheduling model to optimize transition routes towards 100% renewable urban districts". In: *accepted by International Journal of sustainable energy planning and management* (2017).

[RvL:7] K.X. Perez, M. Baldea, T.F. Edgar, G. Hoogsteen, R.P. van Leeuwen, T. van der Klauw, B. Homan, J. Fink and G.J.M. Smit. “Soft-islanding a Group of Houses through Scheduling of CHP, PV and Storage”. In: *Proceedings IEEE Energycon 2016*. 2016. DOI: 10.1109/ENERGYCON.2016.7513972.

[RvL:8] R. P. van Leeuwen, J. Fink and G. J. M. Smit. “Central model predictive control of a group of domestic heat pumps, case study for a small district”. In: *4th International Conference on Smart Cities and Green ICT Systems (SMARTGREENS 2015), Lisbon, Portugal*. Lisbon, Portugal: Insticc Institute for Systems, Technologies of Information, Control and Communication, 2015, pp. 136–147.

In this paper we investigate optimal control of a group of heat pumps. Each heat pump provides space heating and domestic hot water to a single household. Besides a heat pump, each house has a buffer for domestic hot water and a floor heating system for space heating. The paper describes models and algorithms used for the prediction and planning steps in order to obtain a planning for the heat pumps. The optimization algorithm minimizes the maximum peak electricity demand of the district. Simulated results demonstrate the resulting aggregated electricity demand, the obtained thermal comfort and the state of charge of the domestic hot water storage for an example house. Our results show that a model predictive control outperforms conventional control of individual heat pumps based on feedback control principles.

[RvL:9] R. P. van Leeuwen, J. B. de Wit, J. Fink and G. J. M. Smit. “Thermal storage in a heat pump heated living room floor for urban district power balancing - effects on thermal comfort, energy loss and costs for residents”. In: *SMARTGREENS 2014 - Proceedings of the 3rd International Conference on Smart Grids and Green IT Systems, Barcelona, Spain*. Barcelona, Spain: INSTICC Institute for Systems, Technologies of Information, Control and Communication, 2014, pp. 43–50.

For the Dutch smart grid demonstration project Meppelenergie, the effects of controlled thermal energy storage within the floor heating structure of a living room by a heat pump are investigated. Storage possibilities are constrained by room operative and floor temperatures. Simulations indicate limitations for floor heating storage due to absorption of solar energy within the house. To balance power for district renewable energy supply, substantial energy can be stored into the floor without violating comfort limits. Heat loss to the outside due to floor heating storage is small in case of low energy houses and can be financially compensated. This may result in a proposition for residents which is equivalent to heating without thermal storage for power balancing purposes.

[RvL:10] R. P. van Leeuwen, J. B. de wit, J. Fink and G. J. M. Smit. “House thermal model parameter estimation method for Model Predictive Control applications”. In: *IEEE PowerTech Eindhoven 2015, Einhoven, The Netherlands*. Einhoven, The Netherlands: IEEE Power & Energy Society, 2015, pp. 1–6.

In this paper we investigate thermal network models with different model orders applied to various Dutch low-energy house types with high and low interior thermal mass and containing floor heating. Parameter estimations are performed by using data from TRNSYS simulations. The paper discusses results in relation to model order and the order which yields a sufficient level of accuracy is determined. The paper presents a semi-physical estimation method which is used to improve correlation of model parameters with physical determined values. The thermal network model can be used for various simulation studies or for Model Predictive Control (MPC) of house heating or cooling systems. The paper investigates accuracy of the model for MPC by comparing MPC-results with results from TRNSYS simulations, including ventilation heat losses.

[RvL:11] R. P. van Leeuwen, J. Fink, G. J. M. Smit and J. B. de Wit. “Upscaling a district heating system based on biogas cogeneration and heat pumps”. In: *Energy, sustainability and society* 5.16 (2015). ISSN: 2192-0567.

The energy supply of the Meppel district Nieuwveense landen is based on biogas cogeneration, district heating, and ground source heat pumps. A centrally located combined heat and power engine (CHP) converts biogas from the municipal wastewater treatment facility into electricity for heat pumps and heat for district heating purposes. Development of the urban district is influenced by the current economic and building decline. For the district heating energy concept, a migration strategy for the required infrastructure is required. The migration spans the district’s small-scale starting phase involving 40 houses up to a scale of 176 houses. An optimization model which maximizes profitability is developed which includes data from district heating and cooling demand patterns. With the optimization model, optimal CHP size, boiler size, and operational hours are determined for various scenarios. From the scenario analysis, a migration strategy is developed which starts with a simple system concept supported by boilers to a larger system which includes a CHP. Sustainability in terms of CO2 emission savings of the energy concept is compared with other possible energy concepts.

About the author:

Richard received a cum laude bachelor degree in Mechanical Engineering from the Rotterdam University of Applied Sciences and a master degree in Automotive Engineering from the Eindhoven University of Technology. He started his career as entrepreneur in the field of Renewable Energy and design engineer. He worked for seven years as consultant at Nedtrain consulting and Lloyd's Register Rail Europe on Railway Rolling Stock Safety, Reliability and Asset Management projects. From 2007 he works for Saxion as lecturer and project manager in the field of Renewable Energy and he recently succeeded Jan de Wit as Professor Renewable Energy Systems. The Research of the group includes Bio-Energy, Smart Energy for Buildings and Integration of Renewable Energy in the Built Environment.

His PhD-Research took place from 2013 to 2017 at the University of Twente in the area of Smart Multi Commodity Grids and Integration of Renewable Energy.